



**HAL**  
open science

## Generating whole body movements for dynamic anthropomorphic systems under constraints.

Layale Saab

► **To cite this version:**

Layale Saab. Generating whole body movements for dynamic anthropomorphic systems under constraints.. Robotics [cs.RO]. Université Paul Sabatier - Toulouse III, 2011. English. NNT: . tel-00667668

**HAL Id: tel-00667668**

**<https://theses.hal.science/tel-00667668>**

Submitted on 8 Feb 2012

**HAL** is a multi-disciplinary open access archive for the deposit and dissemination of scientific research documents, whether they are published or not. The documents may come from teaching and research institutions in France or abroad, or from public or private research centers.

L'archive ouverte pluridisciplinaire **HAL**, est destinée au dépôt et à la diffusion de documents scientifiques de niveau recherche, publiés ou non, émanant des établissements d'enseignement et de recherche français ou étrangers, des laboratoires publics ou privés.



# THÈSE

En vue de l'obtention du

## DOCTORAT DE L'UNIVERSITÉ DE TOULOUSE

**Délivré par** *l'Université Toulouse III - Paul Sabatier*  
**Discipline ou spécialité :** *Robotique et Informatique*

---

**Présentée et soutenue par** *Layale SAAB*  
**Le** *31 octobre 2011*

**Titre :** *Generating Whole Body Movements for Dynamic Anthropomorphic Systems under Constraints*

---

### JURY

*Abderrahmane Kheddar*  
*Yoshihiko Nakamura*  
*Michel Courdesses*  
*Nicolas Mansard*

---

**Ecole doctorale :** *Systèmes (EDSYS)*  
**Unité de recherche :** *LAAS - CNRS*  
**Directeur(s) de Thèse :** *Philippe Souères, Jean-Yves Fourquet*  
**Rapporteurs :** *Abderrahmane Kheddar, Yoshihiko Nakamura*

## Abstract

This thesis studies the question of whole body motion generation for anthropomorphic systems. Within this work, the problem of modeling and control is considered by addressing the difficult issue of generating human-like motion.

First, a dynamic model of the humanoid robot HRP-2 is elaborated based on the recursive Newton-Euler algorithm for spatial vectors. A new dynamic control scheme is then developed adopting a cascade of quadratic programs (QP) optimizing the cost functions and computing the torque control while satisfying equality and inequality constraints. The cascade of the quadratic programs is defined by a stack of tasks associated to a priority order. Next, we propose a unified formulation of the planar contact constraints, and we demonstrate that the proposed method allows taking into account multiple non coplanar contacts and generalizes the common ZMP constraint when only the feet are in contact with the ground.

Then, we link the algorithms of motion generation resulting from robotics to the human motion capture tools by developing an original method of motion generation aiming at the imitation of the human motion. This method is based on the reshaping of the captured data and the motion editing by using the hierarchical solver previously introduced and the definition of dynamic tasks and constraints. This original method allows adjusting a captured human motion in order to reliably reproduce it on a humanoid while respecting its own dynamics.

Finally, in order to simulate movements resembling to those of humans, we develop an anthropomorphic model with higher number of degrees of freedom than the one of HRP-2. The generic solver is used to simulate motion on this new model. A sequence of tasks is defined to describe a scenario played by a human. By a simple qualitative analysis of motion, we demonstrate that taking into account the dynamics provides a natural way to generate human-like movements.

## Résumé

Cette thèse étudie la question de la génération de mouvements corps-complet pour des systèmes anthropomorphes. Elle considère le problème de la modélisation et de la commande en abordant la question difficile de la génération de mouvements ressemblant à ceux de l'homme.

En premier lieu, un modèle dynamique du robot humanode HRP-2 est élaboré à partir de l'algorithme récursif de Newton-Euler pour les vecteurs spatiaux. Un nouveau schéma de commande dynamique est ensuite développé, en utilisant une cascade de programmes quadratiques (QP) optimisant des fonctions cots et calculant les couples de commande en satisfaisant des contraintes d'égalité et d'inégalité. La cascade de problèmes quadratiques est définie par une pile de tâches associée à un ordre de priorité. Nous proposons ensuite une formulation unifiée des contraintes de contacts planaires et nous montrons que la méthode proposée permet de prendre en compte plusieurs contacts non coplanaires et généralise la contrainte usuelle du ZMP dans le cas où seulement les pieds sont en contact avec le sol.

Nous relient ensuite les algorithmes de génération de mouvement issus de la robotique aux outils de capture du mouvement humain en développant une méthode originale de génération de mouvement visant à imiter le mouvement humain. Cette méthode est basée sur le recalage des données capturées et l'édition du mouvement en utilisant le solveur hiérarchique précédemment introduit et la définition de tâches et de contraintes dynamiques. Cette méthode originale permet d'ajuster un mouvement humain capturé pour le reproduire fidèlement sur un humanode en respectant sa propre dynamique.

Enfin, dans le but de simuler des mouvements qui ressemblent à ceux de l'homme, nous développons un modèle anthropomorphe ayant un nombre de degrés de liberté supérieur à celui du robot humanode HRP2. Le solveur générique est utilisé pour simuler le mouvement sur ce nouveau modèle. Une

série de tâches est définie pour décrire un scénario joué par un humain. Nous montrons, par une simple analyse qualitative du mouvement, que la prise en compte du modèle dynamique permet d'accroître naturellement le réalisme du mouvement.

To my parents, who were always present in good and in bad times, who  
taught me everything and made today possible ...

## Acknowledgements

I would like to acknowledge everyone who helped me achieve this thesis and accompanied me throughout several years of work. It is due to their support that this thesis is completed.

I sincerely thank Abderrahmane Kheddar and Yoshihiko Nakamura for their examination of this thesis. I am honored by their close insight, their constructive feedback and the interest they had in my work. I am also grateful to Michel Courdesses and Vincent Padois for accepting to be members of the jury.

My first gratitude goes to my thesis supervisors Philippe Souères and Jean-Yves Fourquet, for their patience, their guidance and the experience they brought to me during my research work. I have learned how to deal with problems with wisdom and motivation. I had the chance to improve my research skills because they believed in my ideas. A very special thanks goes to Nicolas Mansard for whom I owe most of my achievements. I was supported by his knowledge and guidance on many scientific and technical topics.

I am lucky that I have encountered such wise and open-minded people in the amazing research group of Gepetto, where the teamwork is fundamental. During my thesis, I worked with many PhD students and discussed with them scientific and technical issues. The cheerful atmosphere was always inside the laboratory also in our outings. I am especially grateful for Oussama who helped me from the beginning of this journey in the master's internship. Special thanks to Sovan and Oscar for their collaboration in this thesis. I am thankful for Manish, Sebastien, Thomas, Duong and Antonio who have always supported me morally and helped me in technical problems. Thanks to the former students of Gepetto, Alireza, Mathieu, Minh, Anh, Francesco, David, for the good working environment. I also would like to thank all the members of the group RIA for making my journey easier inside a nice atmosphere.

Warm and big thanks to my parents, my brother and sister, my brother-in-law and my niece, for their support and their confidence in me during all my studies, and for the encouragement brought to me permanently. I also appreciate my grandmother's prayers and thoughts and for filling my life with love and strong beliefs.

Special thanks to my companion Georges for his moral support and motivation especially in the moments of doubts, his help and patience during the difficult periods of my work, and most importantly for the love, care and joy he brings to me.

My last thanks are for my friends in Toulouse who made my evenings and week-ends enjoyable, and my friends in Beirut who motivated me throughout my thesis and especially for those who made the effort to come all the way to Toulouse to attend my defence.

# Contents

<b>List of Figures</b>	<b>vii</b>
<b>List of Tables</b>	<b>xi</b>
<b>1 Introduction</b>	<b>1</b>
1.1 Problem statement . . . . .	1
1.2 Chapter organization . . . . .	4
1.3 Publications . . . . .	5
<b>2 State of the art</b>	<b>7</b>
2.1 Problem statement . . . . .	7
2.2 Methods for motion generation . . . . .	8
2.2.1 Geometric motion planning . . . . .	10
2.2.2 Inverse kinematics . . . . .	12
2.2.3 Inverse dynamics . . . . .	15
2.2.4 Numerical optimization . . . . .	16
2.2.5 Imitation by motion capture . . . . .	18
2.3 Methods for motion analysis . . . . .	20
2.3.1 Biomechanics . . . . .	23
2.3.2 Neurosciences . . . . .	27
2.4 Ergonomic analysis of motion . . . . .	32
2.4.1 Problem definition . . . . .	32
2.4.2 Existing tools . . . . .	34
2.4.2.1 Methods for the evaluation of risks of MSD . . . . .	35
2.4.2.2 Digital models and simulation tools . . . . .	35
2.4.2.3 Norms . . . . .	36
2.4.3 Link with Robotics . . . . .	37

## CONTENTS

---

<b>3</b>	<b>Dynamic motion generation</b>	<b>39</b>
3.1	Problem statement . . . . .	39
3.2	Inverse Kinematics . . . . .	42
3.2.1	Task function approach . . . . .	42
3.2.2	Hierarchy of tasks . . . . .	43
3.2.3	Inverse kinematics formulation . . . . .	44
3.2.4	Projected inverse kinematics . . . . .	44
3.2.5	QP cascade resolution . . . . .	45
3.2.5.1	Generic formulation . . . . .	46
3.2.5.2	Application to inverse kinematics . . . . .	48
3.3	Inverse Dynamics . . . . .	48
3.3.1	Task-space formulation . . . . .	48
3.3.2	Consistency with the generic template . . . . .	49
3.3.3	Projected inverse dynamics . . . . .	50
3.3.4	Application of the QP solver to the dynamics . . . . .	50
3.4	Inverse dynamics under contact constraints . . . . .	51
3.4.1	Insertion of the contact forces . . . . .	51
3.4.2	Sufficient condition for rigid planar contacts . . . . .	52
3.4.3	Including the contact forces within the QP Solver . . . . .	53
3.4.3.1	A first way of modeling the problem . . . . .	54
3.4.3.2	Using contact forces as variables . . . . .	55
3.4.3.3	Reducing the size of the variable $f$ . . . . .	56
3.4.4	Application to the particular case of the ZMP . . . . .	57
3.4.5	Generalization to multiple contacts . . . . .	58
3.5	Experiments . . . . .	59
3.5.1	HRP-2: the humanoid robot . . . . .	60
3.5.2	Experiment A: Swing posture . . . . .	61
3.5.2.1	Description . . . . .	61
3.5.2.2	Results . . . . .	63
3.5.3	Experiment B: sitting in the armchair . . . . .	65
3.5.3.1	Description . . . . .	65
3.5.3.2	Results . . . . .	66
3.5.4	Experiment C: 3D stepping . . . . .	68
3.5.4.1	Description . . . . .	68
3.5.4.2	Results . . . . .	69

3.6	Discussion . . . . .	70
3.7	Conclusion . . . . .	72
<b>4</b>	<b>Imitation and editing of dynamic motion capture</b>	<b>75</b>
4.1	Problem definition . . . . .	75
4.1.1	Motion imitation . . . . .	75
4.1.2	Motion editing . . . . .	77
4.2	The motion capture system description . . . . .	80
4.3	Kinematic adaptation of captured motion . . . . .	82
4.3.1	Multibody motion acquisition . . . . .	82
4.3.1.1	Kinematic optimization problem formulation . . . . .	83
4.3.1.2	Calibration of the body frame . . . . .	85
4.3.2	Virtual skeleton for motion validation . . . . .	86
4.3.3	Kinematic reshaping and imitation of motion by HRP-2 . . . . .	87
4.4	Dynamic processing of motion . . . . .	89
4.4.1	Posture Task . . . . .	89
4.4.2	Addition of arbitrary tasks . . . . .	91
4.4.3	Foot Sliding . . . . .	92
4.5	Results . . . . .	93
4.5.1	Knee oscillation . . . . .	95
4.5.1.1	Right hand motion . . . . .	96
4.5.2	Foot sliding introduction . . . . .	98
4.6	Conclusion . . . . .	98
<b>5</b>	<b>Generation of human-like motion</b>	<b>99</b>
5.1	Motivation . . . . .	99
5.2	Experimental setup . . . . .	101
5.2.1	The real captured motion . . . . .	101
5.2.1.1	Tools and softwares . . . . .	101
5.2.1.2	Description of the scenario . . . . .	102
5.2.2	The human model . . . . .	105
5.2.3	The simulated motion . . . . .	106
5.3	Parameters variation . . . . .	109
5.3.1	Mathematical description of tasks . . . . .	109
5.3.2	The gain tuning . . . . .	110

## CONTENTS

---

5.4	Results . . . . .	112
5.4.1	Kinematics vs Dynamics . . . . .	114
5.4.1.1	Visual comparison . . . . .	114
5.4.1.2	Technical comparison . . . . .	115
5.4.2	Qualitative comparison of torques . . . . .	118
5.4.2.1	Kinematics vs dynamics . . . . .	119
5.4.2.2	Dynamics vs real motion . . . . .	123
5.4.3	Synthesis . . . . .	127
5.4.4	Retargeting of motion vs Generation of motion . . . . .	128
5.5	Conclusion . . . . .	128
<b>6</b>	<b>Conclusion and Perspectives</b>	<b>131</b>
6.1	Contributions . . . . .	131
6.2	Perspectives . . . . .	132
<b>1</b>	<b>Introduction</b>	<b>135</b>
1.1	Contexte . . . . .	135
1.2	Répartition de la thèse . . . . .	139
<b>2</b>	<b>État de l'art</b>	<b>141</b>
2.1	Contexte . . . . .	141
2.2	Méthodes de génération de mouvement . . . . .	142
2.3	Méthodes d'analyse de mouvement . . . . .	144
2.4	Analyse ergonomique du mouvement . . . . .	146
2.4.1	Lien avec la Robotique . . . . .	147
<b>3</b>	<b>Génération de mouvement dynamique</b>	<b>149</b>
3.1	Contexte . . . . .	149
<b>4</b>	<b>Imitation et édition de mouvement dynamique capturé</b>	<b>153</b>
4.1	Définition du problème . . . . .	153
4.1.1	Imitation de mouvement . . . . .	153
4.1.2	édition de mouvement . . . . .	155
<b>5</b>	<b>Génération de mouvement similaire à l'humain</b>	<b>157</b>
5.1	Motivation . . . . .	157
5.2	Conclusion . . . . .	159

<b>6 Conclusion et Perspectives</b>	<b>161</b>
6.1 Contributions . . . . .	161
6.2 Perspectives . . . . .	162
<b>A Mathematical proof</b>	<b>165</b>
A.1 Control scheme . . . . .	165
A.2 Proof of equivalence . . . . .	166
<b>B Visual Task (2D Task)</b>	<b>167</b>
B.1 Interaction Matrix . . . . .	167
B.2 Frame system relations for the humanoid robot . . . . .	168
B.3 2D task specification . . . . .	169
<b>Bibliography</b>	<b>171</b>

## CONTENTS

---

# List of Figures

2.1	The modeling, analysis and synthesis loop relating humans to humanoids modeling and control . . . . .	8
2.2	An example of a kinematic chain with 2 revolute joints having one degree of freedom each denoted by $q_1$ and $q_2$ . . . . .	12
2.3	2 cases of robotic chain models . . . . .	13
2.4	The sequence of the different control inputs starting from the brain commands to the desired targets . . . . .	22
3.1	Successive orthogonal projections that lead to $\dot{q}^*$ given 2 compatible tasks: The first linear system is resolved, then the second linear system is solved within the solution space of the first linear system. . . . .	45
3.2	Two targets are given $e_1$ and $e_2$ . In the left figure, no prioritization is defined then the chain is free to move trying to reach both targets but none of the targets are reached. Prioritization is required to ensure the achievement of the prior task and to avoid failing both tasks. This is represented in the figure on the right where priority is given to $e_1$ . . . . .	46
3.3	Illustration in 3D space of the optimal sets for prioritization problems involving both equality and inequality linear systems. The line represents the equality system and the cube forms the set of inequalities. . . . .	47

## LIST OF FIGURES

---

3.4	Random sampling of the reached support region. The actual support polygon is the encompassing rectangle. The point clouds display the ZMP of random admissible forces: random forces $\phi_c$ are shot, and the corresponding $f = X^\# \phi_c$ are computed. If $\phi_c$ respects (3.29), the corresponding center of pressure is drawn. Each sub-figure displays the admissible forces $\phi_c$ for a different weighted inversion (the Euclidean norm is used on the top left, and random norms are used for the three others). Only a subregion of the support polygon can be reached, experimentally illustrating the fact that (3.29) is a too-restrictive sufficient condition. . . . .	55
3.5	Illustration of the application of a Jacobian inverse on a $2D$ system. . . . .	56
3.6	The humanoid robot HRP-2 with its specifications. . . . .	60
3.7	Experiment A: Top: Snapshots of the oscillatory movements at high frequency. Bottom: relative feet and ZMP positions at the corresponding time instants. The ZMP saturates on the front when the robot head is reaching its maximum amplitude and is breaking to go backward. Similarly, the ZMP nearly saturates on the back when the robot head is reaching its minimum amplitude and breaks to go forward. . . . .	61
3.8	Experiment A: Evolution of the $x$ coordinate of the ZMP during the low frequency 3.8(a) and the high frequency 3.8(b) tests. . . . .	62
3.9	Experiment A: Trajectory of the ankle, knee, hip and chest joints during the postural swing generated by the tracking by the head of a target moving back and forth with an amplitude of $10\text{ cm}$ at two different frequencies. . .	63
3.10	Experiment A: Joint torques variation during the whole experiment realized at high frequency with respect of the torque limit constraints on the chest 3.10(a) and the right leg 3.10(b) tests. . . . .	64
3.11	Experiment B: The sequence of tasks for the sitting experiment in terms of the iteration number which corresponds to the sampling period of $1\text{ms}$ . .	65
3.12	Experiment B: Front and side view of the sitting motion of HRP-2. These snapshots show respectively: the robot at the initial configuration; the position after one hand contact; the position after the second contact; and the final sitting position. . . . .	67

## LIST OF FIGURES

---

3.13	Experiment B: Evolution of the position of the center of mass (COM) during the motion. The three phases which correspond to changes in the number of contact are displayed by different colors. In the first part only the feet are in contact, then the contact of the left hand is added, finally the right hand is also in contact. . . . .	68
3.14	Experiment B: Joint angular variation with and without joint limits constraint . . . . .	69
3.15	Experiment C: Snapshots of the 3D stepping movement starting from a double contact state then showing, the chest and the hand's forward movement, and ending by the 3-contact configuration. . . . .	70
3.16	Experiment C: Timeline of the tasks involved in the bending experiment. . . . .	70
3.17	Experiment C: Trajectory of the projected COM on the planar ground. . . . .	71
4.1	Motion capture system with infra-red cameras and markers. . . . .	80
4.2	Transformation of the nodes from the human reference frame to the robot's frame. . . . .	85
4.3	Orientation of nodes and links. . . . .	86
4.4	Robot model and the skeleton created with the motion capture data. . . . .	87
4.5	Results of the kinematic optimization. . . . .	88
4.6	Results for the robot imitating the dance performed by a human. . . . .	93
4.7	Timeline showing the task sequence. . . . .	95
4.8	Scalogram of the right knee joint evolution. . . . .	95
4.9	Time evolution of the right knee. . . . .	96
4.10	Right hand evolution in the operational space. . . . .	97
4.11	Modification of the hand position adding an operational task. . . . .	97
4.12	Evolution of the ZMP with only the posture task. . . . .	98
5.1	The human MS model developed in YNL. . . . .	102
5.2	Front and back views of the human standing on the force plates and having the circular markers and rectangular electrodes attached to the different bodies. . . . .	104
5.3	The MS model in simulation of the recorded data using sDIMS simulator. The snapshots are taken at the initial configuration and at the end of each reaching task. The red arrow from the ground towards the model represents the resulting contact force. . . . .	105

## LIST OF FIGURES

---

5.4	Frame orientation of both systems ( $X$ is depth) . . . . .	107
5.5	Time sequencing of tasks defined for reproducing the captured motion with no usage of the recorded data itself . . . . .	108
5.6	The human model reaching the target in front and touching the ground with its left knee and foot. . . . .	111
5.7	Front view of the real human behavior, and the corresponding motion of the human model in kinematic and dynamic simulations. These snapshots show both the human and the model, respectively at the initial configuration, the convergence time of the first target, the configuration after reaching the second target, and the final posture when the third target is reached. .	113
5.8	Back and side views of the human model in dynamic simulation taken during the visualization of the same target from two different desired image points. . . . .	116
5.9	Postures of the human model in kinematic simulation while the vision target is modified three times with fixed desired image points, in the top figures, and changed desired image points according to the target, in the bottom figures. . . . .	117
5.10	The torques variation of the legs. . . . .	120
5.11	The torques variation of the torsos. . . . .	121
5.12	The torques variation of the arms. . . . .	122
5.13	The torques variation of the human legs and torso. . . . .	124
5.14	The norm of the torques exerted on both arms of the subject computed from sDIMS. . . . .	125
5.15	The posture of the human model in dynamic simulation when reaching the first target with a flexion of the right knee. . . . .	125
B.1	Projection of a 3D point onto the image plane . . . . .	168
B.2	Orientation of the camera frame $\{C\}$ and the robot's head frame $\{H\}$ . . .	169

# List of Tables

3.1	Computation time and real time of the experiments . . . . .	71
4.1	Segments and Nodes Hierarchy. . . . .	83
4.2	Joints for the posture tasks using the augmented HRP-2 model. . . . .	90
5.1	Joints of the human model. . . . .	105
5.2	Dynamic gain and corresponding kinematic gain values . . . . .	112
5.3	Time sequencing of the simulations. . . . .	119

## LIST OF TABLES

---

# 1

## Introduction

**Humans** and **Humanoids** can be compared and even more, the new trends in humanoid robotics work on making humanoids truly resemble humans. However, there is a big difference between making a robot look like a human and providing it the ability to act like one. As robots are more introduced into today's society, new issues arise like the anthropomorphism of robot movements. These issues concern different research fields. On the one hand, some works deal with the human-robot interaction, where the focus is on making the robot sensitive to the human and also move like a human, for instance, to generate an amicable exchange. On the other hand, other researches employ humanoid robotics developments to serve in many human fields as help for rehabilitation issues or ergonomic evaluation of work stations.

Humanoid robots are anthropomorphic systems with the particularity of having a redundant structure. Redundancy refers to the ability of a robot to reach a goal in more than a unique way. Therefore, there are a lot of challenges involved in generating motion for a humanoid robot. The solutions proposed by roboticists aim at realizing whole-body behavior. On a level of abstraction, one function that humanoids of the future are expected to satisfy is to move in a human-like manner. The most obvious source of inspiration is the human by studying his movements in order to extract useful information that can be used to generate humanoid motion.

### 1.1 Problem statement

The main subject of this thesis is to generate motion on anthropomorphic systems. Since we are interested in anthropomorphic systems that present similarities with humans, we

## 1. INTRODUCTION

---

are concerned with the generation of human-like behaviors and movements. From this context, different questions are derived:

- Why choose human motion? The humanoids role in our society is beyond the scientific and technological innovation. It consists of an increasing research and application sector where humanoids should get in control in some situations instead of only being controlled. This applies in the case of assistance of elderly, entertainment shows or replacement of workers in heavy or risky missions. In most of these services, friendly interaction with humans is a must. Another practical field of applications concerns the human motion analysis. By applying robotic tools and algorithms on humanoids and thus deriving movements similar to the humans', it is possible to help in medical diagnosis, to resolve rehabilitation problems and to achieve ergonomic analysis of motion.
- How to generate the motion? Anthropomorphic systems, particularly humanoid robots, are difficult to control due to their complex tree-like structure. Motion generation methods developed in robotics rely on algorithms and tools that deal with such issue. These methods either depend on motion planning, or tasks definition or optimization of criteria and constitute what we call model-based techniques. Other methods rely on imitation of real humans and can be defined as data-driven. From these methods, we can choose to simulate a motion from scratch depending on modeling and control of mechanical systems, or to replay a reference motion based on motion captured data.

In this thesis, we tackle first the issue of automatic motion generation. This constitutes the heart of this work where multiple steps need to be realized. Among the available motion generation methods, we choose to adopt a model-based approach. This choice is justified by our goal which is to provide a *fast, reliable* and *autonomous* software for producing motion. In particular, we focus on the generation of motion by resolving a set of defined tasks in order to produce a desired behavior. This leads to find a way to relate the task to whole-body movements that should respect some properties like balance and naturalism of motion. For simulation of such a motion, we have to account for three major problems:

- The redundancy of the human model.
- The generation of whole-body motion while satisfying multiple constraints.

- The realization of human-like motion.

A task is defined as a desired kinematic or dynamic property of the robot. By considering the dynamics, we seek to achieve a dynamically stable motion which could result in natural movements which resemble those of humans. Dynamics allows to take into account masses and inertia while modeling the anthropomorphic system. Moreover, contact forces can be integrated in the resolution of the dynamic equation of motion. This resolution defines the joint torques that are necessary to accomplish the desired tasks. Having a highly redundant system, we can find an infinity of possible solutions to choose from. This issue can be resolved either by applying an optimization problem and considering the task as the cost function to be minimized or by adopting techniques of numerical inversion [Nakamura and Hanafusa, 1986; Khatib, 1987]. In order to benefit from the redundancy, we can set multiple tasks and therefore minimize the sum of the costs functions associated with the tasks. However, if the tasks become conflicting, the numerical algorithm could lead to a robot state where none of them are satisfied. In order to encounter this problem, it is proposed to give for each task a corresponding priority order so that the system realizes the most prior task(s). At best, all the tasks can be accomplished. One important type of tasks that needs to be considered is the inequality task. The classical prioritization algorithms do not allow to take into account such type of constraints. However, they have been developed to consider inequalities by resolving a cascade of Quadratic Programs (QPs) on the kinematics level.

Seeking to compare the humanoids motion to a real human behavior, we intend to develop a dynamic hierarchical solver based on the kinematic formulation of QPs [Kanoun et al., 2009; Escande et al., 2010]. To this purpose, we adopt a dynamic model of the humanoid robot HRP-2 available at LAAS. We believe that by considering the dynamics, we can produce a more accurate and human-like motion. Therefore, we implement a solver that is composed of multiple optimization problems ordered in an hierarchical pile under dynamic constraints. The cost functions are prioritized and resolved while respecting the defined order of priority, in order to execute the expected task while taking into account the dynamics. The tasks and constraints can be expressed as equalities or inequalities allowing to consider any kind of behavior. Thus, the cascade of optimization problems set as quadratic programs is resolved iteratively, to compute, at each time step, the new control parameters that realize the given tasks and that respect the dynamic constraints. The first contribution of this thesis is the development of a method for whole-body motion generation considering the dynamics and conserving the balance of the humanoid robot

## 1. INTRODUCTION

---

while being subject to bilateral and unilateral constraints. In particular, we consider multiple non-coplanar contacts by defining a generic formulation for any kind of planar contact.

The second part of this work treats the issue of naturalism of motion. Since humanoids and humans present similar shapes, even if the human body is much more complex, we are interested in replaying captured motion by reshaping the acquired data for more accurate results. Using our developed software for the generation of motion based on a dynamic model, we apply this solver to edit and simulate a reference human motion on the robot. Instead of only imitating the motion, the recorded data is treated to compute reference joint trajectories of the humanoid model. Then, these pre-computed trajectories are defined as a reference task which is considered as a primary task in the stack. Finally, additional tasks can be added to edit the resulting motion in order to reproduce exactly the same original motion. The second outcome of this work is an original technique for blending motion that could possibly lead to feasible and human-like motion of the humanoid, based on a real captured motion.

After having coupled both techniques of stack of tasks definition and imitation of captured motion, we intend to simulate a human-like motion on a human model with no retargeting of data, but only by describing a set of tasks that can reliably reproduce an observed motion on a human. This aims at the validation of the generic nature of our software and the simulation of similar human behaviors. The idea behind this work is to be able to apply the developed method on any anthropomorphic model and to analyze the simulated motion results compared to the reference human motion.

The hierarchical dynamic solver of equality and inequality tasks is a promising tool to resolve the problem of generation of whole-body motion on dynamic anthropomorphic systems. Different applications in the field of human motion analysis constitute a motivation for this study. Nowadays, one important concern of the working society is the evaluation of workplaces on both the levels of ergonomics and prevention from accident risks and efficiency at work.

## 1.2 Chapter organization

This thesis is composed of four main chapters. In chapter 2, we recall the various existing methods of motion generation. Then, we explain how the combination between life sciences studies on human motion, and robotics algorithms and simulation tools could lead

to the generation, analysis and understanding of human motion. Then, we explain how to benefit from this knowledge to feed interesting applications to serve humans.

Chapter 3 sets the foundations and the development of the generic hierarchical dynamic solver of tasks under multiple types of constraints. Different scenarios defined by various stacks of tasks and constraints with multiple contact forces are resolved. This method allows to produce motion automatically while conserving dynamic balance, satisfying constraints and verifying coplanar or non-coplanar contact conditions. Simulations on the humanoid robot HRP-2 are presented to illustrate the validity of the method.

In chapter 4, we use the same solver to reshape and edit motion capture data. It allows to create a new blending technique which ensures the accuracy of the resulting motion along with the quickness of the editing method. These two chapters constitute the main contribution of the thesis.

An application on a human model, which verifies the generic nature of the approach, is presented in chapter 5. Here, we address the problem of reproducing a real motion being based only on the definition of a set of tasks. We establish a qualitative analysis of the simulated motion. We aim at providing a human-like motion generation tool for the analysis of human motion.

## 1.3 Publications

The different works we realized in this thesis led to the following publications:

- L.Saab, P.Souères and J.-Y.Fourquet: *Coupling manipulation and locomotion tasks for a humanoid robot*, Advances in Computational Tools for Engineering Applications (ACTEA) June 2009.
- L.Saab, N.Mansard, F.Keith, P.Souères, J.-Y.Fourquet, *Generation of Dynamic Motion for Anthropomorphic Systems under Prioritized Equality and Inequality Constraints*, IEEE Conference on Robotics and Automation (ICRA) May 2011.
- L.Saab, N. Mansard, O. Ramos, P. Souères and J-Y. Fourquet: *Generic Dynamic Motion Generation with Multiple Unilateral Constraints*, International Conference on Intelligent Robots and Systems (IROS), September 2011.
- O. Ramos, L. Saab, S. Hak. and N. Mansard: *Dynamic motion capture and edition using a stack of tasks*, IEEE Conference on Humanoid Robotics (Humanoids), October 2011.

## 1. INTRODUCTION

---

- L.Saab, N. Mansard, O. Ramos, P. Souères and J-Y. Fourquet: *Dynamic Whole-Body Motion Generation under Rigid Contacts and other Unilateral Constraints*, submitted to IEEE Transactions on Robotics (T-RO).

# 2

## State of the art

### 2.1 Problem statement

The humanoids of today share similarities with humans [Kaneko et al., 2009; Nakaoka et al., 2009]. However, this controversial innovation has few applications so far, which are mainly concerned by entertainment. Another important contribution could be developed in the field of interaction with humans, for example for assistance of elderly, which makes the human appearance of the robot more friendly for interaction. Yet, this is still work in progress. Alternatively, tools developed for humanoid robotics could serve in many human fields as help for rehabilitation issues [Venture et al., 2007] or ergonomic evaluation of work stations [Hue, 2008]. From those different kinds of physio-social applications, a close binding is created between humans and humanoid robots which are controlled by motion generation methods that should realize human-like behaviors on the basis of the properties of the human motion. These properties are derived from life sciences, as biomechanics or neurosciences, and they constitute norms to be respected while generating motion on humanoid robots. Under these constraints, researchers were able to develop human-like motion which could be compared to the human's on many levels. Our main concern is the development of an automatic simulation methodology to generate whole-body anthropomorphic movements respecting the dynamics of the bodies in motion. The ultimate goal is to be able to realize human-like behaviors respecting as much as possible constraints of different types and therefore apply this generic method of motion generation to the fields of human motion analysis. Different methods exist for the **generation**, **analysis** and **evaluation** of the human motion and will be discussed later on. Figure 2.1 represents these methods in different blocks, and shows the different links between

## 2. STATE OF THE ART

---

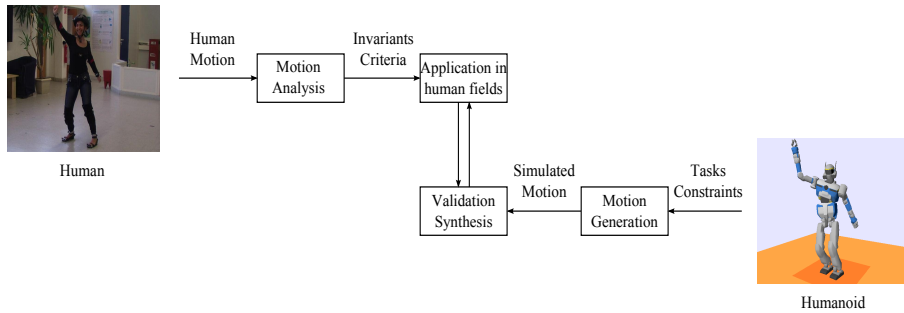


**Figure 2.1:** The modeling, analysis and synthesis loop relating humans to humanoid modeling and control

them. Given a human motion, many techniques from life sciences propose to analyze this motion and to synthesize corresponding properties. Whereas, developers from the fields of robotics, intend to model a humanoid robot, to generate and simulate its motion. First, we are concerned by implementing a complete algorithm for the resolution of the dynamic equation of motion on a multibody system, then by generating dynamic whole-body motion on the humanoid robot HRP-2 in simulation and finally by validating the generic nature of this method by applying it on any type of anthropomorphic model in order to demonstrate the human-like nature of the motion along with the possible benefits we could get with such a tool.

### 2.2 Methods for motion generation

Motion generation consists of the elaboration of control laws to be applied on different systems as manipulators, mobile robots, legged robots, or any avatar and more specifically anthropomorphic systems as humanoid robots. In our work, we are interested in generating human movements in order to generate behaviors of humans in different situations or actions that could especially reveal the capacity of conserving dynamic stability while accomplishing challenging tasks. To this purpose, we had an overview of the various existing methods and their specifications. In fact, human motion generation has been an increasing topic of research dealing either with the walking patterns only or with the movements of the upper parts of the body, then with the coordination of both upper and lower limbs, to finally obtain whole-body stable motions. Some researchers resolved only manipulation issues and thus were only concerned by the upper body movements for the execution of tasks requiring arms and torso motion, as in [Fourquet et al., 2007]. These works considered a model with moving upper limbs and fixed lower limbs. Other

researches involved biped locomotion and treated behaviors needing coordination between the different parts of the body, for example the works of [Kajita et al., 2003]. In this field of research, difficult problems arise due to the unstable nature of a biped structure and to the complexity of the mechanical structures.

Human figures as avatars or humanoid robots are thus difficult to animate or to control because of the need for choreographing many degrees of freedom so that they move in a coordinated and human-like fashion. Two classes of semi-automatic techniques have been developed for creating motion generation methods:

- model-based approaches which use simulation, search and optimization to generate character motion by restricting the space of possible motions via kinematics or dynamics in case of robotics applications or biomechanical models for medical, rehabilitation or entertainment applications:
  - Geometric motion planning
  - Inverse kinematics
  - Inverse dynamics
  - Numerical optimization
- data-driven approaches which take captured motion as a reference to create the movements of the model, these data contain the subtle movement details recorded from a human actor:
  - Imitation of captured motion

Actually, making a robot realize the movements that it has been assigned for can be achieved by different methods, depending on the context, the application and the complexity of the tasks that need to be executed. For ad-hoc and complex tasks that can hardly be further decomposed, the method usually adopted is to directly compute the trajectory that will be tracked by the robot. This is especially interesting in constrained environments, where the robot should move and accomplish tasks while avoiding obstacles [Kuffner, 1998]. For multiple tasks that concern different end effectors, and where it is important to guarantee the accomplishment of some prior task, even if the scenario becomes conflicting, the task-function formalism [Samson et al., 1991] is useful. This formalism is based on the prioritization schemes [Siciliano and Slotine, 1991; Baerlocher and Boulic, 1998] and defines the most interesting tool to deal with highly redundant systems.

## 2. STATE OF THE ART

---

It is applied on both levels of kinematics [Nakamura and Hanafusa, 1986] and dynamics [Khatib, 1987] modeling. For extreme motions, such trajectories can be computed using an optimization-based method – like kicking motions and throwing motions presented in [Miossec et al., 2006; Lengagne et al., 2010] – or by copying and adapting an observed trajectory, as the “aizu-bandaisan odori” dance that has been reproduced by the HRP-2 humanoid robot [Kaneko et al., 2004] based on the performance of a human grand master [Nakaoka et al., 2005].

### 2.2.1 Geometric motion planning

As cited earlier, different aspects and objectives are driven in the available generation methods. The main goals behind generating realistic and dynamic motions for humanoid robots may range from producing machines for assistance of people with reduced mobility to creating graphic animation for entertainment. On the other hand, many researchers claim that the humanoid robots constitute fantastic platforms for testing and validating algorithms in a wide spectrum of research fields. Among these algorithms, interesting *motion planning* methods are developed to resolve the problem of finding a feasible path for any model moving in a constrained environment, in order to reach a goal position.

This relates to the problem of moving an object between two positions in the environment by avoiding the collision with obstacles. A famous example is the Piano Mover’s problem which was stated by Schwartz and Sharir [Schwartz and Sharir, 1982]. This pioneer work has led to the development of the *motion planning* research field described extensively in [Latombe, 1991; Laumond, 1998; Choset et al., 2005; LaValle, 2006]. In the early 80’s, Lozano-Pérez introduced the concept of configuration-space, hereafter denoted by  $\mathcal{C}$ , which is the set of all possible configurations that a mechanism can attain. Since then, this has been a key concept in motion planning for it allows to change the problem of moving a *body* in a space  $\mathcal{W} \in SO(3)$ <sup>1</sup> into the problem of moving a *point* in another space  $\mathcal{C} \subset \mathbb{R}^n$ ; with  $n$  denoting the number of independent variables or degrees of freedom whose values at an instant  $t$  specify a configuration. In the configuration space, an obstacle region  $\mathcal{C}_{obstacle}$  corresponds to the set of configurations where the robot is in collision and thus, becomes forbidden. Then, the free region  $\mathcal{C}_{free} = \mathcal{C} - \mathcal{C}_{obstacle}$ . In this context, a motion planning problem is re-stated as the problem of finding a continuous

---

<sup>1</sup> $SO(3)$  the special orthogonal space of rotation matrices in 3D is  $SO(3) = \{R \in \mathbb{R}^{3 \times 3} | R^T R = I, \det(R) = 1\}$ .

curve or *Path*,  $p : [0, 1] \rightarrow \mathcal{C}_{free}$ , that connects an initial configuration  $p(0) = q_{init}$  to a final configuration  $p(1) = q_{end}$ .

During the following years, several planners have been developed to construct an explicit and exact representation of  $\mathcal{C}_{obstacle}$  [Canny, 1988; Indyk and Matousek, 2004]. In order to provide a practical resolution for the planning problem, sampling-based methods have been developed over the last fifteen years. These methods have proven their efficiency for solving difficult problems in high-dimensional spaces [Kavraki et al., 1996; Hsu et al., 1999; Kuffner and LaValle, 2000].

Though the described methods resolve the problem of path planning, they constitute only a part of the motion generation act, since the resulting draft path is only concerned with geometry. In order to transform this path into a feasible motion, a parameterized trajectory following the planned path, should be computed either by inverse kinematics or inverse dynamics or by optimization. Researchers in the field of motion planning were interested in applying their results on real robots, therefore they adapted their algorithms in order to make the conversion from paths to trajectories. Trajectory planning is the problem of determining a feasible time-parameterized path  $p(t)$ . In this perspective, steering methods verifying the small-time controllability property have been developed to guarantee that two closed random configurations can be jointed by a collision-free trajectory i.e. a trajectory that remains in  $\mathcal{C}_{free}$ . This small connection is called a local path and can be executed instantaneously by the robot. This result is particularly interesting for planning the movement of systems that are not able to move instantaneously in any direction, such as non holonomic systems (for example the cars). They were introduced in the context of motion planning in [Laumond, 1987] and since then have been extensively discussed in [Li and Canny, 1992; Laumond, 1998].

Motion planning techniques allow to determine collision-free trajectories for complex systems. However, they are only concerned with geometry. To control polyarticulated systems, it is necessary to synthesize models describing the changes in the robot configuration that are induced by the variation of joints. Then, depending on whether we need to consider masses or not, a model of the kinematics or the dynamics is required. Furthermore, our aim is to generate human-like motion and to reproduce complex behaviors while taking into account the static and dynamic balance of the systems. To this end, it is necessary to have a reference motion. This reference could be based on motion captured data or on a definition of multiple tasks that constrain one or more body of the robot. In case of direct application of desired tasks, a reference behavior needs to be defined and a corresponding control law needs to be applied. To this purpose, a task should be defined

## 2. STATE OF THE ART

---

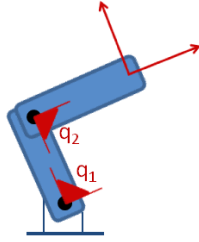


**Figure 2.2:** An example of a kinematic chain with 2 revolute joints having one degree of freedom each denoted by  $q_1$  and  $q_2$

as a desired kinematic or dynamic measure of one or multiple body of the robot. Inverse kinematics and inverse dynamics are then the fundamental models that allow to describe the robot motion. They are described in the next two subsections.

### 2.2.2 Inverse kinematics

*Kinematics* describes how the position and orientation of each body usually denoted by  $e$  is related to the angular value  $q$  of each joint [Sciavicco and Siciliano, 2009; Nakamura and Hanafusa, 1986]. Therefore, it studies the motion of connected solids without the consideration of their inertia and the forces acting on them. The rigid bodies are connected by prismatic or revolute joints to form a kinematic chain. Usually, humanoid robots only contain revolute joints which allow relative rotations between successive bodies. Figure 2.2 shows the kinematic chain of a 2R robot which consists of a manipulator arm presenting 2 rotational degrees of freedom. Actually, the kinematics of polyarticulated robots can be divided into two classes:

- Single-chain model with fixed base: **Manipulator**
- Tree-like model including multiple connected chains and free-space motion: **Humanoid robot**

Examples on both models are shown in figure 2.3. The direct model  $e = f(q)$  maps  $q \in R^n$  to  $e \in R^m$ , where  $R^m$  represents the task space (or operational space),  $m$  denotes the size of the task constraining the position and/or the orientation of the frames attached to the controllable bodies that we call the end effectors;  $R^n$  represents the joint space and  $n$  is the number of independently actuated joints that we call the degrees of freedom (DOF) which defines the *posture* or *configuration* of the system. Since the task is usually defined

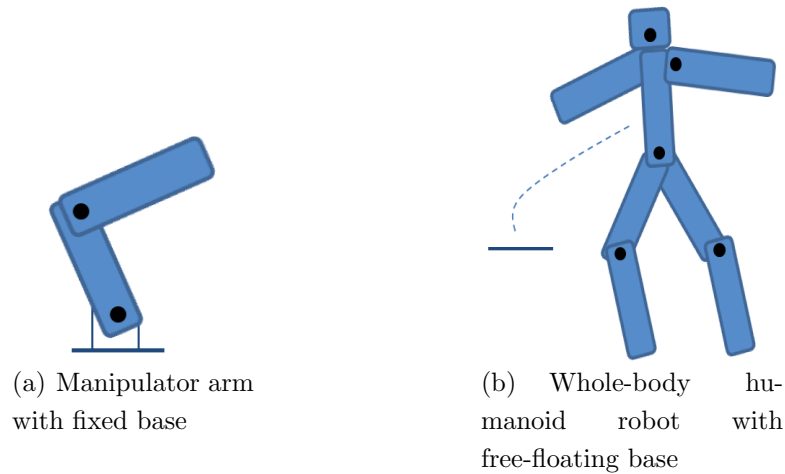


**Figure 2.3:** 2 cases of robotic chain models

by a reference point or a reference trajectory in the task space, the control problem is to determine the appropriate evolution of the joint vector  $q$  that realizes the task. This could be resolved by the inverse geometric model. However, a task is often a nonlinear function of  $q$  that does not admit a trivial inverse. In addition to that, when considering complex kinematic structures such as humanoid robots, the degrees of freedom relevant to a given task often exceed in number the dimension of the task ( $n \geq m$ ). For such systems we resort to numerical methods to solve *inverse kinematics* problems which are linear instead of nonlinear inverse geometric models.

Therefore, the mathematical representation that substitutes to the direct geometric model is the direct kinematic model which maps the joint velocity  $\dot{q}$  to the operational velocity  $\dot{e}$ . At each configuration, the direct kinematic model is linear and enables to compute systematically the vector  $\dot{e}$ . However, we are also interested in resolving the inverse relation in order to compute the rate of motion of the joints. This is called the inverse instantaneous kinematics [Siciliano and Khatib, 2008] which is based on a numerical resolution method to compute the joint velocities along a trajectory that could realize a given velocity of one or more end effectors. One can define the inverse kinematics as a velocity control law since it only constrains the joint velocities and then enables the update of the configuration iteratively.

For robotic arms with a few degrees of freedom, we may find analytical formulas giving the unique control satisfying a desired task. Whereas, for highly-articulated systems like humanoid robots, the kinematic structure is often redundant with respect to a specific

## 2. STATE OF THE ART

---

task which dimension is smaller than the number of degrees of freedom ( $m \leq n$ ). In this case, the robot is said to be under-constrained. Thus, the resolution of inverse kinematics offers infinite number of feasible solutions, i.e. the joint updates, that achieve the same task. In order to benefit from the *redundancy* of the system, multiple tasks could be assigned and resolved either simultaneously or iteratively.

One efficient way of solving the problem of redundancy is by applying numerical optimization algorithms such as minimizing the sum of the cost functions associated with the tasks. However, if the tasks become conflicting, finding a global solution that satisfies all the tasks at the same time becomes infeasible, which could lead to an undesired robot state. To avoid such situations, different solutions have been proposed. They all deal with defining a set of tasks by either giving a weight to each task or strictly prioritizing tasks so that, when such a conflict occurs, the algorithm should privilege the task with the biggest weight or the highest priority. The weighting strategy could be adopted by fixing a proper weight associated to the pseudo-inversion of the Jacobian. Recently, a technique of weighting of tasks has been proposed by [Salini et al., 2009], where a continuous variation of the weight values is associated to each task relatively to its importance. The disadvantage of such a prioritization is that the tasks are all defined in one multi-task, therefore when a conflict occurs, none of the tasks is fully satisfied. Whereas the hierarchy of tasks, which has been modeled in [Liégeois, 1977], works as the control of a less prior task within the set of controls satisfying more prior tasks. The first attempts were concerned by multiple equality constraints at the kinematic level in Resolved Motion Rate Control schemes. Thus, one way of resolution of the inverse kinematics problem is to compute the joint updates by successive orthogonal projections in the null-space of the Jacobian of the prior tasks [Nakamura, 1991]. In this case, in order to obtain the joint updates knowing the task velocities, the Jacobian needs to be inverted, and since it is not a square matrix, a generalized inverse <sup>1</sup> of the Jacobian is chosen upon request. This method is called the multiple priority-order resolution method where priorities are associated to tasks and resolved within the solutions of the prior tasks. This framework of resolution of tasks by order of priority was also developed by [Samson et al., 1991] and extended to any number of tasks in [Siciliano and Slotine, 1991; Baerlocher and Boulic, 1998]. These techniques have been adopted and applied in case of velocity-based [Yoshida et al., 2006; Mansard and Chaumette, 2007; Neo et al., 2007] and torque-based [Khatib et al., 2004] control of humanoid robots.

---

<sup>1</sup>More details will be given in chapter 3

### 2.2.3 Inverse dynamics

Defining the motion based on the kinematics only is sufficient at low speed and under additional stability criteria. Yet, whenever the effects of masses and nonlinear terms, such as Coriolis and Centrifugal forces, cannot be neglected, the full robot dynamics must be considered. Using a dynamic model seems also to be necessary to reproduce human-like behaviors requiring contact with the environment.

As mentioned previously, the robot is considered as a kinematic tree for which the dynamics can be easily developed. The classical approach to expressing the equations of motion was based on a Lagrangian formulation of the problem [Kahn and Roth, 1971; Uicker, 1967]. In the field of the dynamics of mechanisms, the robotics community has especially focused on the problem of computational efficiency for the simulation and control of increasingly complex systems operating at high speeds. Thus, recursive algorithms have been developed [Walker and Orin, 1982; Featherstone, 1987, 1999; Featherstone and Orin, 2000] for the Newton-Euler formulation of the equations of motion and for important dynamic properties computations.

At the level of dynamics, the tasks are defined in terms of the desired accelerations of the end effectors. Similarly as in the kinematics, the dynamics are developed in direct and inverse models. In *direct dynamics*, the current control torques are given as input and then the resulting accelerations are computed. Whereas in *inverse dynamics*, the process is inverted. The input of the system being the joint positions, velocities and accelerations, while the unknowns are the torques required to realize this given state. The problem of resolving the control parameters in order to satisfy the tasks is of our interest and could be referred to as a torque control based approach where the actuation torques required for the motion have to be determined.

A distinction needs to be made at this level, since the inverse dynamics can be resolved using 2 formulations: The *joint space* formulation which computes the torques  $\tau$  corresponding to the joint accelerations  $\ddot{q}$ , or the *operational space* formulation where the resulting torques correspond to  $\ddot{q}$  that will produce the Cartesian reference acceleration  $\ddot{e}$  of the end effectors. In the latter case, the variable  $\ddot{q}$  is a side variable, that does not require to be explicitly computed during the resolution. Contrarily to the kinematic case, the mapping to the task space control input is obtained in two stages. Yet, equivalently, in order to benefit from redundancy, several approaches consider prioritization techniques within a dynamic formulation written in the task space.

## 2. STATE OF THE ART

---

Moreover, since humanoid robots are known to have free-motion in space, they actually possess a free-floating base, and are supposed to be in contact with the environment. It is then feasible to add contact forces within the dynamic formulation. These forces are integrated in the joint space formulation, and could be also taken into account in the operational space. A unified framework for controlling the dynamics of humanoid robots in the operational space, with multiple constraints and contacts was proposed and developed by Khatib et al. [Sentis, 2007; Khatib et al., 2008]. A description of existing operational space dynamic-control approaches is given in [Nakanishi et al., 2008]. A study of the different formulations of the inverse dynamics and the transition between them will be detailed in chapter 3.

Classical mechanics allow to define the mapping between the joint torques and the muscle forces. Thus, many works have extended the dynamic models to musculo-skeletal models. Actually, many researchers in the fields of robotics in collaboration with biomechanists were interested in the human motion analysis. Applications concerned rehabilitation or diagnosis issues based on human musculo-skeletal models, for low limbs only [Thelen et al., 2003; Anderson and Pandy, 2001a,b] or complete models [Yamane and Nakamura, 2007; Demircan and Khatib, 2010]. Also, they were interested in the computation of the muscle forces exerted during a dynamic motion by applying optimization problems.

### 2.2.4 Numerical optimization

Applying *optimization* techniques to resolve motion is useful to fill the gaps in the motion generation methods based on geometric, kinematic or dynamic models.

On the one hand, geometric motion planning algorithms search only for feasible paths for a robot surrounded by obstacles. Then, it is necessary to apply optimization techniques in order to change the initial feasible solution into a movement resembling those of humans. Thus, it is possible to find a path but the question is how to make the correspondence between paths and trajectories? In other terms, how to compute the joint angles variation in time in order to generate the motion that achieves the calculated displacements. As previously explained, the motion planning methods only take into account geometric constraints. However, the motion of a system like a humanoid robot is subject to kinematic or dynamic constraints which are not easily considered in the path-planning methods. Thus, optimization problems, resolved offline, can be used to generate such constrained movements when considering full or complex models and where the environment

is supposed to be known. Then, optimizing a cost function in order to define the optimal joint angles, under some constraints, is the solution to find an optimal trajectory. This trajectory constitutes a reference that should be followed by the robot using generally simple controller as PD or PID, etc.

On the other hand, the classical prioritization algorithms adopted at the kinematic and the dynamic levels present the important restriction that unilateral constraints cannot be considered. These approaches, based on pseudo-inversion and iterative projections in the null space of prior constraints, are well fitted to cope with equality constraints [Baerlocher and Boulic, 2004]. However, they do not allow to explicitly take into account inequality constraints. Physical systems are always subject to such constraints, due to bounded control values as joint or torque limits, or limits in the workspace because of obstacles, etc. Such tasks are described by inequalities. For instance, many techniques were proposed to guarantee that unilateral constraints, as obstacle avoidance or joint limits, can be satisfied. Potential field approaches which generate control forces pushing away from the constraint, have been applied [Khatib, 1986; Marchand and Hager, 1998]. Damping functions have also been used to cope with joint limits or obstacle avoidance [Chang and Dubey, 1995; Raunhardt and Boulic, 2007]. Yet, inequality constraints would then appear with the lowest priority. To address this problem, it has been proposed [Mansard et al., 2009a] to calculate a weighted sum of controls, each one corresponding to a stack of prioritized tasks, where a subset of inequality constraints is treated as equality constraints. The main problem with the algorithm is its exponential complexity in the number of inequalities. In a third approach, a Quadratic Program (QP) is used to optimize a sum of cost functions, each one associated with a desired task, under strict equality and inequality constraints [Hofmann et al., 2009; Zhao and Badler, 1994; Salini et al., 2009]. However, this approach can consider only two priority levels, the level of tasks that appear as strict constraints of the QP, and the level of tasks that appear in the optimized cost function. In fact, the kinematic formulation with equality constraints is naturally written as a QP, from which the pseudo-inversion scheme provides an explicit resolution. QP can also account directly for inequalities, but are limited to two stages of priority, where inequalities must be at the top level. This limitation was surpassed in [Kanoun et al., 2009], where it was possible to define a set of prioritized linear equality and inequality systems, in any order of priority, and solve them as a sequence of QP in cascade. This approach was successfully applied to control the whole-body movements of a humanoid robot in a constrained environment. In [Escande et al., 2010], this cascade of QPs was performed by means of a dedicated

## 2. STATE OF THE ART

---

optimization solver reducing the computation time. Analogically, solvers of dynamic and static quadratic problems for multi-contact were designed in [Collette et al., 2007].

In this thesis, we will expand the QP developed by Escande et al. [Escande et al., 2010] to a generalized expression in order to apply it later, on the same dedicated solver for a hierarchy of tasks, while taking into account the full dynamics of the robot.

Usually, the methods that are based on the resolution of an optimization problem are used in two cases:

- For repetitive movements, to produce an optimal motion minimizing a certain criterion like energy, in order to increase the autonomy of the robot.
- For complex movements, the optimization provides a way to deal with highly redundant systems having a complex number of degrees of freedom and multiple constraints e.g. non-collision, static/dynamic balance, joint/torque limits etc.

On this basis, different researchers have implemented algorithms for motion optimization. [Miossec et al., 2006, 2008] computed analytically the dynamic model and its derivative for resolving movements with single or double foot contact with the ground. Similarly, [Suleiman et al., 2007, 2008b] used Lie groups for the computation of the model and its derivation in terms of the optimization parameters in order to increase the fluidity and the stability of the pre-computed movements. Kanehiro obtained very fast movements in a very constrained environment using a double-step method [Kanehiro et al., 2008].

The optimization methods are also used in the case of discontinuous dynamic models, such as impacts during the motion, where the generated motion is decomposed into three phases: the instantaneous posture and velocity at the moment of impact, before the impact and after it [Tsujita et al., 2008a,b; Konno et al., 2008; Arisumi et al., 2007, 2008].

### 2.2.5 Imitation by motion capture

So far, we have presented model-based generation methods either based on geometry or on kinematic or dynamic models. Another widely used technique for animation of human-like characters is *Motion capture*.

This approach is motivated by research on human-robot interaction, or tools for rehabilitation and medical diagnosis or entertainment utilities. Though this method is based on a set of recorded data and not on a definition of a set tasks, it is always necessary to replay the motion captured data on the humanoid robot or any other avatar by using

kinematic or dynamic models. The imitation of human motion by humanoids has been studied actively from various standpoints [Schaal, 1999]. Another process called Learning from Observation (LFO) was defined [Ikeuchi and Suehiro, 1994] as a paradigm that enables a robot to acquire a way of doing a task just by observing demonstrations of a human instructor. Different researchers were interested in reproducing various types of whole-body motions. [Riley et al., 2000] produced a dancing motion of a humanoid robot by converting a captured human motion into joint trajectories of the robot. For the same purpose, a method was proposed in [Pollard et al., 2002] for constraining given joint trajectories within mechanical limits. Since these studies mainly focused on the constraints of joints, the methods were not sufficient to maintain the dynamic balance. In this perspective, [Yamane et al., 2003] developed a method for controlling a marionette so that it follows a captured human motion, but the mechanism of marionettes is quite different from that of biped humanoid robots. For biped humanoid robots, [Tamiya et al., 1999] proposed a method that enables a robot to follow given motion trajectories while keeping its dynamic body balance. However, this method can deal only with motions in which the robot is standing on one leg. [KAGAMI et al., 2000] extended the method so that it allows changes of supporting leg. However, both methods cannot achieve dynamic walk motions. Nakaoka et al. [Nakaoka et al., 2003, 2007] proposed a study that especially focuses on leg motions to achieve a novel attempt for replaying a recorded motion. The biped-type robot can imitate not only upper body motions but also leg motions including steps that are dependant of the captured data on both feet and waist. Low-level tasks in leg motion are modeled so that they clearly provide the essential information required for keeping dynamic stability and important motion characteristics. A Japanese dance motion has been generated and executed on the humanoid Robot HRP-2 [Kaneko et al., 2004].

Another main contribution in reproducing captured data consists of the elaboration of a dynamic filter by [Yamane and Nakamura, 2003a]. This work offers a general framework for converting a physically inconsistent motion for a given body into a consistent one. Since the inconsistency caused by the difference between a human body and an existing robot like HRP-2 is significant, it would be difficult for the filter to convert a human dance motion into robot motion without losing the stability and other important characteristics.

These researches mainly focused on the imitation or preservation of the original motion data as precise as possible. [Miura et al., 2009] suggested an approach that differs from the conventional capture based motion generation methods, in the sense that it proposes derivation from the original captured motion. This methodology allows for both

## 2. STATE OF THE ART

---

preservation of the characteristics and modification of the original human motion and it has been applied on the humanoid robot HRP-4 [Kaneko et al., 2009] where walking and turning motion are created based on the motion obtained from a professional model. This approach can reduce the difficulties of real problems on motion generation from motion capture data such as time-consuming capturing process, physically demanding trials for performers, tough cleaning works of enormous quantity of captured data.

Another contribution in this field of imitation by motion capture with respect to some constraints is presented in [Suleiman et al., 2007]. It provides an optimization framework to generate the upper body motion of humanoid robot from human captured motion. The generated motion imitates the original one and, at the same time, it respects the physical limits of the humanoid robot.

In the concept of generation of human-like motion, motion captured data is still used in humanoid robotics as a supporting role, only to enhance the natural appearance of the motions synthesized by other methods. Since humanoid robotics is concerned with producing physically feasible movements, inverse kinematics or inverse dynamics computations and direct kinematics or dynamics simulations are yet unsurpassed.

In conclusion, different motion generation methods have been developed and then adopted by the researchers according to their interest. Yet, we are concerned by the generation of human-like motion. Therefore, it is quite mandatory to understand how humans move their body when a target is specified and why they choose certain movements among different possibilities. On the other hand, different fields of life sciences such as biomechanics and neurosciences, have studied the human behaviors and their properties. Thus, a link could be built between robotics and motion analysis methods. In the following, we will show an overview of these existing methods, and we will discuss how the analysis of motion is linked to the robotics generation methods.

### 2.3 Methods for motion analysis

As mentioned earlier, the motion executed in the joint space in response to a given reference in the task space is not unique. Thus it is required to choose between the possible movements in order to generate a solution automatically. To find such a solution, it is interesting to study the nature of the human motion. In this perspective, many researches in the fields of physiology, neurosciences and biomechanics were based on the comprehension of cognitive mechanisms involved during the motion, the study of motor control or

the prediction of the motion. Actually, it is preferred to reduce the number of solutions by conserving the ones that are most-likely possible to be realized by a human. In other words, the problem is to identify properties and criteria by observing humans and then to use them to generate new movements on anthropomorphic systems.

However, it is still an open research issue to understand the mechanism for generating and coordinating human motions. In the brain science community, researchers try to analyze and model how the brain coordinates the whole-body motion [Flash and Hogan, 1985; Kawato et al., 1990]. In the biomechanics community, on the other hand, the dynamics computation and motion analysis using musculo-skeletal models have been investigated [Delp and Loan, 2000; Bhargava et al., 2004; Rasmussen et al., 2003; Anderson and Pandy, 2001b]. Both approaches are complementary but still can not provide the complete solution to the problem.

In fact, the human body is largely complex since it is composed of a large number of bones and tissues which organization remains partly unknown. Moreover, there's an additional complexity due to the neuro-muscular system and its relation with the brain. It would be then necessary to acquire an important knowledge to understand the human motion. The central nervous system (CNS) cannot control everything in a unified way, and seems to use simplifications to reduce the complexity, for example, by decreasing the number of degrees of freedom to be controlled [Bernstein, 1967; Vereijken et al., 1992]. The different models proposed in literature, in any scientific field, rely on simplifications of the real human system. In fact, an admitted hypothesis indicates that there exists a sort of hierarchized system of control [Berthoz, 2003]. We can actually represent the control of the human movement hierarchically in figure 2.4.

Physically, it is common to represent the human body by a system of rigid bodies (generally the bones or group of bones) articulated through mechanical links allowing mainly rotations. We add to this skeletal modeling, the muscles wrapping the bodies. The muscles are activated through the neural commands. Then, since the muscle forces are related to the joint torques through mechanical laws, the dynamics can be computed and the accelerations derived. By integration, the velocity, the trajectory and finally the path to the goal are synthesized. The more we get down in the hierarchy, the more we lose in causality since decisions start from the brain and most commands on the bodies motion are given at the neural level. The more we go up in the hierarchy, the more we gain in redundancy, knowing that with each level, the number of DOF increases while the dimension of the known input is smaller, which leads to many possible solutions to reach the same target. Additionally, the human being is open to the external environment.

## 2. STATE OF THE ART

---

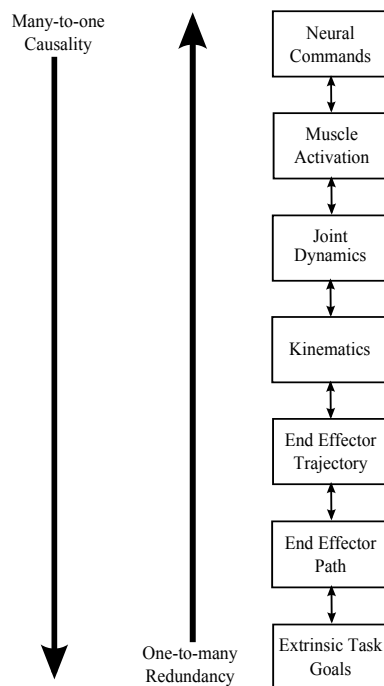


**Figure 2.4:** The sequence of the different control inputs starting from the brain commands to the desired targets

From the information received by its different sensors, numerous mechanisms help him to adapt to its environment, in order to execute complex tasks. These mechanisms are generally involved within the loop of perception, decision and action.

Based on the analysis and study of the human motion, the knowledge and understanding of the human movements are thus useful in numerous application fields. In the medical field, for example, disciplines as biomechanics and neurosciences tend to comprehend and interpret to the best, the human motion. In health problems, the fight against obesity, the treatment and integration of handicaps are key points in the modern society. The physical exercise has become a well-know way of treatment of these troubles and motivates a big number of researchers. In the field of sports, the study of any movement or gesture has been accorded a big importance in order to improve the performances of the players. More recently, the multimedia domains e.g. video games, animated movies etc., seeking to animate virtual avatars in a realistic way, are also interested in human motion analysis. These studies aimed at understanding the cognitive mechanisms which are elaborated during a considered motion, the motor control or the prediction of movements. The computer science has obviously an important role in this field by providing analysis tools for comprehension and treatment, implying an important communication

between the different scientific disciplines: nutrition, physiology, medicine, biomechanics, neurosciences, sport science, physics, mechanics, control etc. These results led to the recognition of existing invariants, characteristics and parameters of the human motion, e.g. the shape of the trajectory of an end effector; the optimization of a certain criterion. In addition to these technical and technological factors, the psychological state of the subjects perceiving the animation also plays a role [Slater and Usoh, 1993].

Next we will show a description of the strategies developed in life sciences particularly in biomechanics and neurosciences, for the extraction of invariants of the human movement.

### 2.3.1 Biomechanics

As explained, it is important to analyze the human motion in order to define some corresponding properties and characteristics, which are useful for various applications. *Biomechanics* offers a wide range of studies where invariants are extracted and explained. At this level, it is considered that there are multiple types of constraints that restrict the choices of computation of natural motion. Biomechanics has successfully developed methodologies for measuring various properties of the human body [Watts et al., 1986; Kearney and Hunter, 1990; Oatis, 1993; Stroeve, 1996; Y. and Hollerbach, 1998; Osu and Gomi, 1999; Lee et al., 2002; Lloyd and Besier, 2003; Valle et al., 2006]. These properties serve for robotics as well as for medical applications and ergonomics.

Many attempts have been made in the biomechanics and robotics literature to create a general model/theory of human-like motion. The earliest systematic study of human and animal (loco)motion principles appears to be due to Marey. His basic revolutionary idea, adopted in the 1880s, was to record several phases of movement on one photographic surface. Marey's chronophotographic gun was made in 1882, this instrument was capable of taking 12 consecutive frames a second, and the most interesting fact is that all the frames were recorded on the same picture. Using these pictures, he studied the motion of different animals [Marey, 1872] and also human locomotion [Marey, 1894]. Real dynamic analysis of human (loco)motion was first proposed by Chow and Jacobson in 1971 via optimal programming [Chow and Jacobson, 1971]. Bernstein and his followers Moreinis and Gritzenko, developed and investigated the mathematical and physical model of the human locomotor system in 1974 in order to learn about the dynamic characteristics of both, a healthy man and one using a prosthesis. Vukobratović, finally solved the inverse problem of anthropomorphic locomotion by developing methods for automatic-setting of

## 2. STATE OF THE ART

---

mathematical models of anthropomorphic mechanisms [Vukobratović et al., 1982–1988]. The biped nature of locomotion has been also tackled in [Alexander, 2004] where a comparison to the human was proposed. The literature of biomechanics and palaeoanthropology agree that the locomotion mode is naturally chosen in a way that minimizes the metabolic cost, which corresponds to the consumption of oxygen that is normalized by the traveled distance and the mass of the subject [Alexander, 1997, 2004]. The most common approach consists in computing the work of the active forces supposing that it is highly related to the metabolic energy spent by the subject to achieve its movement [Norman, 1976; Winter, 1979; Pierrynowski et al., 1980; Williams and Cavanagh, 1983; Caldwell and Forrester, 1992]. Even if other phenomena interfere in the generation of the human locomotion, as the control of the head movements or the gaze [Berthoz, 1997], the energetic aspects have been largely studied. However, many works have demonstrated the importance of the stabilization of the head during locomotion [Pozzo et al., 1990].

For a big number of hypotheses, as the minimization of energy [Alexander, 1997, 2004] or the existence of coordination laws between the joints [Bianchi et al., 1998], it is quite necessary to go beyond postures. The methods of adaptation of motion are better fitted to this type of hypothesis. They actually enable the deformation of postures while taking into account these hypotheses and proving the realism of the result. Among all possible solutions, one could select the ones that verify the general criteria of motor control. F. Multon [Multon, 2006] proposed a quick method (compatible with the interactive applications) allowing to test many types of hypothesis (biomechanical, neuro-physiological or behavioral) on the control of human motion. The motion is a resultant of numerous constraints that could be formalized, in the same time, at the cognitive and mechanical plan. Finely analyzing the role of energy minimization in the production of movements could lead to generating a complete behavior instead of adapting one from a database. In fact, one question should be always asked: a motion that economizes energy for a given subject, is it directly applied and adapted to a different one? Despite the differences in mass and dimension, the anatomical structure and articulations of humans could be considered as unique. Thus, it seems reasonable to apply only geometrical adaptations to the captured motion. A hybrid method of adaptation and blending of captured motion was developed by [Multon, 2006] for the validation of some biomechanical properties of the human motion. Criteria as the minimization of the work of the internal forces and of the jerk<sup>1</sup> were studied and it would be possible to consider other criteria, as the laws of

---

<sup>1</sup>derivative of the acceleration

the planar covariance [Bianchi et al., 1998] or the works based on probabilistic approaches [Kording and Wolpert, 2006]

Researchers in the fields of robotics and biomechanics have also considered the forward dynamic problem: given the forcing functions (joint torques and reaction forces), the objective is to determine the resulting joint kinematics in various simple tasks of human motion. Much of this research is summarized in [Hatze, 1981]. Afterwards, the most important research in the dynamics of anthropomorphic motion has moved to the realm of artificial intelligence.

Alternatively, the kinematic models are used to compute joint trajectories which are based on sample trajectories derived from biomechanics [Zeltzer, 1982; Bruderlin and Calvert, 1989; Boulic et al., 1990; Multon, 1998; Sun and Metaxas, 2001]. For example, the joint trajectories are modeled by parametric curves [Zeltzer, 1982] passing through limit values (key positions) coming from publications in biomechanics [Alexander, 1984]. The main problem consists in synthesizing a controller that is capable of satisfying the constraints while producing natural motion. One of the proposed methods is about defining graphs of key postures [Hodgins et al., 1995; Hodgins, 1996; Brogan et al., 1998; Yang et al., 2004]. These graphs indicate the sequence of key postures to be respected for a motion and to use closed-loop controllers that make the system converge to the next posture. However, the gains corresponding to these controllers still remain difficult to obtain even if the solutions accounting, for example, for the person's morphology (change of dimension and mass of the bodies) [Hodgins and Pollard, 1997], exist. These models also bring the problem of extraction of relevant posture keys (in number and quality). These approaches do not allow to identify the fundamentals of the natural movements but they try to reproduce known trajectories. In addition to that, the improvement of the measurement techniques enabled the elaboration of numerous works that identified the evolution of the kinematic variables (positions, velocities, accelerations, angles) for the different body segments [Alexander, 1983]. In biomechanics, this study has been used in many works [Nilsson et al., 1985].

Moreover, the knowledge of the biomechanical properties is widely used in ergonomic design of products. For determining standard values of these properties, it is required to have well calibrated measuring equipments and to average the data of many subjects. The equipments need mechanical stiffness and accuracy, which make them heavy and bulky in nature. Such equipments are unfortunately not applicable to everyone, especially those who are under rehabilitation and medical treatments. The viscoelastic properties of human-limb joints are sometimes used by medical doctors for diagnosis of

## 2. STATE OF THE ART

---

neuropathic and myopathic diseases such as Huntington's, Parkinson's, and progressive muscular dystrophy. The means to measure the patient-specific viscoelastic properties of limb joints without pain and constraint are useful to make quantitative diagnosis. With those objectives in mind, researches led in the biomechanics field aim at understanding and describing mechanically the human motion. [Amarantini et al., 2010] presents a study of a two-step EMG-and-optimization method for muscle force estimation in dynamic condition. This study could offer interesting advantages for various applications in many fields, including rehabilitation, clinical and sports biomechanics, ergonomics and therapy. Also many researchers in both fields of robotics and biomechanics were interested in a common study for elaborating motion analysis tools. [Venture et al., 2006, 2007] presented a design of a new experimental process that allows to record the human limbs movement in a painless constraint-free environment and to perform the identification of the limbs joints passive dynamics in a large experimental context as the diagnostic of the Parkinson disease performed by a clinician. In the spirit of filling the gap between neurosciences and biomechanics [Murai et al., 2007] developed a whole-body neuromuscular system, which was build on top of the musculo-skeletal human model for somatosensory calculation [Nakamura et al., 2005; Yamane et al., 2005].

Based on all these studies, we can say that human-like biomechanics is a modern scientific approach to human-like motion dynamics and control. [Ivancević, 2010] made the link between mathematical biomechanics and humanoid robotics. The term *human-like biomechanics* is used to denote this unified modeling and control approach based on: theoretical mechanics, differential geometry and topology, nonlinear dynamics and control as well as modern path-integral methods. From this *geometry-mechanics-control* perspective, 'human' and 'humanoid' means the same. This unified approach, enables both, design of humanoid systems of immense complexity and prediction/prevention of subtle neuro-musculo-skeletal injuries. The dynamics of human motion is extremely complex, multi-dimensional, highly nonlinear and hierarchical. Human skeleton has more than two hundred rigid bones, connected by rotational joints, which have up to three rotation axes. Nevertheless, in classical biomechanics the main analytical tool was "translational vector" geometry [Ivancević and Ivancević, 2006], which consists of representing the force vectors and their corresponding lever arms. The skeleton is driven by a synergistic action of its 640 muscles. Each of these muscles has its own excitation and contraction dynamics, in which neural action potentials are transformed into muscular force vectors. On the other hand, the robotic approach for human-like motion dynamics and control has been

developed in the last three decades [Vukobratović and Borovać, 2004; Vukobratović et al., 2004; Nakamura et al., 2006].

Since the dynamics of the human and consequently the humanoid motion is becoming widely used, [Ivancević and Ivancević, 2005] refer to biodynamics instead of biomechanics. Humanoid robots are human-like, anthropomorphic mechanisms with complex, muscle-driven biodynamics with many activated degrees of freedom and hierarchical brain-like control. In other words, humanoid biodynamics is supposed to closely resemble biodynamics of human motion. According to [Ivancević and Ivancević, 2005], it is an encapsulated level of biomechanics concerned with the dynamic properties of the human model, and thus it covers both *biomechanically-realistic human dynamics* and *biologically similar humanoid dynamics* [Ivancević and Ivancević, 2005]. The biodynamics is extremely complex, multi-dimensional, highly nonlinear and hierarchical. The control of such a system, having so many degrees of freedom, would at first seem beyond analytical treatment. The task is made even more difficult by the fact that, apart from the basic feedback mechanisms, the brain control mechanism is still largely unknown. Therefore, it is quite important to understand the human motion from the neurosciences point of view.

### 2.3.2 Neurosciences

Learning how the body moves from the biomechanics side is not a unique way of understanding the human motion. Actually, the brain makes all the choices of movements and then these choices guide the different parts of the body to move following a certain control law. The *human motor control* is very complex and is divided into different levels. The first one concerns the brain which transmits control signals to the muscles through the spinal cord. The muscles are then activated by the motor neurons which lead to their contraction that induces the movement of the rigid bodies connected with the muscles through the musculo-skeletal system. The coordinated activity of a group of muscles enables the execution of motion planned by the brain in order to achieve a desired task. During the corresponding movement of the bodies, the sensory feedback delivered by different sensors e.g. the eyes, is returned to the brain, therefore, the motion originally planned could be modified or rectified. The exchanged signals between the different modules implied in this process of motion generation rely on a set of complex chemical and physical mechanisms. Thus, different elements are involved in producing a motion and they are all controlled by the central nervous system (CNS).

## 2. STATE OF THE ART

---

Despite the complexity of the motor control planning problem, the brain is able to resolve it easily. Facing an infinity of solutions for a motor task, the brain selects only one. It is interesting to note that the choice of the solution is always the same independently of the person. Many experiments that were realized in the field of *neurosciences*, have demonstrated properties of the human motion from which invariants were defined. For example, for pointing tasks, it has been proven that the trajectory of the finger is approximatively a line with small curve and the velocity profile of the hand is bell-shaped [Atkeson and Hollerbach, 1985; Soechting and Lacquaniti, 1981; Morasso, 1981; Abend et al., 1982]. We should point out that these main characteristics of the human motion remain unchanged even if the initial position, velocity and/or amplitude of the movement are modified, and when the dynamic properties as the weight are also changed [Flanders et al., 1996; Papaxanthis et al., 2003]. It has been also demonstrated that the final posture of the movement is independent of the velocity of the movement [Atkeson and Hollerbach, 1985; Soechting and Lacquaniti, 1981; Nishikawa et al., 1999; Flanders et al., 1999].

Different theories of motor control have been developed during the last decades.

- Look-up table: This theory assumes that the central nervous system has learned every movement and that the brain memorizes this set of movements in a table. When a movement is required, it's only sufficient to look it out in the table [Albus, 1971; Marr, 1969].
- Elimination of DOF: This second theory proposes that the CNS resolves the redundancy by using only the necessary DOF to achieve the task while the others are frozen [Bernstein, 1967; Vereijken et al., 1992; Newell, 1991].
- Equilibrium point hypothesis: Hypothetically, the posture of a rigid body is represented by an equilibrium point of agonist and antagonist muscles (the opposite forces are null). When the stiffness of a muscle is changed, the body moves towards the equilibrium point. Therefore, a movement can be considered as the gradual change of the stiffness of muscles along a certain trajectory of the equilibrium points [Feldman, 1966].
- Muscular synergies: This approach is introduced in [Bernstein, 1967]. It consists in activating simultaneously a group of muscles due to one signal of control. Due to their small number and their possible combination to produce complex movements, synergies allow to resolve the problem of redundancy at the muscular level and

facilitate the computation of the motor control. They actually define the general concept of motor primitives which constitute the basic elements of the motor control.

- **Internal models:** One important problem is to deal with the relation between the sensory feedback and motor control. The concept of internal model comes from the idea that the brain disposes of transformation models between the required control and the desired behavior of the system, as well as the inverse transformation [Wolpert and Ghahramani, 2000]. These models enable the CNS to plan a priori the necessary forces for the movement.
- **Optimal control:** The theory of optimal control is a developed mathematical theory that presents many applications in the engineering fields. Since this theory aims at choosing the best solution among all possible solutions, depending on a cost criteria, it seems to be ideal to resolve the problem of motor control. In addition to that, it also resolves the problem of redundancy of the sensory-motor system by imposing constraints on the movement. In this area of optimal control theory, many researchers have synthesized the hypothesis that the movements minimize a certain cost related to the kinematics or the dynamics of the motor system. Under the basis of this hypothesis, they have found, more or less, some good characteristics of the human motion observed during experimentations. Among a variety of optimal control models proposed in literature, we will cite three of the most well-known models representing three different types of optimality criteria:
  - **Minimum jerk:** This criteria was proposed in [Flash and Hogan, 1985]. The smooth characteristics of the human movements results in the minimization of the acceleration variations or jerk, of the end effector, expressed in the task space. For the CNS, this minimization could be an interesting advantage for achieving the movement with good precision while protecting the joints and the tendons.
  - **Minimum torque-change:** Uno et al. [Uno et al., 1989] suggested another type of optimality criteria based on the dynamics of the system. According to this criteria, the best way for the CNS to produce smooth movements that protect the musculo-skeletal system is to minimize the torque variations acting on the joints.
  - **Minimum variance:** The theory of the minimum variance is located at the level of the neural signal to explain the motion planning [Harris and Wolpert, 1998].

## 2. STATE OF THE ART

---

The idea is about the noise in the neural control signal which will disturb and deviate the desired movement. These deviations are accumulated during the movement and induce a variance in the final position of the hand. This theory argues that the amplitude of the neural noise is proportional to the amplitude of the control signal (signal-dependent noise).

More models have been exploited in literature, and diverse optimization criteria have been equally proposed: The criterion of minimum time [Nelson, 1983], the criteria derived from the minimum-jerk [Dingwell et al., 2004; Richardson and Flash, 2002], the dynamical criteria [Nakano et al., 1999; Kashima and Isurugi, 1998], and the energy criteria [Soechting et al., 1995; Alexander, 1997; Kang et al., 2005; Nishii and Murakami, 2002; Guigon et al., 2007]. Syntheses on these criteria are found in [Engelbrecht, 2001; Todorov, 2004]. Inspired from the principles of motor control, an application to the field of humanoid robotics was presented in [Minh, 2009], where the focus was on realizing human-like reaching tasks.

As mentioned earlier, one of the main theories of the motor control lies on the hypothesis that the CNS disposes of elementary components of control known as the motor primitives. This approach suggests that the motor system is able to elaborate more complex movements while combining these primitives. This organization offers a way of simplification of the computations and record of movements. In particular, it could solve the problem of redundancy of the musculo-skeletal system. The existence of motor primitives has been suggested by a huge number of biological experimentations frequently cited in literature [Flash and Hochner, 2005].

On the joint kinematic level, the primitives are considered as simultaneous variations of the joint variables of the movement.

The existence of primitives has been equally studied on the muscular level. In this case, the authors tend to highlight the coordinated activation of group of muscles described as muscular synergies.

The idea of structuring the control from motor primitives, as proposed by neurobiologists, is of evident interest for roboticists. It synthesizes a canonical base of movements from which more complex movements could be generated. The benefit of such approach is to reduce the complexity of the control problem. Once a set of motor primitives is characterized, this problem is no more about the direct definition of control signals, but it is about the identification of factors representing the contribution of each primitive in the construction of these signals.

For robotic systems including a high number of DOF, such as humanoid robots, the principle of human inspired motor primitives, seems to be relevant for simplifying the problem of control. Taking into account the important differences between the biological systems and the actual robotic systems, at the structure level as well as the actuating mode, the primitives that are considered by roboticists are essentially of kinematic nature e.g. the joint trajectories, or dynamic nature e.g. the forces applied on the joints. Hence, it is possible to use motor control primitives to reproduce a large record of movements. However, as far as they are defined in open-loop, these primitives are simply dependent of the time signal and do not enable the interaction, during the motion, with the environment via a sensory feedback. Aware of this problem, certain authors have proposed a new definition of primitives. Todorov et al. [Todorov and Ghahramani, 2003], for example, have considered sensory-motor primitives in which the perception and control are linked. These primitives allow to couple the control with the sensory feedback. Therefore, a control law defined by such primitives constitutes a closed-loop control.

Hence, the analyses of human motion derived from biomechanics or neurosciences allow to propose a set of hypotheses and properties of motor control, based on experimental data. It is then interesting to use models of anthropomorphic systems and to develop simulators capable of testing the influence of these hypotheses on a computed movement. This yields to both analysis and synthesis of motion by verifying if the properties of the resulting simulated motion are comparable to the ones from experimental data. A big number of research works have been proposed based on this coupling between analysis and synthesis of motion. For example, F. Yeadon focused on the aerial movements of gymnasts [Yeadon et al., 1990]. In the same spirit, in the field of neurosciences and cybernetics, [Alexander, 1997] verified that the simulated trajectory of a 2D arm which minimizes the metabolic energy is the closest one to the experimental measurements. Many authors from the biomechanics field have also adopted this type of approach. [Delp et al., 1990; Nakamura et al., 2005] developed a model of an anthropomorphic system composed of skeleton and muscles. Thanks to this model, S. Delp [Delp et al., 1990] tries to predict which surgical act is the most appropriate for a pathology and for a given subject to improve its gestural. The main goal of this thesis is to provide a novel methodology for the resolution of dynamic motion and new tools for the automatic generation of whole-body motion while having a generic formulation in order to be adopted on different anthropomorphic models. The validation of the simulated motion by judging the realism of this motion and by comparing with properties of the real human motion consists a primary

## 2. STATE OF THE ART

---

point of discussion. This creates the loop of analysis-synthesis of motion based on two steps:

- Finding models and invariants of the human motion from biomechanics or neurosciences.
- Simulating the human motion using a humanoid or an avatar: Modeling and Control.

An interesting future application would be to tackle the problem of design of work stations, starting from a motion of a worker and realizing an analysis of this motion then a synthesis using the developed simulator from robotics.

### 2.4 Ergonomic analysis of motion

The growing research in the fields of biomechanics and neurosciences enhanced the development of tools for measuring different parameters related to the human motion. This enables the robotics community, and more specifically, the one related to the humanoid robotics field, to compare their results with similar actions taken from real humans. Moreover, it allows the elaboration of synthetic methods to find appropriate solutions to apply on humanoids in order to achieve human-like behaviors.

#### 2.4.1 Problem definition

In the field of robotics, many researchers were interested in generating realistic whole-body motion for different purposes, among other the conception and design of workplaces. To this end they used the criteria and invariants of human movement identified by the biomechanical and neuro-physiological communities to generate movements likely to those realized by humans. By accomplishing such objectives, the issues of *ergonomics* were tackled. The International Ergonomics Association defines ergonomics as follows: *Ergonomics* is the scientific discipline concerned with the understanding of interactions among humans and other elements of a system, and the profession that applies theory, principles, data and methods to design in order to optimize human well-being and overall system performance. In other words, it is the study of designing equipment and devices that fit the human body, its movements, and its cognitive abilities. Ergonomics is employed to fulfill both the goals of health and productivity. It is relevant in the design of safe working environment and easy-to-use interfaces to machines. Proper ergonomic

design is necessary to prevent repetitive strain injuries, which can increase over time and can lead to long-term disability.

Among the multiple reasons behind work pathologies, the most common ones are related to the musculo-skeletal disorders (MSD). Actually, the ergonomic analysis of motion has a social and economical origin due to the explosion of number of MSD at work. They represent a major health problem at work especially in the industrial countries. The MSD of the higher limbs as the shoulder, elbow and wrist, represent 68% of the compensated professional illness in France. Different methods and tools have been developed and used for the evaluation of workplace design. To this end, norms have been also identified. The appearance of MSD is explained by the combination of multiple independent factors:

- Biomechanical factors as the joint values, the maintenance of postures (static work), the efforts required for the execution of a task and the repetitiveness of gestures.
- Psycho-sociological factors that could affect the psychology of the operator: the pressure and stress, the inter-professional relations and the atmosphere of work, the professional dissatisfaction due to the work conditions, the lack of recognition, the negative perception of work.
- Factors of organization of work such as the production organization modes (just on time, Kanban, MRP etc.), the procedures of work imposed on the operator, the used equipments and the remuneration of the operator.
- Individual factors of the operator as the age, sex and health.

However, the evaluation of the action coupled with all these different factors, is a complex task. The increase of the number of MSD since the early 80's has led to the development of a certain number of methods and tools for the sake of better consideration of human as a whole during the analysis or re-design of work stations. Järvinen & Karwowski [Järvinen and Karwowski, 1992], Lauring [Lauring, 2004] then Marsot & Claudon [Marsot and Claudon, 2006], for example, introduced a state of the art of the different tools and identify different families of ergonomic evaluators. The development of new software packages aiming at taking into account the human factors in the design of work stations is growing. It involves particularly a better estimation of criteria used for the evaluation of work stations, at the early stage of the design, and from the ergonomic point of view as well as the prevention from the risks of accident. The recommended prevention strategy is focused on the a priori estimation of risks. It fixes as an objective for the conceiver

## 2. STATE OF THE ART

---

of equipments for work, to get the lowest residual risk level possible accounting for the technical status.

In conclusion, given a description of pieces to assemble, of used tools and different operations to execute, these preventive strategies aim at optimizing the position of the different components of the work station in order to minimize the constraints of the operator in terms of posture, magnitude and repetitiveness of gestures as well as costs that are related to the assembly time. These software tools enable the designer of the assembly stations to evaluate certain ergonomic aspects of the workplace and to try different solutions in order to find the ones that satisfy the qualifications of the production and solicits less the operator. The ergonomic evaluation can be based on various norms that will be discussed later on. But the design and analysis rest, to a large extent, on the experience and the expertise of the designer and enough little on a systematic quantification of ergonomic aspects. New tools of simulation, generally integrated into the software suites of PLM (Product Life-Cycle Management), allow to simulate the presence of the human operator in an environment of production and supply a software version of the most known evaluation forms. Nevertheless, the real challenge is to develop software products that allow to simulate automatically realistic movements of the human in its workplace. Another source of data for the generation of movements is the literature stemming from physiology and biomechanics [Wang, 1999]. Despite the huge amount of data collected in ergonomics and human motion studies, no ‘fundamental principle of human motion’ emerges. Nevertheless, some invariants are known in a number of case studies and different tools are associated with them.

### 2.4.2 Existing tools

The tools are organized in three big families:

- The methods devoted to reducing the risks of MSD
- The digital models and numerical simulation tools
- The timecycle analysis methods

The input data are relative characteristics of the operator (anthropometry, age, gender), of the manipulated object (dimension, weight, height and distance of the start and end positions) and of the frequency of the manipulation. From the computation of efforts acting on the backbone, the energy dissipation and the comparison with data coming

from the literature, these tools provide as output either a level of risk or recommendations concerning the weight limits and the frequency of manipulation if the latter was not indicated in the input. The most well-known are ErgonLIFT [Vedder and Laurig, 1994], LIFTAN [KARWOWSKI et al., 1986], ERGON-EXPERT [Rombach and Laurig, 1990], MMH-EXPERT [Kayis and Alimin, 1992] and the works of Jung and Freivalds [Jung and Freivald, 1990]. The evaluation tools are listed in [Marsot and Claudon, 2006], where 2 types have been distinguished:

- the “heavy” equipments requiring a complex instrumentation and expertise in biomechanics and/or physiology. They concern the experimental laboratories.
- The “easy” means used without any instruments on the field.

### 2.4.2.1 Methods for the evaluation of risks of MSD

To evaluate factors of risk of occurrence of MSD, two groups of methods are proposed:

- One group deals with equations, indicators, tables or graphs that are defined relatively to the physiological data and aim at identifying risk factors. For example, the revised equation of NIOSH (National Institute of Occupational Safety and Health) [NIOSH, 1991] that allows to compute the maximum permissible load in terms of many factors as frequency and quality of hold [Waters et al., 1993]. Or the the tables of MITAL [Mital et al., 1993] or of SNOOK & CIRIELLO [Snook and Ciriello, 1991] that determine the maximum permissible weight, that persons could carry during manipulation tasks.
- A second group of methods is mainly based on the observation and evaluation of professional activity. These methods, allowing to accomplish postural analysis, are usually presented as evaluation grids and attribute a score to a posture at work described by the observation of joint positions in proximity to body segments e.g. the arm, the forearm or the neck. [Aptel et al., 2000] provides a bibliographical synthesis of existing tools and an analysis of the assets and drawbacks of these techniques.

### 2.4.2.2 Digital models and simulation tools

The simulation must reproduce, as accurately as possible, a work scene in which the operator could execute his activity according to the pre-planned conditions and it should

## 2. STATE OF THE ART

---

allow the estimation of criteria that are used for the evaluation of workplaces on both levels of ergonomics and prevention from accident risks. The new tools of numerical simulation allow the visualization of future workplaces and their operators starting from the phase of design. Particularly, a certain number of software editors for CAD (Conception Aided Design) and/or PLM (Product Lifecycle Management) have developed products that could include and animate a digital actor in an industrial environment. It is quite the case of the editors of the software series PLM which contain a package dedicated for the ergonomics in their integrated library of packages. We can distinguish two big families of products that are concerned by the animation of digital actors in the design process of an industrial work station. On the one hand, we can cite the tools that are designed for a particular application and can be used in a generic industrial context. Fourquet et al. [Fourquet et al., 2007; Hue et al., 2007] developed the software tool OLARGE for simulating and analyzing seated repetitive work tasks that constitute a large part of repetitive industrial tasks. On the other hand, other tools are specifically conceived for a precise type of application, as for example the conception of the inside of vehicles.

These soft solutions, generic or specific, mostly provide an animation of the model by direct and inverse kinematics. Some of these solutions also enable the animation of the model based on motion captured data. Additionally, some of these software solutions afford basic ergonomic analysis, based on the previously cited methods as the equation of NIOSH or the equations of SNOOK. These digital models enable non-specialists of ergonomics to realize a whole series of pre-studies as the evaluation of the visibility, accessibility, and other constraints of a work station. Yet, these software solutions present some disadvantages: first, these expensive solutions are relatively difficult to be used by a non-specialized person. Second, there is still many things to develop in the sake of generation of realistic motion. From all the existing evaluators, different norms were extracted in order to unify or standardize the analysis. They are described below.

### 2.4.2.3 Norms

Different norms on the French, European and international levels, regulate the conception, ergonomics and evaluation of the workstations. The norms NF EN 614-1 [nor, 2006] and NF EN 614-2 [nor, 2000b] concern the ergonomic principles of conception. The anthropometry and the measures of the bodies are equally normalized. Also, other norms exist for the evaluation of postures at work as the norm ISO 11226 [nor, 2000a].

### 2.4.3 Link with Robotics

As explained earlier, the human motion analysis is related to robotics, and more specifically humanoid robotics, depending on the application fields and considering the analogy between humanoids and humans modeling. This link constitutes a straight connection with my work and an immediate extension of my thesis. Aiming at developing a generic, automatic, and dynamic motion generation tool and elaborating anthropomorphic models, the resulting whole-body motion is expected to be human-like. Thus, the extraction of syntheses on the human motion by comparing with its properties is of my primary interest. This study can be exploited for different applications like rehabilitation and ergonomics. In order to realize this study, an interdisciplinary collaboration of specialists from the fields of life sciences, ergonomics and robotics, must take place. The kinematic and dynamic models of polyarticulated systems that come from robotics offer an interesting basis for the elaboration of numerical simulators that aim at reproducing and anticipating critical situations that generate muscular pathologies. This is a part of the general problem of the design of work stations for short term efficiency in productivity and time cycle, and long term performances with minimization of MSD risks. The objective is to afford a realistic prediction of movements, and eventually of certain efforts, required for certain manipulation or locomotion tasks.

Actually, even though a big number of workplaces with repetitive work consider tasks that are done in sitting positions or fixed standing positions, the real work is usually the combination of locomotion and manipulation actions. We aim at developing methods and solutions in response to this issue, while considering a double condition. On the one hand, the simulation of repetitive tasks that require the operator's movement between different areas of manipulation in a standing position on single or double support. On the other hand, the coordination of the upper and lower limbs of the body, while realizing tasks in the environment and changing the number of contacts.

Robotics provides the foundations and concepts for modeling the human mechanics and setting the relations between the task to be accomplished and the possible movements in the general framework of motion generation of articulated chains. For a numerical model derived from the mechanics, there exist infinitely many motor behaviors that produce the same given task. In robotics, this redundancy does not cause trouble. The main specificity of the proposed theme comes from the necessity of producing sequences of realistic movements chosen within a set of plausible solutions. Therefore, applying the models coming from robotics and the motion generation methods that are based on

## 2. STATE OF THE ART

---

prioritization in order to deal with redundancy, comes as a start point to accomplish whole-body motion. Then, the development of a generic framework, that is simple for the users and that produces a human-like motion comes next. Afterwards, comparing or adapting the simulated motion to a real human captured motion affords a good way for the validation of the framework and the analysis of the simulated motion. Therefore, this study implies applications in the different fields of life sciences.

# 3

## Dynamic motion generation under prioritized equality and inequality constraints

### 3.1 Problem statement

How to generate stable whole-body motions for humanoid robots in a generic way? Due to the complexity of the tree-like structure of these robots and the instability of their bipedal posture, this question is very challenging. As these polyarticulated systems include many degrees of freedom, they are generally highly redundant with respect to usual tasks, and therefore difficult to control. Moreover, constraints of different sorts need to be considered when designing the movement. These constraints may arise from internal dynamics, task definition or interaction with the environment. Depending on the situation, they are strict constraints, that should have priority over any task, or slack constraints, to be respected at best to optimize the dynamical properties of the motion. These constraints are of two kinds : equalities (for example, zero velocity at rigid-contact points), and inequalities (for example, joint position, velocity and torque within given bounds). Different developments concerning redundancy and task priority have been proposed in the robotics literature and discussed in chapter 2.

Since whole-body motion is naturally concerned with dynamics and contact forces, a dynamic modeling is thus necessary. The tasks need also to be defined at the dynamic level in order to determine the actuation torques required for executing the motion. Several approaches, as explained in § 2.2.3, consider priority techniques within a dynamic

### 3. DYNAMIC MOTION GENERATION

---

formulation written in the task space or *operational* space. In this family of methods, the unilateral constraints are described as potential functions and treated as a lower-priority constraint. The most generic formulation, so far, was proposed by Sentis et al. [Sentis, 2007], while setting a hierarchy of tasks for the resolution of multiple constraints and contacts. However, the contact constraints are not explicitly taken into account. On the other hand, many approaches were developed to explicitly consider inequality constraints with the dynamical model. An original scheme to compute a generic dynamic control law from a hierarchical set of both unilateral and bilateral constraints was proposed in [Mansard et al., 2009a]. A double-stage solver based on static and dynamic quadratic problems is designed in [Collette et al., 2007] for achieving a dynamic stable control of humanoid robots considering multiple grasps and non-coplanar frictional contacts. This solver is a part of a global architecture of low-level (the QP solver) and high-level controllers. In the high level, the robot analyzes its state and subsequently chooses a strategy, either by reacting to a disturbance or by realizing a task sequence, for keeping its balance and satisfying the constraints. This method seems to be effective to control any humanoid robot with important number of DOF. Yet it is quite complex and interdependent since a before-hand stage of static QP needs to be resolved, then a higher level of control should make a posteriori decisions. Note that the solver does not adopt prioritization of constraints, they are all resolved simultaneously which could make the problem infeasible. In this perspective of developing controllers for the simulation or demonstration of humanoid robot motion subject to multiple variable contacts, many researchers combined dynamical models with motion planning techniques in a double stage framework of contact-before-motion planning. It consists of planning a sequence of multi-contact stances with corresponding static postures that brings a humanoid robot from an initial configuration to a desired stance/configuration. In [Escande et al., 2006], the planner is based on building successively and iteratively a tree of nodes defining a sequence of contact switches and states, then generating corresponding postures to these states that result in a continuous motion. The tree builder is inspired from the Best First Planning Algorithm which is a potential field based algorithm presented in [Latombe, 1991]. The posture generator, taking as input the initial set of contacts, resolves the motion by optimizing a geometrical criteria under dynamical constraints. Therefore, the motion was restricted to respect only quasi-static equilibrium. Similar approach was adopted in [Hauser et al., 2005]. Due to the geometric nature of such techniques, which is not suited for the integration of dynamic motion constraints in the planning, different solutions were

proposed in the motion planning research area. Adapting kinodynamic planning or dynamic filtering techniques [Kuffner et al., 2002; Belousov et al., 2005; Yoshida et al., 2005] are considered to overcome this limitation. Recently, [Bouyarmane and Kheddar, 2011b], investigated a different approach that directly synthesizes dynamically consistent motion. This method is decomposed into two levels forming the global contact-before-motion planning approach. First, getting the information carried out by the stage where a sequence of multi-contact stances is planned [Bouyarmane and Kheddar, 2011a, 2010]. Second, generating the motion between these stances by applying a multi-objective controller that minimizes a weighted sum of objectives. These objectives are defined by an intermediate stage of a finite state machine, subject to dynamic equality and inequality constraints. Despite the fact that this method allows the generation of dynamic motion considering multiple contacts, the formulation is not yet generic since it not possible to define manipulation tasks or other constraints as collision avoidance, and to resolve them simultaneously. Another approach considering this issue of motion generation in multi-contact stances was presented in [Lengagne et al., 2010]. This approach generates full dynamic motion between sequences of contacts including dynamic transitions by formulating the motion-planning problem as a semi-infinite optimization problem [Reemtsen and Ruckmann, 1998] expressing the joint trajectories as parameterized B-spline functions. This approach requires yet very high computation times. Similarly, in this kind of motion planning based methods, the motion for specific tasks are computed and optimized, but no explicit definition of tasks is possible. However, our concern is more about the liberty of choice and resolution of any kind of task and the adaptation to any constraint. Thus, we need to adopt a task formalism to generate the motion with the required behavior, while satisfying the desired constraints and considering the possibility that any link of the robot gets into contact with any point of the environment. In [Saab et al., 2011a], we extended to the dynamics the method involving a cascade of QP initially developed for the kinematics in [Kanoun et al., 2009; Escande et al., 2010]. This method allowed to generate a minimum-norm whole-body dynamic movement satisfying at best a list of prioritized equality and inequality constraints. However, the preliminary solution that was proposed in that paper for modeling the unilateral contacts of feet with the floor was rather conservative and could not be easily applied to other kinds of contacts. Then, in [Saab et al., 2011b] we extended our preceding results by introducing a standard modeling of unilateral rigid contacts that can be processed, within the stack of tasks (SOT) formalism [Mansard et al., 2009b], similarly as other equality or inequality constraints. A generic framework, that enables the resolution of various types of dynamic constraints

### 3. DYNAMIC MOTION GENERATION

---

with an arbitrary order of priority, including single or multiple non-coplanar contacts, is then stated. We show that the proposed approach generalizes the classical balance condition given by the Zero Moment Point (ZMP) [Kajita et al., 2003].

The chapter is organized as follows: First, section 3.2 recalls the classical schemes for inverse kinematics and introduces the alternative and generic formulation of the hierarchized set of QP that is drawn from these schemes. Then, the dynamic formulation without contacts is described in Section 3.3. Section 3.4 is devoted to the standard formulation of contacts and shows that the classical ZMP stability condition is a particular case of this formulation. The efficiency of the method is finally illustrated in section 3.5, where the simulations of three complex tasks, performed with the dynamical model of HRP-2 and involving non-coplanar contacts, are presented.

## 3.2 Inverse Kinematics

### 3.2.1 Task function approach

The task-function approach [Samson et al., 1991], or operational-space approach [Khatib, 1987; Nakamura and Hanafusa, 1986], provides a mathematical framework to describe tasks in terms of specific output functions. This approach offers an elegant way to bind the planning and the execution of a mission. On the one hand, it defines both the high level specification of the action expressed in formal logic causes (planning); on the other hand, it details the low level formulation allowing to compute the control (execution). The task space is an output space such that the error to regulate can be easily expressed and measured. The usual approach consists in designing a reference behavior of the error in the task space and then applying an inverse transformation to express this reference in the configuration space.

A task is defined by three elements: a vector  $e \in R^m$ , a mapping matrix  $Q$ , and a reference evolution of the task function  $\dot{e}^*$ . Simply it could be represented by the triplet  $(e, \dot{e}^*, Q)$ , where  $e$  is the task function that maps the configuration space to the task space. Typically, the vector  $e$  corresponds to the error between a signal  $s$  and its desired value:

$$e = s - s^*$$

$\dot{e}^*$  is the reference behavior expressed in the tangent space to the task space at  $e$ , and  $Q$  is the differential mapping between the task space and the configuration space of the

robot which verifies the relation:

$$\dot{e} + \mu = Qu, \quad (3.1)$$

where  $u$  is the control and  $\mu$  is the drift of the task. To compute a specific robot control  $u^*$  that performs the reference  $\dot{e}^*$ , any numerical inverse of  $Q$  can be used. The generic expression of the control law is then :

$$u^* = Q^\#(\dot{e}^* + \mu) + Pu_2 \quad (3.2)$$

where  $Q^\#$  is a generalized inverse operator as defined in [Ben-Israel and Greville, 2003],  $P = I - Q^\#Q$  is the corresponding projector in the null space of  $Q$  and  $u_2$  is any arbitrary vector in the space of the robot control, that can be used as a secondary control input to fulfill another control objective [Liégeois, 1977].

The interest of defining the robot motion inside a task space rather than directly at the joint level is double. First, the task space is chosen such that the control law can be easily designed, making the link between sensor feedback and control direct. Typically, in visual servoing the task space is the space of measurable visual features [Espiau et al., 1992]. Second, the interference between two task spaces can be prevented using the projection operator  $P$ , that allows to decouple concurrent simultaneous objectives.

### 3.2.2 Hierarchy of tasks

Most of the time, the command as defined in (3.2) controls only some part of the robot, giving the possibility to realize other tasks simultaneously when the robot presents enough redundancy. In this purpose, tasks are usually organized into a hierarchy, so that tasks of lower priority do not perturb the realization of higher priority tasks [Siciliano and Slotine, 1991]. Tasks of high priority usually aim at preserving the security of the robot (balance, collision avoidance), while motion tasks have lower priority. Different methods to build such a hierarchy have been proposed in the literature and were detailed in chapter 2. In summary, there are two families of methods: the first one applies pseudo-inversion projection techniques ensuring the realization of the prior tasks, while the second defines a cascade of optimization problems, relying each on a cost function subject to constraints, that also guarantee the feasibility of the priority problems.

First, we will discuss the reasoning of the projection techniques and then make the analogy with the resolution method of the optimization problems, at the kinematics level as well as the dynamics level. Now, considering the projector  $P$  from (3.2), we can say

### 3. DYNAMIC MOTION GENERATION

---

that it is intrinsically related to the redundancy of the robot with respect to the task  $e$ . If a secondary task  $(e_2, \dot{e}_2^*, Q_2)$  has to be performed, then  $u_2$  can be used as a new control input. Introducing (3.2) in  $\dot{e}_2 + \mu_2 = Q_2 u$  gives:

$$\dot{e}_2 + \tilde{\mu}_2 = \widetilde{Q}_2 u_2 \quad (3.3)$$

with  $\tilde{\mu}_2 = \mu_2 - Q_2 Q^\#(\dot{e}^* + \mu)$  and  $\widetilde{Q}_2 = Q_2 P$ . This last equation fits the template (3.1), and can be solved using the generic expression (3.2) [Siciliano and Slotine, 1991]:

$$u_2^* = \widetilde{Q}_2^\#(\dot{e}^* + \tilde{\mu}_2) + P_2 u_3, \quad (3.4)$$

where  $P_2$  enables to propagate the redundancy to a third task using the input  $u_3$ . By recurrence, this generic scheme can be extended to any arbitrary hierarchy of tasks.

#### 3.2.3 Inverse kinematics formulation

In inverse kinematics, the control input  $u$  is simply the robot joint velocity  $\dot{q}$ . The differential link  $Q$  between the task and the control is the task Jacobian  $J$ . In that case, the drift is generally null, and (3.1) is written:

$$\dot{e} = J\dot{q} \quad (3.5)$$

Most of the time, the generalized inverse is the pseudo inverse (denoted by  $\cdot^+$ ) which gives the least Euclidean norm of both  $\dot{q}$  and  $\dot{e}^* - J\dot{q}$  [Ben-Israel and Greville, 2003; Golub and Van Loan, 1996]. The control law is then:

$$\dot{q}^* = \dot{q}_1^* + P\dot{q}_2 \quad (3.6)$$

where  $\dot{q}_1^* = J^+ \dot{e}^*$ . A typical reference behavior is an exponential decay of  $e$  to zero:  $\dot{e}^* = -\lambda e, \lambda > 0$ . Figure 3.1 shows a representation of 2 linear systems that are compatible and of the solution satisfying both systems obtained by successive pseudo-inversions.

#### 3.2.4 Projected inverse kinematics

Consider a secondary task  $(e_2, \dot{e}_2^*, J_2)$ . The template (3.1) is written:

$$\dot{e}_2 - J_2 \dot{q}_1^* = J_2 P \dot{q}_2 \quad (3.7)$$

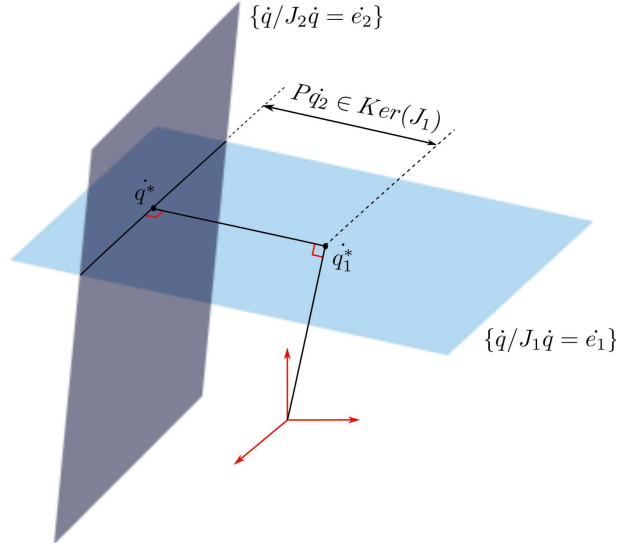


**Figure 3.1:** Successive orthogonal projections that lead to  $\dot{q}^*$  given 2 compatible tasks: The first linear system is resolved, then the second linear system is solved within the solution space of the first linear system.

In this case, the differential link is the projected Jacobian  $Q = J_2 P$ , and the drift is  $\mu = -J_2 \dot{q}_1^*$ . The control input  $\dot{q}_2^*$  is obtained once more by numerical inversion [Siciliano and Slotine, 1991; Baerlocher and Boulic, 2004]:

$$\dot{q}_2^* = (J_2 P)^+ (\dot{e}_2 - J_2 \dot{q}_1^*) + P_2 \dot{q}_3 \quad (3.8)$$

where  $P_2$  is the projector into the null space of  $J_2 P$ . The same scheme can be reproduced iteratively to account for any number of tasks until  $P_i$  is null. The choice of the task order should respect some priority in order to realize feasible movements that correspond to desired behaviors. Figure 3.2 shows the importance of prioritization in case of 2 targets to be reached.

### 3.2.5 QP cascade resolution

In [Kanoun et al., 2009], it was proposed to use a QP solver to compute the inverse kinematics, instead of using a pseudo inverse as previously described. For only one task, the resolution by QP is strictly equivalent to a pseudo inverse resolution. However, the great advantage of the QP resolution is that it allows to take into consideration constraints defined by linear equalities and/or inequalities. Indeed the classical pseudo-inverse resolution scheme, based on successive projections, cannot explicitly handle inequalities. The

### 3. DYNAMIC MOTION GENERATION

---

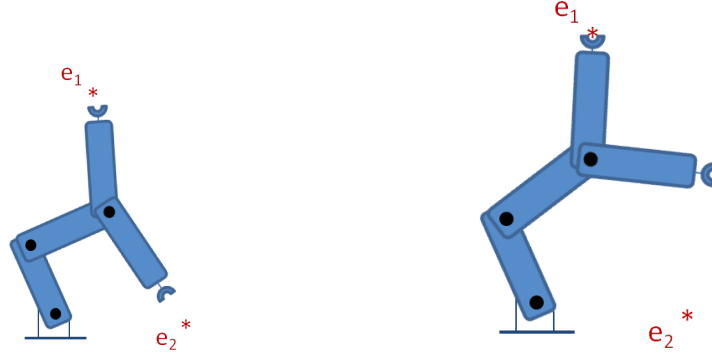


**Figure 3.2:** Two targets are given  $e_1$  and  $e_2$ . In the left figure, no prioritization is defined then the chain is free to move trying to reach both targets but none of the targets are reached. Prioritization is required to ensure the achievement of the prior task and to avoid failing both tasks. This is represented in the figure on the right where priority is given to  $e_1$ .

extension in [Kanoun et al., 2009] allows to generalize the QP formulation to a hierarchy of several equalities and inequalities. In fig. 3.3, we show an illustration of the resolution method of the QP considering equality and inequality systems with different choices of prioritization.

#### 3.2.5.1 Generic formulation

In applied mathematics, the QP resolution algorithm based on the active set method was first given in [Fletcher, 1971]. It works as a double-stage hierarchized set, where inequalities can only be expressed at the top priority level. The introduction of slack variables is then a classical solution to circumvent this limitation [Boyd and Vandenberghe, 2004]. In [Kanoun et al., 2009; Escande et al., 2010], it was proposed to extend the use of slack variables to handle more than two stages of priority.

In the following, a task is defined by the two boundary inequalities  $(e, (\underline{r}^*, \bar{r}^*), Q)$ , where  $\underline{r}^*$  and  $\bar{r}^*$  are respectively the lower and upper bounds on the reference behavior. Specific cases can be immediately implemented:  $\underline{r}^* = \bar{r}^*$  in the case of equalities, and  $\underline{r}^* = -\infty$  or  $\bar{r}^* = +\infty$  to handle single-bounded constraints. At stage  $k$ , the cascade algorithm solving the hierarchy of tasks is expressed by the following QP:

$$\begin{aligned}
 & \min_{u_k, w_k} \|w_k\|^2 \\
 \text{s.t.} \quad & \underline{r}_{k-1}^* \leq Q_{k-1}u_k + w_{k-1}^* \leq \bar{r}_{k-1}^* \\
 & \underline{r}_k^* \leq Q_k u_k + w_k \leq \bar{r}_k^*
 \end{aligned} \tag{3.9}$$

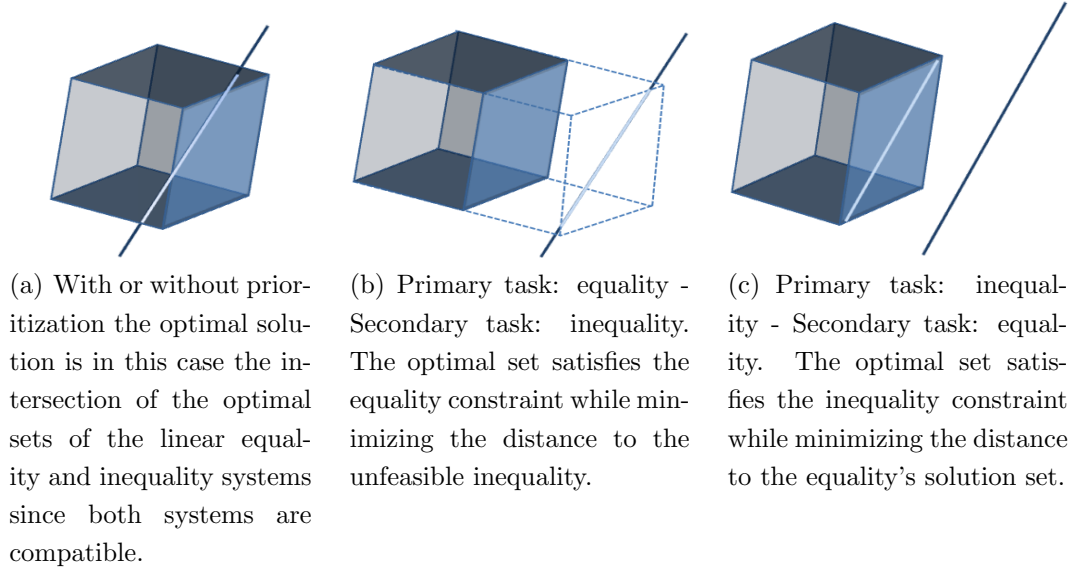


**Figure 3.3:** Illustration in 3D space of the optimal sets for prioritization problems involving both equality and inequality linear systems. The line represents the equality system and the cube forms the set of inequalities.

where  $Q_{k-1}, (\underline{r}_{k-1}^*, \bar{r}_{k-1}^*)$  are the constraints at all the previous stages, from 1 to  $k - 1$ , and  $Q_k, (\underline{r}_k^*, \bar{r}_k^*)$  is the constraint at stage  $k$ .

The slack variable<sup>1</sup>  $w_k$  is used to add some freedom to the solver if no solution can be found when the constraint  $k$  is introduced, under the  $k - 1$  previous constraints. Whereas  $w_{k-1}^*$  has a fixed value due to the result of the optimization of the  $k - 1$  first QPs,  $w_k$  is variable and can be used by the solver to relax the last constraint. A solution to the *strict*  $k - 1$  constraint  $Q_{k-1}$  is then always reached, even if the *slack* constraint  $Q_k$  is not feasible, which corresponds to the definition of the hierarchy between tasks.

In the following, a set of tasks with a hierarchy order (or stack of tasks) will be denoted by using the lexicographic order as follows:  $(i) \prec (ii) \prec (iii) \prec \dots$  which means that task  $(i)$  has the highest priority.

<sup>1</sup>  $w$  is an implicit optimization variable whose explicit computation can be avoided when formulating the problem as a cascade. It does not appear in the vector of optimization variables  $u$ . See [Escande et al., 2010] for details.

### 3. DYNAMIC MOTION GENERATION

---

#### 3.2.5.2 Application to inverse kinematics

When considering a single task, inversion (3.6) corresponds to the optimal solution to the problem:

$$\min_{\dot{q}} \|J\dot{q} - \dot{e}^*\|^2 \quad (3.10)$$

By applying the QP resolution scheme, both equalities and inequalities can be considered. Replacing  $r$  by  $\dot{e}$ , the reference part is then rewritten:

$$\underline{\dot{e}^*} \leq \dot{e} \leq \bar{e}^* \quad (3.11)$$

For instance, in the case of two tasks with priority order  $e_1 \prec e_2$ , the expression of the QP is given by:

$$\begin{aligned} & \min_{\dot{q}, w_2} \|w_2\|^2 \\ s.t. & \quad \underline{\dot{e}_1^*} \leq J_1\dot{q} + w_1^* \leq \bar{e}_1^* \\ & \quad \underline{\dot{e}_2^*} \leq J_2\dot{q} + w_2 \leq \bar{e}_2^* \end{aligned} \quad (3.12)$$

Most of the time, unilateral constraints have priority over any other constraint: typically, joint limits and obstacle avoidance have a higher priority than a grasping task. However to handle less-common cases (like insuring visibility when performing a visually-guided grasping), a stack of tasks including inequalities at any level can be considered.

In the sequel, we will show that the QP cascade accounting for linear equalities and inequalities can be easily extended to the dynamics.

## 3.3 Inverse Dynamics

In this section we consider the case of a contact-free dynamical multi-body system without free-floating root.

### 3.3.1 Task-space formulation

As previously stated, a task is defined by a task function  $e$ , a reference behavior and a differential mapping. At the dynamic level, the reference behavior is specified by the expected task acceleration  $\ddot{e}^*$ . Given such a reference, the operational-space inverse-dynamics problem comes down to finding the torque control input  $\tau$  that produces the necessary joint acceleration  $\ddot{q}$ . The variable  $\ddot{q}$  is then a side variable, that does not require to be explicitly computed during the resolution. Contrary to the case of kinematics, the mapping between the control input  $\tau$  and the task space is obtained in two stages. First,

the link between accelerations in the configuration space and in the task space is obtained by deriving (3.5):

$$\ddot{e} = J\ddot{q} + \dot{J}\dot{q} \quad (3.13)$$

Then, the dynamic equation of the system is deduced from the mechanical laws of motion [Featherstone, 2008].

$$A\ddot{q} + b = \tau \quad (3.14)$$

where  $A = A(q)$  is the generalized inertia matrix of the system,  $\ddot{q}$  is the joint acceleration,  $b = b(q, \dot{q})$  gathers all the nonlinear effects including Coriolis, centrifugal and gravity forces and  $\tau$  is the actuation torque. Finally, the classical resolution of the task-space inverse-dynamics problem requires a reformulation to remove  $\ddot{q}$  by merging (3.13) in (3.14) [Khatib, 1987]:

$$\ddot{e} - \dot{J}\dot{q} + JA^{-1}b = JA^{-1}\tau \quad (3.15)$$

Thus, the problem of finding the torque control  $\tau$  that ensures the given reference acceleration  $\ddot{e}^*$  can be solved by inverting this linear expression, for example by using a pseudo inverse. When a first task is solved, a secondary task can be introduced using the null space of the first Jacobian. Then, iteratively, a stack of tasks can be considered, with the lower-priority tasks being executed at best without disturbing the tasks having higher priority [Siciliano and Slotine, 1991; Sentis, 2007].

#### 3.3.2 Consistency with the generic template

Eq. (3.15) is of the form of the template (3.1) with  $Q = JA^{-1}$ ,  $\mu = -\dot{J}\dot{q} + JA^{-1}b$  and  $u = \tau$ . The inverse dynamics control law can then be directly obtained by inverting  $Q$ . To cope with the dynamics of the system, the use of the generalized inverse operator weighted<sup>1</sup> by  $A$ , denoted by  $\cdot\#^A$ , was proposed in [Khatib, 1987]. This weighted inverse gives the least norm solution  $\|\tau\|_A = \sqrt{\tau^\top A^{-1}\tau}$  respecting the constraint (3.15) [Doty et al., 1993]. This norm corresponds to a minimization of the acceleration pseudo energy  $\dot{q}^\top A\dot{q}$  [Park, 2006; Peters et al., 2008]. Introducing  $\tau_2$  as the torque devoted to a secondary objective we get:

$$\tau^* = \tau_1^* + P\tau_2 \quad (3.16)$$

where,  $\tau_1^* = (JA^{-1})\#^A(\ddot{e} - \dot{J}\dot{q} + JA^{-1}b)$  and  $P$  is the projector into the null space of  $JA^{-1}$ .

---

<sup>1</sup>Dealing with a redundant system, the Jacobian matrix is full row rank. The weighted generalized inverse of a full row matrix  $X$  by a matrix  $W$  takes the following form:  $X\#^W = WX^\top(XWX^\top)^{-1}$ .

### 3. DYNAMIC MOTION GENERATION

---

#### 3.3.3 Projected inverse dynamics

As before, the differential link is obtained by replacing (3.16) into the robot dynamics equation associated to a second task  $\ddot{e}_2 - \dot{J}_2\dot{q} + J_2A^{-1}b = J_2A^{-1}\tau^*$ :

$$\ddot{e}_2 + \mu_2 = Q_2\tau_2 \quad (3.17)$$

with  $\mu_2 = -\dot{J}_2\dot{q} + J_2A^{-1}b - J_2A^{-1}\tau_1^*$ , and  $Q_2 = J_2A^{-1}P$ . The same weighted inverse is used to inverse  $Q_2$  [Park, 2006; Sentis, 2007]. Accordingly, any number of tasks can be added iteratively until the projector becomes null. As for the kinematics, the main drawback of the pseudo-inverse-based resolution is the limitation to tasks defined by equalities. In order to deal with inequalities, we propose to extend the QP cascade that was previously introduced for the kinematics.

#### 3.3.4 Application of the QP solver to the dynamics

When resolving a given task  $e$  by taking into account the dynamics, both (3.13) and (3.14) must be fulfilled. There are two ways of formulating the QP. First,  $\ddot{q}$  can be substituted from (3.13) into (3.14), to obtain the single reduced equation (3.15). In that case, the QP is used to solve the system in  $\tau$ , the variable  $\ddot{q}$  being not explicitly computed. Alternatively, (3.13) can be solved under the constraint (3.14). Using the hierarchy notation, the cascade of QPs is thus (3.14)  $\prec$  (3.13), or using the standard QP notation:

$$\begin{aligned} & \min_{\tau, \ddot{q}, w} \|w\|^2 \\ \text{s.t.} \quad & A\ddot{q} + b = \tau \\ & \ddot{e}^* + w = J\ddot{q} + \dot{J}\dot{q} \end{aligned} \quad (3.18)$$

In that case, both  $\tau$  and  $\ddot{q}$  are explicitly computed. They constitute the vector of optimization variables  $u = (\tau, \ddot{q})$ .

Comparing both formulations, expressing some constraints using the reduced QP could be difficult. However, as shown in (3.18), the explicit QP has a straightforward formulation. In [Saab et al., 2011a], we proposed to use the reduced QP formulation, and proved that it is equivalent to the solution obtained by using pseudo inverses as in [Sentis, 2007]. After testing on various experimental setups, we measured that there is no significant computation-cost differences between reduced and exhaustive QP formulation. Since exhaustive-QP formulation is easier to write, we will use it in the following computations.

## 3.4 Inverse dynamics under contact constraints

### 3.4.1 Insertion of the contact forces

In the previous section, we considered a polyarticulated system in free space, *i.e.* with no free-floating root and without contact forces. For humanoid robots, the contacts with the environment have to be considered. In addition, the degrees of freedom corresponding to the root are not actuated since it is considered to be free-floating.

First, let us consider a contact between a single body of the robot and the environment. The dynamic equation is:

$$A\ddot{q} + b + J_c^\top \phi_c = S^\top \tau \quad (3.19)$$

where  $A$  and  $b$  are defined as before,  $\ddot{q}$  is the vector of generalized joint accelerations<sup>1</sup>,  $\phi_c = (f_c, \tau_c)$  is the generalized 6D contact force applied to the body in contact, expressed at the points  $x_c$ ,  $J_c = \frac{\partial x_c}{\partial q}$  is the Jacobian matrix of the body in contact at point  $x_c$ , and  $S = [0 \ I]$  is a matrix that allows to select the actuated joints.

The rigid contact condition implies that there is no motion of the robot contact points  $x_c$  *i.e.*  $\dot{x}_c = 0$ ,  $\ddot{x}_c = 0$ . For a given state, it implies the linear equality constraint:

$$J_c \ddot{q} = -\dot{J}_c \dot{q} \quad (3.20)$$

By multiplying (3.19) by  $J_c A^{-1}$  and substituting the expression of  $J_c \ddot{q}$  given by (3.20), the link between the torque and the contact force takes the following form, in which the acceleration no longer appears explicitly:

$$J_c A^{-1} J_c^\top \phi_c = J_c A^{-1} (S^\top \tau - b) + \dot{J}_c \dot{q}, \quad (3.21)$$

where  $J_c A^{-1} J_c^\top$  is invertible, and  $\phi_c$  can be deduced [Khatib et al., 2008]:

$$\phi_c = (J_c^\top)^\# A^{-1} (S^\top \tau - b) + (J_c A^{-1} J_c^\top)^{-1} \dot{J}_c \dot{q} \quad (3.22)$$

since  $J_c^\top$  is a full column rank matrix. This expression of  $\phi_c$  can be re-injected in (3.19), to obtain an expression of the dynamic equation in which the contact force does not appear explicitly anymore.

$$A\ddot{q} + b_c = P_c S^\top \tau, \quad (3.23)$$

---

<sup>1</sup>To be exact,  $\ddot{q}$  should be written  $\begin{bmatrix} \dot{v}_f \\ \ddot{q}_A \end{bmatrix}$ , where  $v_f$  is the 6D velocity of the robot root and  $q_A$  the position of the actuated joints. For the ease of notation  $q$ ,  $\dot{q}$  and  $\ddot{q}$  will be used in the sequel.

### 3. DYNAMIC MOTION GENERATION

---

where  $P_c = (I - J_c \#^{A^{-1}} J_c)^\top = (I - (J_c A^{-1}) \#^A J_c A^{-1})$  is the projection operator of the contact, and  $b_c = P_c b + J_c^\top (J_c A^{-1} J_c^\top)^{-1} \dot{J}_c \dot{q}$ . As previously, the differential link between the task and the torque input is expressed through the intermediate variable  $\ddot{q}$  by using (3.13):

$$\ddot{e} + \mu_c = Q_c \tau \quad (3.24)$$

with  $\mu_c = -\dot{J}_c \dot{q} + J_c A^{-1} b_c$  and  $Q_c = J_c A^{-1} P_c S^\top$ . By inverting (3.24) and choosing a proper weighted inverse, it is possible to show that this formulation is equivalent to the operational-space dynamic equation developed in [Sentis et al., 2010] (see Appendix A).

As before, Eq. (3.24) follows the template (3.2) and can be directly formulated as a QP. The QP can be expressed under a reduced form as proposed in [Saab et al., 2011a]. Or, more simply, the QP cascade (3.18) can then be directly reformulated to take into account the dynamics in contact. Using the cascade notation, the program for one task is (3.19)  $\prec$  (3.20)  $\prec$  (3.13). The variables  $\phi_c$  and  $\ddot{q}$  are then explicitly computed. The optimization variables are  $u = (\tau, \ddot{q}, \phi_c)$ . This explicit QP-cascade formulation was proved to be equivalent to the reduced inversion in [Saab et al., 2011a].

#### 3.4.2 Sufficient condition for rigid planar contacts

For a single point in rigid contact with a surface, there are two complementary possibilities: either the force along the normal to the contact surface is positive (the robot pushes against the surface and does not move), or the acceleration along the normal is positive (the robot is just starting to move). Both possibilities are said to be complementary since one and only one of them is fulfilled. By writing (3.19) and (3.20), we implicitly consider that the robot is in the first case: positive normal force and no movement. Thus, the generated control must fulfill this condition.

Very often, only the non-motion condition constraint (3.20) is considered [Khatib et al., 2008]. This allows to generate a dynamic motion. However, this motion may not be feasible since the condition of positivity of the normal contact forces is not explicitly verified. A first solution can be to saturate the part of the control that does not correspond to gravity compensation when the positivity condition is not satisfied [Sentis, 2007]. However, such a solution is very restrictive compared to the motions that the robot can actually perform. Checking this second constraint is not possible without a generic way of handling inequalities. What we propose in the following is to use the possibilities offered by the cascade of the QP to cope with this problem.

### 3.4 Inverse dynamics under contact constraints

---

We consider the case of a rigid contact between two planar surfaces, one being a face of one body of the robot, the other one belonging to the environment. In case the robot is touching two or more planar surfaces at the same time, several planar contacts are to be considered. The point  $c$  denotes the arbitrary origin of the reference frame attached to the robot body in contact (for example,  $c$  can be chosen at the center of the joint with the previous body in the chain). To guarantee a rigid planar contact, at least three points of the body  $p_i$ ,  $i = 1, \dots, l$  ( $l \geq 3$ ), not aligned, define the boundaries of the polygon of contact. For  $i = 1, \dots, l$ ,  $f_i$  denotes the contact force applied at the vertex  $p_i$ . Following the notation used in (3.19),  $\phi_c$  is related to the vector  $f$  of the contact forces  $f_i$  by the relation:

$$\phi_c = \begin{bmatrix} f_c \\ \tau_c \end{bmatrix} = \begin{bmatrix} \sum_i f_i \\ \sum_i p_i \times f_i \end{bmatrix} = X \begin{bmatrix} f_1 \\ \vdots \\ f_l \end{bmatrix} = Xf, \quad (3.25)$$

with

$$X = \begin{bmatrix} I & I & \dots & I \\ \hat{p}_1 & \hat{p}_2 & \dots & \hat{p}_l \end{bmatrix},$$

where  $\hat{p}_i$  is the matrix of pre-product defined by:

$$\hat{p}_i = \begin{bmatrix} 0 & -p_{i_z} & p_{i_y} \\ p_{i_z} & 0 & -p_{i_x} \\ -p_{i_y} & p_{i_x} & 0 \end{bmatrix}$$

Using this notation, a sufficient condition to guarantee a rigid contact between the body of the robot and the planar surface is that all the normal components  $f_i^\perp$  of the contact forces  $f_i$  are positive, expressing the fact that the reaction forces of the surface is directed toward the robot:

$$f^\perp \geq 0 \quad (3.26)$$

with  $f^\perp = (f_1^\perp, f_2^\perp, \dots, f_l^\perp)$  the vector of the normal components of the forces at the contact points.

#### 3.4.3 Including the contact forces within the QP Solver

Condition (3.26) must now be introduced in the QP cascade proposed at the end of Section 3.4.1.

### 3. DYNAMIC MOTION GENERATION

---

#### 3.4.3.1 A first way of modeling the problem

The constraints should be written with respect to the optimization variables, while (3.26) depends on  $f$ . A first way of writing (3.26) with respect to the optimization variables is to use the linear map  $X$  between  $\phi_c$  and  $f$  given by (3.25). In order to compute  $f$ , (3.25) should be inverted by using a particular generalized inverse  $X^\#$ :

$$f = X^\# \phi_c \quad (3.27)$$

The normal component  $f^\perp$  is then given by:

$$\begin{aligned} f^\perp &= S^n X^\# \phi_c \\ &= F \phi_c \end{aligned} \quad (3.28)$$

with the selection matrix  $S^n$  defined by:

$$S^n = \begin{bmatrix} 001000000 \dots 0000000 \\ 000001000 \dots 0000000 \\ \dots & \dots & \dots \\ 000000000 \dots 0001000 \\ 000000000 \dots 0000001 \end{bmatrix}$$

The condition of positivity of  $f^\perp$  is then written with respect to the optimization variables:

$$F \phi_c \geq 0 \quad (3.29)$$

The QP cascade is then (3.19)  $\prec$  (3.20)  $\prec$  (3.29)  $\prec$  (3.13), with the vector of optimization variables being  $u = (\ddot{q}, \tau, \phi_c)$ .

However, (3.29) is only a sufficient condition of (3.26), that is too restrictive. In fact, the map  $X$  is not invertible. Thus, by choosing a specific inversion  $^\#$ , we made a too strong a priori assumption, and it may happen that an admissible  $\phi_c$  produces a negative  $f^\perp = S^n X^\# \phi_c$ . For example, Fig. 3.4 displays the domain reached by the center of pressure: for a necessary and sufficient condition, the whole support polygon should be reached. Using the Euclidean norm, only the included diamond inside the support polygon is reached, as presented in fig. 3.4. Various included quadrilaterals are reached when using other norms for the inversion operator  $^\#$ . We can also illustrate this problem by the following mathematical example. Suppose we have only two positive forces in 2D with one linear constraint  $\phi_c$ :

$$\begin{cases} f_1 = 2 \\ f_2 = 4 \end{cases} \quad (3.30)$$

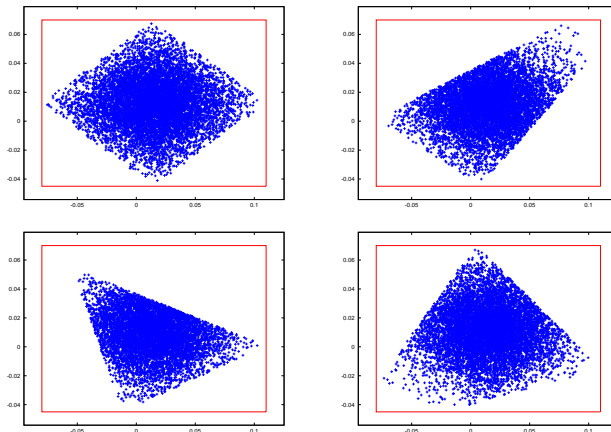


**Figure 3.4:** Random sampling of the reached support region. The actual support polygon is the encompassing rectangle. The point clouds display the ZMP of random admissible forces: random forces  $\phi_c$  are shot, and the corresponding  $f = X^\# \phi_c$  are computed. If  $\phi_c$  respects (3.29), the corresponding center of pressure is drawn. Each sub-figure displays the admissible forces  $\phi_c$  for a different weighted inversion (the Euclidean norm is used on the top left, and random norms are used for the three others). Only a subregion of the support polygon can be reached, experimentally illustrating the fact that (3.29) is a too-restrictive sufficient condition.

If we define  $\phi_c = -f_1 + f_2$  as shown in figure 3.5(a), the solution obtained by the minimization of the distance to the origin is included in the dashed zone. This solution gives a negative force  $f_1$  as opposed to the hypothesis. Whereas, figure 3.5(b) represents the case where  $\phi_c = f_1 + f_2$ . In this example, the zone corresponding to the minimum solution gives positive forces  $f_1$  and  $f_2$ . We conclude that depending on the form of the linear application between  $\phi_c$  and the contact forces, the minimization induced from the weighted pseudo-inversion gives solutions of positive or negative forces.

#### 3.4.3.2 Using contact forces as variables

The problem is that the forces  $f_i$  cannot be uniquely determined from  $\phi_c$ , while it is possible to determine  $\phi_c$  from  $f_i$ . To cope with this problem we propose to take the contact forces  $f$  among the optimization variables of the QP resolution. Condition (3.26) is then directly written with respect to the variables  $u = (\tau, \ddot{q}, \phi_c, f)$ . The cascade is then: (3.19)  $\prec$  (3.20)  $\prec$  (3.25)  $\prec$  (3.26)  $\prec$  (3.13). Since  $\phi_c$  can be determined from  $f$ , it would be possible to express all the QPs in terms of  $f$  and without  $\phi_c$ . However, this increases considerably the size of the Jacobian of the contact points, and thus the whole complexity

### 3. DYNAMIC MOTION GENERATION

---

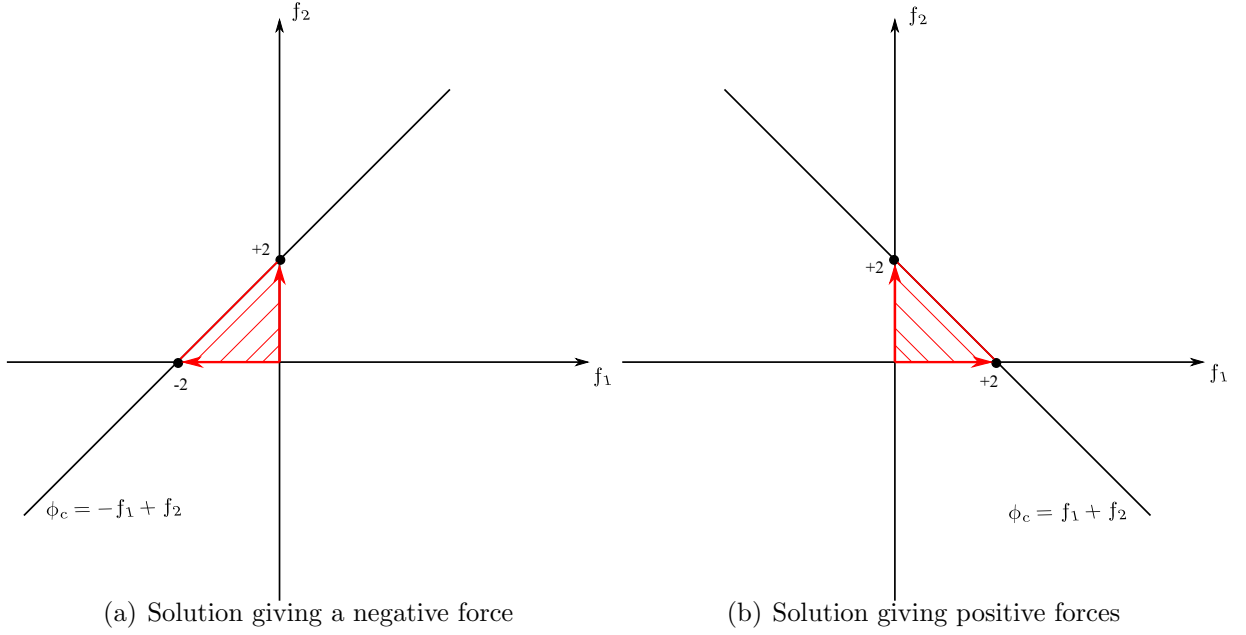


**Figure 3.5:** Illustration of the application of a Jacobian inverse on a  $2D$  system.

of the cascade. Keeping  $\phi_c$  inside the variables acts as a proxy on the bigger-dimension variable  $f$ . The contact forces only appear for the positivity condition (3.26) and for the link with  $\phi_c$  (3.25).

#### 3.4.3.3 Reducing the size of the variable $f$

It is possible to rewrite (3.25) to decouple the link between  $\phi_c$  and the tangent components of  $f$ . Consider the point  $o$  chosen at the interface of contact (for example,  $o$  is the projection of  $c$  on the surface of contact). The point  $o$  belongs then to the support polygon. Let us denote by  $\phi_o$  the expression of the vector of forces and torques at  $o$ , expressed in terms of  $\phi_c$  as follows:

$$\phi_o = \begin{bmatrix} f_o \\ \tau_o \end{bmatrix} = \begin{bmatrix} I_3 & 0_3 \\ {}^o\hat{c} & I_3 \end{bmatrix} \phi_c = {}^oX_c \phi_c, \quad (3.31)$$

where  ${}^o c$  are the coordinates of the point  $c$  in the referential centered at  $o$ , having its  $z$ -axis normal to the surface of contact, and  ${}^o\hat{c}$  is the associated pre-product matrix.

### 3.4 Inverse dynamics under contact constraints

---

From (3.25) and (3.31), it comes:

$$f_{o_x} = \sum_i f_{i_x} = f_{c_x} \quad (3.32a)$$

$$f_{o_y} = \sum_i f_{i_y} = f_{c_y} \quad (3.32b)$$

$$f_{o_z} = \sum_i f_{i_z} = f_{c_z} \quad (3.32c)$$

$$\tau_{o_x} = \sum_i -{}^o p_{i_z} f_{i_y} + \sum_i {}^o p_{i_y} f_{i_z} = -c_z f_{c_y} + \tau_{c_x} \quad (3.32d)$$

$$\tau_{o_y} = \sum_i {}^o p_{i_z} f_{i_x} - \sum_i {}^o p_{i_x} f_{i_z} = c_z f_{c_x} + \tau_{c_y} \quad (3.32e)$$

$$\tau_{o_z} = \sum_i -{}^o p_{i_y} f_{i_x} + \sum_i {}^o p_{i_x} f_{i_y} = \tau_{c_z} \quad (3.32f)$$

where  ${}^o p_i$  are the coordinates of the contact points expressed in the frame centered at  $o$ . Since  $o$  is coplanar with the  $p_i$ , the  ${}^o p_{i_z}$  are null. Then, the previous expression reveals a decoupling in  $\phi_c$ : the forces  $f_{o_{x,y}}$  and the torque  $\tau_{o_z}$  are expressed in terms of  $f_{i_{x,y}}$ . The force  $f_{o_z}$  and the torques  $\tau_{o_{x,y}}$  are function of  $f_{i_z}$ . In the QPs, there are consequently no constraints to choose the value of  $f_{o_{x,y}}$  and  $\tau_{o_z}$ . It is thus possible to remove these variables and the associated constraints (3.32a), (3.32b) and (3.32f). Then, the rigid-contact constraint can be expressed as follows:

$$Q_c \begin{bmatrix} \phi_c \\ f^\perp \end{bmatrix} = 0 \quad (3.33)$$

$$f^\perp \geq 0$$

with

$$Q_c = \begin{bmatrix} 0 & 0 & -1 & 0 & 0 & 0 & 1 & 1 & \dots & 1 \\ 0 & c_z & 0 & -1 & 0 & 0 & p_{1_y} & p_{2_y} & \dots & p_{l_y} \\ -c_z & 0 & 0 & 0 & -1 & 0 & -p_{1_x} & -p_{2_x} & \dots & -p_{l_x} \end{bmatrix}$$

The cascade is then (3.19)  $\prec$  (3.20)  $\prec$  (3.33)  $\prec$  (3.13) and the optimization variables are  $u = (\tau, \ddot{q}, \phi_c, f^\perp)$ .

#### 3.4.4 Application to the particular case of the ZMP

In this section, we consider the particular case where the sole contact is the contact of feet with the floor. We will show that the sufficient condition of rigid planar contact introduced in section 3.4.2 is equivalent to the usual ZMP constraint.

Suppose, as previously, that the robot is in single support, but consider now that the contact surface is horizontal. We consider the frame centered at  $o$  with the z-axis upward vertical. As stated in [Kajita et al., 2009; Vukobratović and Borovac, 2004], the ZMP can be defined as the barycenter of the contact points  $p_i$  delimiting the contact surface of the

### 3. DYNAMIC MOTION GENERATION

---

foot with the horizontal floor, weighted by the normal component  $f_{i_z}$  of the contact forces  $f_i$  at these points<sup>1</sup>. The ZMP coordinates are thus:

$$z = \left( \frac{\sum_i^o p_{i_x} f_{i_z}}{\sum_i f_{i_z}}, \frac{\sum_i^o p_{i_y} f_{i_z}}{\sum_i f_{i_z}}, 0 \right)$$

In affine geometry, it is a well known result that the convex hull of a set of points is the set of barycenters of these points weighted by positive coefficients (Proposition 5.6 page 29 in [Audin, 2002]). The rigid contact condition defined by (3.26) guarantees that the normal component  $f_{i_z}$  of each contact force  $f_i$  is positive. As a consequence, the condition (3.26) guarantees that the ZMP belongs to the convex hull of the contact points  $p_i$  which, by definition, is equal to the support polygon.

On the other hand, if the ZMP belongs to the support polygon, there always exists a distribution of contact forces  $f_i$  at the points  $p_i$ , having positive components  $f_{i_z}$ , and such that the ZMP is the barycenter of the  $p_i$  weighted by the  $f_{i_z}$ . Note that, if the support polygon is defined by four or more contact points  $p_i, i \geq 4$ , the ZMP can be defined as the barycenter of the  $p_i$  with an infinite number of weight combinations  $f_{i_z}$ . In particular, one  $f_{i_z}$  can be negative. However, the necessary and sufficient condition insures that if the ZMP belongs to the support polygon, there always exists a distribution of forces  $f_i$  such that the ZMP can be written as the barycenter of the  $p_i$  weighted by positive normal components  $f_{i_z}$ .

Therefore, in the case of contact with a horizontal floor, the rigid contact condition defined by (3.26) is equivalent to the well known dynamic stability condition which requires that the ZMP belongs to the support polygon.

**Theorem 1:**

*if  $f_{i_z} \geq 0$  then  $ZMP \in SP(p_i)$ ;*

*if  $ZMP \in SP(p_i)$  then there exist a set of  $f_{i_z}$  that are all positive.*

#### 3.4.5 Generalization to multiple contacts

Eq. (3.19) only considers one body in planar contact. If more than one body is in contact, or if one body is in contact with more than one surface, several forces  $\phi_i$  have to be introduced for each couple plane-body in contact:

$$A\ddot{q} + b + \sum_i J_i^T \phi_i = S^T \tau \tag{3.34}$$

---

<sup>1</sup>Usually the foot is considered as a rectangle delimited by four vertices  $p_i, i = 1, \dots, 4$ , but any shape, delimited by three or more contact points, can be considered as well.

For each body in contact, the same reasoning can be applied separately. Support polygons and normal forces  $f_i^\perp$  have to be introduced. For each contact,  $f_i^\perp$  can be linked to the generalized force  $\phi_i$  with the same constraint (3.31), and the normal forces are constrained to be positive. For each contact  $i$ , we denote by (3.20. $i$ ) the non-motion constraint and (3.33. $i$ ) the positivity constraint.

Similarly, if several tasks are considered, we denote by (3.13. $j$ ) the constraint for each task  $j$ . Finally, the task-function formalism requires the system to be fully constrained to ensure its stability in the sense of Lyapunov (Lyapunov stability, [Samson et al., 1991]). A very last stage is then introduced to cope with the case of an insufficient number of tasks and constraints to fulfill the full-rank condition:

$$\ddot{q} = -K\dot{q} \tag{3.35}$$

Various full-rank constraints could have been considered (minimum acceleration, distance to a reference posture, etc). The choice of using the damping constraint is arbitrary.

Finally, the complete cascade for  $n$  contacts and  $k$  tasks is written: (3.19)  $\prec$  (3.20.1)  $\prec$  (3.33.1)  $\prec$  ...  $\prec$  (3.20. $n$ )  $\prec$  (3.33. $n$ )  $\prec$  (3.13.1)  $\prec$  ...  $\prec$  (3.13. $k$ )  $\prec$  (3.35), with the optimization variables  $u = (\tau, \ddot{q}, \phi_1, f_1^\perp, \dots, \phi_n, f_n^\perp)$ .

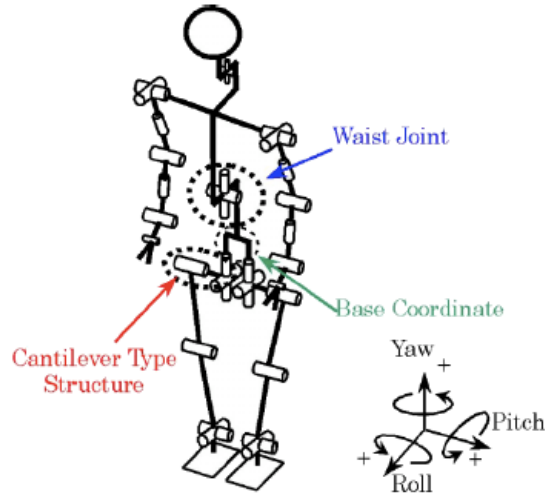
## 3.5 Experiments

This section presents different experiments that were conducted on the HRP-2 humanoid robot to validate our approach. However, as a torque-feedback control cannot be implemented on this robot, the experiments were performed in simulation at a sampling rate of  $1ms$ . We used the dynamic simulator AMELIF [Evrard et al., 2008] to resolve the direct dynamics and process the integration of  $\ddot{q}$ . The integration solver is a classical Runge-Kutta of fourth order. Our objective was to make the robot execute various tasks involving whole-body movements while keeping its dynamic balance. To this end, we selected three experimental protocols, including different kinds of constraints, that we expressed as sequences of tasks to be resolved by a QP cascade. The control law was integrated in the control framework SoT [Mansard et al., 2009b], using the dedicated solver [Escande et al., 2010] and applied on-line to the robot.

Besides showing that the proposed approach allows to perform complex dynamic movements on a humanoid robot, another objective of these experiments was to see if the simulated robot movement are resembling those of humans. The validation of realism of the

### 3. DYNAMIC MOTION GENERATION

---



Dimensions		Height: 1540 mm; Width: 620 mm
Mass (including batteries)		58 kg
Degrees of freedom		30 axes
Walking speed		0 – 2km/h
Hand grip		2 kgf (per hand)
Sensors	Torso	3-axes vibration gyro 3-axes velocity sensor
	Arms	6-axes force sensors
	Legs	6-axes force sensors
Motor drivers		48V 20A (I max) 2 axes/driver ×16
Power system		NIMH battery DC 48V 14.8Ah

**Figure 3.6:** The humanoid robot HRP-2 with its specifications.

motion and the resemblance with real human movements would enable us to take an initial step towards ergonomic analysis, in the perspective of reproducing human repetitive tasks and behaviors in different work stations.

Before discussing the different experimental setups, it is important to describe the humanoid robot HRP-2 which was the model used in our simulations.

#### 3.5.1 HRP-2: the humanoid robot

The humanoid robot HRP-2, represented in fig. 3.6 was developed by Kawada Industries in collaboration with the National Institute of Advanced Industrial Science and Technology (AIST)[Kaneko et al., 2004]. This robot is first modeled as a tree-like kinematic

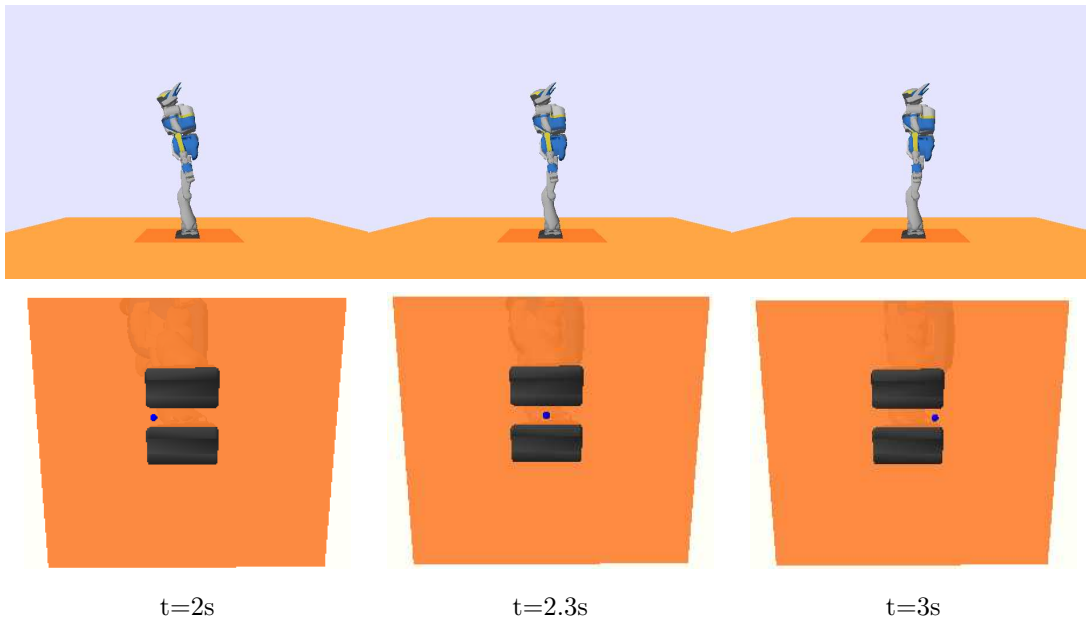


**Figure 3.7:** Experiment A: Top: Snapshots of the oscillatory movements at high frequency. Bottom: relative feet and ZMP positions at the corresponding time instants. The ZMP saturates on the front when the robot head is reaching its maximum amplitude and is breaking to go backward. Similarly, the ZMP nearly saturates on the back when the robot head is reaching its minimum amplitude and breaks to go forward.

structure including several single chains of bodies connected by revolute joints. The free-floating base, or the root of the robot, is considered at the waist. This model presents 30 DOF each one being a revolute joint controlled by one actuator. Each body in the model has a shape, a mass and an inertia matrix. The joint is characterized by the parameters  $q$ ,  $\dot{q}$  and  $\ddot{q}$  that determine respectively the position, velocity and acceleration of each body with respect to the parent body.

### 3.5.2 Experiment A: Swing posture

In the first experiment, we evaluate the possibility to reproduce with the robot a behavior that was previously observed in humans [Bardy et al., 2002]. It concerns the coordination of postural joints during a swinging movement induced by the tracking of a visual target.

#### 3.5.2.1 Description

During this task, the robot is standing up in double support in front of a visual target. A postural swing is obtained by only controlling the position and orientation of the robot

### 3. DYNAMIC MOTION GENERATION

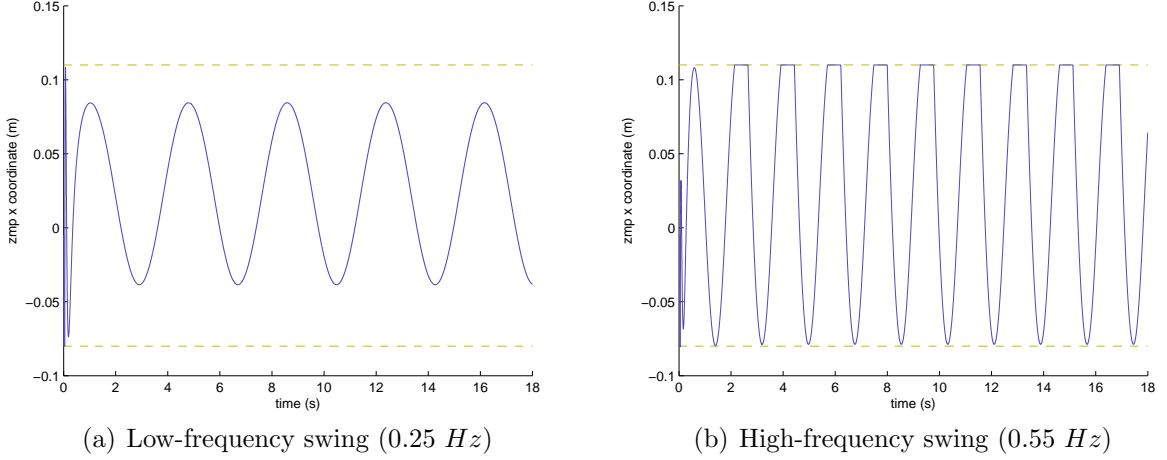


**Figure 3.8:** Experiment A: Evolution of the  $x$  coordinate of the ZMP during the low frequency 3.8(a) and the high frequency 3.8(b) tests.

head in order to track the target. For this motion, the tracking task which concerns the head motion is written under the form defined in (3.13). The task function  $e_{head}$  is defined as the error between the current and the expected head pose (position and orientation):

$$e_{head} = \begin{bmatrix} p - p^* \\ r\theta \ominus r\theta^* \end{bmatrix}, \quad (3.36)$$

where  $p$  and  $p^*$  are respectively the current and the reference position of a point in the head,  $r\theta$  and  $r\theta^*$  are respectively the current and the reference head orientation, and the symbol  $\ominus$  represents a distance operator in the matrix group. To ensure a proper convergence of this task function, the reference acceleration is designed as a proportional-derivative (PD) control law:

$$\ddot{e}_{head}^* = -\lambda_p e_{head} - \lambda_d \dot{e}_{head} \quad (3.37)$$

where  $\dot{e}_{head}$  is the velocity in the task space ( $\dot{e}_{head} = J\dot{q}$ ) and the gains  $\lambda_p$ ,  $\lambda_d$  allow to adjust the convergence velocity.

In addition to the task  $e_{head}$ , a torque limit constraint is added in order to enforce the limit values of the actuators. Since the torques are included in the vector of optimization variables, it is trivial to express the torque limits by a simple inequality equation constraining only these variables:

$$\underline{\tau} \leq \tau \leq \bar{\tau} \quad (3.38)$$

with  $\bar{\tau} = -\underline{\tau}$  the maximum torque value. The cascade of tasks then becomes: (3.19)  $\prec$  (3.20)  $\prec$  (3.33)  $\prec$  (3.38)  $\prec$  (3.37)  $\prec$  (3.35).

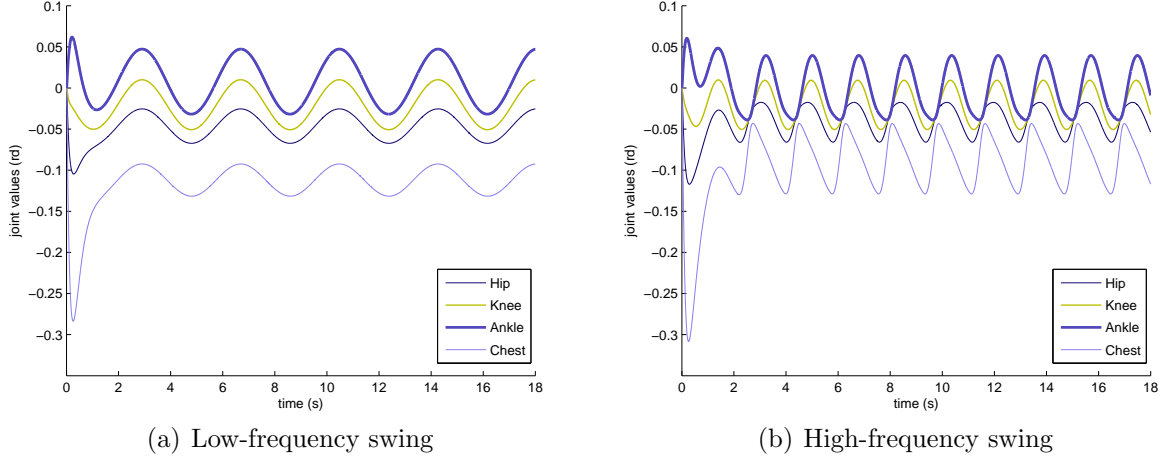


**Figure 3.9:** Experiment A: Trajectory of the ankle, knee, hip and chest joints during the postural swing generated by the tracking by the head of a target moving back and forth with an amplitude of 10 *cm* at two different frequencies.

In this experiment, the task function  $e_{head}$  was used to track a reference sinusoidal trajectory in order to generate a swing of the robot posture. Two reference movements of the target are successively considered. In both cases the target moves back and forth in front of the robot, along a sinusoidal trajectory of amplitude 10 *cm*, but the frequency differs. In the first test, called low frequency, the reference target oscillates at 0.25 *Hz*, whereas, in the second test, called high frequency, the target oscillates at 0.55 *Hz*.

### 3.5.2.2 Results

The experiment is summed up in figures 3.7 - 3.10. An overview is given in Fig. 3.7: the robot oscillates forward and backward to follow the target. The ZMP is computed and displayed as a point on the ground; it reaches the front limit when the robot is bending forward. Figure 3.8 shows the evolution of the ZMP in both low-frequency and high-frequency cases. At low frequency, the ZMP moves inside the support polygon without reaching the limits. However, at high frequency, the ZMP is saturated. As said upper, this saturation, if not written explicitly, is a direct consequence of constraint (3.33). The resulting joint trajectory during the low and high-frequency movements are respectively presented in figures 3.9(a) and 3.9(b). In both cases, the trajectories are mainly a sinusoid following the same phase and frequency than the head target motion. We could also observe that before attaining the steady state, a transient state occurs. In the low-frequency case, the amplitude of joint oscillations is maximum at the ankle and

### 3. DYNAMIC MOTION GENERATION

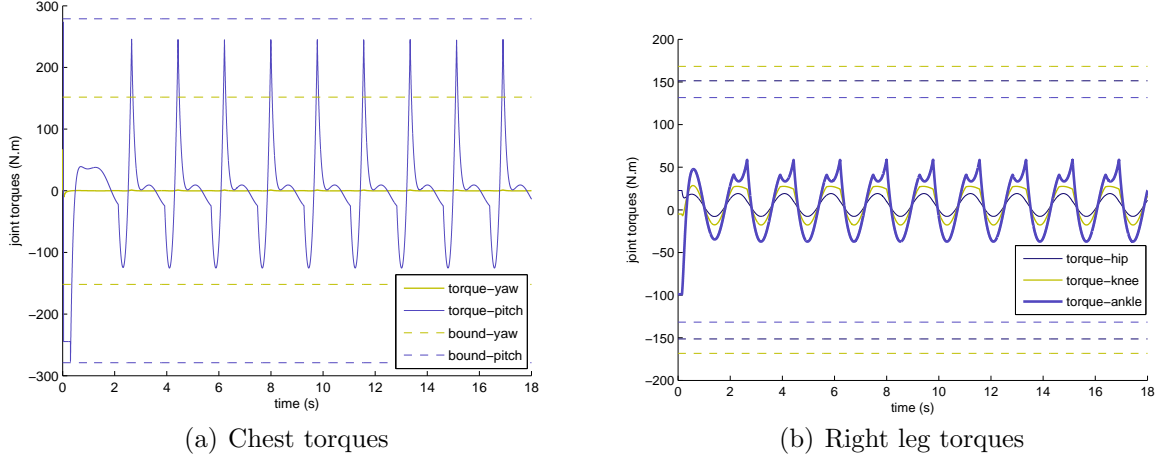


**Figure 3.10:** Experiment A: Joint torques variation during the whole experiment realized at high frequency with respect of the torque limit constraints on the chest 3.10(a) and the right leg 3.10(b) tests.

decreases progressively while moving up along the kinematic chain until the chest. In the high-frequency case, the amplitude of the in-phase joint oscillations still increases from the ankle to the hip. However, a certain relative phase between the ankle and the hip, and even a larger one between the ankle and the chest, appear. This shows that for high frequencies an anti-phase mode occurs. The anti-phase mode corresponds to the extra correction due to the ZMP saturation. Interestingly, these results are comparable to the ones observed in humans which are described in [Bonnet et al., 2008].

The torque values for the low-frequency case are a direct mapping of the joint trajectory: oscillation exactly at the same phase as the target motion. Figure 3.10 displays the torque values and limits for the high-frequency movement. Figure 3.10(a) shows the joints of the chest with clear efforts on the pitch joint which is the one constrained by the lateral swing motion. These torques reach periodic peaks due to the compensation of saturation of the ZMP. Actually, since the system does not allow anticipation or prediction, thus when the ZMP saturates, the acceleration of the chest suddenly increases which leads to the exertion of high torques. These values could be smoothed when the prediction is taken into account which is not easily applied in our case since we compute the joint trajectories instantaneously. In figure 3.10(b), the torques corresponding to the hip, knee and ankle joints are visualized with maximum effort at the ankle, then less effort at the knee, and finally with minimum effort at the hip. Similarly to the chest, which exerts small efforts on the yaw joint, the leg torques of the yaw joints are also small. Therefore,

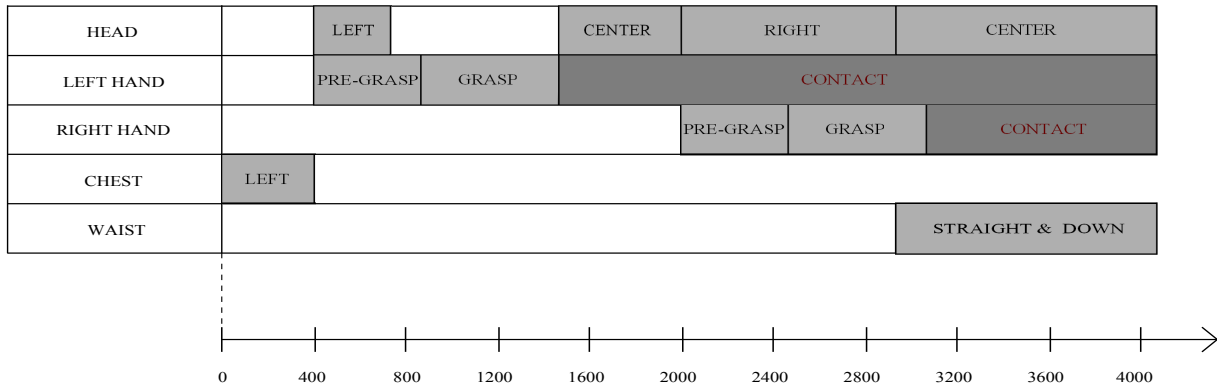


**Figure 3.11:** Experiment B: The sequence of tasks for the sitting experiment in terms of the iteration number which corresponds to the sampling period of  $1ms$ .

in Fig. 3.10(b), we show only the torques corresponding to the pitch joints of the hip, knee and ankle. The anti-phase movement due to the ZMP saturation is indeed clearer on the torque plot, since torques are directly linked with the ZMP. The chest is strongly used to stop the forward momentum when the ZMP reaches the limit. Once more, this is consistent with [Bonnet et al., 2008].

### 3.5.3 Experiment B: sitting in the armchair

The second experiment aims at showing that complex movements involving several non-coplanar contacts can be performed by using the proposed approach.

#### 3.5.3.1 Description

The scenario consists in making HRP-2 sit in an armchair, using the contact of hands with the armrests. Four bodies of the robot reach a contact during the motion: both feet are in contact with the ground and each hand comes in contact with the armrest located on its side. A contact surface of four points is defined for each contact: the sole of each foot, and the grasp surface inside the hands. Two different mathematical expressions are associated with the tasks: a first order Taylor development for the joint limits task and a classical PD law for the operational tasks which drives the motion of the end effectors as previously explained. The joint-limit constraints are imposed by a set of linear inequalities on joint positions. For a given state  $(q, \dot{q})$ , this constraint is equivalent to the linear inequalities

### 3. DYNAMIC MOTION GENERATION

---

on joint accelerations:

$$\underline{q} \leq q + \Delta T \dot{q} + \frac{\Delta T^2}{2} \ddot{q} \leq \bar{q} \quad (3.39)$$

where  $\underline{q}$  and  $\bar{q}$  represent the lower and upper joint-limits respectively, and  $\Delta T$  is the sampling period.

The task functions, the target points and the reference behavior are designed in order to achieve the successive steps of the sitting movement. Two classes of tasks are considered: the control of the pose (position and rotation) of an operational frame attached to one body and the direction of the gaze. Four operational tasks are used. To control the movements of the left hand and the right hand, the task functions  $e_{lh}$  and  $e_{rh}$  are respectively defined. For these two tasks, two references are successfully used: the pre-grasp (target point located above the armrest) and the grasp (contact point on the armrest). The task function  $e_{chest}$  is used to constrain the rotation of the chest. Finally,  $e_{waist}$  is introduced to control the orientation of the waist in the sagittal plane and its position along the vertical axis. A task  $e_{gaze}$  is also introduced to control the direction of the robot gaze using a 2D visual servo task B. It consists in moving the robot head to make the projection  $s$  of a specific point of the scene reach the center  $s^*$  of the image of the right camera:

$$e_{gaze} = s - s^* \quad (3.40)$$

Three points of the scene are successively visualized: the left and right armrests, and a point in front of the robot.

#### 3.5.3.2 Results

The experiment is summed up in figures 3.11 - 3.14. Figure 3.11 presents the time line of the motion, indicating when each task is added and removed from the stack. Basically, the motion is decomposed into three steps: look left and grasp the left armrest, then do the same on the right, then sit. At the beginning of the motion,  $e_{chest}$  is first added to the QP cascade when the chest is requested to turn to the left side. Next,  $e_{gaze}$  and  $e_{lh}$  are simultaneously resolved to control the gaze and the left hand reaching movement. When this manipulation task is achieved, the left hand contact is added, and the robot gaze is directed back toward the central reference point. Afterwards, the same gaze and reaching tasks are applied on the right side of the robot, with a final right hand contact. At the end, the robot gaze is once again driven toward the central point and the task  $e_{waist}$  is activated to move the waist down in order to achieve the sitting movement. The order of the tasks in the stack is determined according to the chronological order: first in, top

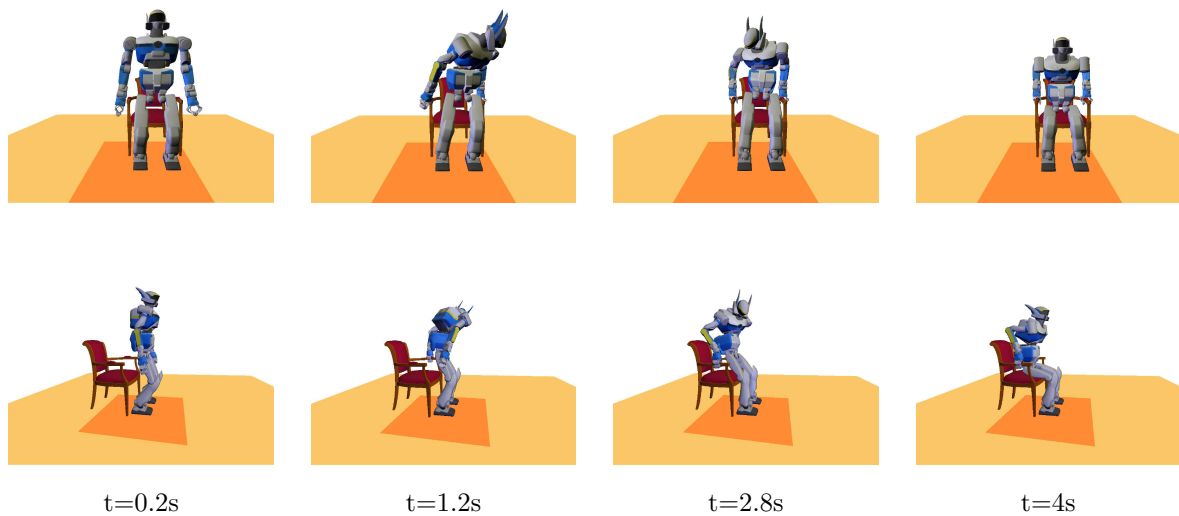


**Figure 3.12:** Experiment B: Front and side view of the sitting motion of HRP-2. These snapshots show respectively: the robot at the initial configuration; the position after one hand contact; the position after the second contact; and the final sitting position.

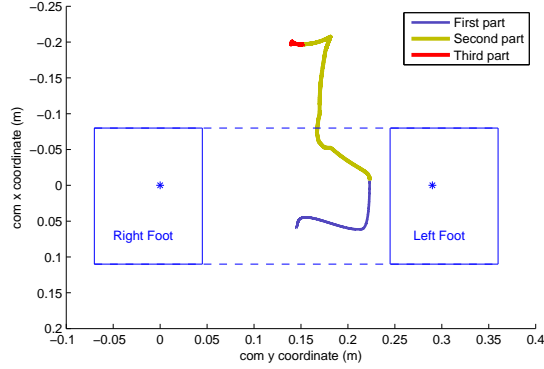
priority, with the joint limits constraint at the top priority. Note that during the whole movement, the center of mass (COM) is not constrained and remains free to move.

Figure 3.12 presents a chronological sequence of four snapshots of the movement of HRP-2 sitting in the armchair. As the dynamics is taken into account, the motion is naturally smooth, without having to consider any additional criterion. The robot keeps its dynamic balance while grasping the right armrest, having already one contact with the left hand.

Fig. 3.13 shows the projected COM trajectory on the ground. The trajectory is divided into three parts. At the beginning, the COM starts from a point in the middle of both feet, inside the support polygon. From the beginning of the second part, the contact points are no longer coplanar. Keeping the COM inside the contact polygon is a classical equilibrium condition, that cannot be applied as soon as the first hand reaches the contact. Similarly, the classical ZMP constraint cannot be considered to describe the balance, since it is not defined when the hands are in contact. Instead, the proposed approach does not constraint the COM, sparing the degrees of freedom, to make the motion smoother and to increase the space reachable by the robot.

Figure 3.14 presents a comparison of the motion obtained with and without accounting for the joint limits task (3.39) in the cascade. Figure 3.14(a) represents the evolution of

### 3. DYNAMIC MOTION GENERATION



**Figure 3.13:** Experiment B: Evolution of the position of the center of mass (COM) during the motion. The three phases which correspond to changes in the number of contact are displayed by different colors. In the first part only the feet are in contact, then the contact of the left hand is added, finally the right hand is also in contact.

the head joint. The joint limit is reached, but not violated, thanks to (3.39). The same sequence of tasks was run without the joint-limit constraint. The limit is violated when the constraint is not considered. The same applies for the left-hand joint, as shown in Fig. 3.14(b). In that case, some oscillation can be noticed due to an excessive gain on the joint limits task. The gain of each task can be either fixed or variable with the error. We can try to find a good tuning of the gain to avoid the oscillations. A description of the gain tuning is given in 5.3.2.

#### 3.5.4 Experiment C: 3D stepping

The aim of the third experiment is to show that the proposed dynamic motion generation method allows to stabilize the robot movement by adding a new contact when necessary. The motion corresponds to a dynamic 3D step from a stable 2-contacts configuration to a stable 3-contacts configuration.

##### 3.5.4.1 Description

In this last experiment the robot is standing up in front of a wall. First, it bends its trunk forward until reaching a non-statically stable configuration. Then, it stabilizes its movement by reaching out the wall with its left hand to create a rigid contact. A closed chain between the floor and the wall is then generated to stabilize the robot posture.

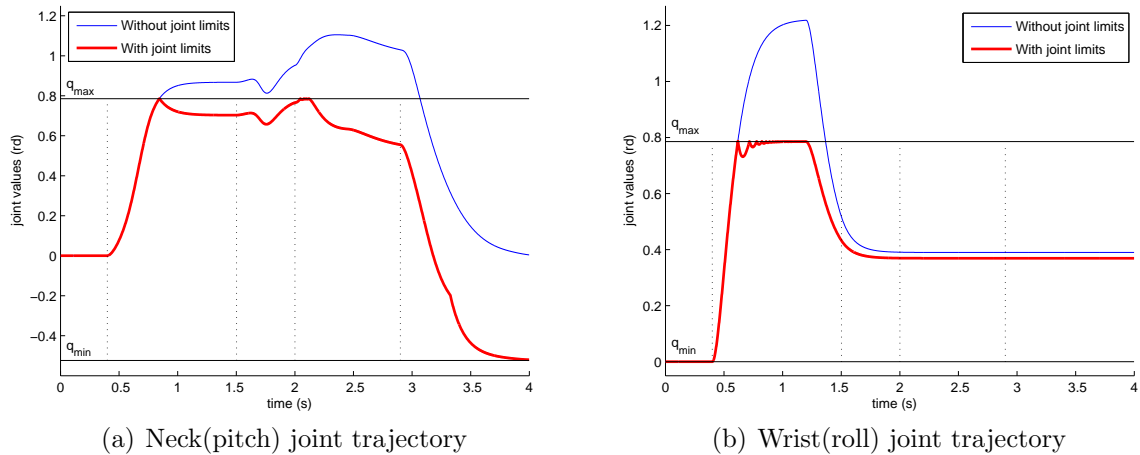


**Figure 3.14:** Experiment B: Joint angular variation with and without joint limits constraint

The movement is defined by the following sequence of tasks. At the beginning, the robot is in the usual half-sitting configuration. Two operational tasks are used to perform the movement:  $e_{chest}$  is used to control the chest position in order to make it lean forward, whereas  $e_{lh}$  is used to make the hand reach the expected position and orientation. Finally, the contact condition is added when the hand reaches the wall.

### 3.5.4.2 Results

The experiment is summed up in figures 3.15 - 3.17. Figure 3.15 gives an overview of the motion. Figure 3.16 describes the temporal setting of the proposed scenario. An initial phase was necessary at the beginning of the motion to change the configuration of the robot from the half-sitting position to a more suitable configuration before bending. Figure 3.17 shows the trajectory of the COM projection on the ground during the whole movement, knowing that this point was not constrained. Since the movement is highly constrained and the final posture is critical, the relaxation of the COM is important to extend the domain of accessibility of the robot. Indeed, as shown in Fig. 3.17 the projected COM starts between the robot feet and evolves continuously towards the front space following the motion of the upper body of the robot. If the COM stay unconstrained the robot would fall. Thus, a solution to gain stability is by stepping (with the hand) towards the wall. Because of non-coplanar contacts, the condition of stability cannot be expressed in terms of COM or ZMP positions. The only constraint is to preserve the

### 3. DYNAMIC MOTION GENERATION

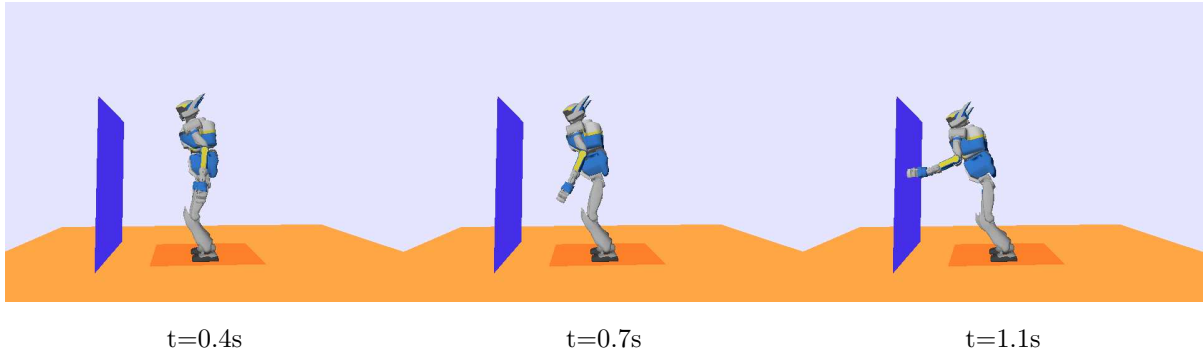


**Figure 3.15:** Experiment C: Snapshots of the 3D stepping movement starting from a double contact state then showing, the chest and the hand’s forward movement, and ending by the 3-contact configuration.

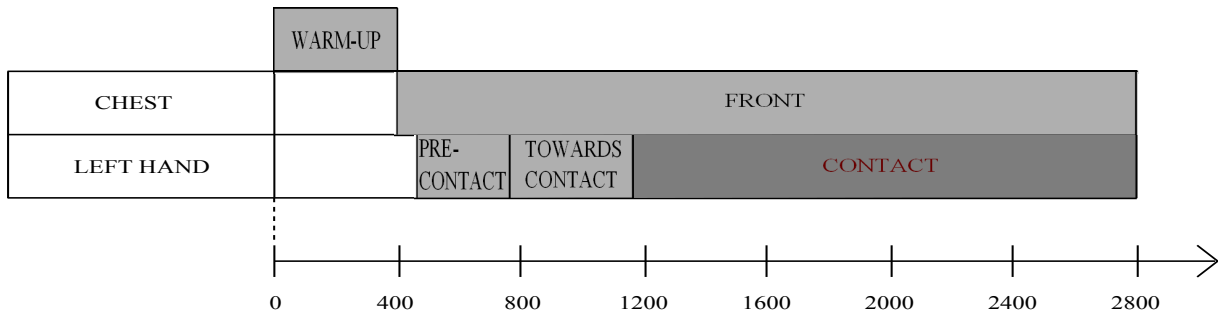


**Figure 3.16:** Experiment C: Timeline of the tasks involved in the bending experiment.

rigid-contact condition at the feet and at the left hand until the end of the movement and guarantee a stable configuration at the end.

Finally, the table 3.1 summarizes the computation time and real time for experiments A, B and C. For all the experiments, illustrating movies can be found at : <http://homepages.laas.fr/lisaab/tro-movies>.

## 3.6 Discussion

The results presented earlier show that the developed method is generic enough to generate the motion of a dynamic model while conserving stability. Moreover it allows to consider the contact of any body of the robot with any surface of the environment. The multiplicity of optimization variables gives the possibility to express different tasks and constraints at the operational level or at the joint level. Despite the complex nature of the problem

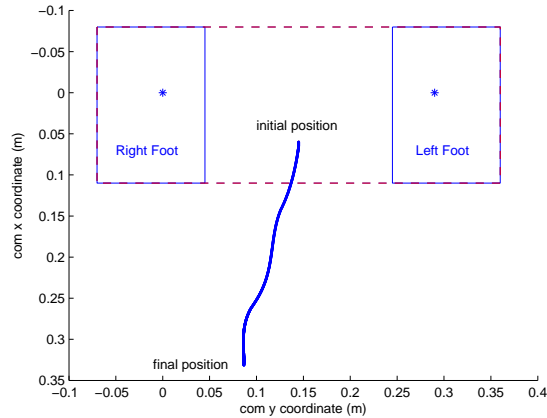


**Figure 3.17:** Experiment C: Trajectory of the projected COM on the planar ground.

**Table 3.1:** Computation time and real time of the experiments

Experiment	Number of iterations	Computation time	Real time
A	18000	9mn 37s	18s
B	4000	4mn 5s	4s
C	2800	1mn 06s	2.8s

formulation, there are still many points that need to be clarified or improved. First of all, the collision avoidance should be integrated in the set of constraints to ensure both no self-collision and no collision with the environment. As this point was not in our primary field of interest, we plan to consider it afterwards. However it could be easily implemented by computing the distance between 2 objects and preventing the shortest distance between them to become null. Second, the contact constraint is chosen to respect the case of rigid contact with no motion of the contact point, no sliding effect, and positive normal forces. Actually, the contact forces applied on the vertices of the contact surface are decomposed into 2 components: a normal force  $f^\perp$  and a tangential force  $f^\parallel$ . Thus, the forces that are necessary to hold a desired contact state e.g. prohibiting from possible detachment or sliding of the body in contact, should lie inside the Coulomb cone [Liu and Wang, 2005]. This constraint is written as:

$$\begin{cases} f^\perp \geq 0 \\ \|f^\parallel\|^2 \leq \eta^2 f^{\perp 2} \end{cases}$$

### 3. DYNAMIC MOTION GENERATION

---

where  $\eta$  is the friction coefficient. In our case, we only consider the first part of the force constraint which concerns the normal component of this force. Actually, in the case of HRP-2, as the friction coefficients are very high, the second part of the constraint is always respected. Then, we could guarantee that the contact force lies inside the Coulomb cone.

One restriction of this solver is imposed by the choice of the final stage task which is defined by the velocity damping task of (3.35). As described earlier, this task is introduced to get a full-rank constraint which controls the motion of the remaining free DOF, if any, to stop moving. More interesting constraints can be considered instead, as the minimization of torques which could lead to more natural behaviors.

Another important point to discuss is the effect of the transition between tasks when adding or removing tasks or contacts. Sometimes discontinuities appear and the motion is affected. Actually, this shows disturbances in the acceleration of the COM and consequently, the position of the ZMP. Although this does not disturb the resulting motion of the robot in simulation, it might cause trouble when playing the motion on the real robot. Possible solutions were suggested in section 3.5.4 to avoid this problem. This issue does not concern the real focus of this thesis since the main objective is to develop a human-like motion generation software that is easy to manipulate and for applications in human motion analysis.

This leads us to discuss about the fact of having developed an open loop control. For roboticists, it is usually important to apply a closed loop control relying on real feedback of sensors in order to rectify the motion. However, since the stability of the robot is taken into account during the whole motion in addition to joint and torque limits constraints, and as the disturbances that could occur are smoothed in case they appear, the generated motion could be directly applied on HRP-2.

Finally, from the computation point of view, the computation time is still a bit slow, but yet rather reasonable. The improvement of the computation time exceeds the scope of this work, but should be considered later on.

## 3.7 Conclusion

Based on a normalization of both inverse-kinematics and inverse-dynamics control schemes, a cascade of QPs was proposed to design the torque control while taking into account unilateral and bilateral constraints. A generic formulation of multi-contact constraints was also integrated into the approach. In particular, this formulation enables tasks with non-coplanar contacts generalizing stability conditions beyond the ZMP criterion. This

solution provides an efficient framework to generate motions in a wide variety of robotic tasks. The effectiveness of this novel formulation is illustrated through three experiments including various tasks, multi-contact, joint or torque limits.

### 3. DYNAMIC MOTION GENERATION

---

# 4

## Imitation and editing of dynamic motion capture using a stack of tasks

### 4.1 Problem definition

#### 4.1.1 Motion imitation

In robotics, generating motion by imitation has become an active research area during these recent years. The easiest way to make a humanoid robot behave like a human, is to simply copy human movements. The connoted simplicity is with regard to how much we need to understand the human movements in order to reproduce them. Even without requiring to understand these movements, motion imitation for a humanoid robot is more than just a straightforward transfer. Human motion imitation by a humanoid robot is a challenging task involving coordination, control and stabilization of the robot. This imitation paradigm that allows the robot to learn the way of performing a task by observing human demonstrations has been called *learning from observation (LFO)* [Nakaoka et al., 2007]. It was initially introduced for robotic manipulators with the name *assembly plan from observation (APO)* [Ikeuchi and Suehiro, 1994]. The challenges here arise due to the kinematic and dynamic disparity between the human and the humanoid. Moreover, coordination problems are inherent to kinematically redundant robots, as it is the case of humanoids. Control difficulties emanate from the complex tree-like structure of such robots, as well as their unstable nature due to their vertical position. The robot must not only reproduce some captured behavior, but it should not fall while performing the motion, keeping its dynamic balance. These constraints make imitation of captured motion a more complicated problem in robotics than in computer animation.

## 4. IMITATION AND EDITING OF DYNAMIC MOTION CAPTURE

---

A classical approach for motion imitation in computer graphics is inverse kinematics [Gleicher, 1998; Grochow et al., 2004] since the characters usually do not possess physical dynamic characteristics. The main tools are related to motion editing and retargeting [Yamane and Nakamura, 2003b]. Stéphane Ménardais [Ménardais, 2003] has proposed a software architecture for the rectification, combination and adaptation of captured motion. Richard Kulpa [Kulpa, 2005] proceeded with these implementations and included new functionalities of adaptation to kinematic, kinetic and dynamic constraints. This led to a motion simulation method called MKM for “Manageable Kinematic Motion” (MKM). One of the major interests of this approach is the use of an independent representation of the morphology to carry out almost all operations. Thus, independently from the subject on which the motion capture is done or the avatar to be animated, this method is an abstraction to the problems of adaptation which imply high computation time. MKM presented a possible way for defining models of movements capable of adapting to the environment while respecting at best the style contained in the original data. This approach gives systematically a link between the biomechanical analysis and its consideration in the kinematic model. To help conceiving such models, [Multon, 2006] have developed a tool for the definition of models, the “S4D Maker” to which a certain number of necessary constraints could be parameterized. One of the applications of these works is the animation of virtual avatars for interactive applications. For the generation of pre-computed animations, it is possible to use other approaches that take more computation time as for example the dynamic simulators. Some commercial software products have been developed to produce this type of operations and ensure the coherence with captured trajectories (for example, Endorphin of Natural Motion or the products of Havok company). For this type of application, MKM is more dedicated to animate secondary characters or crowds for whom it is desired to obtain intuitive and quick results. Accordingly, this type of approaches is adapted to simulated environments in which it is desired, for example, to test a spatial planning for a neighborhood or a building or to simulate the behaviors of users inside sub-stations to improve the quality of service. This requires a high number of characters to be animated simultaneously and interactive visualization. The adaptation method with MKM is able to resolve this issue, however it is necessary to develop a level of reciprocal coordination between the behaviors and the adaptation of captured motion. Even though sometimes dynamics is taken into account [Popović, 2000], its main objective is to give more realism to the animation rather than to make the motion feasible. The motion generated with computer animation methods is not guaranteed to be suitable for a direct reproduction on a robot.

Like a human, a humanoid robot has two hands, two legs, a torso, a head, etc. While the overall similarity can be quite convincing at first glance, the organization of how each joint moves with respect to the other, and by how much, is very different. Additionally, the number of DOF in a human's body exceeds even the most technologically advanced humanoids. This kinematic disparity is magnified by the fact that humans do not obey to standard shapes and sizes. Thus, any imitation framework has first to be intelligent enough to appropriately scale human motion and then map this motion onto the appropriate robot joints. The second problem is that of dynamics. Agility in humans is not only the ability to move fast, but doing so while maintaining dynamic balance at the same time. Walking and running are examples of dynamic movements, but humans are capable of a lot more. In the case of humanoid robots, often the dynamics of the system is simplified. A consequence of the relative mechanical and computational simplicity is that the humanoids of today are well behind human capabilities in terms of agility and dynamics. This brings us back to the problem of imitating human movements which are possibly beyond the dynamic capabilities of the humanoid. Several studies have tried to solve these issues in motion imitation using a variety of approaches, that will be presented in section 4.1.2.

In our work, we were particularly interested in a dynamic motion, precisely dancing, since it reveals dynamic movements. To this purpose, we propose to use a generic hierarchical optimization solver to consider simultaneously the dynamic reshaping and the motion editing. This solver consists of the inverse-dynamics control cascade proposed in chapter 3. The flexibility of the scheme allows the addition of arbitrary tasks in the operational space that modify the trajectory of the joints, to generate a more similar motion, or to change some part of it. This work is a part of a collaboration with a PhD student, Sovannara Hak, concerned by motion imitation for the transfer of the captured motion to kinematic joint data, and a master student, Oscar Ramos, for adapting the motion and resolving the technical issues [Ramos et al., 2011]. My contribution was in proposing the project, managing it and developing some parts, notably, producing the reference movements by motion capture and using the solver presented in chapter 3.

### 4.1.2 Motion editing

As mentioned previously, many researchers that were interested in replaying captured motion, were also interested in reshaping these data for more accuracy or generality. The starting point is usually the motion acquired from a human using a motion capture

#### 4. IMITATION AND EDITING OF DYNAMIC MOTION CAPTURE

---

system. The information gathered from a human motion capture system can further be organized into a database which can be used for categorization of motion based on human behaviors, and for the synthesis of robot motion [Yamane et al., 2011]. The database concept has been widely used for recognizing human motion and synthesizing humanoid motions. The information directly obtained from the motion capture system consists of a certain continuous representation (usually the position) of the markers without any explicit a priori knowledge about when a certain type of motion starts or ends. Databases for robotics applications are required for different usages as the classification of human motion into distinct behaviors, the recognition of behaviors of newly observed motion and the synthesis of a robot motion that adapts to the current situation. Motion capture data must then be organized so that the planner can effectively extract candidates of motions and/or configurations. The solution proposed by [Yamane et al., 2011] is to decompose the whole motion into primitives and establish the transitions between these primitives to generate a type of motion describing a behavior. The method consists in developing an efficient clustering algorithm [Ward, 1963] for dividing a set of sample frames into two descendant nodes to construct a binary tree from human motion data. Algorithms for basic statistical computations are based on the binary tree structure. Using these algorithms, it is possible to recognize a newly observed motion sequence, estimate the current state and predict future motions, and plan new sequences that satisfy given constraints. The purpose of that study is to dispose of a highly hierarchical data structure for human motion database.

Alternatively, optimization is a classical solution for reshaping the captured motion before imitation. For example, upper body motion is produced by solving a separate optimization problem for each frame of the motion in [Safonova et al., 2003]. A constraint that uses trajectory optimization and filtering to preserve the main characteristics of the original motion and to respect at the same time the physical limitations of the humanoid robot is proposed in [Ruchanurucks et al., 2006]. A similar approach is proposed in [Suleiman et al., 2008a] where the modifications improve the conformity of the movement with respect to the kinematics or/and the dynamics. In that work, the recorded motion was the one of a boxer which was outside the robot limits. The problem consists in minimizing the difference between the angular values of the humanoid robot's joints and those of the virtual actor, considering a dynamic model subject to joint and torque limits. This optimization is applied on the upper body of the robot, and a further control of the ZMP trajectory using the cart table model [Kajita et al., 2003] is applied to ensure

dynamic stability. Due to the physical limitations of a humanoid robot, the acquired motion can be slowed down to better fit these restrictions.

To benefit from the advantages of both approaches, the dynamic simulation and the adaptation of captured motion, some researchers found it interesting to couple both. Yamane and Nakamura [Yamane and Nakamura, 2003a] developed dynamic filters to be applied on kinematic trajectories. Others proposed to rectify the resulting movements from the motion capture by verifying specific mechanical laws as the respect of the gravity in the air phase [Pollard and Behmaram-Mosavat, 2000].

Real-time imitation adds an additional level of challenges that were tackled in the studies by [Dariush et al., 2008; Yamane and Hodgins, 2009; Montecillo-Puente and Sreenivasa, 2010]. Generally, robotic applications for motion imitation are wide and include industrial assembly [Ikeuchi and Suehiro, 1994], humanoid walking [Miura et al., 2009], yoyo playing [Mombaur and Sreenivasa, 2010], Chinese Kungfu [Zhao et al., 2004], etc. In particular, one of the interesting applications is the imitation of a dance. One of the pioneering works for robot dancing is described in [Nakaoka et al., 2003, 2004, 2005, 2007]. The humanoid robot HRP-2 imitated the complicated Japanese dance of Aizu-Bandaisan. Since the original dancing movements were outside the dynamic limits of the robot, the movements themselves were modified such that they conformed to the robot's limitations while still being close to the original template. For the upper body, the motion is directly reproduced, but for the lower body, it cannot be directly applied since the dynamics of a person and a robot are not the same. Thus, three tasks are defined in [Nakaoka et al., 2007] to present the legs behavior:

- *Step*: It can be applied to any leg and consists in lifting the swing foot and landing it back, with the support foot fixed. This task is detected by analyzing the trajectory of the foot.
- *Stand*: It consists in having both feet on the ground and is assumed to be present in those segments in which no step was detected.
- *Squad*: It consists in raising and lowering the waist and is detected by analyzing the trajectory of the waist.

Another Japanese dance was reproduced in [Shiratori et al., 2007] with modifications to the upper body motion. In the same field of application, another sequence of motion resembling a dance was presented in [Pollard et al., 2002]. The captured joint trajectories were adapted to generate a feasible motion by the robot.

## 4. IMITATION AND EDITING OF DYNAMIC MOTION CAPTURE

---

After discussing some important existing techniques developed for editing captured motion, it is time to present the method adopted in this work for transferring the motion on the robot and realizing a satisfactory imitation. Knowing that the collected data from the motion capture tool, is simply geometrical, and since we are concerned with the dynamics and realism of the motion, two phases need to be realized. First, the kinematic adaptation, in order to apply the motion on the humanoid robot. Second, the dynamic processing of the motion for ensuring the stability of the robot and then editing the motion by defining multiple prioritized tasks using the stack of tasks by resolving a cascade of dynamic QPs. This chapter is organized as follows. In section 4.2, we describe the motion capture device available in LAAS for recording the movements. Section 4.3 presents the method used to reshape the observed human motion to the robot kinematics using an optimization algorithm. The tasks used for motion imitation and editing, that are integrated in the dynamic solver, are introduced in Section 4.4. The results obtained in simulation for the humanoid robot HRP-2 imitating a dance motion are presented in Section 4.5. Finally, a conclusion of this contribution is given in section 4.6.

### 4.2 The motion capture system description

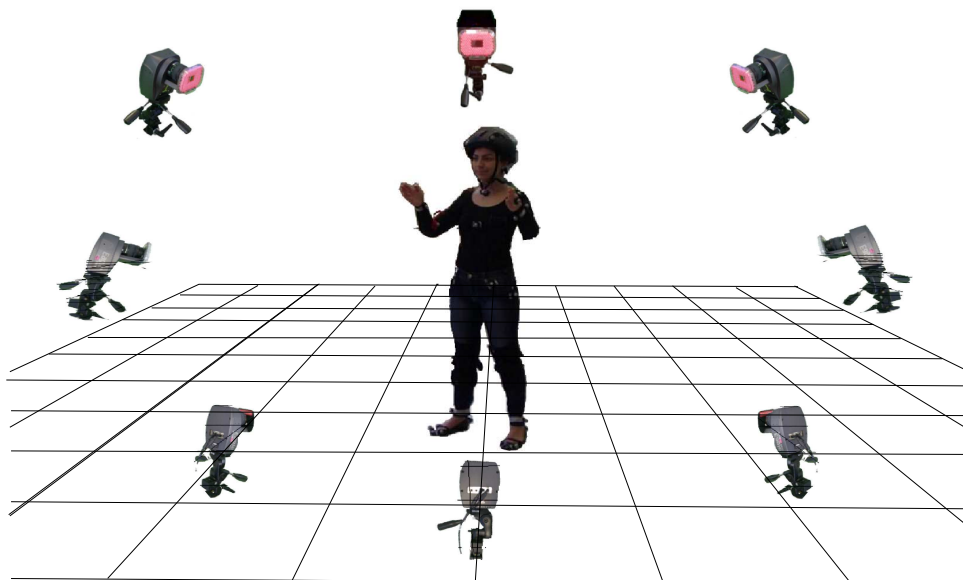


**Figure 4.1:** Motion capture system with infra-red cameras and markers.

Before transferring the human movements to the humanoid robot and realizing the imitation, we need first to record these movements. In this section, we will introduce the

## 4.2 The motion capture system description

---

tool that was used for the motion capture.

Actually, there are many ways for recording the movements of a human. Several options exist in this regard and the final choice depends on the intended accuracy, recording environment, ease of instrumenting the participants etc. Probably the least intrusive of these options is the reconstruction of motion from video cameras, for example that was used in the studies by [Dariush et al., 2008]. The advantage here is that one can simply record a person's movements without having to modify the hardware or outfitting the actor with special equipment. Of course the downside is the difficulty in computing individual joint rotation angles and the associated errors in position accuracy. At the other end of the spectrum, is completely instrumenting a human using Inertial Measurement technology (IMU). Recent technological and algorithmic advances in using IMUs allow them to be used with relatively low drift over extended periods of time. Specialized suits with embedded IMUs can be used to record accelerations and rotation rates of human joints. The motion can then be reproduced in real-time, for example the Xsens inertial motion capture suit [Roetenberg et al., 2009]. However, outfitting many participants in an experiment may be a time consuming and cumbersome process, as would be finding the correct suit sizes.

A popular form of motion capture is based on recording the distinct infrared signature of reflective markers. Our choice is made on this tool since it is available at LAAS. This infrared-camera based motion capture system is able to reconstruct the 3D motion of a set of marked bodies with a high frequency and a very good accuracy. These bodies can constitute a bigger entity and the whole motion thus becomes very complex. Using several cameras (usually 6+) are used to estimate the 3-D position of the markers. These markers can be a part of special suits or just attached to the bare skin or clothes of a human. Cameras specially equipped with infrared filters track the movement of these markers. Fig. 4.1 shows an illustration of the motion capture setup. In order to identify specific markers, we have to pre-define partial or complete skeletons consisting of fixed length joints. The system then uses this initial template to match the current marker data with the correct pose of the skeleton. For tracking non-human data we can also define models corresponding to rigid manipulable bodies (sticks, balls, boxes etc). This technology has already found extensive use in medical diagnosis and popular public mediums like movies, video games and virtual reality applications. The drawbacks of motion capture are a substantial initial investment in time and infrastructure. Additionally, the recordable area is limited by the space enclosed within the cameras. But most research on human gait uses relatively small movement space (in the order of several meters) and requires

## 4. IMITATION AND EDITING OF DYNAMIC MOTION CAPTURE

---

repeated measurements. Thus, the ease of infrared-camera based motion capture and the advantages it offers have made it the favored choice among many gait research studies. In the motion capture experiments conducted as part of this thesis, we use 10 infrared tracking cameras (MotionAnalysis, CA, USA) to record the motion. The accuracy of marker positions was about  $2mm$  and the recording rate was  $200Hz$ . Motion was streamed online or stored offline using the software Cortex (MotionAnalysis, CA, USA). During the recording of human movements via motion markers, it is possible to lose some data due to self-occlusions. In offline applications, this is generally acceptable and motion can be recovered using specialized methods like 3-D spline interpolation.

The capture and analysis of motion is an active research area due to its complexity and potential applications [Moeslund et al., 2006]. The capture of whole-body human motion is an example of this complexity and as we said, we choose to imitate a dynamic dance motion. The difficulty of reproducing exactly the captured motion on humanoid robots, in particular HRP-2, leads us to search and adopt editing techniques. The inverse dynamics control scheme described in chapter 3 will be used to reproduce a dynamically consistent motion of the robot. The contribution of this work is to propose a complete methodology to quickly reshape a dynamic motion demonstrated by a human expert, and to adapt the dynamics of the human body to the robot body own dynamics. In the next section we will describe the first step of transforming the data into kinematic trajectories that could be transferred on the robot.

### 4.3 Kinematic adaptation of captured motion

#### 4.3.1 Multibody motion acquisition

As described earlier, our motion capture system is a 10-camera with marker tracking system [Motion]. A set of 35 markers is usually used for recording the data of the human. The motion capture system provides the 6D pose of a set of unconstrained bodies in space, typically the limbs of the demonstrator. From these data a virtual skeleton that matches the kinematic hierarchy of the robot is built. For the set of 6D pose, we need to recompute the joint position of the demonstrator, knowing its geometric model. This is achieved by solving a nonlinear optimization problem, which will be described in paragraph 4.3.1.1, and where the geometric model of the demonstrator is known, and the joint position is the optimization variable. The number of markers is not directly related to the number of joints in the skeleton since a subset of markers can be used to gather

**Table 4.1:** Segments and Nodes Hierarchy.

Segment	Parent node	Child node
Right Hip	waist	Rleg1
Right Thigh	Rleg1	Rleg2
Right Leg	Rleg2	Rfoot
Left Hip	waist	Lleg1
Left Thigh	Lleg1	Lleg2
Left Leg	Lleg2	Lfoot
(Same node)	root	waist
Abdomen	waist	chest
Thorax	chest	head
Right Shoulder	chest	Rarm1
Right Forearm	Rarm1	Rarm2
Right Arm	Rarm2	Rhand
Left Shoulder	chest	Larm1
Left Forearm	Larm1	Larm2
Left Arm	Larm2	Lhand

robust information of a single joint. The output obtained from the motion capture system for each node  $m_j$  attached to each body of the geometric model, consists of the 6D pose:  $W_m[T_{xi} T_{yi} T_{zi} R_{xi} R_{yi} R_{zi}]$  representing the translation and orientation with respect to the motion capture system's reference frame that will be referred to as  $\{W_m\}$ . For the position, Cartesian coordinates (in mm) are obtained and for the orientation, roll, pitch and yaw angles (in degrees) are given. This output defines a coordinate system for each node. The skeleton is represented by links joining the parent and child node, as shown in Table 4.1. The waist is considered as the root and all the segments are defined with respect to it.

### 4.3.1.1 Kinematic optimization problem formulation

Having to deal with two different models, one corresponding to the subject and the other to the robot, we will define each one by a tree of bodies and nodes. Each node represents a frame attached to the body at the level of the markers position in case of the subject model, denoted by  $m_j$ , and at the level of the center of the joint in case of the robot, denoted by  $r_j$ ; with  $j \in \{1, \dots, m\}$  nodes. The robot's forward kinematics (or the geometric

#### 4. IMITATION AND EDITING OF DYNAMIC MOTION CAPTURE

model) gives the pose of each body with respect to the robot's world reference frame  $\{W\}$ , denoted by the transformation matrix  ${}^W T_{r_j}(q)$  which is a function of the joint vector  $q$ . Whereas, the motion capture system gives the 6D pose of the body  $m_j$  during the whole movement represented by  ${}^W \tilde{T}_{m_j}(t)$ . This is illustrated in figure 4.2. Then, the problem of finding the suitable joint values  $q^*(t)$  for the robot at a time  $t$  can be reduced to minimizing the difference between these transformation matrices as:

$$q^*(t) = \arg \min_q \sum_j^m \| {}^W \tilde{T}_{m_j}(t) \ominus {}^W T_{r_j}(q) \|^2 \quad (4.1)$$

$$s.t. \quad \underline{q}_i \leq q_i \leq \overline{q}_i \quad (4.2)$$

where  $\underline{q}_i, \overline{q}_i$  are the minimum and maximum angular values of a joint  $i$ , respectively, for  $i \in \{1, \dots, n\}$ . We used a weighted norm of the translation-axis-angle vectorial writing of the transformation matrices given as follows. The homogeneous matrices are expressed as:

$${}^W \tilde{T}_{m_j}(t) = \begin{bmatrix} \tilde{R}_{m_j}(t) & \tilde{p}_{m_j}(t) \\ 0 & 1 \end{bmatrix} \quad (4.3)$$

$${}^W T_j(q) = \begin{bmatrix} R_{r_j}(q) & p_{r_j}(q) \\ 0 & 1 \end{bmatrix}, \quad (4.4)$$

where  $R$  and  $p$  represent the rotation and translation part respectively. For the part corresponding to the position, the difference to minimize is directly represented by the  $L2$  norm as  $\| \tilde{p}_{m_j}(t) - p_{r_j}(q) \|_2$ . For the orientation part, the difference is measured by the rotation angle  $\theta_i$ , which is obtained by using the axis/angle representation of the product  $R_{d_i} = R_{r_j}(q) \tilde{R}_{m_j}(t)^{-1} \in SO(3)$ . When the rotation matrices are close to each other, the angle of  $R_{d_i}$  about the arbitrary axis is very small and  $R_{d_i}$  is close to the identity matrix. Representing the product of the rotation matrices as:

$$R_{d_i} = \begin{bmatrix} n_x & o_x & a_x \\ n_y & o_y & a_y \\ n_z & o_z & a_z \end{bmatrix} \quad (4.5)$$

the angle will be:

$$\theta_i = \text{atan2}(s_a, c_a) \quad (4.6)$$

where

$$s_a = \frac{\sqrt{(n_y - o_x)^2 + (n_z - a_x)^2 + (o_z - a_y)^2}}{2} \quad (4.7)$$

$$c_a = \frac{n_x + o_y + a_z - 1}{2}. \quad (4.8)$$

### 4.3 Kinematic adaptation of captured motion

The angle  $\theta_i$  is always between 0 and  $\pi$ . Finally, the operator  $\ominus$  in (4.1) is given by:

$${}^W\tilde{T}_{m_j}(t) \ominus {}^W T_{r_j}(q) = w_{p_i} \| \tilde{p}_{m_j}(t) - p_{r_j}(q) \|_2 + w_{o_i} \theta_i \quad (4.9)$$

where  $w_{p_i}$  is the weight corresponding to the position part of the joint  $i$  and  $w_{o_i} = 1 - w_{p_i}$  is the weight for the orientation part. These weights are included to provide more flexibility to the model and are experimentally determined to give more priority to one of the parts.

The  ${}^W T_{r_j}(q)$  should be computed from the geometric model of the demonstrator. In our case, we used directly the model of the robot to compute  ${}^W T_{r_j}(q)$ . The optimization method has proved to be robust enough to handle the approximation, and the dynamic solver is sufficient to recover all the resulting noise and inaccuracy.

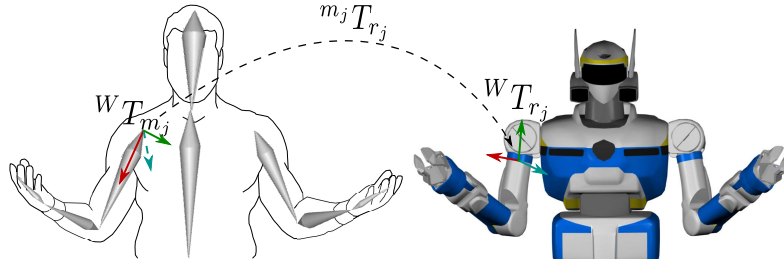


**Figure 4.2:** Transformation of the nodes from the human reference frame to the robot's frame.

#### 4.3.1.2 Calibration of the body frame

In equation (4.1) it is supposed that the same frames are used to express both the motion capture observation and the geometric model. This is of course not the case in practice, since the motion capture system uses its own arbitrary frames to express the multi-body motion. Then the observation of the motion capture has to be reformulated in the proper frame. To this end, the person whose motion has to be captured starts with a position that is well known for the robot. Using this known configuration, the transformation matrices between each node  $m_j$  of the subject and the corresponding node  $r_j$  of the robot is obtained as a “calibration” step and represented by  ${}^{m_j} T_{r_j}$ , which remains constant during all the process, as long as the markers do not have relative motion with respect to the body they are attached to. The matrix  ${}^{m_i} T_{r_j}$  includes the differences in orientation between the frames attached to the markers and the frames defined in the forward kinematics for each joint, as well as the differences in segment lengths between the robot and the dancer. Another matrix that is obtained during the calibration process is the one relating the

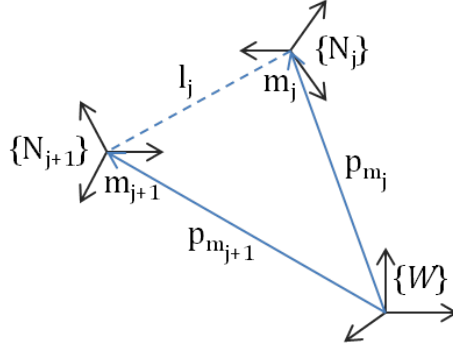


**Figure 4.3:** Orientation of nodes and links.

reference frame of the motion capture system  $\{W_m\}$  and the robot's reference frame  $\{W\}$  represented by  ${}^W T_{W_m}$ . Let the position and orientation of each node  $m_j$ , with respect to the motion capture reference frame, be represented by the homogeneous transformation  ${}^{W_m} T_{m_j}(t)$ , which varies in time according to the motion of the dancer. Then, to express the reference transformation in the robot's world frame we apply the following change of coordinate system:

$${}^W \tilde{T}_{m_j}(t) = {}^W T_{W_m} {}^{W_m} \tilde{T}_{m_j}(t) {}^{m_j} T_{r_j} \quad (4.10)$$

### 4.3.2 Virtual skeleton for motion validation

To verify the results of the kinematic optimization process, a skeleton model that reproduces the motion obtained from the motion capture system in the virtual environment of the robot was implemented. Let  $m_j$  represent the  $j$ -th parent node,  $m_{j+1}$  its children node and  $l_j$  the link joining both nodes. As figure 4.3 shows, the orientation of each node is not related to the link that joins them, but the direction of that link can be obtained as  $p_{l_j} = p_{m_{j+1}} - p_{m_j}$ , where  $p$  is the position with respect to the world reference frame. In the virtual environment used for the robot, the elements are specified by their position and orientation in roll-pitch-yaw angles, and even though  $p_{l_j}$  represents the orientation of the link, it cannot directly specify the needed orientation angles.

To obtain these angles, a fictitious frame having its  $X$  axis coincident with the direction of  $p_{l_j}$  is introduced. Such a frame is fully described by a rotation matrix  $R_{l_j} \in SO(3)$  whose columns constitute an orthonormal basis in  $\mathbb{R}^3$ . To this end, the Gram-Schmidt process was used. The initial basis is  $\{v_1, v_2, v_3\}$ , with  $v_1 = p_{l_j}$ , and  $v_2, v_3$  being random vectors. The orthonormalization process gives a new orthonormal basis  $\{e_1, e_2, e_3\}$  that can be directly used as the columns of  $R_{l_j}$ . The first vector is directly obtained as  $e_1 = \frac{v_1}{\|v_1\|}$ .

### 4.3 Kinematic adaptation of captured motion

For the second vector, first  $u_2 = v_2 - (v_2 \cdot e_1)e_1$  is obtained and then  $e_2 = \frac{u_2}{\|u_2\|}$ . For the third vector,  $u_3 = v_3 - (v_3 \cdot e_1)e_1 - (v_3 \cdot e_2)e_2$  and  $e_3 = \frac{u_3}{\|u_3\|}$ . Using this basis, the fictitious frame describing the link  $l_i$  is represented as

$$T_{l_i} = \begin{bmatrix} e_1 & e_2 & e_3 & p_{l_i} \\ 0 & 0 & 0 & 1 \end{bmatrix} \quad (4.11)$$

from which the needed roll, pitch and yaw angles can be computed.

The implemented skeleton, in the same environment of the robot, is shown in Figure 4.4. From our observations, we realize that the dimensions of the robot and the

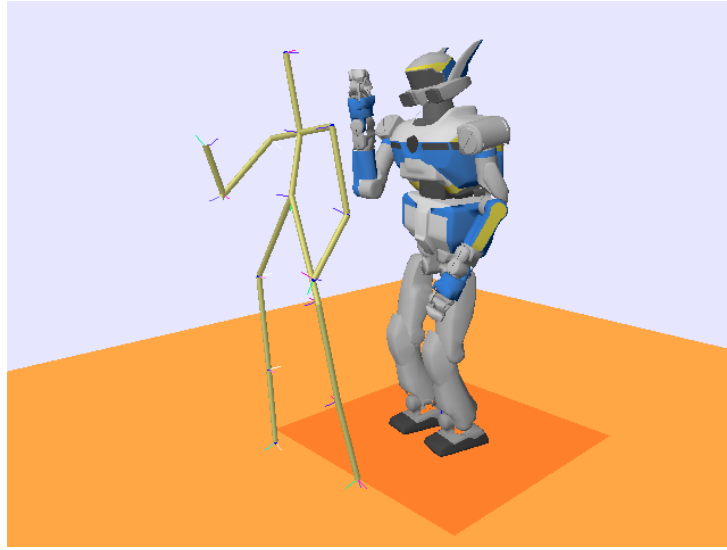


**Figure 4.4:** Robot model and the skeleton created with the motion capture data.

skeleton are not the same as the model of the demonstrator. The skeleton shown was built up by using directly the matrices  ${}^W_m\tilde{T}_{m_j}(t)$ . There is an offset between the two models as the world frame for the motion capture is not the same as the world frame for the robot. The matrix  ${}^{m_j}T_{r_j}$  maps the nodes of the motion capture system to the ones of the robot. However, the method described in this section can also be applied by taking into account for the differences between the nodes of the model and the joints of the robot, if the matrix  ${}^{r_j}T_{m_j}$  relating them is also considered.

#### 4.3.3 Kinematic reshaping and imitation of motion by HRP-2

While observing the motion of the real dancer, we detect that it includes movements of the head and chest laterally (around the x-axis), which are not feasible by HRP-2 N.14

#### 4. IMITATION AND EDITING OF DYNAMIC MOTION CAPTURE

---

since it does not possess the corresponding degrees of freedom at the head and chest. To overcome this problem and to reproduce the motion more precisely, it was decided to add 2 additional DOF to the model, one for the head and the other for the chest. Thus, the model considered for the study presented in this chapter has 32 DOF but used HRP2 N.14 as a reference. This model will be referred to as the *augmented* HRP-2 N.14 model. Even though this is physically not possible on the real HRP-2, it could be physically implemented on a robot having these capabilities, like HRP-4 [Kaneko et al., 2009].

The results of the kinematic optimization process in the augmented model of HRP-2 are shown in figure 4.5. It is noted that, since there are no contact constraints, the

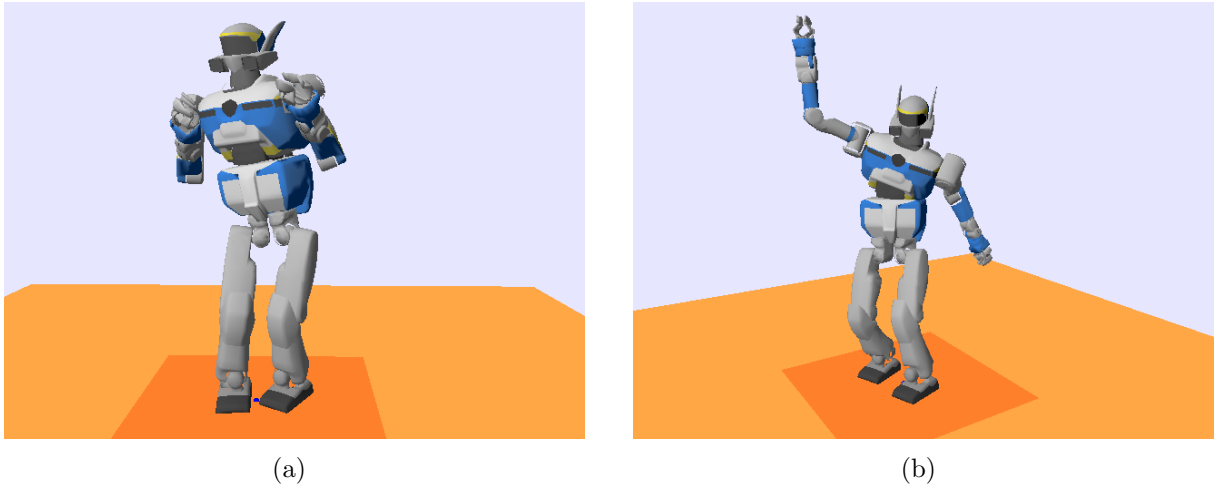


**Figure 4.5:** Results of the kinematic optimization.

feet are not restricted to stay in contact with a certain point of the ground but they can move freely within the ground plane to yield a better optimization of their position and orientation and eventually “compensate” the errors in some other nodes, due to the complexity and variety of the motion. These feet motions are also due to the real motion of the dancer that did some involuntary feet motions according to the music or sliding movement of one the feet. Figure 4.5(a) shows clearly an unwanted rotation of the left foot and figure 4.5(b) shows both feet having the same relative orientation but being not properly oriented with respect to the reference frame.

## 4.4 Dynamic processing of motion

As explained, the robot's dynamic model differs from the human's one. Moreover, the motion that was recovered using only kinematic methods, does not necessarily guarantee the stability of the robot. As a result, the robot can fall down trying to follow directly the joint trajectories obtained, if no dynamic modeling is adopted. In addition to that, the executed dance is an example of a very dynamic and complex motion where the arms movements can easily destabilize the robot when the dynamics is not considered. This is the reason why the motion obtained with the kinematic optimization was further "validated" dynamically using the cascade scheme represented in chapter 3. The objective is to reproduce the dancer's motion and at the same time to satisfy the restrictions imposed by the dynamics of the robot. To this end, a global posture task was implemented using the angular trajectory given by the motion capture as the reference to be followed by the robot. The contact constraints with the ground were added at each foot, since mainly, the motion was executed in double support. This satisfies the dynamic stability criterion. The cascade of QP is then formulated based on our developed solver. As we progress in the dynamic generation of motion and as we get results, more operational tasks are added to better accomplish the imitation of the dancer's motion and eventually to include some additional movement. For the purpose of imitation and editing, we have mainly used four types of tasks:

- The first task regulates the posture (actuated part of the robot configuration) to follow the motion of the demonstrator.
- The other tasks were used to edit the motion and to include respectively: the control of the position and orientation of an operational point, the control of the trajectory of a particular joint, and the control of the position on the ground plane of one foot for sliding.

These tasks are described in detail here below.

### 4.4.1 Posture Task

The desired trajectory for the joint angles is obtained using the motion capture system (as explained in section 4.3.1.1). This acquired motion can be directly replayed on a human-like character used in the field of computer graphics. However, it is not straightforward to regenerate the data by a robot as it does not consider the dynamic model or the

#### 4. IMITATION AND EDITING OF DYNAMIC MOTION CAPTURE

---

constraints associated with it. In this case, the inverse dynamics control scheme can be used as it considers the contact constraints and the dynamic stability conditions. More precisely, a task that follows the joints evolution as closely as possible while satisfying the prior dynamic conditions is implemented and will be called the *posture task*. Let  $q_{jk} = (q_j, \dots, q_k) \in \mathbb{R}^{k-j+1}$  with  $k, j \in \mathbb{N}$ ,  $1 \leq j \leq k \leq n$  represent the vector containing the angular values that need to be controlled, and  $q_{jk}^*$  the corresponding desired configuration. A posture task is expressed as  $e = q_{jk} - q_{jk}^*$ . At the velocity level, this will lead to  $\dot{e} = J_{jk}\dot{q}$  with the Jacobian  $J_{jk} \in \mathbb{R}^{(k-j+1) \times (6+n)}$  selecting only the desired joints:

$$J_{jk} = \begin{bmatrix} 0_{(k-j+1) \times (6+j-1)} & I_{k-j+1} & 0_{(k-j+1) \times (n-k)} \end{bmatrix} \quad (4.12)$$

where  $I_{k-j+1} \in \mathbb{R}^{(k-j+1) \times (k-j+1)}$  is the identity matrix and  $0_{k_1 \times k_2} \in \mathbb{R}^{k_1 \times k_2}$  are zero matrices. In the special case of controlling all the actuated joints, the identity matrix will have its largest size, lying in  $\mathbb{R}^{n \times n}$ . Finally, the reference acceleration is given as a tracking of the joint trajectory obtained by the motion capture system, using a PD controller:

$$\ddot{q}_{jk} = -\lambda_p(q_{jk} - q_{jk}^*) - \lambda_d(\dot{q}_{jk} - \dot{q}_{jk}^*) \quad (4.13)$$

with  $\lambda_p$  the proportional gain and  $\lambda_d$  the derivative gain, allowing to adjust the convergence velocity.

The posture task was split into separate parts to give more freedom in the choice of the PD gain for each part of the body. Table 4.2 shows these parts as well as the joints implied in each one. There is an overlap between the arms and the grippers but those

**Table 4.2:** Joints for the posture tasks using the augmented HRP-2 model.

Part	Joints
Right Leg	1-6
Left leg	7-12
Chest	13-15
Head	16-18
Right Arm	19-25
Left Arm	26-32
Right Gripper	25
Left Gripper	32

tasks are never performed simultaneously. The task for the grippers is usually added when the arm posture task is removed and an operational space task is executed instead.

When only the joints are to be directly followed, all the tasks presented in Table 4.2 are used, except the ones corresponding to the grippers.

#### 4.4.2 Addition of arbitrary tasks

The posture task reproduces the desired motion at the joint level satisfying the dynamic constraints. However, the PD acts as a low-pass filter, generating non desired movements at some points or erasing some delicate or very dynamic movements, typically due to fast oscillatory motions. Nevertheless, the structure of the stack of tasks can be used to overcome this problem by adding operational tasks that enhance or even modify the original motion. Moreover, the priorities of the tasks can be modified to better achieve the desired motion.

An operational task controls directly the position and/or orientation of different operational points. In our case, we consider the head, chest, waist, feet and hands of the robot as the controlled end-effectors. Each operational point  $x_i = (p_{ix}, p_{iy}, p_{iz}, \varphi_{ix}, \varphi_{iy}, \varphi_{iz}) \in \mathbb{R}^6$  is expressed in Cartesian coordinates to specify its position and the roll, pitch, yaw angles for its orientation. Despite this 6D representation, we are free to control either both position and orientation, or only some axis of interest. For this sake, a diagonal selection matrix  $S_x$  is defined as:

$$\begin{bmatrix} s_1 & 0 & 0 & 0 & 0 & 0 \\ 0 & s_2 & 0 & 0 & 0 & 0 \\ 0 & 0 & s_3 & 0 & 0 & 0 \\ 0 & 0 & 0 & s_4 & 0 & 0 \\ 0 & 0 & 0 & 0 & s_5 & 0 \\ 0 & 0 & 0 & 0 & 0 & s_6 \end{bmatrix} \quad (4.14)$$

where  $s_j$  is a binary, 1 or 0, the former one to control that particular element of position or orientation, and the latter one to leave it unconstrained. Thus, the differential relation is expressed as:

$$S_x \dot{e}_i = S_x J \dot{q} \quad (4.15)$$

and the reference  $x_i^*$  to be followed only considers the controlled elements of position and/or orientation, with  $e_i = x_i - x_i^*$ .

We use this operational task to edit the motion in two cases:

- *Specification of target points:* A new desired target for a chosen operational point can be specified without defining the desired trajectory to reach it. This point can be determined using forward kinematics to compute its position from the kinematic optimization, described in section 4.3.1.1, or it can be arbitrarily set.

## 4. IMITATION AND EDITING OF DYNAMIC MOTION CAPTURE

---

- *Specification of a trajectory:* Let the trajectory for the operational point  $x$  be called  $x_o(t)$ . The new trajectory  $x_n(t)$  that will be set as the desired trajectory for that operational point will be  $x_n(t) = x_o(t) + x_m(t)$ , where  $x_m(t)$  is the trajectory modification that can be done on any of the six degrees of freedom of  $x$ . This trajectory modification  $x_m(t)$  can be time varying or constant, according to the requirements.

It is important to point out that the added operational task must have higher priority than the joints posture task it would interfere with. For instance, if an operational task is added to the hand, the priority of the arm posture task must be reduced. Alternatively, the task can be removed, but it is preferred to be kept, as it will serve as a “guide” for the new trajectory. If these priority considerations are not taken into account, the desired motion would be blinded by the solutions satisfying the posture task with higher priority, then the desired effect would not be achieved. Other tasks (typically, the gaze) could be considered, even if not meaningful in our case of pop dancing.

### 4.4.3 Foot Sliding

At some points, the observed motion revealed slight changes in the contact which becomes not exactly rigid. Thus, to let a foot slide, the rigid contact constraints stating  $\dot{x}_c = 0$  and  $\ddot{x}_c = 0$  can be relaxed constraining the motion to the horizontal  $XY$  plane. For the contact  $i$ , this restriction at the velocity level can be formulated as  $v_z = 0$ ,  $\omega_x = 0$ ,  $\omega_y = 0$  allowing the other velocity elements to take arbitrary values. This guarantees no translation along the vertical axis  $Z$  or rotation about it. To take into account these constraints, the dynamic model would need to be reformulated. Alternatively, another simpler and more flexible approach is to remove the contact constraint and add a task that restricts the motion in the  $Z$  direction, imposing no restrictions to the  $X$  or  $Y$  axis, which will limit the motion to the  $XY$  plane. Considering  $x^*$  as the desired task, this particular case of the 6D task (4.15) is:

$$x^* = \begin{bmatrix} 0 \\ 0 \\ T_z \\ 0 \\ 0 \\ 0 \end{bmatrix} \quad S_x = \begin{bmatrix} 0 & 0 & 0 & 0 & 0 & 0 \\ 0 & 0 & 0 & 0 & 0 & 0 \\ 0 & 0 & 1 & 0 & 0 & 0 \\ 0 & 0 & 0 & 1 & 0 & 0 \\ 0 & 0 & 0 & 0 & 1 & 0 \\ 0 & 0 & 0 & 0 & 0 & 0 \end{bmatrix} \quad (4.16)$$

where  $S_x$  is the selection matrix defined in (4.14) and  $T_z$  is the known height of the foot operational point with respect to the world frame. When the foot is in contact with the

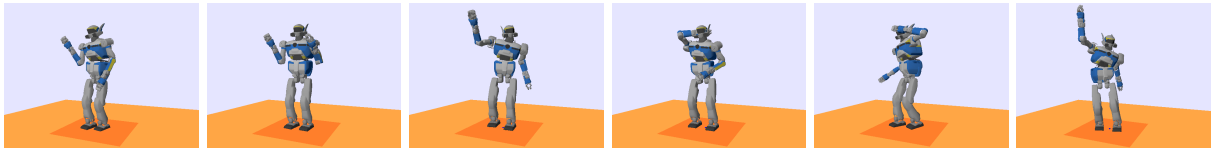
ground, this constraint restricts the height of the foot to remain constant, and the rotation about the  $X$  and  $Y$  axis to be null. The translation in the lateral plane and the rotation around the  $Z$  axis are not constrained.

This task does not exactly correspond to a sliding, since sliding can accept forces orthogonal to the motion. The proposed solution is thus more restrictive than necessary. However, the visual effect would be the same, and it will keep the motion feasible and dynamically consistent.

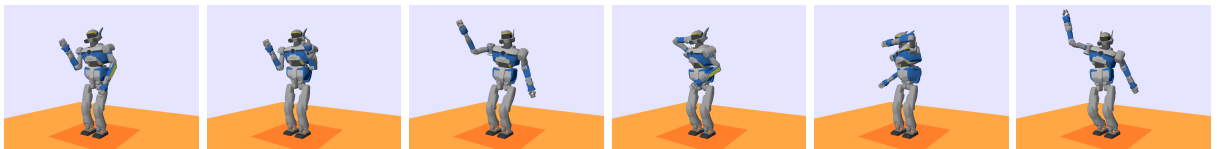
## 4.5 Results



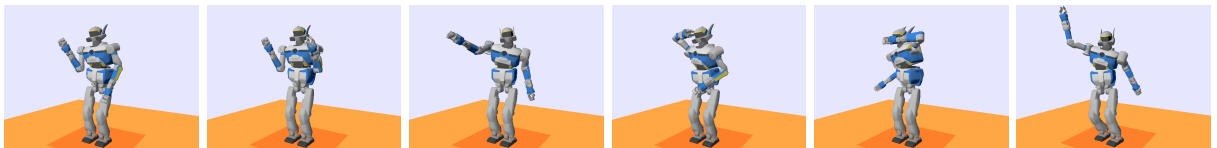
(a) Motion performed by the dancer (<http://homepages.laas.fr/nmansard/humanoid11-ramos-mocap/initial.avi>)



(b) Motion obtained with the geometric model (<http://homepages.laas.fr/nmansard/humanoid11-ramos-mocap/geometric.avi>)



(c) Motion resulting from the dynamic posture task (<http://homepages.laas.fr/nmansard/humanoid11-ramos-mocap/dynamic.avi>)



(d) Final dynamic and edited motion (<http://homepages.laas.fr/nmansard/humanoid11-ramos-mocap/final.avi>)

**Figure 4.6:** Results for the robot imitating the dance performed by a human.

To validate the proposed method, the motion of a dancer was acquired using the motion

## 4. IMITATION AND EDITING OF DYNAMIC MOTION CAPTURE

---

capture system, which provides the position and orientation of the frames associated with each node. The motion was retargeted to a modified-HRP-2 model (i.e we added one degree of freedom to both chest and neck joints, obtaining a kinematic structure closer to the one of HRP-4 [Kaneko et al., 2009], to obtain a nicer final motion), and edited to correct the retargeting error and introduce new non demonstrated features.

The kinematic optimization was applied to obtain the corresponding joint trajectories, which were then validated dynamically using the posture task in the inverse dynamics solver. The joint trajectory is first obtained from the motion capture, and it is, of course, not stable nor dynamically consistent as figure 4.6(b) shows. A first dynamic motion is then obtained using only the joint trajectory as reference. This motion is displayed in figure 4.6(c). The motion is stable; however, the geometric and dynamic retargeting have lost some data and produced some errors compared to the initial demonstrated trajectory. Since the frequency of the motion capture system was 200 Hz and the period used to dynamically generate the motion is 1 ms, the new desired joint values are changed every 5 iterations, and the exponential decreasing behavior is not always completed as a new desired value appears before the previous one has been completely reached. For motions with slow rate of change, the previous and next desired values are close enough and they can be properly followed. However, for motions with fast increments between consecutive frames, the desired joint values are not reached and the system acts as a low-pass filter on the joints evolution. This is particularly noticeable when there are oscillations, like the arm moving up and down consecutively or the knees moving continuously forward and backward. Three editions were thus applied:

- The knee oscillations (smoothed by the PD) were enhanced.
- The right hand motion was corrected.
- An additional motion of the left foot consisting in sliding on the ground, which was not present in the initial demonstration, was introduced.

The final results of the whole body motion after the dynamic processing are shown in figure 4.6(d). It is observed that the feet remain in a constant position due to the rigid contacts constraint imposed to the dynamic model. However, by the end of the motion there is an intended sliding on the foot as described in section 4.4.3.

The sequence showing the time of integration of the different tasks and modifications shown in figure 4.7. The following subsections provide more details on the three modifications cited above.

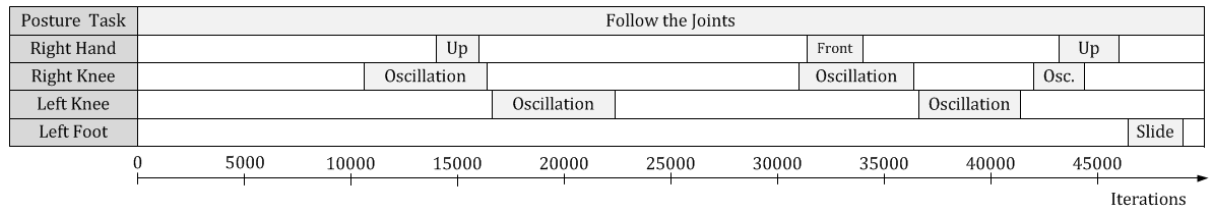


Figure 4.7: Timeline showing the task sequence.

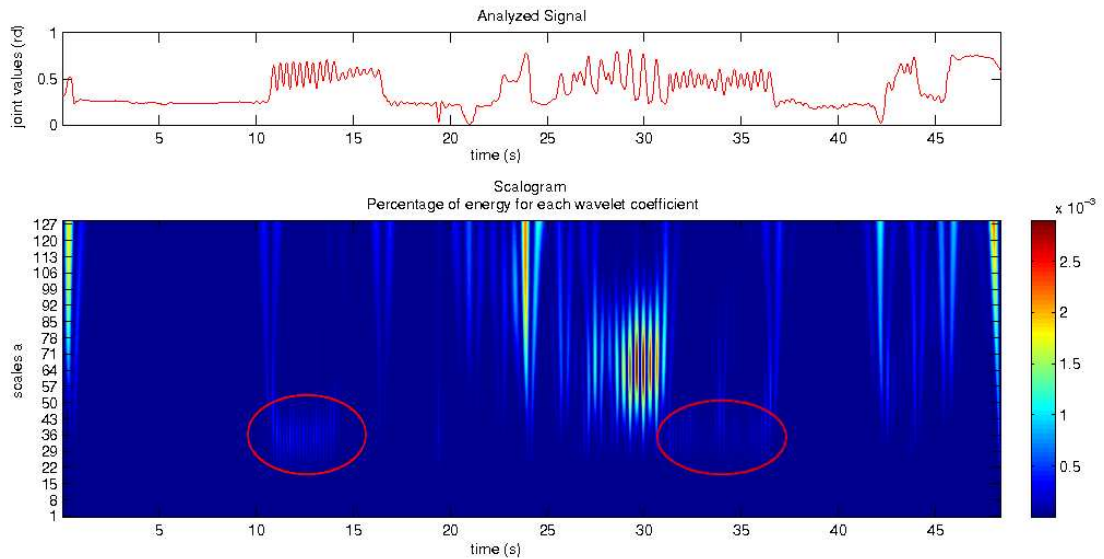


Figure 4.8: Scalogram of the right knee joint evolution.

### 4.5.1 Knee oscillation

The knees constitute a particular case as the dancer permanently moved them but at the dynamic level this motion was strongly weakened. To correct this problem we referred to the task approach where the motion of the knee joint was analyzed. On the top of figure 4.8, the joint evolution obtained after the kinematic optimization for the right knee is drawn. Between  $t = 10s$  and  $t = 14s$ , and between  $t = 31s$  and  $t = 36.5s$ , the motion of the joint is oscillatory. These moments of oscillation correspond exactly to the observed motion of the dancer's right knee. A scalogram using the Gaussian wavelet was constructed and it is shown in the bottom of figure 4.8, where it is observed (in red circle) that there are salient frequencies at those points. It was determined that the scale  $a$  corresponding to the maximum values at the desired positions is 36. The frequency and the scales are related by  $f = \frac{f_s f_w}{a}$ , where  $f_s$  is the sampling frequency and  $f_w$  is the center frequency of the wavelet. For the Gaussian derivative of order 4,  $f_w = 0.5Hz$ ,

## 4. IMITATION AND EDITING OF DYNAMIC MOTION CAPTURE

and considering that the sampling frequency used during the acquisition is  $200Hz$ , the resulting frequency is  $2.7\text{ Hz}$ . Then, a task on the knee was added at that frequency to resemble more the motion.

Figure 4.9(a) shows the time evolution of the right knee joint, and figure 4.9(b) shows the evolution in the  $x$  coordinate of the right knee operational point. Note that there is a difference in the time scale of figure 4.8 and figure 4.9, since the former one corresponds to the kinematic optimization of the motion sampled at  $200Hz$  and the latter corresponds to the dynamic level that runs at  $1000Hz$ . The red line shows the evolution of the joint when only the posture task is applied to the leg, and the blue line shows the evolution when the operational task is added to the knee, but both lines are obtained using the dynamic control scheme. Even though the joint is not directly controlled, it is observed in fig. 4.9(a) that with the operational task addition, the knee joint presents an oscillation with higher amplitude, whereas by applying only a posture task, the oscillation is weak. The results of the  $x$  coordinate variation in the operational space show a clear consistent oscillation with similar amplitude when the knee task was added. Both the joint space and the operational space show the effect of the task at the knee.

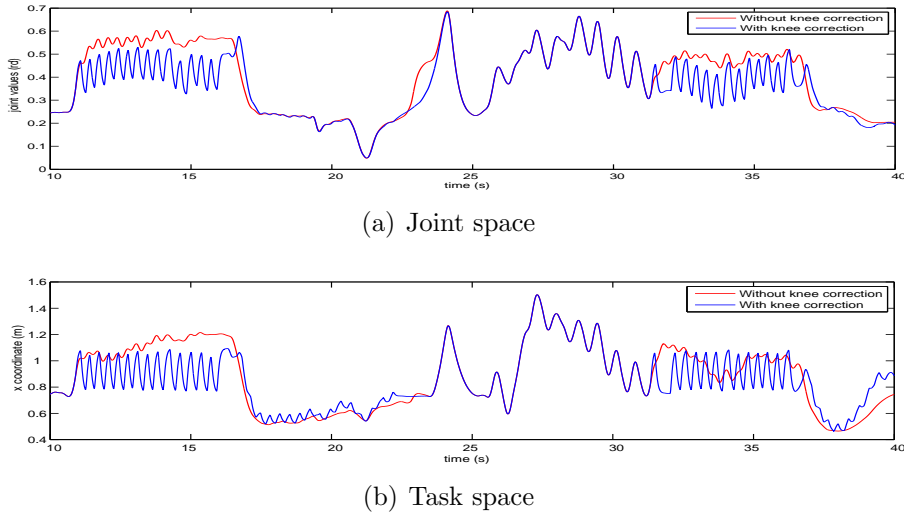


**Figure 4.9:** Time evolution of the right knee.

### 4.5.1.1 Right hand motion

The fast up and down motion of the right arm was also smoothed as a consequence of the applied PD controller. This was especially noted when the arm could not reach the upper

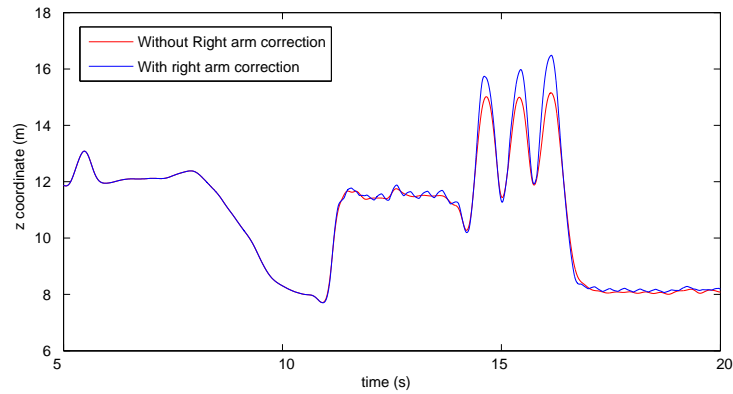


**Figure 4.10:** Right hand evolution in the operational space.

positions that the dancer performed. Then, an operational task to raise more the arm was introduced. The result is shown in figure 4.10. The trajectory of the  $z$  coordinate of the right arm using only the posture task and the trajectory with the operational correction are shown in this figure. The corrected trajectory, improved the upper positions of the right hand. The task of the right hand was also used to avoid the auto collision of the hand with the head, as it can be noticed in fig. 4.6, by comparing the position of the hand in the fourth thumbnail. The changes obtained for the right hand are shown in figure 4.11. As observed, the hand has been moved to a higher position using an operational task.

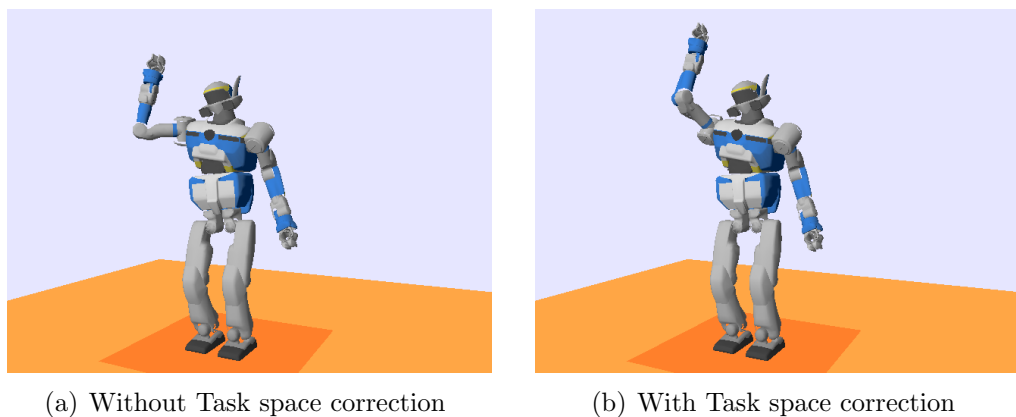


**Figure 4.11:** Modification of the hand position adding an operational task.

## 4. IMITATION AND EDITING OF DYNAMIC MOTION CAPTURE

### 4.5.2 Foot sliding introduction

We artificially introduced a sliding movement of the right foot, to prove that extra features can be added as desired. To introduce the sliding effect on a foot, the ZMP of the motion obtained using only the dynamic posture was analyzed. Figure 4.12 shows (in blue) the trajectory of the ZMP  $y$  coordinate. The wide red lines show the limits of the support polygon, and the dashed red lines show the boundaries of the foot (inside the support polygon). Between  $t = 46.94$  and  $t = 48.31$ , the ZMP lies completely in the area corresponding to the right foot. Then, it was possible to introduce the sliding task for the left foot in this interval, guaranteeing the dynamic stability of the robot, as the sliding foot cannot be considered anymore as a part of the support polygon. The support changes from double to single.

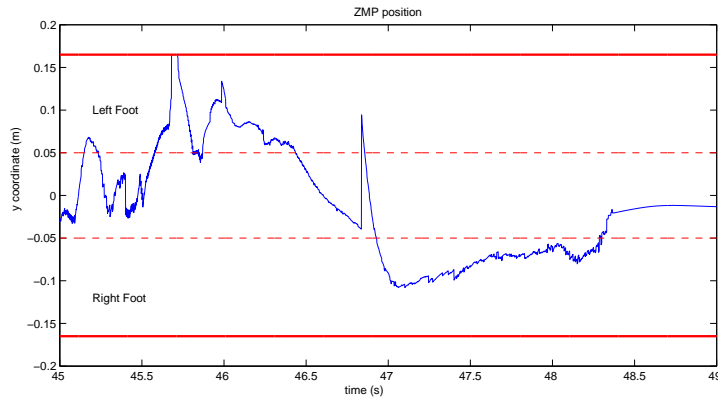


**Figure 4.12:** Evolution of the ZMP with only the posture task.

## 4.6 Conclusion

A method for the imitation of whole-body motion for humanoid robots has been presented. The contribution of this work is to propose a complete methodology to quickly reshape a dynamic motion demonstrated by a human expert, adapt the dynamics of the human body to the own dynamics of the robot and modify or edit as desired the initial motion to introduce extra features that were not demonstrated. It allows to build complex dynamic behaviors, based on a composition of tasks and constraints that are used as basic bricks for motion generation. The method was successfully applied to the imitation of a dancing motion, but generally, it can be used for the imitation of any type of motion. The obtained motion is dynamically consistent, and could be directly replayed by a real humanoid robot.

# 5

## Application of the inverse dynamics solver to the generation of human-like motion

### 5.1 Motivation

Motivated by the growing concern of human motion analysis, and knowing that robotics tools and algorithms could serve for such a study, we are interested in applying our developed solver to generate a motion on a human model. Knowing that the existing tools are rather limited, our aim is to elaborate and provide a software for the realization of such analysis. On the one hand, robotics serves for the development of tools for automatic motion generation. On the other hand, the invariants of the human movement that are derived from life sciences are required to set a reference for the comparison and validation of the simulated motion. Moreover, one important motivation of this work comes from the collaboration of the Gepetto Group of LAAS-CNRS with the Yoshihiko Nakamura Laboratory (*YNL*) of the University of Tokyo. Actually, the Japanese laboratory is concerned with the capture of human motion and the simulation of the corresponding complete musculo-skeletal (MS) activity using the software *sDIMS* they have developed. In addition to the motion capture system, they use more specific measurement tools as Electromyography (EMG), for identifying and measuring the muscular activation, and ground force plates, for measuring the contact forces of the supporting foot/feet. Their research is wide and combines multiple areas. One of their main concern is to estimate the human muscular efforts exerted during some movements or in case of injuries. This

## 5. GENERATION OF HUMAN-LIKE MOTION

---

brings us to a common point of interest which is at the basis of the collaboration between *LAAS-CNRS* and *YNL*. On the general level, the goal of this collaboration is to exchange the developments in the field of humanoid robotics and anthropomorphic motion in both laboratories. During my stay at *YNL*, my research work was to learn their tools and to understand the nature and characteristics of the human motion. Our goal was to combine the research and technological developments of both laboratories in two main steps. The first step is to record the motion of a human executing some manipulation tasks while satisfying other constraints. Then, the second step is to simulate the motion, not by imitation of the motion capture data, but by setting a stack of equality and inequality tasks that represent the human actions and that could reproduce the original scenario. We propose to resolve this stack of tasks using the inverse dynamics hierarchized solver developed in chapter 3. Then, we seek to compare the human motion and the one simulated on the human model at different levels, starting with a simple visual comparison and then extending it to analyze qualitatively the torques exerted during the motion. We also want to compare the movements obtained based on kinematics and dynamics. Since we have shown in chapter 3, that both formulations follow a generic expression, it is interesting to generate the same motion using a kinematic and a dynamic human model, and then search for the differences in order to synthesize and evaluate the effect of dynamics. This chapter adds to the context of chapter 3 some important characteristics:

- Development of a human model and application of the hierarchical solver to this new model.
- Capture of a human motion and extraction of the stack of tasks corresponding to his movements.
- Application of the same scenario to resolve the kinematics and dynamics of the motion.
- Study, analysis and comparison of the results obtained from both simulations and reference motion.

The chapter starts in section 5.2 by describing the recorded motion along with the motion capture tools available at the *YNL*. Then, the corresponding stack of tasks are described. Some parameters, as the gain of the tasks, needed to be chosen carefully. Section 5.3 is dedicated to the description of the tasks and the parameters values. Finally a double stage comparison is developed in section 5.4 for analyzing the human motion regarding the simulations.

## 5.2 Experimental setup

### 5.2.1 The real captured motion

In this section we describe the tools and equipments of the YNL that were used to capture the original human motion, and then we present the original scenario.

#### 5.2.1.1 Tools and softwares

Many researches focused on motion analysis and simulation of human musculo-skeletal model in the field of sports science and medicine [Kaya et al., 1995; Komura et al., 2000; Suzuki and Takatsu, 1997]. The purpose of these researches is to analyze the human somatosensory data,<sup>1</sup> then to use it to improve motion styles of athletes, to evaluate movements of disabled and to support rehabilitation planning. However, the models that are developed are simplified or limited to some parts of the body because of the high complexity of whole body motion. On the other hand, robotics provides efficient algorithms to compute the dynamic equation of motion that were applied to whole-body models for generating motions, as for example the MS model shown in fig. 5.1 from [Yamane and Nakamura, 2007]. This kind of model includes a model of the skeleton and the muscular system. The skeleton is made of a set of bones which constitute the rigid links with specific masses and inertia. The muscular model wrapping the bones contains a set of muscles, tendons, ligaments, which are active wires, and cartilages, which are passive elements [Nakamura et al., 2005; Yamane et al., 2005; Nakamura et al., 2003]. By setting an origin, via-point(s) and an end for each wire, the modeling of each component of the muscular model is precise. Computations of inverse kinematics and inverse dynamics are applied to the complex MS system using the motion capture data that allows to derive the proprioceptive information. The motion capture data is coupled to EMG and force sensors measurements for more accuracy in the inverse dynamics computation in the following way. First, the captured motion is treated by inverse kinematics, where the joint angular variations are computed from the markers position data, then the joint trajectories are integrated. By differentiating the joint velocities, the system defines at each time step the current joint positions, velocities and accelerations. Thus, Newton-Euler inverse dynamics algorithm [Featherstone, 1987] is applied for the computation of the generalized torques which include the effect of both external contact forces and internal muscle forces required

---

<sup>1</sup>The somatosensory information includes tension, length, and velocity of the muscles, tension of the tendons, and ligaments, pressure of the cartilages, and stress of the bones.

## 5. GENERATION OF HUMAN-LIKE MOTION

---

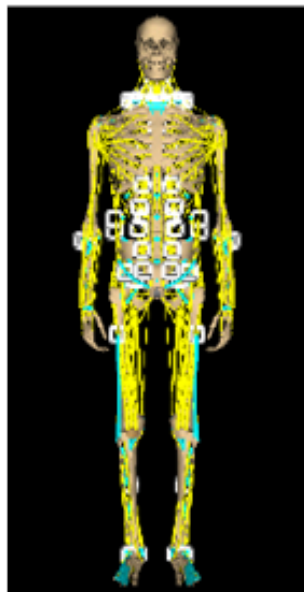


**Figure 5.1:** The human MS model developed in YNL.

to accomplish the given motion. Then, the mapping between the generalized torques and the muscle forces is computed using the principle of virtual work and knowing that the generalized torques are produced by the internal wire tensions and the contact forces. Since the number of wires is greater than the number of DOF, computing the forces from the torques is a highly redundant problem [Nakamura et al., 2005]. Therefore the muscle forces are obtained by applying an optimization problem, linear or quadratic, subject to equality and inequality conditions that are formulated, knowing the joint torque data along with the measurements recorded during the motion capture, as the muscle activation data from EMG, and the ground contact forces measured by the force sensors.

### 5.2.1.2 Description of the scenario

The purpose of this section is to describe the original human motion and the motion capture experimental setup. First, we start by the motion capture settings. The initial phase consists of the calibration of the motion capture system. Then, the subject needs to be equipped with markers and EMG electrodes. The EMG electrodes are coupled and chosen to be attached to 4 joints of the human body, shoulder - elbow - knee - foot, on the left and right sides. Since each EMG electrode is composed of two pins, input and output, they are attached on the front and back sides. Synchronization between the motion capture system and the analog system of EMG measurements is required.

By applying the physiological model of muscle proposed by Hill [Hill, 1938] and Wilkie [Wilkie, 1956], which was later formulated by Stroeve [Ritchie and Wilkie, 1958], the muscle force can be computed from the measured EMG signal. The integrated EMG signal, called IEMG [Merletti and di Torino, 1999], gives directly the activity level  $u$  of the motor neuron. The muscle activity level  $a$  is then computed from  $u$  by the following equation:

$$\dot{a} = \frac{u - a}{T};$$

where  $T$  is a constant parameter used to adjust the time delay. The muscle force  $f^*$  is then computed by:

$$f^* = aF_l(l)F_v(\dot{l})F_{max};$$

where  $F_{max}$  is the maximum force of the muscle measured on each subject,  $F_l(l)$  and  $F_v(\dot{l})$  represent the relationship between the normalized force and the muscle length  $l$  and its velocity, respectively [Yamane et al., 2005; Yamane and Nakamura, 2007]. The measurements of the marker positions, EMG signals and ground contact forces are simultaneously obtained by using an in-house optical motion capture system of 35 markers (Motion Analysis) and commercially available, 16-channel EMG and two force plates (Skitter company). The motion capture system and the data acquisition computers for EMG and force plates are connected via the network. The acquisition of the markers positions is realized at  $200Hz$  along with the data from EMG and force plates measured at  $1KHz$ . Figure 5.2 shows a subject standing on force plates and on whom EMG electrodes and markers are attached.

After we went through the preparations for recording the motion, we will describe the played scenario. The original human motion needs to be chosen carefully to reflect challenging behaviors as reaching far objects while being subject to stability constraints and other limiting or conflicting tasks. The purpose is to be able to reproduce this motion later on with our developed software. The subject was asked to be in single support by standing on his right foot and to hold a cup with his left hand at around  $1m$  high off the ground. Then, three consecutive reaching tasks were executed simultaneously with a gaze task, based on three different targets. From the initial posture of single support and left hand up, the subject reaches by his right hand a target placed on the ground in front of him. Then, the subject moves his right hand to reach the second target on his right. Finally, the third target point is placed behind the subject and should be pointed out. While executing these manipulation tasks, the subject must direct his eyes towards the targets. During all the motion, the subject is supposed to conserve

## 5. GENERATION OF HUMAN-LIKE MOTION

---

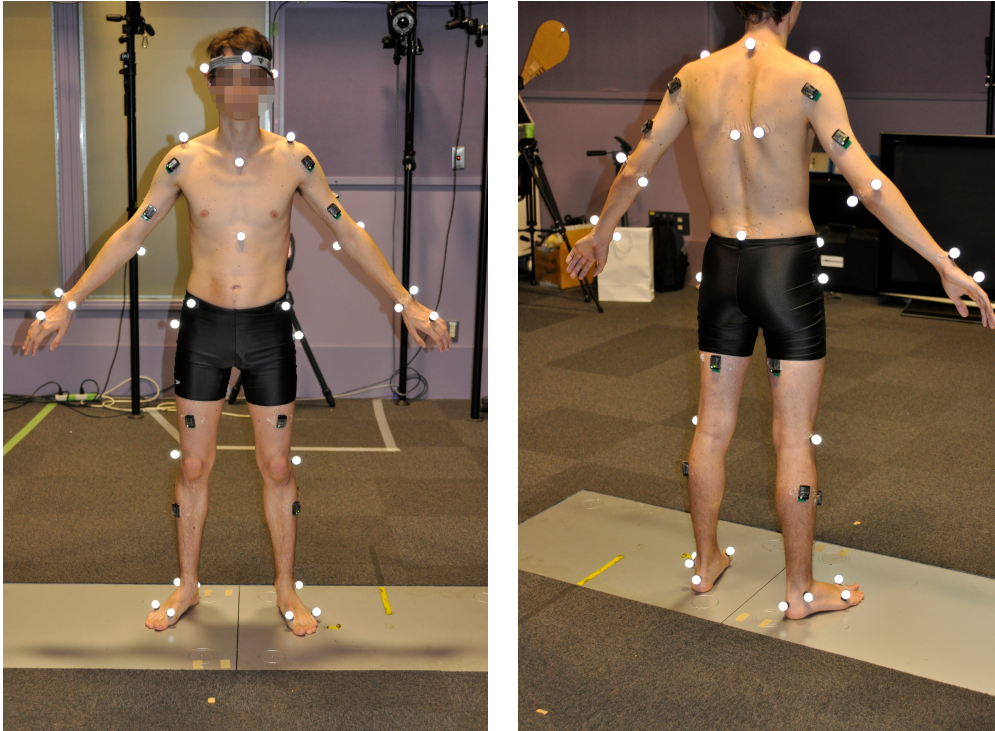


**Figure 5.2:** Front and back views of the human standing on the force plates and having the circular markers and rectangular electrodes attached to the different bodies.

its balance keeping only one supporting foot and maintaining his left hand up with free motion inside an admissible circle. Snapshots of this motion are shown in figure 5.7(a). This motion is first simulated with the sDIMS software developed by the YNL, in order to get the muscle force data. The MS model has 155 DOF and 997 muscles. This software allows to perform kinematic and dynamic simulations. First, the inverse kinematics is resolved with the motion capture data as reference behavior. Then the output of the kinematics computations are given as input to the dynamic system which includes the inverse dynamics for the computation of torques. The simulated motion by sDIMS is presented in figure 5.3. The human motion also constitutes a reference for our inverse dynamics solver. However, at this time, the recorded data is not used. Instead, we define a set of equality and inequality tasks corresponding to the real motion, to be simulated on a human skeletal model developed to this purpose.

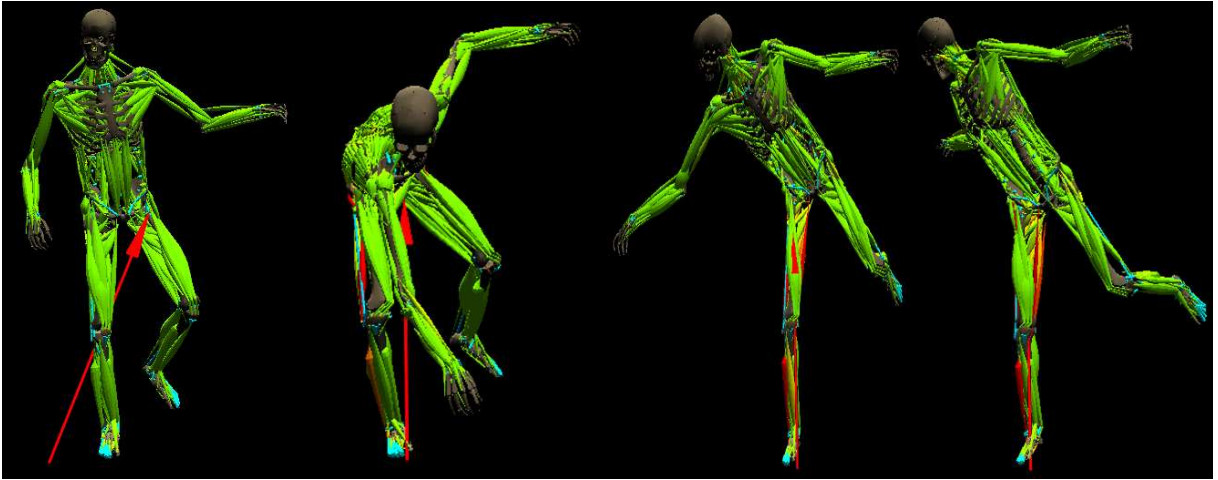


**Figure 5.3:** The MS model in simulation of the recorded data using sDIMS simulator. The snapshots are taken at the initial configuration and at the end of each reaching task. The red arrow from the ground towards the model represents the resulting contact force.

### 5.2.2 The human model

In order to simulate the motion more accurately and as close as possible to the human behavior, we designed a human model including more degrees of freedom than the HRP-2 model. This new model is based on the humanoid model, but includes additional DOF at the head, chest, ankle and 3 new revolute joints between the chest and the waist associated to one body that we call abdomen. The table 5.1 shows the different bodies with their corresponding joint numbers. This human model has 37 controllable DOF which enables

**Table 5.1:** Joints of the human model.

Part	Joints
Right Leg	1-7
Left leg	8-14
Abdomen	15-17
Chest	18-20
Head	21-23
Right Arm	24-30
Left Arm	31-37

more redundancy in motion. The length of each segment was computed from the existing MS model of the sDIMS software. The designed model strongly differs from the actual

## 5. GENERATION OF HUMAN-LIKE MOTION

---

human MS model in its nature and dimension, being only geometrical (bodies and joints) and having a smaller number of DOF. Despite this fact, we will consider it as a first step for simulating human-like motion using our developed software. Considering such a simplified model allows to reduce first, the pre-process time consumption, and second the computation time of the kinematic and dynamic simulations. However, the simulated motion on the MS model based on EMG information and motion capture data remains more accurate. Since our goal is mainly to develop an “easy” software for automatic generation of complete human-like motion and to be able to add modifications as avoiding obstacles and auto-collisions, the hierarchized inverse dynamics solver can afford solutions to such problems. Moreover, this solver is generic enough to deal with any model with any number of DOF. Thus, developing a more detailed human model with more accurate masses, inertia, and lengths can be considered as a future work.

### 5.2.3 The simulated motion

Having a generation motion tool in hand along with a human model, the next step is to extract a stack of tasks that could reproduce, at least visually and qualitatively, the reference human motion. Therefore, this original motion should be expressed as multiple tasks and constraints.

First, by observing the motion of the left foot and the left hand, it is obvious that both bodies move inside a limited region that was imposed on the subject. Thus, these constraints are formulated as inequality constraints on the left ankle and the left wrist operational points. In this case, we define the upper and lower bounds that compose the 3D polygon of translational motion. Since the orientation of the left foot was not constrained during the reference motion, it should be kept free. However, the subject having to hold a cup during all the experiment, the orientation of the left hand should be constrained. But, since the initial posture of the human model is chosen such that the orientation of the hand is by default the proper one, we assume that the hand’s orientation would not change. Therefore, we choose to constrain only the position of the left hand, but we could easily add a constraint on the rotation of the hand. We define the limits of the hand and foot by computing the distance of the initial 3D pose to the high standard deviation. The standard deviation is a widely used measurement of variability used in statistics and probability theory. It represents the variation or “dispersion” around average or mean. The high standard deviation indicates that the data are spread out over a large range of values. The computation of these bounds will be detailed later on. The

left ankle and wrist are both constrained within the vertical plane. But, the left ankle is chosen to respect only the vertical component bounds.

Beside the inequality tasks, two other equality tasks were defined, one for the manipulation and the other one for the gaze. The manipulation task is defined on the right hand or wrist operational point and constrained the  $6D$  pose by only selecting the translational part since the orientation was not imposed to the human. Three targets were defined according to their actual positions in the original environment. However, since the world frame is not identical in the original environment and the simulator, we apply the corresponding change of coordinates. Both frames have the same orientation but not the same lateral position. Thus, the transformation is only Cartesian and consists in attaching the original frame to the right foot as it is the case in our simulator. Then, the visual tasks are also formulated as equality tasks where the gaze should focus on the target to be reached. We will discuss, in the results section, the modifications that could be made on the visual task. In order to avoid auto-collisions and to increase the resemblance to human movement, intermediary points were defined before reaching the first 2 actual targets. One important task concerning the center of mass is added to conserve the stability.

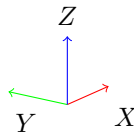


**Figure 5.4:** Frame orientation of both systems ( $X$  is depth)

Actually, the human is naturally able to remain stable but there is no guarantee that the human model will behave the same way. We suppose that by constraining the projection of the center of mass to keep its position inside the support polygon, we could reliably reproduce the stability criteria chosen by the human.

Since the stack of tasks formalism is generic, and since we already dispose of a corresponding kinematic solver, it is interesting to simulate the motion using both inverse kinematics and inverse dynamics solvers. We want to analyze the resulting motions and point out the different strategies and choices of parameters. The figure 5.5 shows the sequence of tasks used for both simulations but with different timelines. IP1 and IP2 define 2 intermediary points (IP) added as pre-pointing tasks in order to avoid an auto-collision between the right hand and the right foot, in the first pointing task. Then, the second IP

## 5. GENERATION OF HUMAN-LIKE MOTION

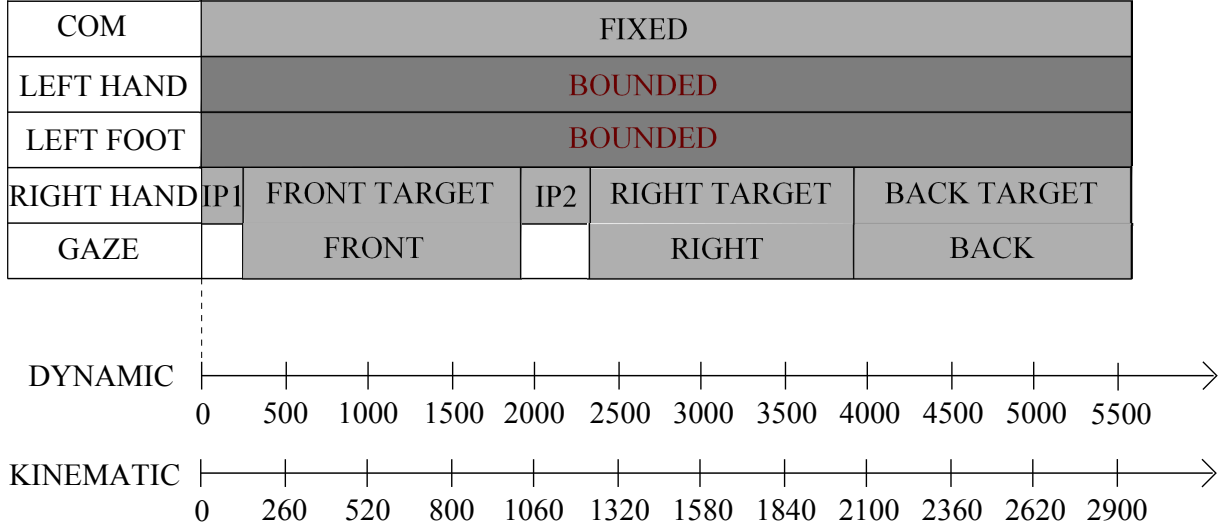


**Figure 5.5:** Time sequencing of tasks defined for reproducing the captured motion with no usage of the recorded data itself

is necessary to avoid the collision of the hand with the ground. The choice of adding intermediary points is simple and does not perturb the realization of the actions neither the realism of the final simulated behavior. Since no obstacle avoidance nor auto-collision are properly taken into account, at this level, these pre-pointing tasks resolve such problems. As explained earlier, the COM is constrained during all the motion. This is a particular case of the previously explained PD task, since we only control the position of the COM,  $p_{com} \in \mathbb{R}^3$ , to the desired position  $p_{com}^* \in \mathbb{R}^3$ . To this end, the task is  $e = p_{com} - p_{com}^*$  and the current position of the COM is computed from the dynamics of the robot. Knowing that the COM is free to move inside the support polygon, we could define a corresponding inequality constraint. We choose instead to constrain its projection to a fixed position. The inequality tasks are also considered during all the simulation and the bounds should be respected in order to have a simulated motion similar to the human motion. The visual task is added simultaneously with the final reaching task. Observing the reference motion, it is quite hard to decide when the human starts looking at the target and whether the vision or the manipulation is first initiated. The idea of coupling the vision tasks with the final targets ensures the relaxation of more DOF during the pre-pointing phase.

## 5.3 Parameters variation

### 5.3.1 Mathematical description of tasks

The equality tasks convergence obey to second order equation in the case of dynamics, and first order equation in the case of kinematics. We will discuss the choice of the gains in the next section, since it is critical to define the values corresponding to a good convergence rate. For the inequality tasks, we need to define a specific task that bounds the operational space velocity or acceleration in the case of kinematics and dynamics respectively. When resolving the kinematics, the inequality constraint is expressed as:

$$\underline{e} \leq e + \Delta T.G\dot{e} \leq \bar{e}$$

In the case of dynamics, this constraint is equivalent to the following linear inequalities on task accelerations:

$$\underline{e} \leq e + \Delta T.G\dot{e} + \frac{(\Delta T.G)^2}{2}\ddot{e} \leq \bar{e};$$

where  $\Delta T$  is the sampling time and  $G$  is the control gain associated with the task. The upper and lower bounds are computed by different expressions. Either, by computing the distance from the mean values of the recorded data to the high standard deviation:

$$[e; \bar{e}] = [\mu_{e_i} - 3\sigma_{e_i}; \mu_{e_i} + 3\sigma_{e_i}] \quad (5.1)$$

Or, by computing the distance from the initial values to the high standard deviation:

$$[e; \bar{e}] = [e_0 - 3\sigma_{e_i}; e_0 + 3\sigma_{e_i}], \quad (5.2)$$

where  $\sigma_{e_i}$  is the square root of the variance of each coordinate  $e_i$  (with  $i = 1, \dots, 3$  denoting each direction of motion) of  $e$ .  $\mu_{e_i}$  represents the mean of the measured positions  $e_i$  of the markers attached to the left ankle and left wrist. These positions are measured in *mm* and expressed in the world frame of the motion capture system. They are then converted into the *m* unit and transformed to the human model world frame in order to be homogeneous with the simulation system.  $e_0$  represents the measured initial position of the left ankle and left wrist or the computed initial position from the initial configuration of the human model. First, we choose to set the bounds for both inequality tasks as in eq. (5.1). Then, for the foot, we decide to constrain only the vertical motion along the  $Z$  axis. We find this constraint sufficient to reproduce the reference motion since the task consists in simply keeping the left foot in the air. For the left hand, the constraint is more complicated, as

## 5. GENERATION OF HUMAN-LIKE MOTION

---

it must hold a cup and keep it inside a region around its original position where it was held on a 1m high pedestal. We choose to control the motion in the frontal plane along the axes  $Y$  and  $Z$ .

Since the initial posture of the human model is not the same as the human's, the simulated behavior, typically for the left foot, is not the same. Both initial configurations are represented in figures 5.7(a) and 5.7(b) at the start time. Actually, the initial posture of the human model is chosen to be a stable one with one supporting foot and an orthogonal rotation of the elbow joint to put the hand up. Therefore, we do not intend to compute exactly the same posture as the human. The human model's initial posture shows a lower distance between the left foot and the ground. Thus, by applying the inequality task with the bounds expressed as in (5.1), a problem of collision of one or more bodies of the leg, i.e. the knee and foot, with the ground occurs. In particular, we observe that the knee touches the ground when the model is bending and trying to reach the first target. This is shown in figure 5.6. This is because we constrain the ankle position to move inside an acceptable zone without controlling the movement of the other joints of the leg. Moreover, in this work, we do not deal with obstacle avoidance. One direct solution is to compute the minimum height of the subject's left ankle in the real experiment and to apply it as a lower bound. This pushes the human model to raise his left foot at the first iterations in order to compensate for the gap with the minimum bound imposed since the model starts with an initial posture that does not fit the bounds.

### 5.3.2 The gain tuning

The control gains for the dynamic and kinematic tasks differ and each value can be chosen as constant or variable. The variable gain is adaptative according to the norm of the error. The adaptative gain  $G_a$  can be set with one of the following definitions:

$$G_a = k_0 e^{(k_\infty \|e\|)} + \beta \quad (5.3)$$

or

$$G_a = (k_0 - k_\infty) e^{(-\frac{\beta}{(k_0 - k_\infty)} \|e\|)} + k_\infty; \quad (5.4)$$

where  $k_0$  and  $k_\infty$  constitute the values of the initial gain and the final gain respectively,  $\beta$  is the slope corresponding to the error,  $\|e\|$  is the norm of the error. We choose to define the gain according to (5.4). In order to make a comparison on both levels, we needed to build a certain correspondence between the gain values in kinematics and in dynamics. Seeking to simulate a similar motion with the same convergence rate, a way to define the

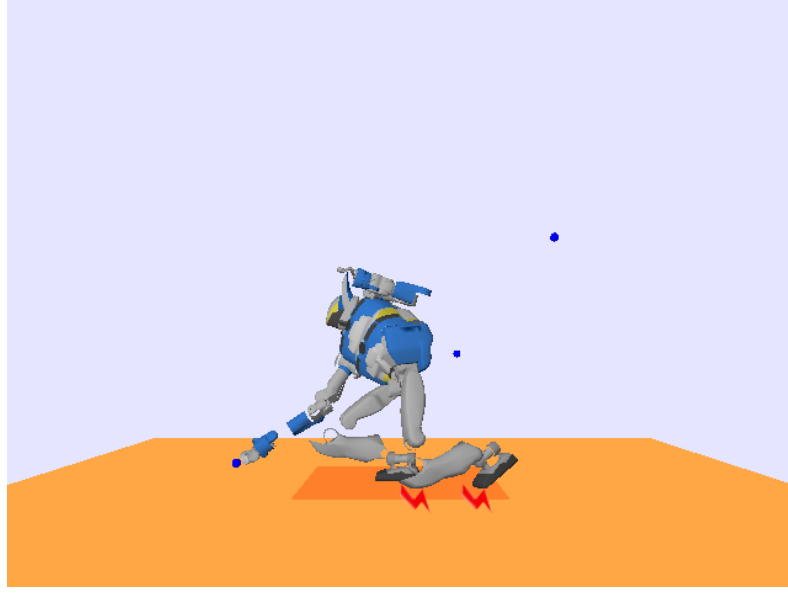


**Figure 5.6:** The human model reaching the target in front and touching the ground with its left knee and foot.

gains in both cases is by an identification of the error expressed in both systems and by a numerical computation of the values of the gain. First, we set the convergence rate to 80%. Thus, we want to define the gain that corresponds to 80% of the convergence of the task. Then, we resolve both equations of errors in kinematics and dynamics.

- kinematic error: The expression of the velocity control law in kinematics is a first order differential equation of the form  $\dot{e} = -\lambda e$ . The error is then derived as:

$$e(t) = e_0 e^{-\lambda t} \quad (5.5)$$

- dynamic error: In this case, the error is computed from the PD equation  $\ddot{e} = -\lambda_p e - \lambda_d \dot{e}$  which constitutes a second order differential equation. We consider that this equation has a double root and the corresponding solution has the following form:

$$e(t) = (At + B)e^{-kt} \quad (5.6)$$

Knowing the initial and final conditions, the final expression of the error is:

$$e(t) = e_0 \left( \frac{\lambda_d}{2} t + 1 \right) e^{-\frac{\lambda_d}{2} t} \quad (5.7)$$

For a given set of values of the derivative gain  $\lambda_d$ , we define:

$$e_0 \left( \frac{\lambda_d}{2} t + 1 \right) e^{-\frac{\lambda_d}{2} t} = \frac{1}{5} e_0;$$

## 5. GENERATION OF HUMAN-LIKE MOTION

---

**Table 5.2:** Dynamic gain and corresponding kinematic gain values

$\lambda_d$	$\lambda$
10	2.7
50	13.4
100	26.8
500	134.1
1000	268.2

where  $\frac{1}{5}e_0$  is the remaining 20% of the total convergence of the task. Then, we deduce the time corresponding to the gain  $\lambda_d$  that realizes this convergence. Accordingly we can compute  $\lambda$  from:

$$\lambda = \frac{\ln 5}{t}$$

We can compute a corresponding set of values for the kinematic gain that is homogeneous to the given values of the dynamic gain. The table 5.2 shows some of these values.

Finally, we choose  $k_0 = 10$  and  $k_\infty = 100$  for the dynamic equality task of manipulation, and the corresponding kinematic gains would be  $k_0 = 2.7$  and  $k_\infty = 26.8$ . For the other tasks, we choose corresponding relative constant gains.

### 5.4 Results

This section presents the simulation results from kinematics and dynamics compared to the real human motion simulated by sDIMS. In the following, we will always refer to the results from sDIMS, using the MS model, as the real motion in order to avoid confusion with the kinematic and dynamic simulations realized by applying our hierarchical solver. The subject will be referred to as H, and the human model as HM. First of all, we will propose a technical and visual analysis of the kinematic and dynamic simulations on the human model. Then, we intend to compare the norm of the efforts exerted in simulation and in real motion, knowing that both models have comparable masses and inertia of the common bodies.

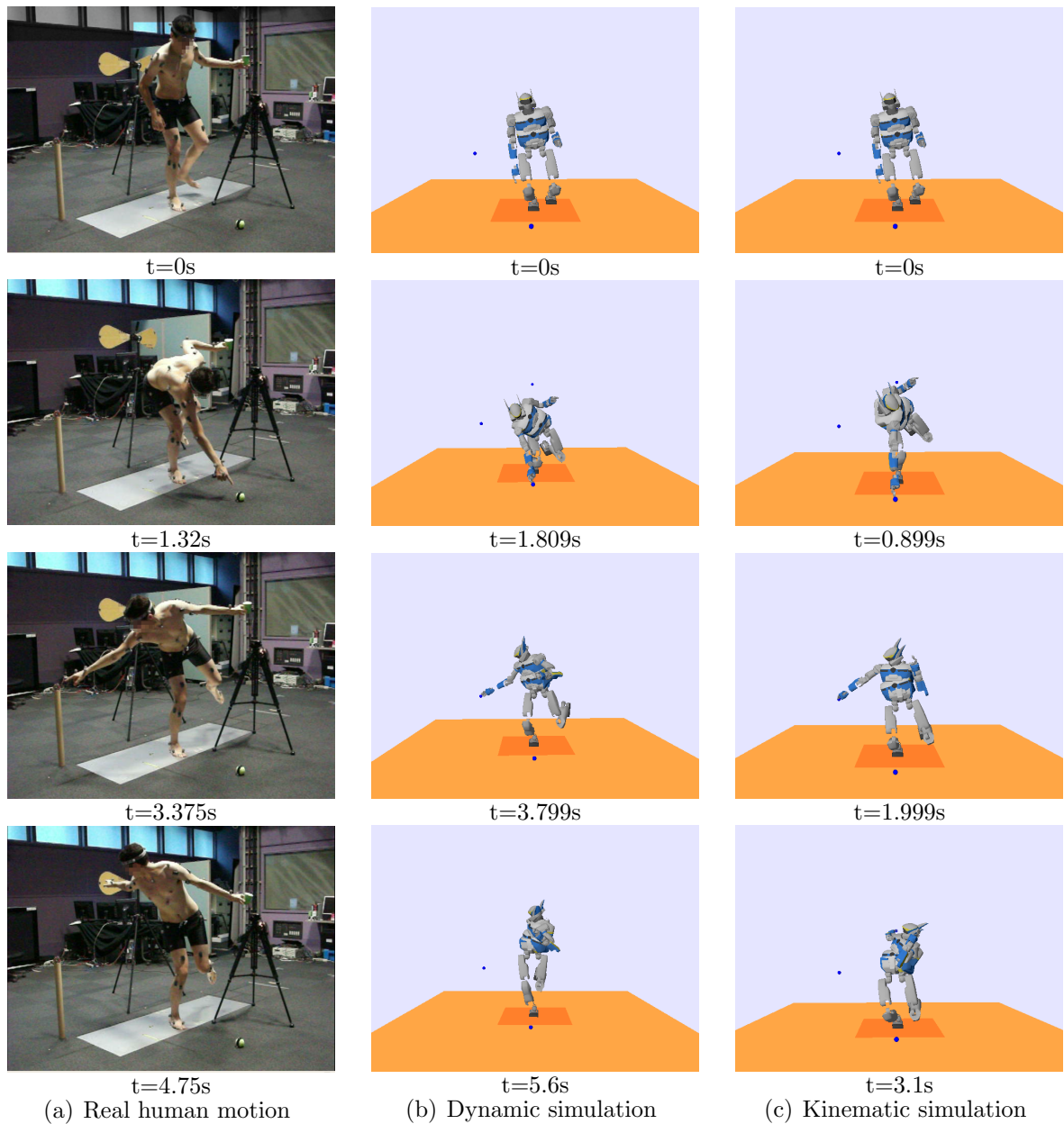


**Figure 5.7:** Front view of the real human behavior, and the corresponding motion of the human model in kinematic and dynamic simulations. These snapshots show both the human and the model, respectively at the initial configuration, the convergence time of the first target, the configuration after reaching the second target, and the final posture when the third target is reached.

## 5. GENERATION OF HUMAN-LIKE MOTION

---

### 5.4.1 Kinematics vs Dynamics

#### 5.4.1.1 Visual comparison

Figure 5.7 shows snapshots from the human captured motion and from our simulations. We notice that for the initial posture, the human H is looking towards the first target since he has already visualized the scene. Moreover, knowing a priori the next move that should be made, H anticipates by pointing his eyes towards the target. It is quite normal at this stage for the model to have a different head position since this anticipation was not taken into account when computing the initial configuration. Actually, we start by an arbitrary posture that is stable and that satisfies the single foot support. We also want to have a similar position of the left hand compared to the human one. Figures 5.7(a), 5.7(b) and 5.7(c) show the postures at the end of each reaching task. The major differences are related to:

- The right hand's pose.
- The orientation of the head.
- The left foot and left hand positions.
- The upper body posture.

In the following, we will give a detailed description of the similarities and differences between the resulting simulations for each given configuration in 5.7.

When moving to reach the first target, the posture of the human model HM given by the dynamic simulation looks more natural than the kinematic one. Looking at the left leg, we can see that with the dynamics, HM lifts his foot in a comparable way to H. Whereas the foot is risen very high when only the kinematics is used. Similarly, the left hand is higher in the kinematic simulation than with the dynamics. Another different behavior concerns the right hand that is too much extended in the kinematic motion and gives an unnatural look. Moreover, the head is more rotated in case of the kinematics, whereas, the pose of the head obtained with the dynamic model seems quite comparable to the human one.

In the next configuration, when the second target on the right is reached, also we could point out many differences. The right knee is more flexed in the case of kinematics yielding to a lower position of the right foot compared to the real motion, while the dynamic simulation gives also a better resulting motion. The left hand position is also

quite different in the case of the kinematics while it is quite similar to the real motion in the case of dynamics. The right hand pose, typically the orientation, taken by the kinematic model is completely unnatural, while the dynamic model moves his hand and arm in the same orientation as the human arm. Finally, the head orientation also differs in the kinematic model compared to the dynamic model and to the human.

For the final target, we notice similar differences at the level of the extension and flexion of the right knee. However, the left arm in both simulations takes a different posture but the fixed bounds are always respected. Despite this difference, the configuration obtained with the dynamic model is closer to the one of the human than with the kinematic model. Finally, we observe that the upper body of the kinematic model moves in an opposite direction to the target while H seems to go towards the target. This also appears on the dynamic HM posture but with less intensity.

For clearer comparison, a video combining these three motions is available on: <http://homepages.laas.fr/lisaab/human-motion>. Even though the differences are only visual, we can say that the configurations obtained with the dynamic model are more resembling the human ones than the configurations resulting from kinematics only.

#### 5.4.1.2 Technical comparison

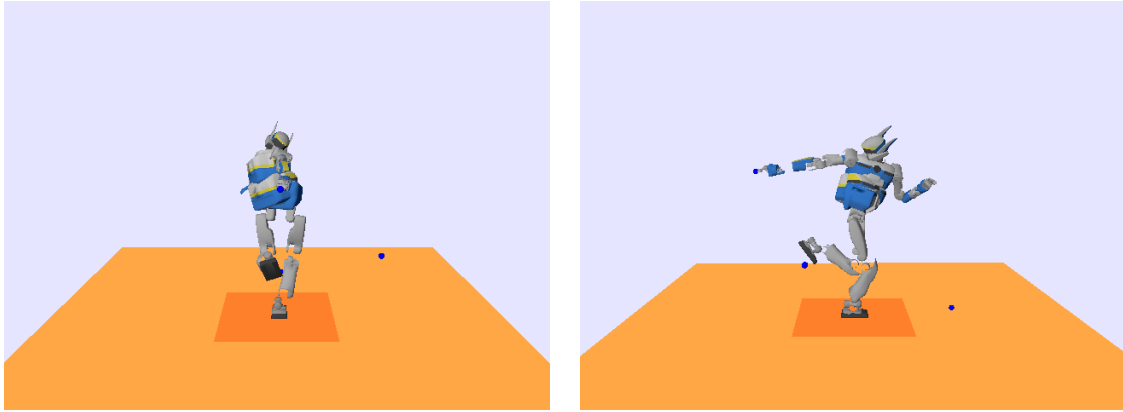
As explained in the appendix B, the visual task shows that a point in the world frame is projected into the image plane of the camera. The coordinates of the projected point  ${}^i p$  are computed, and the desired position on the image plane is given by  ${}^i p^*$ . By default, this desired point is set at the center of the image plane. Then the error between  ${}^i p$  and  ${}^i p^*$  defines the visual task error and the head attached to the camera moves towards this desired point. During the simulations, the choice of the desired point seemed to be restrictive because it caused some unnatural moves of the head and auto-collisions during the visualization of some of the targets. Recall that the purpose of the visual task is to make HM looks natural while reaching the target and tracking it visually. This is due to the equality definition type of the visual task. In addition to that, we did not impose joint limits constraint in this scenario.

**Dynamic simulation:** The only target that led to an unnatural posture of the head was the one in the back. Figure 5.8(a) shows the snapshots taken in two cases:

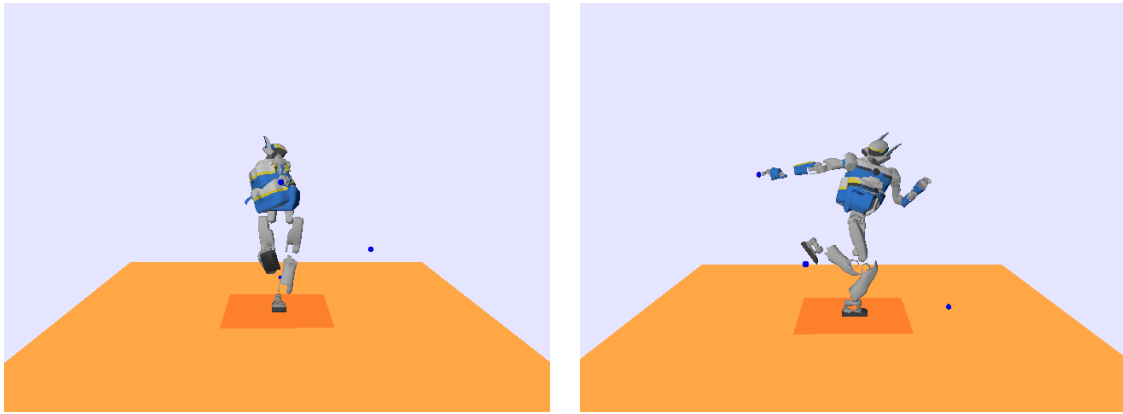
- The default case as shown in fig. 5.8(a).

## 5. GENERATION OF HUMAN-LIKE MOTION

---



(a) Desired image point set as default to the center of the image plane



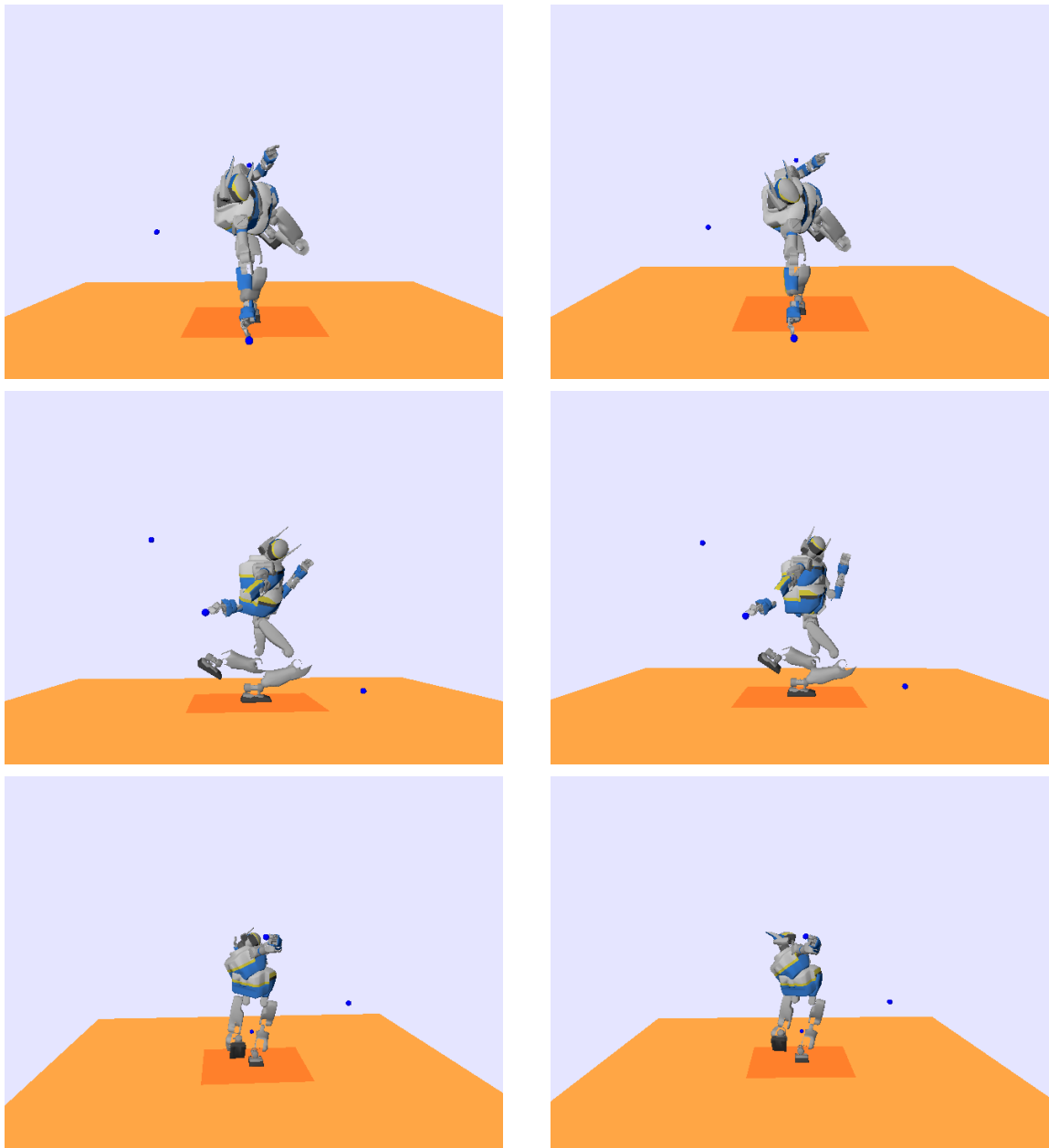
(b) Desired image point shifted to the right of the center of the image plane

**Figure 5.8:** Back and side views of the human model in dynamic simulation taken during the visualization of the same target from two different desired image points.

- The rectified case where a new desired image point is set in such a way that the position of the head is relaxed, inducing a more natural movement. This is presented in fig. 5.8(b).

The original  ${}^i p^*$  is set to  $[0, 0]$ , which makes HM turn his head orthogonally to its default orientation in order to visualize the target from the center of the image plane. The resulting behavior gives an unnatural look and the motion of the head exceeds the corresponding joint limits. Observing the human look, we deduced that the vision point in the image plane can be shifted in a way that makes HM look from his right “eye”.

**Kinematic simulation:** The three targets in this case induced unnatural behaviors and auto-collisions. Similarly to the dynamic simulation, for each target, the desired image



(a) Desired image point set as default to the center of the image plane  
 (b) Desired image point shifted to different positions in the image plane

**Figure 5.9:** Postures of the human model in kinematic simulation while the vision target is modified three times with fixed desired image points, in the top figures, and changed desired image points according to the target, in the bottom figures.

point is chosen according to the expected behavior.

For all the visual tasks, the tuning of these image points was made by assumption.

## 5. GENERATION OF HUMAN-LIKE MOTION

---

Another technique can also be applied to relax the head pose while looking, by identifying a vision cone that bounds the visual target. Thus, we could define the visual task as an inequality task.

### 5.4.2 Qualitative comparison of torques

After running the simulations of the captured human motion on sDIMS, we obtain the torques exerted by H. Extracting the corresponding task sequence and executing kinematic and dynamic simulations based on the hierarchical solver, makes it interesting to compare the torques executed by the main joints of the body during the motion in these three simulations. Since it is not straightforward to compute the torques from the kinematic simulation, we implemented a test based on the Recursive Newton Euler Algorithm (RNEA) for spatial variables. First, we derive the joint velocities obtained from the kinematic simulation. Then we compute the corresponding contact forces by applying an identification problem. From (3.19), we can select the first 6 rows corresponding to the number of contact variables involved with single contact only.

$$S_c(A\ddot{q} + b + J_c^T \phi_c) = 0, \quad (5.8)$$

where  $S_c = [I_{6 \times 6} \ 0]$  is a matrix that allows to select the non-actuated joints. Therefore, we run the RNEA for each state described by a current position, velocity, acceleration, and the contact forces are added as external forces at the ankle joint. Thus, we obtained the torques exerted during the motion from three different simulations. As explained, the MS model is much more detailed and accurate, but both models have comparable masses and inertia which enable us to compare the torques, at least from a qualitative point of view. Since the resulting motions possess different simulation times, which affect the acceleration rates and therefore the torques, we will not establish a quantitative analysis. In the following, we will discuss our observations and analysis of the resulting simulations. All the resulting graphs are divided into three phases of motion:

- From the start of the motion until reaching the first target.
- From the posture at the first target until the achievement of the second manipulation.
- From the second convergence until the accomplishment of the final reaching task.

**Table 5.3:** Time sequencing of the simulations.

State	Kinematic simulation	Dynamic simulation	Human motion
Start Configuration	0	0	0
First target reached	0.899s	1.999s	3.1s
Second target reached	1.809s	3.799s	5.6s
Final target reaches	1.32s	3.375s	4.75s

The time sequencing is shown in table 5.3, and vertical lines are drawn on the graphs to separate each sequence. By the gain tuning, we try to realize similar convergence times in kinematics, dynamics and real motion. Yet, the choice of setting the gains automatically does not give exact timelines. We can rather vary the gains by studying the convergence of each sequence separately. However, this choice will not truly affect the analysis of the torques evolutions. Since the simulation on sDIMS was based on the motion capture data, the recorded motion was longer than the scenario reproduced by our solver. Therefore, the total time of the simulated motion by sDIMS exceeds the time of convergence of the final task. In figures 5.13(a), 5.13(b) and 5.14, we show the torque trajectories corresponding to this extended time in lighter colors.

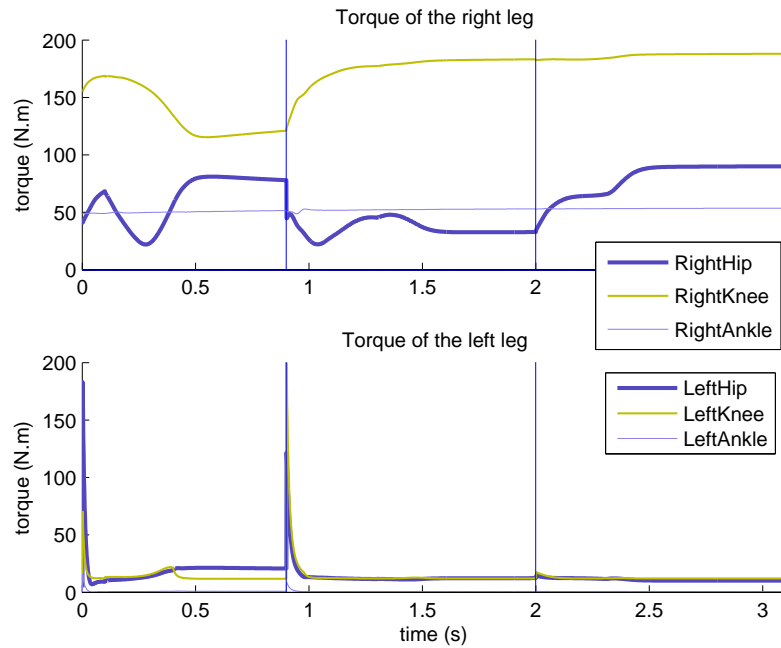
#### 5.4.2.1 Kinematics vs dynamics

In this section, we will compare the resulting torques from dynamics and kinematics. Even if it is improper to obtain torques from kinematics modeling, the reconstruction of the torques gives the efforts that could possibly be induced from kinematics. This enables us to examine the effect of the dynamic resolution of motion. Dividing the body into legs, torso and arms, and comparing their torque trajectories, we deduce some characteristics:

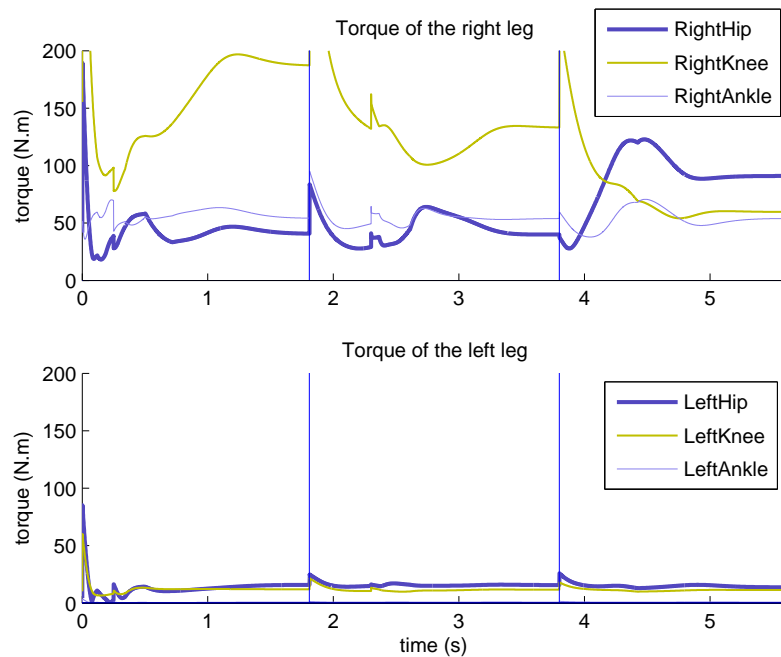
- In the lower body, the knees exert the highest efforts.
- In the upper body, the abdomen and the shoulders present maximum torques.
- Both simulations present discontinuities of the torques due the stabilization of the system before each transition.
- The dynamic simulation gives smoother results.

Figures 5.10(a) and 5.10(b) show respectively the evolution of the norm of the torques of both legs in the kinematic and dynamic simulations. We choose to cut the axes to

## 5. GENERATION OF HUMAN-LIKE MOTION

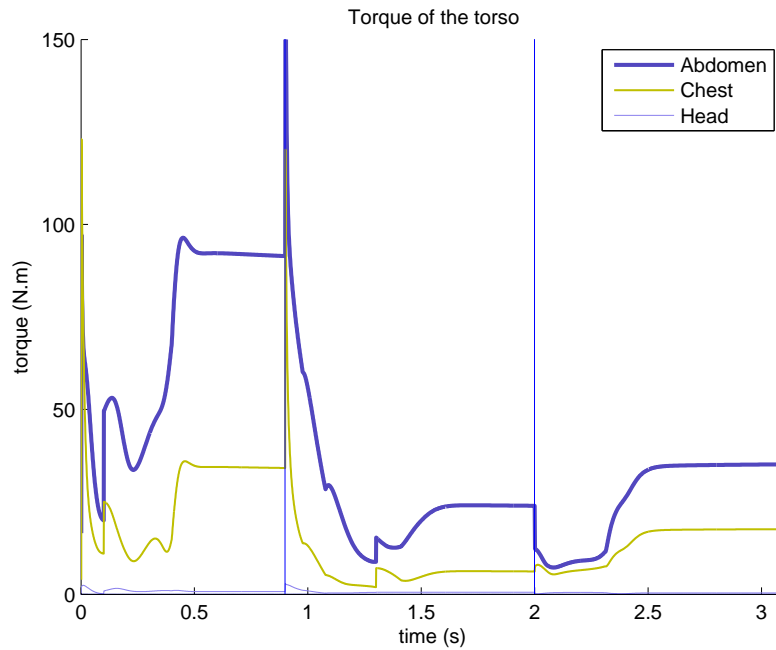


(a) The norm of the torques exerted on both legs of the human model computed from the Recursive Newton-Euler Algorithm by deriving the joint velocities obtained from the kinematic simulation.

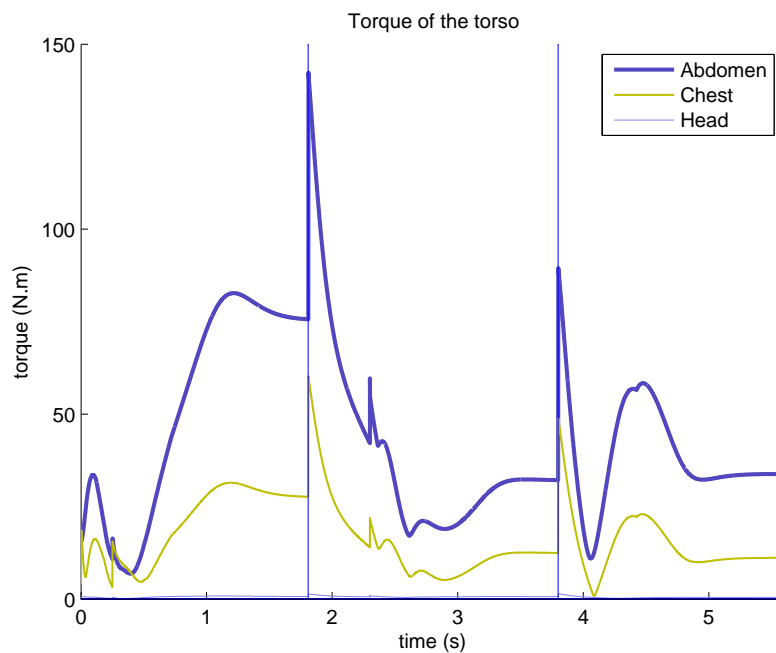


(b) The norm of the torques exerted on both legs of the human model computed from the dynamic simulation.

**Figure 5.10:** The torques variation of the legs.



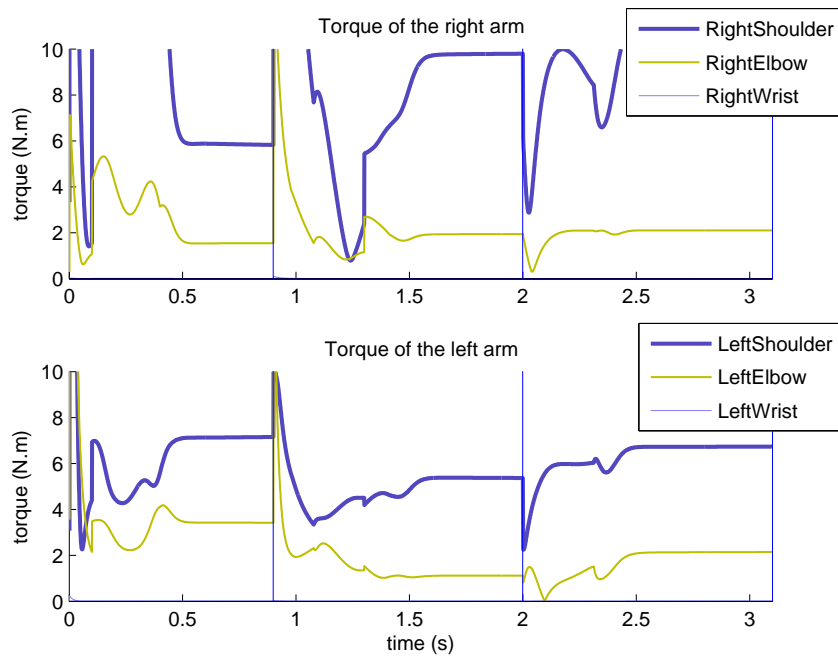
(a) The norm of the torques exerted on the torso of the human model computed from the Recursive Newton-Euler Algorithm by deriving the joint velocities obtained from the kinematic simulation.



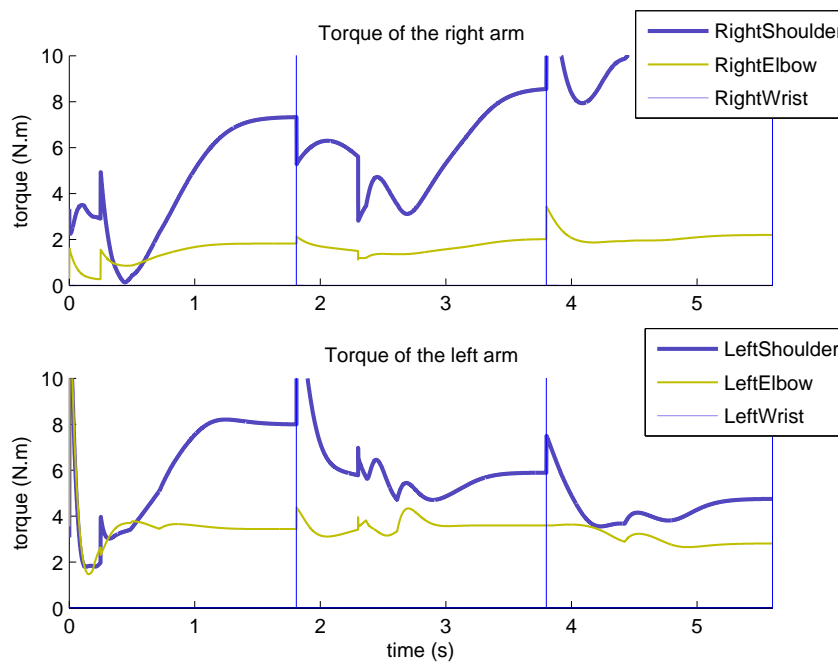
(b) The norm of the torques exerted on the torso (waist, abdomen, chest) of the human model computed from the dynamic simulation.

**Figure 5.11:** The torques variation of the torsos.

## 5. GENERATION OF HUMAN-LIKE MOTION



(a) The norm of the torques exerted on both arms of the human model computed from the Recursive Newton-Euler Algorithm by deriving the joint velocities obtained from the kinematic simulation.



(b) The norm of the torques exerted on both arms of the human model computed from the dynamic simulation.

**Figure 5.12:** The torques variation of the arms.

the norm of  $200N.m$  just to have the same scale for all the plots of the legs. However, no normalization neither scaling are done. Considering the right leg which is in contact with the ground, we notice that the knee exerts the most important torques in both cases. However, we observe that the torques of the knee joint in the kinematic simulation reaches a maximum value and conserves it during the last two phases. Instead, in the dynamic simulation, the knee tends to exert less efforts when the task is achieved. This shows that, by taking into account the masses and inertia of the bodies of the model, the torques are minimized. The ankle and the hip exert similar torques. Comparing with the left leg, moving in the air with less constraints than the right leg, the torques are quite smaller. However, in the bottom of figure 5.10(a) we see higher peaks at each transition, compared to the ones observed in figure 5.10(b) for the left leg. This is mainly due to the derivations computed at the kinematics level. Taking into account the dynamics allows to obtain smoother motion.

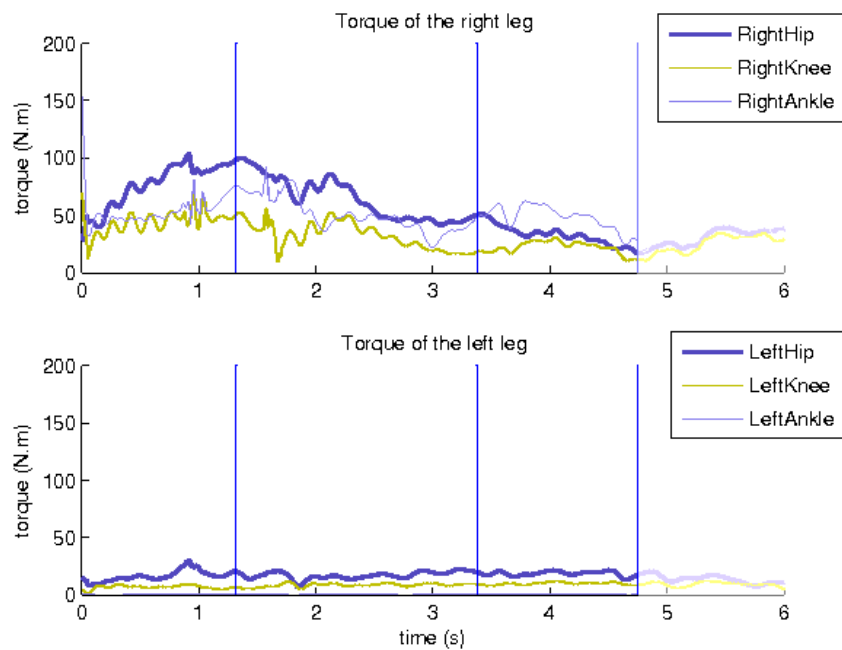
Observing the motion of the upper body and considering the chain from the waist to the head, figures 5.11(a) and 5.11(b) show that the biggest effort is at the abdomen and by moving up in the chain, the efforts decrease from the chest to the head. This applies on both simulations. The resemblance seems to be due to the task of the COM which leads the motion of the torso. For the arms movements, we can see in figures 5.12(a) and 5.12(b) that the shoulders exert the highest torques for both arms and in both simulations. Also, exploring the kinematic tree towards the leaf node, the elbow and the wrist employ lower efforts.

In general, we observe a transient state, in both simulation results, at each transition between a target and another. This result was expected since the tasks follow either a second order law or an exponential decay during the convergence phase to stability. Thus, the system tries to regulate the error of the task. In addition to that, since no prediction is considered, when making a commutation to the next phase high peaks appear. We can notice that the dynamic simulation gives smoother torques evolution. Yet the torques from kinematics are only a reconstruction and therefore, they are not as precise as the dynamic resulting torques. Thus, it is more interesting to compare the dynamic simulation results to the real motion.

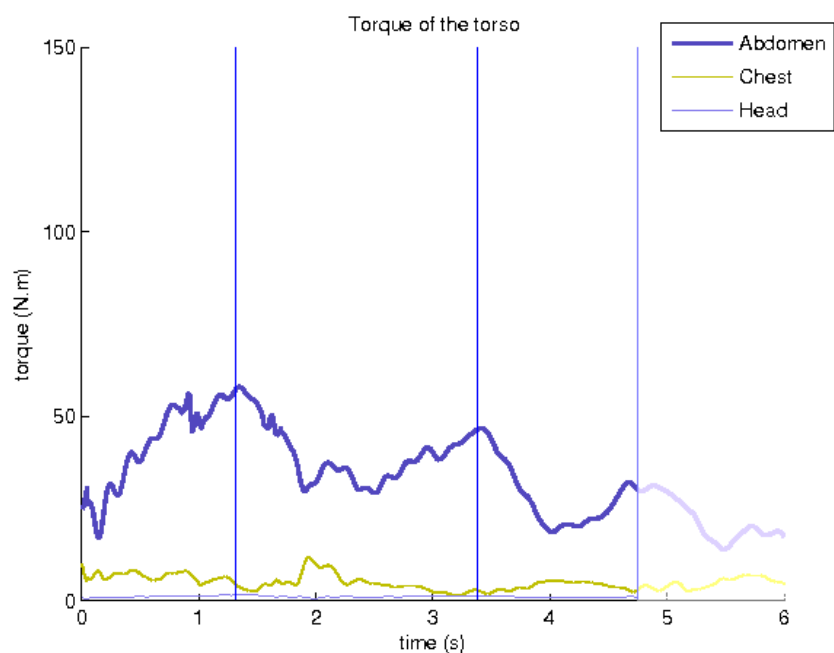
#### 5.4.2.2 Dynamics vs real motion

By observing the torques resulting from the real motion, we can point out the main similarities and differences with the simulated motion.

## 5. GENERATION OF HUMAN-LIKE MOTION



(a) The norm of the torques exerted on both legs of the subject computed from sDIMS.



(b) The norm of the torques exerted on the upper body of the subject computed from sDIMS.

**Figure 5.13:** The torques variation of the human legs and torso.

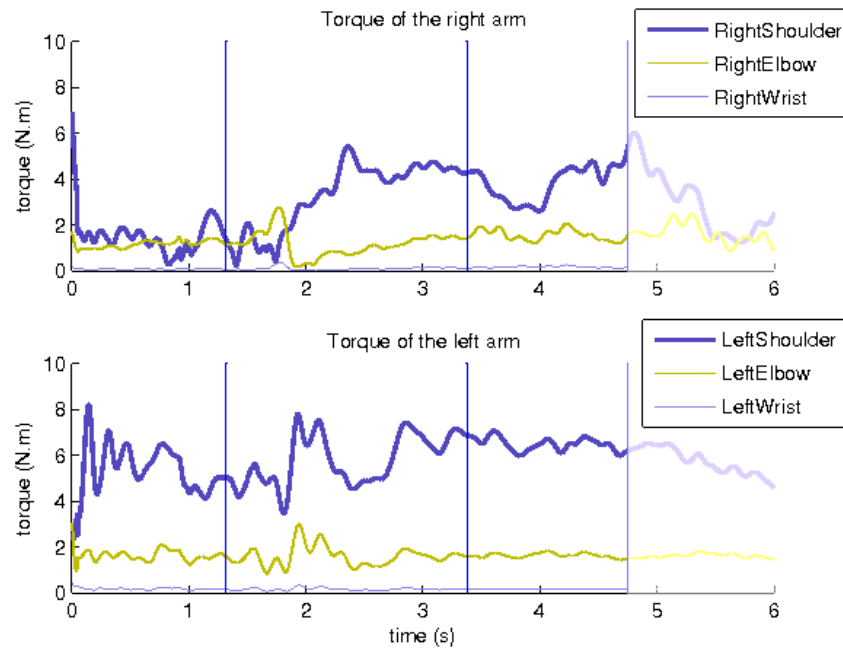


**Figure 5.14:** The norm of the torques exerted on both arms of the subject computed from sDIMS.

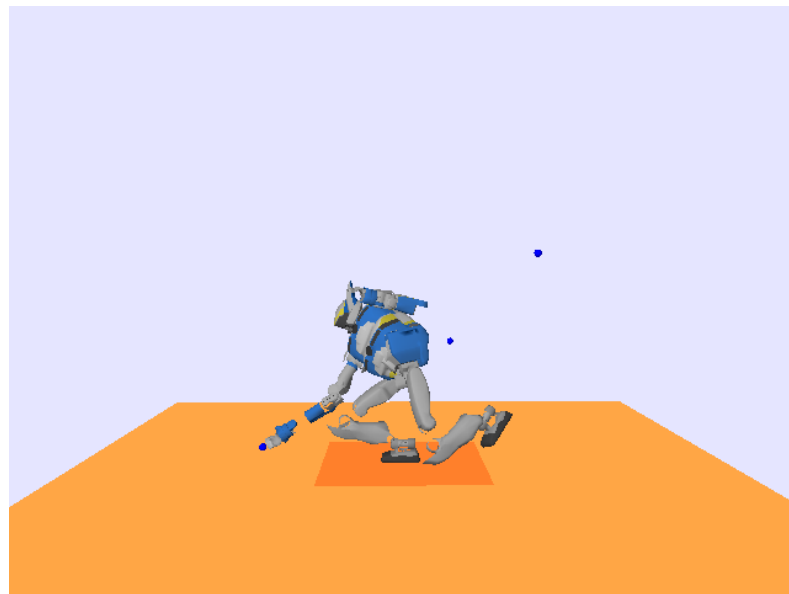


**Figure 5.15:** The posture of the human model in dynamic simulation when reaching the first target with a flexion of the right knee.

## 5. GENERATION OF HUMAN-LIKE MOTION

---

- Similarities:
  - Similar distribution of efforts on the joints of both lower bodies.
  - Similar torque trajectories for both upper bodies.
- Differences:
  - Smoothness of the trajectories obtained in the real motion as opposed to high peaks appearance in the dynamic simulation.
  - Maximum torques corresponding to different joints of both lower bodies.

Analyzing closely the torques variations of H and HM and considering first the right leg, we can give the following interpretations. In the first phase of the motion, it is shown in figure 5.13(a), that the ankle and the knee exert similar efforts while the hip reaches the maximum torque. Comparing with the motion of HM in figure 5.10(b), the efforts at the ankle and the hip are similar, while the highest torque is exerted by the knee. It seems there is a similar decomposition of the efforts in both results, however there is no clear explanation why more efforts appear at the knee instead of the hip. As shown in figure 5.15, the posture of HM shows a flexion of the knee that is more important compared to the human posture of figure 5.7(a) when the first target is reached. At the moment of transition to the second target, we notice a rise of the torques of all joints in both cases, with continuous motion of H as opposed to sudden peaks realized by HM. At the last phase, there is an exchange of the distribution of the right leg torques in both cases. In the dynamic case, the knee and the ankle present the same torques, and the hip becomes dominant. Whereas in the real motion, the hip and the knee exert lower efforts than the ankle. At this stage, the similarity of the knee efforts can be explained by the extension of the right leg in the dynamic simulation. This is presented in figure 5.7(b) where HM posture corresponds to the final posture of H shown in figure 5.7(a), when reaching the final target. It seems that there is always a distribution of torques on all joints of the supporting foot in both resulting behaviors, even if the corresponding higher torques are not exerted by the same joints. The left leg has quite the same torque evolution as shown in figures 5.13(a) and 5.10(b). Certainly, the motion of H is again smoother and does not present peaks as in the dynamic simulation.

The same observation is made on the torso part of H as shown in figure 5.13(b). Also, we can see high efforts at each transition. By exploring the chain from the abdomen to the head, the torques are employed decreasingly. We also notice high peaks in figure

5.11(b) at the moments of transition which are the result of the sequencing of tasks. The torque variations of the arms present also high peaks as seen in figure 5.12(b). Compared to figure 5.14, the right shoulder exerts higher torques in the dynamic simulation. This is due to the push of the chest against the direction of the target in order to keep the balance of the model and to satisfy the COM constraint, which leads to higher efforts on the shoulder to reach the target in the back.

We can conclude that the most important distinction of both motions concerns the *smoothness* of the torque trajectories compared to the dynamic simulation. This is clearly shown in figures 5.13(a), 5.13(b) and 5.14. This interesting characteristic can be related to the natural capacity of the humans to anticipate their movements. The behavior is smoother than with HM since the human already prepares for the next move, knowing beforehand the next target to be reached. However, the torques evolution is globally continuous in the dynamic simulation. The insertion and removal of a task, or the swap in the order of priority, and the change of the target, are events that could create a discontinuity. In our case, we only modify the desired position of the hand and the gaze. Thus at each new convergence, the task error regulates to 0, the system being stabilized. After achieving the task convergence, the definition of a new target would create a big output torque.

### 5.4.3 Synthesis

After describing the similarities and differences in the real motion and the dynamic simulation we can summarize our results and conclude on some properties of both motions.

- Human motion analysis: The real motion is smooth and continuous. Actually, the brain of the human enables anticipation of motion. Knowing a priori the sequence of moves to make, the human can predict the amount of effort that is required for the next movement. Therefore, during some transition phases, we detect an increase of the torque following a growing curve, then a smooth decrease is observed by the decay of the curve.
- Dynamic motion analysis: The human model that we developed does not represent exactly the same human measurements i.e. the masses and inertia, therefore the simulated motion does not reliably reproduce the real one. However, the dynamic simulation gives in general a comparable behavior to the human one. Yet, the motion is not always continuous and it shows peaks at each transition due to the

## 5. GENERATION OF HUMAN-LIKE MOTION

---

new command applied to reach the new target and to visualize this target. Actually, the stack of tasks is modified whenever the defined goals are accomplished. Applying a PD control law for the convergence of the task induces a phase of stabilization by the end of each sequence.

### 5.4.4 Retargeting of motion vs Generation of motion

In this chapter, we presented simulation results that were obtained from “scratch” by defining only a reliable stack of tasks that could reproduce the original human motion. In chapter 4, the goal was to retarget the captured motion and then to edit it, if needed, by adding necessary tasks that made the motion similar to the recorded one. At this stage, we also used the stack of tasks formalism, but mostly for editing. The prior task was defined at the joint level by tracking the actual joint variations of the subject. The retargeting phase that consists of applying an optimization problem to compute these angular values was processed separately. This makes the retargeting and editing of motion more accurate than only applying an equivalent stack of tasks to the desired behavior. However, the post-process of the recorded data is a time consuming process and always needs to be edited to get to a final motion that resembles the reference motion. Moreover, the motion capture procedure itself consumes a lot of time and costs a lot if we want to be fully equipped i.e. with force plates and EMG. In the case of adapting a complete stack of tasks to this reference motion, for automatic generation of motion, the procedure is much faster. Some tuning is always required in order to set the parameters of the tasks, as the gain values and the desired poses. Therefore, we seek to produce a natural and human-like motion by a fast and simple method and without the need of a reference motion. Our dynamic solver is a promising tool for such a purpose.

## 5.5 Conclusion

In this chapter, we validate the application of our software to any anthropomorphic model. The simulation results show that taking into account the dynamics along with a fast definition of prioritized tasks could reproduce more natural movements than considering only kinematics. Visually, we can see that the dynamic model presents better postures than the kinematic model. However, when analysing the torque variations compared to the real motion, we detect some differences typically in the shape of the torque trajectories and their smoothness. This is mostly due to the limitations of our human model.

Therefore, is it interesting to develop a more complete anthropomorphic model like the musculo-skeletal model used in the sDIMS simulator. However, the MS model is very complex and useful for the computation of muscle forces. In our case, we could limit our modeling to the skeletal phase by adding the same number of degrees of freedom and exact masses, inertia and lengths for the bodies. We find it primary to proceed in the near future with the development of a complete human model. In addition to that, we seek better results concerning the torque trajectories by adopting smoothing techniques and continuous definition of tasks. In [Keith, 2010; Keith et al., 2011], many solutions were proposed to solve this problem. The main solution consists in making insertions and removals of tasks by a succession of smooth swap operations between adjacent pairs of tasks. The swap of priority of adjacent pairs of tasks is realized using a method based on a linear interpolation and the removal and the insertion of the lowest priority task are smoothed by the use of an insertion gain. An elegant approach would consist in solving the entire stack of tasks with a unique minimization problem. However, this method prevents from respecting the hierarchical structure of the stack of tasks.

As a future application, we can benefit from our developed software for the workstation design by reproducing sceneries from the real life of workers. This tool would constitute a motion prediction tool that can be integrated in the PLM software family. Therefore, one direct implication is to realize ergonomic evaluation of risk factors at work, then to synthesize preventive techniques from the resulting disorders leading to suggestions or recommendations for modifications in the existing workplaces.

## 5. GENERATION OF HUMAN-LIKE MOTION

---

# 6

## Conclusion and Perspectives

From robotics to life sciences different techniques and studies have been employed to create the binding between both fields. This corresponds to two independent and evolving chains starting respectively from generation and analysis of motion, then converging to a common node of synthesis of motion.

### 6.1 Contributions

In this thesis we addressed the issues of generation and synthesis of motion. Thus, we were interested in modeling, control and realism of the resulting motion. First, we elaborated a dynamic model of the humanoid robot HRP-2 based on the Recursive Newton-Euler Algorithm using spatial vectors. Then, we designed a new dynamic control scheme composed of cascade of QPs that optimize cost functions and compute the torque command while satisfying equality and inequality constraints. The cascade of QPs is derived from a given hierarchized stack of tasks. The computed torques constitute one of the feasible solutions that are required to accomplish the defined tasks and constraints. Another specification of this work is the formulation of a generic multi-contact constraint that allows to consider multiple non-coplanar contacts generalizing stability conditions beyond the ZMP criterion. We demonstrated the efficiency of the developed motion generation method on the humanoid robot HRP-2 in simulation.

In order to build the bridge between humanoids motion generated by robotic algorithms and human motion recorded by motion capture tools, we developed a generation method combining imitation and stack of tasks formalism. This method relies on reshaping the captured data then editing this motion using the definition of tasks and dynamic

## 6. CONCLUSION AND PERSPECTIVES

---

constraints, then resolving the deduced stack with the implemented hierarchical solver. This original method enables to reshape a dynamic human motion and then to reproduce reliably the motion on a humanoid while respecting the dynamics and editing the motion when necessary.

Finally, to tackle the realism of the simulated motion, we developed an anthropomorphic model with more degrees of freedom than HRP-2. We applied our generic solver to simulate motion on this new model. Therefore, we defined a set of tasks that described carefully a chosen scenario played by a real human. We demonstrated, by a simple qualitative analysis of motion, that by considering the dynamics instead of kinematics only, the resulting motion was more human-like. Thus, we were able to reproduce quite similar motion to the real human without requiring the process of acquisition and reshaping of motion.

### 6.2 Perspectives

Future works will focus in general on realizing and analyzing more complex behaviors that reproduce reliably scenes from the real life of humans and mimic the human movement.

On a short term basis some practical and evident adjustments can be considered. First, from the general robotics point of view, it is always important to validate the results on a real platform thus, we seek to apply the generated motion on the real HRP-2 robot. Even if the available HRP-2 is not torque controlled, however, we can still apply the joint trajectories computed by integration of the joint accelerations. Then, from our observations of the simulated motion we find one immediate and necessary improvement to be made which is to introduce additional constraints, such as obstacle avoidance and self-collision. In addition to that, the formulation that we developed for the contact constraint does not express neither take into account the friction forces assuming that they do not affect the respect of the contact condition. Therefore, for the sake of generality, it is preferred to integrate the model and the condition associated with the friction forces.

At the task definition level, the experiments show that each commutation between tasks could lead to discontinuities and non smooth trajectories. This occurs during insertion, removal, change of priority or change of desired behavior of any task or constraint. Smoothing techniques turn out to be the solution for such discontinuities and could be considered in the future to improve the results. Indeed, the formulation of the cascade of QPs as one big optimization problem would also guarantee the continuity of the control outputs.

When comparing the reproduced simulated motion to the reference human motion, we sense the need for the development of a complete anthropomorphic model that represents more precisely the human body, even if only on the skeletal level. This would enable more accurate and similar results that would make our solver trustworthy for applications in the fields of analysis of human motion. Since the human model cannot predict the next movement, distortions in the control outputs appear at each transition of tasks. Thus, it would be interesting to investigate the possibility of adding anticipation in motion and control. This could consist in applying a 2-step resolution method. The first step for computing the non smooth trajectories and the second for adding anticipation, knowing a priori the time and amount of distortion. This sort of prediction would make the behavior of the model smoother and similar to the human's, yet it would complicate the computations.

On a long term perspective, we plan to apply this framework to generate motion on a human model that uses more complex actuation structures to help conceiving workplaces. This work is based on the need of the working French society to dispose of evaluators of risks of injuries at work and preventive techniques from musculo-skeletal disorders. In order to reduce the bad effects of MSD and other risk factors, the companies started to search for preventive measurements towards these various factors. Mostly, these attempts constitute a possible diagnosis of a certain situation and lead to suggestions or recommendations for modifications in the existing workplaces. We intend to exploit our developed solver to define and simulate human-like behaviors that allow an ergonomic design of workstations.

**Génération de mouvements  
corps-complet sous contraintes pour  
des systèmes dynamiques  
anthropomorphes**

# 1

## Introduction

Les **Humains** et les **Humanoïdes** sont comparables, voire actuellement similaires. Cependant, développer un robot ressemblant à l'humain est différent du fait de fournir au robot la capacité d'agir comment un humain. Comme les robots deviennent plus intégrés dans la société, de nouvelles questions se posent comme l'anthropomorphisme des mouvements du robot. Ces questions concernent différents champs de recherche. D'une part, l'interaction homme-robot qui s'intéresse à réaliser un échange amical entre l'humain et le robot en sensibilisant le robot à la présence de l'humain et en lui amenant à faire des mouvements similaires à ceux de l'humain. D'autre part, les développements de la robotique humanoïde servent dans différents domaines des sciences humaines comme la réhabilitation et l'évaluation ergonomique des postes de travail.

Les robots humanoïdes sont des systèmes anthropomorphes particulièrement redondants. La redondance s'explique par la capacité du robot à atteindre une cible avec différentes manières. Par conséquent, de nombreux défis rentrent en jeu dans la génération de mouvement par un robot humanoïde. Les solutions proposées par les roboticiens visent à réaliser un comportement du corps complet. A un niveau d'abstraction, les humanoïdes du futur sont attendus à se déplacer comme des humains. La source d'inspiration la plus évidente est l'humain en étudiant ses mouvements pour extraire des informations utiles à la génération de mouvements par des humanoïdes.

### 1.1 Contexte

Le sujet principal de cette thèse est la génération de mouvements pour des systèmes anthropomorphes. Puisque nous nous intéressons aux systèmes anthropomorphes présentant

## 1. INTRODUCTION

---

des similarités avec les humains, nous sommes concernés par la génération de comportements et de mouvements humains. À ce propos, différentes questions se dérivent:

- Pourquoi choisir le mouvement humain? Le rôle des humanoïdes dans notre société excède les innovations scientifiques et technologiques. Il consiste un secteur croissant de recherche et d'application où les humanoïdes doivent interagir d'une façon réactive au lieu de simplement subir une commande. Ceci s'applique dans le cas d'assistance de personnes âgées, de participation à des spectacles de divertissement ou de remplacement d'ouvriers dans des missions dangereuses pour l'humain. Dans la plupart de ces domaines, l'interaction amicale avec les humains est une obligation. Un autre domaine d'application à signaler concerne l'analyse du mouvement humain. En adaptant les mouvements des humanoïdes à ceux de l'humain, il est possible d'intervenir aux diagnostics médicaux, de résoudre des problèmes de réhabilitation et de réaliser des évaluations ergonomiques des postes de travail.
- Comment générer le mouvement? Les systèmes anthropomorphes, et en particulier, les robots humanoïdes, sont difficilement contrôlables à cause de leur structure arborescente complexe. Les méthodes de génération de mouvement développées en robotique dépendent d'algorithmes et d'outils qui traitent ce genre de problèmes. Ces méthodes dépendent soit de la planification de mouvement, soit de la définition de tâches ou de l'optimisation de critères, et cela constitue ce qu'on appelle les techniques "basées modèle". D'autres méthodes dépendent de l'imitation des humains et peuvent être définies comme "basées données". Grâce à ces méthodes, la simulation de mouvement peut se faire à partir de zéro en se basant sur la modélisation et la commande des systèmes mécaniques, ou en rejouant un mouvement de référence provenant des données de capture de mouvement.

Dans cette thèse, les problèmes de génération automatique de mouvement sont d'abord adressés. Cela constitue le cœur de ce travail nécessitant plusieurs étapes. Parmi les méthodes de génération de mouvement existantes, nous choisissons d'adopter une approche basée modèle. Ce choix est justifié par notre but de fournir un logiciel de génération de mouvement rapide, fiable et autonome. En particulier, notre travail se concentre sur la génération de mouvement par résolution d'un ensemble de tâches définies par ordre de priorité dans le but de produire un comportement désiré. Ceci amène à trouver un lien entre la tâche et le mouvement du corps complet qui devrait respecter certaines propriétés comme l'équilibre et le naturalisme du mouvement. Pour la simulation d'un tel mouvement, trois problèmes majeurs doivent être pris en compte:

- La redondance du modèle humain.
- La génération du mouvement corps complet en satisfaisant plusieurs contraintes.
- La réalisation de mouvement humain

Une tâche est définie comme une propriété cinématique ou dynamique du robot. En considérant la dynamique du système, nous cherchons à obtenir un mouvement dynamiquement stable pouvant résulter des mouvements naturels. La dynamique permet de considérer les masses et inerties dans la modélisation du système anthropomorphe. De plus, les forces de contact peuvent être intégrées dans la résolution de l'équation dynamique du mouvement. Cette résolution définit les couples articulaires nécessaires pour accomplir les tâches désirées. Ayant un système fortement redondant, une infinité de solutions possibles peuvent être trouvées. Ce problème de redondance est résolu soit en appliquant un problème d'optimisation en considérant la tâche comme une fonction coût à minimiser ou en adoptant des techniques d'inversion numérique. Afin de bénéficier de la redondance, plusieurs tâches peuvent être déterminées ainsi la somme des fonctions coûts associées aux tâches est minimisée. Cependant, si les tâches deviennent contradictoires, l'algorithme numérique peut amener le robot à un état où aucune des tâches n'est satisfaite. Pour contourner ce problème, un ordre de priorité peut être attribué à chaque tâche afin que le système puisse réaliser les tâches les plus prioritaires. Au mieux, toutes les tâches seront accomplies. Un type important de tâches à considérer est la tâche bilatérale. Les algorithmes classiques d'hiérarchisation ne permettent pas de considérer ce type de tâches. Néanmoins, ils ont été développés pour tenir compte des inégalités en résolvant une cascade de Programmes Quadratiques (QPs) au niveau cinématique. Cherchant à comparer le mouvement des humanoïdes au comportement d'un humain réel, nous développons un solveur dynamique hiérarchique basée sur la formulation cinématique des QPs. À cet effet, nous adoptons un modèle dynamique du robot humanoïde HRP-2 présent au LAAS. En considérant la dynamique du système, nous pensons pouvoir produire un mouvement plus précis et similaire à celui de l'humain. Pour cette raison, un solveur est développé et composé de plusieurs problèmes d'optimisation ordonnés dans une pile hiérarchisée sous contraintes dynamiques. Les fonctions coûts sont classées par ordre de priorité et résolues en respectant cet ordre, afin d'exécuter la tâche attendue en respectant la dynamique du système. Les tâches et contraintes peuvent être exprimées comme des égalités ou des inégalités permettant de considérer tout type de mouvement. Ainsi, la cascade de problèmes d'optimisation définis comme programmes quadratiques

## 1. INTRODUCTION

---

est résolue itérativement, pour calculer, à chaque pas de temps, de nouveaux paramètres de commande réalisant les tâches données et respectant les contraintes dynamiques. La première contribution de cette thèse est le développement d'une méthode de génération de mouvement corps complet considérant la dynamique et conservant l'équilibre du robot humanoïde sous contraintes unilatérales et bilatérales. En particulier, nous considérons des contacts multiples non-coplanaires en développant une formulation générique de tout genre de contact planaire.

La deuxième partie de ce travail traite les questions de naturalisme de mouvement. Puisque les humanoïdes et les humains présentent des formes similaires, quoique le corps humain est beaucoup plus complexe, nous nous intéressons à rejouer des mouvements capturés, par recalage des données acquises, afin d'obtenir des résultats plus exacts. En utilisant notre logiciel développé pour la génération de mouvement d'un modèle dynamique, nous appliquons ce solveur pour l'édition et la simulation d'un mouvement humain de référence sur le robot. Au lieu de se limiter uniquement à l'imitation du mouvement, les données enregistrées sont traitées de façon à définir des trajectoires articulaires de référence pour le robot humanoïde. Ensuite, ces trajectoires pré-calculées sont définies comme une tâche de référence considérée comme tâche primaire dans la pile. Après, d'autres tâches supplémentaires peuvent être ajoutées pour éditer le mouvement résultant afin de reproduire exactement et fidèlement le mouvement d'origine. Le second aboutissement de ce travail réside dans l'originalité de la technique développée pour le mélange de mouvement pouvant amener l'humanoïde à exécuter un mouvement faisable et humain, en se basant sur des données de capture de mouvement.

Après avoir couplé les deux techniques de définition de pile de tâches à l'imitation de mouvement capturé, nous proposons de simuler un mouvement d'un humain sur un modèle humain sans passage par le recalage de données mais uniquement par une description d'une pile de tâches pouvant reproduire fidèlement le mouvement observé sur l'humain. Ceci a pour but de valider la généralité de notre logiciel et la simulation de comportements humains similaires. L'idée qui repose à l'origine de ce travail est la capacité de développer une méthode applicable à tout modèle anthropomorphe et d'analyser les mouvements simulés résultants en les comparant au mouvement humain de référence.

Le solveur dynamique et hiérarchique de tâches d'égalités et d'inégalités est un outil prometteur pour la résolution du problème de génération de mouvement corps complet sur des systèmes anthropomorphes dynamiques. Différentes applications dans les domaines d'analyse de mouvement humain constituent une motivation pour cette étude. Actuellement, une préoccupation importante de la population active est l'évaluation des postes

de travail aux niveaux ergonomiques et préventifs des accidents dûs aux risques de travail et l'efficacité du travail.

## 1.2 Répartition de la thèse

Cette thèse est composée de quatre chapitres principaux. Dans le chapitre 2, nous rappelons les différentes méthodes existantes pour la génération de mouvement. Ensuite, nous expliquons comment la combinaison des études des sciences du vivant sur le mouvement humain avec les algorithmes et outils de simulation issus de la robotique peuvent conduire à la génération, analyse et compréhension du mouvement humain. Puis, nous expliquons comment bénéficier de cette connaissance pour nourrir différentes applications afin de servir les humains.

Le chapitre 3 élabore les principes et le développement du solveur dynamique et générique de tâches hiérarchisées sous plusieurs types de contraintes. Différents scénarios définis par diverses piles de tâches et contraintes avec multiples forces de contact sont résolues. Cette méthode permet de produire le mouvement automatiquement en conservant l'équilibre dynamique et en satisfaisant les contraintes et vérifiant les conditions de contact coplanaires et non-coplanaires. Des simulations sur le robot humanoïde HRP-2 sont présentées pour illustrer la validité de la méthode.

Dans le chapitre 4, nous utilisons le même solveur pour recalibrer et éditer les données de capture de mouvement. Ceci permet de créer une nouvelle technique de mélange de mouvement assurant la fiabilité du mouvement résultant par une méthode assez rapide. Ces deux chapitres constituent la contribution principale de la thèse.

Une application à un modèle humain est présentée dans le chapitre 5, permettant de vérifier la généralité de l'approche. Ici, on adresse le problème de reproduction d'un mouvement réel en se basant uniquement sur la définition d'une pile de tâches. Nous établissons une analyse qualitative du mouvement simulé. Nous visons à fournir un outil de génération de mouvement similaire à l'humain pour l'analyse du mouvement humain.

## 1. INTRODUCTION

---

## 2

# État de l'art

## 2.1 Contexte

De nos jours, les humanoïdes deviennent similaires aux humains [Kaneko et al., 2009; Nakaoka et al., 2009]. Cependant, jusqu'à présent, cette innovation controversée présente peu d'applications qui concernent principalement les activités de divertissements. Une autre contribution importante pourrait être développée dans le domaine de l'interaction avec l'homme, par exemple, pour l'assistance des personnes âgées, puisque l'apparence humaine du robot permette un échange amical. Mais c'est toujours un travail en progrès. Alternativement, les robots humanoïdes peuvent rendre service aux humains en intervenant dans la résolution des problèmes de réhabilitation [Venture et al., 2007] ou l'évaluation ergonomique des postes de travail [Hue, 2008]. De ces différents types d'applications physio-sociales, un lien étroit est créé entre les humains et les robot humanoïdes qui sont contrôlés par des méthodes de génération de mouvement devant produire des comportements similaires à ceux des humains sur la base de propriétés de mouvement humain. Ces propriétés dérivent des sciences humaines, comme la biomécanique ou les neurosciences, et elles constituent des normes à suivre en générant le mouvement sur les robots humanoïdes. En respectant ces contraintes, des chercheurs ont pu développer un mouvement comparable à l'humain à différents niveaux. Notre principale préoccupation est de développer une méthodologie automatique de simulation de mouvements anthropomorphiques corps complet respectant la dynamique des corps en mouvement. Le but ultime est d'arriver à réaliser des comportements pareils à ceux de l'humain en tenant compte de différents types de contraintes et par conséquent d'appliquer cette méthode générique de génération de mouvement dans les domaines d'analyse de mouvement humain. Différentes méthodes

## 2. ÉTAT DE L'ART

---

de **génération**, d'**analyse** et d'**évaluation** de mouvement humain existent et seront discutées plus tard. La figure 2.1 représente ces méthodes dans différents blocs, et montre les liaisons entre elles. étant donné un mouvement humain, différentes techniques provenant des sciences humaines proposent d'analyser ce mouvement et de synthétiser des propriétés correspondantes. Tandis que des développeurs dans le monde de la robotique comptent modéliser un robot humanoïde pour générer et simuler son mouvement. Tout d'abord, nous sommes intéressés par l'implémentation d'un algorithme complet pour la résolution de l'équation dynamique du mouvement sur un système multi-corps, ensuite la génération de mouvement dynamique corps complet par le robot humanoïde HRP-2 en simulation et finalement la validation de la généralité de cette méthode en l'appliquant sur tout type de modèle anthropomorphe afin de montrer la nature humaine du mouvement.

### 2.2 Méthodes de génération de mouvement

La méthode de génération de mouvement consiste à l'élaboration de lois de commande applicables sur différents systèmes à l'exemple de manipulateurs, robots mobiles, robots bipèdes ou un avatar quelconque, et spécifiquement des systèmes anthropomorphes comme les robots humanoïdes. Dans notre travail, nous nous sommes intéressés à la génération de mouvement en vue de reproduire des comportements humains dans différentes situations ou actions. Ces situations sont spécifiquement choisies telles qu'elles reflètent la capacité de conservation de l'équilibre dynamique en accomplissant des tâches difficiles. Pour cela, il est utile d'avoir un aperçu général sur les diverses méthodes existantes ainsi que leurs caractéristiques. En fait, la génération de mouvement humain constitue un sujet de recherche croissant donnant soit uniquement des trajectoires de marche ou aussi des mouvements des membres supérieurs du corps, et enfin obtenir des mouvements corps complet stables en gérant la coordination des membres inférieurs et supérieurs. Certains travaux de recherche se focalisent sur des tâches de manipulation nécessitant le mouvement des bras et du torse comme dans [Fourquet et al., 2007]. Dans ces travaux, le modèle considéré possède une partie supérieure du corps mobile et une partie inférieure fixe. D'autres chercheurs s'investissent dans la locomotion bipède et traitent les mouvements de coordination entre les différentes parties du corps, nous en citons par exemple [Kajita et al., 2003]. Dans ce domaine de recherche, des problèmes difficiles surgissent dus à la nature instable de la structure bipède et la complexité des structures mécaniques.

Les modèles anthropomorphes comme les avatars ou les robots humanoïdes sont difficiles à animer ou à contrôler à cause des nombreux degrés de liberté à coordonner afin de

## 2.2 Méthodes de génération de mouvement

---

bouger d'une façon comparable à l'humain. Deux classes de techniques semi-automatiques sont élaborées pour le développement de méthodes de génération de mouvement:

- Les approches basées sur un modèle, se servant de la simulation, recherche et optimisation pour générer le mouvement en restreignant l'espace possible de mouvements via la cinématique ou la dynamique dans le cas d'applications en robotique, ou par des modèles biomécaniques pour des applications médicales, de réhabilitation ou de divertissement:
  - Planification géométrique de mouvement
  - Cinématique inverse
  - Dynamique inverse
  - Optimisation numérique
- Les approches basées sur les données de capture de mouvement considérées comme référence pour reproduire les mouvements sur le modèle. Ces données contiennent les détails de mouvement subtils enregistrés sur un humain:
  - Imitation de mouvements capturés

En fait, afin d'amener un robot à réaliser un mouvement désiré, différentes méthodes peuvent être choisies selon le contexte, l'application et la complexité des tâches à exécuter. Pour des tâches complexes difficilement décomposables, la méthode généralement adoptée est de calculer directement la trajectoire à suivre par le robot. Ceci est intéressant en particulier dans des environnements contraints où le robot doit se déplacer et accomplir des tâches en évitant des obstacles [Kuffner, 1998]. Pour des tâches variées sollicitant différents organes terminaux où il est important de garantir la réalisation de tâches prioritaires, même si les mouvements deviennent contradictoires, le formalisme de la fonction de tâche [Samson et al., 1991] est utile. Ce formalisme se base sur des schémas de priorisation [Siciliano and Slotine, 1991; Baerlocher and Boulic, 1998] et définit l'outil le plus intéressant dans la gestion des systèmes fortement redondants. Il s'applique aux deux niveaux de modélisation, cinématique [Nakamura and Hanafusa, 1986] et dynamique [Khatib, 1987]. Pour des mouvements extrêmes, les trajectoires peuvent être calculées en utilisant une méthode basée sur l'optimisation – comme le mouvement de coup de pied ou de lancement présentés dans [Miossec et al., 2006; Lengagne et al., 2010] – ou en copiant et adaptant une trajectoire observée, comme la danse “aizu-bandaisan odori” reproduite

## 2. ÉTAT DE L'ART

---

par le robot humanoïde HRP-2 [Kaneko et al., 2004] en prenant comme référence une performance d'un professionnel [Nakaoka et al., 2005].

### 2.3 Méthodes d'analyse de mouvement

Comme il a été précédemment mentionné, le mouvement exécuté dans l'espace articulaire en réponse à une tâche référence, définie dans l'espace opérationnel, n'est pas unique. Alors, il est nécessaire de choisir parmi les mouvements plausibles afin de générer une solution automatique. Pour trouver une telle solution, il est intéressant d'étudier la nature du mouvement humain. Dans cette perspective, plusieurs chercheurs dans les domaines de la physiologie, des neurosciences et de la biomécanique se sont basés sur la compréhension des mécanismes cognitifs impliqués durant le mouvement, l'étude du contrôle moteur ou la prédiction du mouvement. En fait, il est préférable de réduire le nombre de solutions en conservant celles qui sont les plus probablement réalisées par un humain. En d'autres termes, le problème est d'identifier les propriétés et les critères en observant les humains et ensuite de s'en servir pour générer de nouveaux mouvements sur des systèmes anthropomorphes.

Cependant, la compréhension du mécanisme de génération et de coordination des mouvements humains s'avère toujours un problème ouvert. Dans la communauté des sciences cognitives, spécifiquement concernée par l'étude du cerveau, les chercheurs tentent d'analyser et de modéliser la façon dont le cerveau coordonne le mouvement du corps entier [Flash and Hogan, 1985; Kawato et al., 1990]. Cependant, dans la communauté de la biomécanique, le calcul de la dynamique et l'analyse du mouvement sont étudiés en utilisant des modèles musculo-squelettiques [Delp and Loan, 2000; Bhargava et al., 2004; Rasmussen et al., 2003; Anderson and Pandey, 2001b]. Les deux approches sont complémentaires mais elles ne peuvent toujours pas assurer la solution complète au problème.

En fait, le corps humain est largement complexe puisqu'il est composé d'un nombre considérable d'os et de tissus dont l'organisation est toujours partiellement connue. En outre, le système neuro-musculaire et ses liens avec le cerveau ajoutent une complexité supplémentaire. Alors il serait nécessaire d'acquérir des connaissances importantes pour comprendre le mouvement humain. Le système nerveux central ne peut pas tout contrôler d'une manière unifiée et semble utiliser des simplifications pour réduire la complexité, par exemple, en réduisant le nombre de degrés de liberté contrôlables [Bernstein, 1967; Vereijken et al., 1992]. Les différents modèles proposés dans la littérature, dans n'importe

## 2.3 Méthodes d'analyse de mouvement

---

quel domaine scientifique, s'appuient sur des simplifications du système humain réel. En effet, une hypothèse admise indique qu'une sorte de système de commande hiérarchisé existe [Berthoz, 2003]. En réalité, nous pouvons représenter le contrôle du mouvement humain hiérarchiquement dans la figure 2.4.

Physiquement, il est commun de représenter le corps humain par un système de corps rigides (généralement les os ou groupe d'os) articulés par des joints mécaniques permettant principalement les rotations. Nous ajoutons à ce modèle squelettique, les muscles enrobant les corps. Les muscles sont activés par des commandes neuronales. Ensuite, comme les forces musculaires sont reliées aux couples articulaires par des lois de la mécanique, la dynamique peut-être calculée et les accélérations sont dérivées. Par intégration, les vitesses, les trajectoires et finalement le chemin pour atteindre la cible sont synthétisés. Plus nous descendons dans la hiérarchie, plus nous perdons de causalité puisque les décisions sont prises au niveau du cerveau et la majorité des commandes sur les mouvement des corps sont données au niveau neuronal. Plus nous montons dans la hiérarchie, plus nous gagnons en terme de redondance, sachant qu'à chaque niveau, le nombre de degrés de liberté augmente tandis que la dimension des entrées connues est réduite, menant à plusieurs solutions possibles pour réaliser une même cible. De plus, l'être humain est en contact avec l'environnement externe. Grâce aux informations reçues par ses différents capteurs sensoriels, de nombreux mécanismes aident l'humain à s'adapter à son environnement en vue d'exécuter des tâches complexes. Ces mécanismes sont généralement impliqués dans la boucle de perception, commande et action.

En se basant sur l'analyse et l'étude du mouvement humain, la connaissance et la compréhension de ces mouvements sont alors utiles dans différents champs d'applications. Dans le domaine médical, par exemple, des disciplines comme la biomécanique et les neurosciences tendent à comprendre et interpréter le mouvement humain au mieux. En ce qui concerne les problèmes de santé, la lutte contre l'obésité, le traitement et l'intégration des handicaps, ils sont considérés comme des points clés dans la société moderne. L'exercice physique est devenu une méthode de traitement bien connue et appréciée par un grand nombre de chercheurs motivés. Dans le domaine de sport, les spécialistes accordent une grande importance à l'étude de tous les mouvements ou gestuels afin d'améliorer les performances des joueurs. Récemment, les domaines de multimédia e.g. les jeux vidéos, les films animés etc., visant à animer des avatars virtuels d'une façon réaliste, s'intéressent aussi à l'analyse du mouvement humain. Ces études ont pour but de comprendre les mécanismes cognitifs élaborés durant un mouvement quelconque, le contrôle moteur et la prédiction des mouvement. L'informatique a un rôle important dans ce domaine en

## 2. ÉTAT DE L'ART

---

fournissant les outils d'analyse, de compréhension et de traitement, impliquant une communication importante entre les différentes disciplines scientifiques: nutrition, physiologie, médecine, biomécanique, neurosciences, sport, physique, mécanique, commande, etc. Ces résultats conduisent à la reconnaissance d'invariants, de caractéristiques et de paramètres existants dans le mouvement humain, e.g. la forme de la trajectoire d'un organe terminal, l'optimisation d'un certain critère. En plus de ces facteurs techniques et technologiques, l'état psychologique des sujets percevant l'animation joue aussi un rôle [Slater and Usoh, 1993].

### 2.4 Analyse ergonomique du mouvement

Dans le domaine de la robotique, plusieurs chercheurs se sont intéressés à la génération du mouvement humain corps complet d'une façon réaliste, pour différentes raisons dont la conception des postes de travail. A cette fin, ils se sont référés aux critères et invariants du mouvement humain identifié par les communautés de biomécanique et neuro-physiologie pour générer des mouvements similaires à ceux réalisés par des humains. En accomplissant tels objectifs, les problèmes de l'*ergonomie* sont adressés. L'*ergonomie* est la discipline scientifique qui étudie les interactions entre les humains et s'intéresse à la conception d'équipements et d'appareils qui s'adaptent au corps humain, ses mouvements et ses capacités cognitives. L'ergonomie est employée pour remplir les objectifs de la santé et de la productivité. Elle est utile pour la conception de l'environnement de travail sécurisé. Une conception ergonomique convenable et correcte est nécessaire pour prévenir des microtraumatismes, qui peuvent s'aggraver avec le temps et mener à des handicaps à long terme.

Parmi les raisons multiples à l'issue des pathologies du travail, les plus communes sont reliées aux troubles musculo-squelettiques (TMS). En effet, l'analyse ergonomique de mouvement possède une origine sociale et économique due à une explosion du nombre de TMS au travail. Ils représentent un problème de santé majeur au travail principalement dans les pays industriels. Les TMS des membres supérieurs comme l'épaule, le coude et le poignet représentent 68% des maladies professionnelles indemnisées en France. Différentes méthodes et normes sont développées et identifiées, ensuite, utilisés pour l'évaluation de la conception des postes de travail. Järvinen & Karwowski [Järvinen and Karwowski, 1992], Lauring [Lauring, 2004] puis Marsot & Claudon [Marsot and Claudon, 2006] ont introduit un état de l'art des différents outils et ont identifié différentes familles d'évaluateurs ergonomiques. Le développement de nouveaux outils qui prennent en compte les facteurs

humains dans la conception des postes de travail est en croissance. Ceci implique particulièrement une meilleure estimation des critères utilisés pour l'évaluation des postes de travail ainsi qu'une prévention des risques d'accident de travail.

### 2.4.1 Lien avec la Robotique

L'analyse du mouvement humain est lié à la robotique, et plus particulièrement à la robotique humanoïde, en fonction des domaines d'application et compte tenu de l'analogie entre la modélisation des humanoïdes et des humains. Ce lien constitue un rapport direct avec mon travail et une extension immédiate de ma thèse. Visant à développer un outil générique, automatique et dynamique pour la génération de mouvement et d'élaborer des modèles anthropomorphiques, le mouvement corps complet résultant devrait ressembler à celui de l'humain. Ainsi, l'extraction de synthèses sur le mouvement humain en comparant avec ses propriétés constitue un principal intérêt. Cette étude peut être exploitée pour différentes applications comme la réhabilitation et l'ergonomie. Afin de réaliser cette étude, une collaboration interdisciplinaire de spécialistes dans les domaines des sciences du vivant, l'ergonomie et la robotique, doit avoir lieu. Les modèles cinématiques et dynamiques des systèmes poly-articulés issus de la robotique offre une base intéressante et rigoureuse pour l'élaboration de simulateurs numériques qui visent à reproduire et anticiper les situations critiques générant des pathologies musculaires. Ceci constitue une partie du problème général de conception des postes de travail pour une efficacité à court terme dans la productivité et le cycle du temps, et des performances à long terme avec minimisation des risques de TMS. L'objectif est de permettre la prévision des mouvements de manière réaliste, et aussi de certains efforts, requis pour des tâches de manipulation ou de locomotion.

En fait, même si un grand nombre de postes de travail répétitif considèrent des tâches effectuées en position assise ou debout et fixe, le vrai travail est habituellement une combinaison d'actions de locomotion et manipulation. Nous visons à développer des méthodes et des solutions en réponse à cette question, tout en envisageant deux conditions. D'une part, la simulation de tâches répétitives nécessitant le mouvement de l'opérateur entre les différentes zones de manipulation en position debout en simple ou double support. D'autre part, la coordination des membres supérieurs et inférieurs du corps, tout en réalisant des tâches dans l'environnement et modifiant le nombre de contacts.

La robotique fournit les fondements et les concepts de modélisation de la mécanique des humains et permet de définir les relations entre la tâche à accomplir et les mouvements

## 2. ÉTAT DE L'ART

---

possibles, dans le cadre général de génération de mouvement des chaînes articulées. Pour un modèle numérique dérivé de la mécanique, il existe une infinité de comportements pouvant produire une même tâche donnée. En robotique, cette redondance ne cause pas de problèmes. La principale spécificité du thème proposé provient de la nécessité de produire des séquences de mouvements réalistes choisis parmi un ensemble de solutions plausibles. Par conséquent, l'utilisation des modèles issus de la robotique et des méthodes de génération de mouvement basées sur l'hierarchisation afin de gérer la redondance, est considéré comme un point de départ pour établir un mouvement du corps complet. Ensuite, l'élaboration d'un cadre générique, à la fois simple pour les utilisateurs et produisant un mouvement réaliste humain, vient en seconde priorité. Puis, en comparant ou en adaptant le mouvement simulé à un mouvement humain réel capturé fournit une bonne base pour la validation du travail et de l'analyse du mouvement simulé. Par conséquent, cette étude implique des applications dans les différents domaines des sciences du vivant.

# 3

## Génération de mouvement dynamique sous contraintes d'égalité et d'inégalité hiérarchisées

### 3.1 Contexte

Comment générer des mouvements corps complet stables pour les robots humanoïdes d'une manière générique? En raison de la complexité de la structure arborescente de ces robots et de l'instabilité de leur posture bipède, cette question est très difficile. Comme ces systèmes poly-articulés comprennent de nombreux degrés de liberté, ils sont généralement fortement redondants par rapport aux tâches habituelles, et donc ils sont difficiles à contrôler. Par ailleurs, toutes les contraintes diverses doivent être considérées lors de la conception du mouvement. Ces contraintes peuvent découler de la dynamique interne, la définition des tâches ou l'interaction avec l'environnement. Selon la situation, ces contraintes sont considérées strictes, devant être prioritaires sur toute autre tâche, ou des contraintes de type mou, devant être respectées au mieux, afin d'optimiser les propriétés dynamiques du mouvement. Ces contraintes sont de deux types: unilatérales (par exemple, une vitesse nulle aux points de contact rigide), et bilatérales (par exemple, la position, la vitesse et le couple articulaires bornés dans des limites données). Différents développements concernant la redondance et la priorité des tâches ont été proposés dans la littérature robotique et discutés dans le chapitre 2.

Puisque le mouvement du corps complet est naturellement dynamique impliquant aussi des forces de contact, une modélisation dynamique est donc nécessaire. Les tâches doivent

### 3. GÉNÉRATION DE MOUVEMENT DYNAMIQUE

---

également être définies au niveau dynamique afin de déterminer les couples d'actionnement nécessaires pour l'exécution du mouvement. Comme expliqué dans la § 2.2.3, plusieurs approches considèrent les techniques de priorité dans une formulation dynamique écrite dans l'espace opérationnel. Dans cette famille de méthodes, les contraintes unilatérales sont décrites comme des champs de potentiels et traitées comme une contrainte de moindre priorité. La formulation existante la plus générique, a été proposé par Sentis et al. [Sentis, 2007], en déterminant une hiérarchie de tâches pour la résolution de multiples contraintes et contacts. Cependant, les contraintes de contact ne sont pas explicitement prises en compte. D'autre part, de nombreuses approches ont été développées pour considérer explicitement des contraintes d'inégalité avec le modèle dynamique. Un schéma original, a été proposé dans [Mansard et al., 2009a], pour calculer une loi de commande dynamique et générique à partir d'un ensemble de contraintes hiérarchisées à la fois unilatérales et bilatérales. Un solveur double-phase, basé sur des problèmes quadratiques statiques et dynamiques, est conçu dans [Collette et al., 2007] pour parvenir à un contrôle dynamique stable de robots humanoïdes envisageant des mouvements de saisies multiples et des contacts de frottement non coplanaires. Ce solveur constitue une partie d'une architecture globale de contrôleurs de bas niveau (le solveur QP) et de haut niveau. Dans le haut niveau, le robot analyse son état et décide par la suite d'agir suivant une stratégie, soit en réagissant à une perturbation ou en réalisant une séquence de tâches, pour garder son équilibre et satisfaire les contraintes. Cette méthode semble être efficace pour contrôler un robot humanoïde avec un nombre important de degrés de liberté. Pourtant elle est assez complexe et interdépendante, dû au calcul réalisé a priori pour la résolution des QPs statiques, ainsi un niveau supérieur de commande devrait prendre les décisions a posteriori. Notez que le solveur n'adopte pas la hiérarchisation des contraintes, elles sont toutes résolues simultanément, ce qui pourrait rendre le problème infaisable. Dans cette perspective de développement de contrôleurs pour la simulation ou la démonstration de mouvements d'un robot humanoïde sujet à de multiples contacts variables, de nombreux chercheurs combinent les modèles dynamiques avec les techniques de planification de mouvement dans un cadre à double étage de contact-avant-mouvement planifié. Il consiste à planifier une séquence de multi-contacts avec les postures statiques correspondantes, qui amène un robot humanoïde d'une configuration initiale à une position/configuration désirée. Dans [Escande et al., 2006], le planificateur est basé sur la construction successive et itérative d'un arbre de nœuds définissant une séquence de contacts commutatifs et d'états, puis la génération de postures correspondant à ces états et résultant en un mouvement continu. à partir d'un ensemble initial de contacts, le générateur de postures résout

le mouvement en optimisant un critère géométrique sous contraintes dynamiques. Par conséquent, le mouvement est contraint uniquement à respecter l'équilibre quasi-statique. Une approche similaire a été adoptée dans [Hauser et al., 2005]. La nature géométrique de ces techniques ne permet pas l'intégration des contraintes de mouvement dynamique dans la planification. Différentes solutions ont été proposées dans le domaine de planification de mouvement comme les techniques de filtrage [Kuffner et al., 2002; Belousov et al., 2005; Yoshida et al., 2005]. Récemment, [Bouyarmane and Kheddar, 2011b], a étudié une approche différente qui synthétise directement un mouvement dynamique consistant. Cette méthode est décomposée en deux niveaux formant l'approche globale de contact-avant-mouvement planifié. Le premier consiste à synthétiser l'information obtenue lors de la planification des positions des multi-contacts [Bouyarmane and Kheddar, 2011a, 2010]. Le second permet de générer le mouvement entre ces positions en appliquant un contrôleur multi-objectif qui minimise une somme pondérée des objectifs. Ces objectifs sont définis à l'aide d'une machine à états finis, sous contraintes d'égalité et d'inégalité. Bien que cette méthode permette la génération de mouvement dynamique compte tenu de multiples contacts, la formulation n'est pas encore générique, puisqu'il n'est pas possible de définir des tâches de manipulation ou d'autres contraintes, comme l'évitement d'obstacles, et de les résoudre simultanément. Une autre approche adressant cette question de génération de mouvement entre les multi-positions de contact a été présentée dans [Lengagne et al., 2010]. Cette approche génère un mouvement complètement dynamique entre les séquences de contacts, y compris des transitions dynamiques, en formulant le problème de planification de mouvement comme un problème d'optimisation semi-infini [Reemtsen and Ruckmann, 1998] et exprimant les trajectoires articulaires comme des fonctions B-splines. Toutefois, cette approche nécessite un temps de calcul très élevée. De même, cette méthode ne permet pas de définir explicitement les tâches. Cependant, notre intérêt porte sur la liberté de choix et de résolution de tout type de tâche et l'adaptation à tout type de contrainte. Ainsi, nous avons besoin d'adopter un formalisme de fonction de tâche permettant de générer le mouvement avec le comportement requis, tout en satisfaisant les contraintes désirées et considérant la possibilité que tout corps du robot puisse entrer en contact avec n'importe quel point de l'environnement. Dans [Saab et al., 2011a], nous avons étendu à la dynamique, la méthode impliquant une cascade de QPs initialement développée pour la cinématique dans [Kanoun et al., 2009; Escande et al., 2010]. Cette méthode a permis de générer un mouvement du corps entier dynamique satisfaisant au mieux, une liste de contraintes d'égalité et d'inégalité hiérarchisées. Cependant, la solution préliminaire qui a été proposée dans ce travail pour la modélisation des contacts unilatéraux des pieds avec le

### 3. GÉNÉRATION DE MOUVEMENT DYNAMIQUE

---

sol était plutôt conservatrice et ne pouvait pas être facilement appliquée à d'autres types de contacts. Puis, dans [Saab et al., 2011b] nous avons étendu nos précédents résultats en introduisant une modélisation standard des contacts rigides unilatéraux de façon à être traités dans le formalisme de la pile des tâches (SOT) [Mansard et al., 2009b] pareillement aux contraintes d'égalité ou d'inégalité. Un cadre générique, qui permet la résolution de différents types de contraintes dynamiques avec un ordre arbitraire de priorité, y compris un ou plusieurs contacts non coplanaires, est alors établi. Nous montrons que l'approche proposée généralise la condition d'équilibre classique donnée par le "Zero Moment Point" (ZMP) [Kajita et al., 2003].

Ce chapitre traite la base de mon travail et présente principalement la méthode générique de génération de mouvement dynamique développée dans cette thèse. Tout d'abord, les schémas de commande de cinématique inverse sont rappelés, ensuite la formulation alternative et générique des cascades hiérarchisées de QP déduite de ces schémas est introduite. Puis, la formulation dynamique sans considération de contacts est décrite. Dans un second temps, la formulation standard de contacts est développée et la condition d'équilibre du ZMP est démontrée qu'elle constitue un cas particulier de cette formulation. L'efficacité de la méthode est enfin illustrée à travers des simulations de trois tâches complexes, réalisées avec le modèle dynamique de HRP-2 et impliquant des contacts non coplanaires, ainsi que des limites des positions ou couples articulaires.

En conclusion, en se basant sur une normalisation des deux schémas de commande d'inverse cinématique et d'inverse dynamique, une cascade de QPs a été proposée pour concevoir la commande en couple en tenant compte des contraintes unilatérales et bilatérales. Une formulation générique des contraintes de multi-contact a également été intégrée dans la démarche. En particulier, cette formulation permet de résoudre des tâches impliquant des contacts non coplanaires généralisant les conditions d'équilibre au-delà du critère du ZMP. Cette solution fournit un cadre efficace pour générer des mouvements dans une grande variété de tâches robotiques.

# 4

## Imitation et édition de mouvement dynamique capturé en utilisant une pile de tâches

### 4.1 Définition du problème

#### 4.1.1 Imitation de mouvement

En robotique, la génération de mouvement par imitation est devenue un domaine de recherche actif au cours de ces dernières années. La meilleure façon de faire un robot humanoïde se comporter comme un humain, est de simplement copier les mouvements humains. La simplicité est connoté à l'égard de combien nous avons besoin pour comprendre les mouvements humains afin de les reproduire. Même sans avoir besoin de comprendre ces mouvements, l'imitation de mouvement par un robot humanoïde n'est pas simplement un transfert direct. L'imitation du mouvement humain par un robot humanoïde est une tâche difficile impliquant la coordination, le contrôle et la stabilisation du robot. Ce paradigme d'imitation permettant au robot d'apprendre la manière d'exécuter une tâche en observant les manifestations de l'homme a été appelé "*learning from observation (LFO)*" [Nakaoka et al., 2007]. Les défis ici parviennent de la disparité cinématique et dynamique entre l'homme et l'humanoïde. Par ailleurs, des problèmes de coordination sont inhérents aux robots à redondance cinématique, comme c'est le cas des humanoïdes. Des difficultés de commande émanent de la complexité de la structure arborescente de tels robots, ainsi que de leur nature instable due à leur position verticale. Le robot ne doit pas seulement reproduire certains comportements capturés, mais il ne doit

#### 4. IMITATION ET ÉDITION DE MOUVEMENT DYNAMIQUE CAPTURÉ

---

pas tomber durant le mouvement, en gardant son équilibre dynamique. Ces contraintes rendent l'imitation du mouvement capturé un problème plus compliqué dans la robotique que dans l'animation par ordinateur.

Comme un humain, un robot humanoïde a deux mains, deux jambes, un torse, une tête, etc. Alors que la similitude globale peut être tout à fait convaincante à première vue, la façon et la norme dont chacune des articulations se déplace par rapport à l'autre, sont très différentes. De plus, le nombre de degrés de liberté dans le corps d'un être humain dépasse même celui des humanoïdes les plus avancés technologiquement. Cette disparité cinématique est amplifiée par le fait que les humains n'ont pas de formes et de tailles standard. Ainsi, toute méthode d'imitation doit d'abord être assez intelligente pour déterminer l'échelle du mouvement humain et le faire correspondre aux articulations appropriées du robot. Le deuxième problème est celui de la dynamique. L'agilité chez les humains ne représente pas seulement la capacité de bouger vite, mais le faire tout en préservant l'équilibre dynamique en même temps. Marcher et courir sont des exemples de mouvements dynamiques, mais les humains sont capables de plus. Dans le cas des robots humanoïdes, souvent la dynamique du système est simplifiée. Une conséquence de la relative simplicité mécanique et informatique est que les humanoïdes actuellement disponibles ont des capacités beaucoup moins développées que les capacités humaines en termes d'agilité et de dynamisme. Cela nous ramène au problème de l'imitation des mouvements humains qui sont éventuellement au-delà des capacités dynamiques de l'humanoïde. Plusieurs études ont tenté de résoudre ces questions d'imitation de mouvement en utilisant une variété d'approches, qui seront présentés dans la section 4.1.2.

Dans notre travail, nous avons été particulièrement intéressés par un mouvement dynamique, précisément la danse, car elle révèle du dynamisme. À cette fin, nous proposons d'utiliser un solveur d'optimisation générique hiérarchique pour considérer simultanément le recalage dynamique et l'édition de mouvement. Ce solveur est composé de la cascade de commande d'inverse dynamique proposée dans le chapitre 3. La flexibilité du programme permet l'ajout de tâches arbitraires dans l'espace opérationnel qui modifient la trajectoire des articulations, de générer un mouvement plus similaire, ou de changer une partie de celui-ci. Ce travail fait partie d'une collaboration avec un doctorant, Sovannara Hak, concerné par l'imitation du mouvement, surtout, par le transfert des mouvements capturés en données cinématiques articulaires, et un étudiant en master, Oscar Ramos, travaillant à adapter le mouvement et à résoudre les problèmes techniques [Ramos et al., 2011]. Ma contribution a été de proposer le projet, le gérer et de développer certaines parties, no-

tamment, la production des mouvements de référence par la capture de mouvement et d'utiliser le solveur présenté dans le chapitre 3.

### 4.1.2 édition de mouvement

Comme mentionné précédemment, de nombreux chercheurs qui s'intéressaient à rejouer des mouvements capturés, se sont aussi intéressés dans le recalage de ces données pour plus d'exactitude ou de généralité. Le point de départ est généralement le mouvement acquis par une personne en utilisant un système de capture de mouvement. Les informations recueillies à partir d'un système de capture de mouvement humain peuvent encore être organisées dans une base de données pouvant être utilisée pour la catégorisation des mouvements basés sur les comportements humains, et pour la synthèse des mouvements des robots [Yamane et al., 2011]. Alternativement, l'optimisation est une solution classique pour recalibrer le mouvement capturé avant imitation. Généralement, les applications robotiques pour l'imitation de mouvement sont larges et comprennent l'assemblage industriel [Ikeuchi and Suehiro, 1994], la marche des humanoïdes [Miura et al., 2009], le jeu de yoyo [Mombaur and Sreenivasa, 2010], le Kungfu chinois [Zhao et al., 2004], etc. En particulier, l'une des applications intéressantes est l'imitation d'une danse. L'une des œuvres pionnières de danse sur un robot est décrite dans [Nakaoka et al., 2003, 2004, 2005, 2007]. Sachant que les données recueillies à partir de l'outil de capture de mouvement, est tout simplement géométrique, et puisque nous sommes concernés par la dynamique et le réalisme du mouvement, deux phases doivent être réalisées. Tout d'abord, l'adaptation cinématique, afin d'appliquer le mouvement sur le robot humanoïde. Deuxièmement, le traitement dynamique du mouvement pour assurer la stabilité du robot et ensuite éditer le mouvement en définissant plusieurs tâches prioritaires à l'aide de la pile de tâches en résolvant une cascade de QPs dynamiques.

Ce chapitre présente les outils nécessaires et disponibles qui sont utilisés pour réaliser la capture, le recalage et l'édition de mouvement. Une description de l'appareil de capture de mouvement disponible au LAAS pour l'enregistrement des mouvements est d'abord réalisée. Ensuite, la méthode utilisée pour recalibrer le mouvement humain observé cinématiquement en utilisant un algorithme d'optimisation, est présentée. Les tâches utilisées pour l'imitation et l'édition de mouvement, qui sont intégrées dans le solveur dynamique, sont aussi introduites. Les résultats obtenus en simulation sur le robot humanoïde HRP-2 imitant un mouvement de danse sont finalement présentés.

#### 4. IMITATION ET ÉDITION DE MOUVEMENT DYNAMIQUE CAPTURÉ

---

La contribution de ce travail est de proposer une méthodologie complète pour recaler rapidement un mouvement dynamique exécuté par un expert humain, d'adapter la dynamique du corps humain à la dynamique propre du robot et de modifier ou d'éditer le mouvement initial comme désiré pour introduire des fonctionnalités supplémentaires qui n'ont pas été démontrées. Elle permet de construire des comportements complexes dynamiques, basée sur une composition de tâches et de contraintes qui sont utilisées comme briques de base pour la génération de mouvement. La méthode a été appliquée avec succès à l'imitation d'un mouvement de danse, mais généralement, elle peut être utilisée pour l'imitation de tout type de mouvement. Le mouvement obtenu est dynamiquement cohérent, et pourrait être directement rejoué par un robot humanoïde réel.

# 5

## Application du solveur de la dynamique inverse pour la génération de mouvement similaire à celui de l'humain

### 5.1 Motivation

Motivée par l'étude croissante de l'analyse du mouvement humain, et sachant que les outils et algorithmes de la robotique pourraient servir à une telle étude, nous nous intéressons à l'application de notre solveur développé pour la génération de mouvement sur un modèle humain. Sachant que les outils existants sont plutôt limités, notre objectif est d'élaborer et de fournir un logiciel pour la réalisation d'une telle analyse. D'une part, la robotique sert pour le développement des outils de génération automatique de mouvement. D'autre part, les invariants du mouvement humain qui sont dérivés des sciences du vivant sont nécessaires pour définir une référence pour la comparaison et la validation du mouvement simulé. En outre, une motivation importante à la base de ce travail provient de la collaboration du groupe de Gepetto du LAAS-CNRS avec le "Yoshihiko Nakamura Laboratory (YNL)" de l'Université de Tokyo. En fait, le laboratoire japonais est intéressé par la capture de mouvement humain et la simulation de l'activité entière musculo-squelettique (MS) correspondante en utilisant le logiciel sDIMS qu'ils ont développé. En plus du système de capture de mouvement, ils utilisent des outils de mesure plus précis tels que l'électromyographie (EMG), pour identifier et mesurer l'activation musculaire, et

## 5. GÉNÉRATION DE MOUVEMENT SIMILAIRE À L'HUMAIN

---

des plaques d'effort, pour mesurer les forces de contact du(des) pied(s) d'appui. Leur recherche est large et elle combine plusieurs domaines. Un de leur principal intérêt est d'estimer les efforts humains musculaires exercés pendant quelques mouvements ou en cas de blessures. Cela nous amène à un point d'intérêt commun qui est à la base de la collaboration entre le *LAAS-CNRS* et *YNL*. Sur le plan général, l'objectif de cette collaboration est d'échanger les développements dans le domaine de la robotique humanoïde et de mouvement anthropomorphe dans les deux laboratoires. Pendant mon séjour au *YNL*, mon travail de recherche était d'apprendre leurs outils et de comprendre la nature et les caractéristiques du mouvement humain. Notre objectif était de combiner la recherche et les développements technologiques des deux laboratoires en deux étapes principales. La première étape consiste à enregistrer le mouvement d'un être humain exécutant certaines tâches de manipulation tout en satisfaisant d'autres contraintes. Ensuite, la deuxième étape consiste à simuler le mouvement, non par imitation des données de capture de mouvement, mais en définissant une pile de tâches d'égalité et d'inégalité qui représentent les actions humaines et qui pourrait reproduire le scénario d'origine. Nous proposons de résoudre cette pile de tâches à l'aide du solveur de la dynamique inverse hiérarchisée développé dans le chapitre 3. Ensuite, nous cherchons à comparer le mouvement humain, et celui simulé sur le modèle humain, à différents niveaux en commençant par une simple comparaison visuelle et s'étendant ensuite à l'analyse qualitative des couples exercés durant le mouvement. Nous tenons également à comparer les mouvements obtenus à partir de la cinématique et la dynamique. Puisque nous avons montré au chapitre 3, que les deux formulations proviennent d'une expression générique, il est intéressant de générer le même mouvement en utilisant un modèle humain cinématique et un dynamique, et ensuite trouver les différences afin de synthétiser et d'évaluer l'effet de la dynamique. Ce chapitre ajoute au contexte du chapitre 3 quelques caractéristiques importantes:

- Le développement d'un modèle humain et l'application du solveur hiérarchique pour ce nouveau modèle.
- La capture de mouvement humain et l'extraction de la pile de tâches correspondante à ces mouvements.
- L'application du même scénario pour résoudre la cinématique et la dynamique du mouvement.
- L'étude, l'analyse et la comparaison des résultats obtenus à partir de deux simulations et du mouvement de référence.

Ce chapitre commence par la description du mouvement enregistré avec les outils de capture de mouvement disponibles au YNL. Ensuite, la pile de tâches correspondante est décrite. Enfin une comparaison à double niveau est développée pour analyser les mouvements humains à l'égard des simulations.

## 5.2 Conclusion

Dans ce chapitre, nous validons la possibilité d'utiliser notre logiciel sur tout modèle anthropomorphe. Les résultats de simulations montrent que la prise en compte de la dynamique avec une définition simple des tâches hiérarchisées pourraient reproduire des mouvements plus naturels que ceux reproduits par la cinématique seulement. Visuellement, on peut voir que le modèle dynamique présente une meilleure posture que le modèle cinématique. Cependant, en analysant les variations des couples par rapport au mouvement réel, nous détectons certaines différences typiquement au niveau de la forme des trajectoires des couples et de leur régularité. Cela est principalement dû aux limitations de notre modèle humain.

Donc, il est intéressant de développer un modèle anthropomorphe plus détaillé pareil au modèle musculo-squelettique du simulateur sDIMS. Cependant, le modèle MS est très complexe et utile pour le calcul des forces musculaires. Dans notre cas, nous pourrions limiter notre modélisation au niveau squelettique en ajoutant le même nombre de degrés de liberté ainsi que les masses, l'inertie et les longueurs des corps exactes. Nous trouvons que c'est primordial de procéder au développement d'un modèle humain complet dans le futur proche. De plus, nous cherchons de meilleurs résultats concernant les trajectoires des couples en adoptant des techniques de lissage et la définition continue des tâches. Dans [Keith, 2010; Keith et al., 2011], de nombreuses solutions ont été proposées pour résoudre ce problème. La principale solution consiste à faire des insertions et retraits de tâches par une succession d'opérations d'échanges entre les paires de tâches adjacentes. Une approche élégante consisterait à résoudre toute la pile de tâches avec un problème de minimisation unique. Cependant, cette méthode empêche de respecter la structure hiérarchique de la pile de tâches.

## 5. GÉNÉRATION DE MOUVEMENT SIMILAIRE À L'HUMAIN

---

# 6

## Conclusion et Perspectives

De la robotique aux sciences du vivant, différentes techniques et études ont été employées pour créer le lien entre les deux domaines. Cela correspond à deux chaînes évoluant indépendamment commençant respectivement par la génération et l'analyse du mouvement, puis convergeant vers un nœud commun de synthèse du mouvement.

### 6.1 Contributions

Dans cette thèse, nous avons adressé les problèmes de génération et de synthèse du mouvement. Alors, nous nous étions intéressés par la modélisation, la commande et le réalisme du mouvement. Dans une première étape, nous avons élaboré un modèle dynamique du robot humanoïde HRP-2 basé sur l'algorithme récursif de Newton-Euler en utilisant des vecteurs spatiaux. Puis, nous avons conçu un nouveau schéma de commande dynamique qui est composé d'une cascade de QPs optimisant les fonctions coûts et calculant la commande en couple en satisfaisant les contraintes unilatérales et bilatérales. La cascade des QPs est dérivée d'une pile de tâches hiérarchisées donnée. Les couples calculés constituent une des solutions plausibles pour accomplir les tâches définies et les contraintes. Une autre spécification de ce travail est de formuler une contrainte générique pour les multi-contacts qui permet de considérer de multiples contacts non-coplanaires permettant de généraliser les conditions de stabilité au-delà du critère du ZMP. Nous avons démontré l'efficacité de la méthode de génération de mouvement développée sur le robot humanoïde HRP-2 en simulation.

Afin de créer le lien entre le mouvement des humanoïdes, généré par des algorithmes issus de la robotique, et le mouvement humain, enregistré par les outils de capture de

## 6. CONCLUSION ET PERSPECTIVES

---

mouvement, nous avons développé une méthode de génération combinant l'imitation et le formalisme de la pile des tâches. Cette méthode repose sur le recalage des données capturées, puis l'édition de ce mouvement, en utilisant la définition des tâches et des contraintes dynamiques, ensuite la résolution de la pile déduite avec le solveur hiérarchique implémenté. Cette méthode originale permet de recalibrer un mouvement dynamique humain et ensuite de reproduire de manière fiable le mouvement sur un humanoïde tout en respectant la dynamique, et d'éditer ce mouvement si nécessaire.

Enfin, pour traiter le réalisme du mouvement simulé, nous avons développé un modèle anthropomorphe ayant plus de degrés de liberté que HRP-2. Nous avons appliqué notre solveur générique pour simuler le mouvement sur ce nouveau modèle. Par conséquent, nous avons défini un ensemble de tâches qui décrit avec précaution un scénario choisi joué par un être humain réel. Nous avons démontré, par une simple analyse qualitative du mouvement, qu'en considérant la dynamique au lieu de la cinématique uniquement, le mouvement résultant ressemble plus à celui de l'humain. Ainsi, nous avons été capables de reproduire un mouvement assez similaire à l'être humain réel sans avoir recours au processus d'acquisition et de recalage du mouvement.

### 6.2 Perspectives

Les travaux futurs porteront en général sur la réalisation et l'analyse de comportements plus complexes reproduisant de manière fiable des scènes de la vie réelle des hommes et imitant le mouvement humain.

À court terme, quelques modifications pratiques et évidentes peuvent être considérées. Tout d'abord, du point de vue robotique général, il est toujours important de valider les résultats sur une véritable plate-forme ainsi, nous cherchons à appliquer le mouvement généré sur le robot physique HRP-2. Même si le robot HRP-2 n'est pas commandé en couple, cependant, nous pouvons toujours appliquer les trajectoires articulaires calculées par l'intégration des accélérations articulaires. Puis, à partir de nos observations du mouvement simulé, nous trouvons une amélioration immédiate et nécessaire à faire qui consiste à introduire des contraintes supplémentaires, telles que l'évitement d'obstacles et l'auto-collision. De plus, la formulation que nous avons développée pour la contrainte de contact n'exprime pas, ni ne prend en compte les forces de friction en supposant qu'elles ne violent pas la condition de contact. Par conséquent, pour des raisons de généralité, il est préférable d'intégrer le modèle et la condition associée aux forces de frottement.

Au niveau de la définition des tâches, les expériences montrent que chaque commutation entre les tâches pourrait conduire à des discontinuités et des trajectoires non lisses. Cela se produit lors de l'insertion, suppression, changement de priorité ou un changement du comportement désiré de toute tâche ou contrainte. Les techniques de lissage s'avèrent être la solution pour contourner telles discontinuités et pourraient être considérées dans l'avenir pour améliorer les résultats. En effet, la formulation de la cascade de QPS comme un seul grand problème d'optimisation pourrait également garantir la continuité des sorties de commande.

En comparant le mouvement simulé reproduit au mouvement humain de référence, nous ressentons la nécessité de développement d'un modèle complet anthropomorphe qui représente plus précisément le corps humain, même si c'est seulement au niveau squelettique. Cela permettrait d'obtenir des résultats plus précis qui rendraient notre solveur fiable pour des applications dans les domaines de l'analyse du mouvement humain. Comme le modèle humain ne peut pas prévoir le prochain mouvement, des distorsions dans les sorties de commande apparaissent à chaque transition de tâches. Ainsi, il serait intéressant d'étudier la possibilité d'ajouter de l'anticipation au mouvement et à la commande. Cela consisterait à appliquer une méthode de résolution à 2 étapes. La première étape pour le calcul des trajectoires non lisses et la deuxième pour l'ajout de l'anticipation, sachant a priori, le temps et la quantité de distorsion. Cette sorte de prédiction rendrait le comportement du modèle lisse et semblable à celui de l'humain, mais elle compliquerait les calculs.

À long terme, nous envisageons d'appliquer cette architecture de génération de mouvement sur un modèle humain qui utilise des structures de commande plus complexes pour aider à concevoir les postes de travail. Ce sujet est basé sur la nécessité de la population active française à disposer d'évaluateurs de risques de blessures au travail et des techniques de prévention des troubles musculo-squelettiques. Afin de réduire les mauvais effets des facteurs de risque des TMS et d'autres facteurs, les entreprises ont commencé à rechercher des mesures préventives envers ces différents facteurs. Généralement, ces tentatives constituent un diagnostic possible d'une certaine situation et conduisent à des suggestions ou recommandations pour des modifications dans les postes de travail existants. Nous avons l'intention d'exploiter notre solveur élaboré pour définir et simuler des comportements humains qui permettent une conception ergonomique des postes de travail.

## 6. CONCLUSION ET PERSPECTIVES

---

# Appendix A

## Mathematical proof

We prove in the following the equivalence between the control scheme proposed in Section 3.4 and the control law proposed in [Sentis, 2007].

### A.1 Control scheme

We recall first the development of the operational-space control law for dynamic systems under rigid contacts [Sentis, 2007]. The task Jacobian knowing a set of contacts is defined by:

$$J_{t|c} = JP_c^\top \quad (\text{A.1})$$

where the subscript  $t|c$  indicates that the task space quantities are projected in the space consistent with the contact constraints. By left multiplying (3.23) by inverse transpose constrained Jacobian  $(J_{t|c} \#^{A^{-1}})^\top = (A^{-1} J_{t|c}^\top (J_{t|c} A^{-1} J_{t|c}^\top)^{-1})^\top$ , the task-space dynamic evolution is obtained:

$$\Lambda_{t|c} \ddot{e} + \mu_{t|c} = Q_{t|c} S^\top \tau, \quad (\text{A.2})$$

with  $\Lambda_{t|c} = (J_{t|c} A^{-1} J_{t|c}^\top)^{-1}$ ,  $Q_{t|c} = (J_{t|c} \#^{A^{-1}})^\top P_c$  and  $\mu_{t|c} = Q_{t|c} b + (J_{t|c} \#^{A^{-1}})^\top J_c^\top (J_c A^{-1} J_c^\top)^{-1} J_c - \Lambda_{t|c} \dot{J} \dot{q}$ . The control torques that perform the reference task are directly computed by inverting numerically (A.2):

$$\begin{aligned} \tau^* &= ((J_{t|c} \#^{A^{-1}})^\top P_c S^\top) \# f^* \\ &= J^{\star \top} f^* \end{aligned} \quad (\text{A.3})$$

where

$$J^* = J_{t|c} (S P_c^\top) \#$$

## A. MATHEMATICAL PROOF

---

and

$$F = \Lambda_{t|c}\ddot{e} + \mu_{t|c}$$

This final form corresponds to the standard force-to-joint-torque mapping, linking the end-effector forces  $f^*$  to the joint torques by the transpose of the robot Jacobian.

### A.2 Proof of equivalence

Control law (A.3) can be shown to be equivalent to the control law proposed in Section 3.4. On the one hand, since  $SP_c^\top$  is full row rank, (A.3) can be rewritten:

$$\tau^* = (SP_c^\top A^{-1}P_cS^\top)^{-1}SP_c^\top A^{-1}P_cJ^\top (JP_c^\top A^{-1}P_cJ^\top)^{-1}\ddot{e}^*, \quad (\text{A.4})$$

On the other hand, the scheme proposed in Section 3.4 can be written:

$$\tau = (JA^{-1}P_cS^\top)^{\#W}\ddot{e}^* \quad (\text{A.5})$$

with  $W$  a user-defined weight matrix. Developing the weighted inverse gives [Doty et al., 1993]:

$$\tau = WSP_c^\top A^{-1}J^\top (JA^{-1}P_cS^\top WSP_c^\top A^{-1}J^\top)^{-1}\ddot{e}^*$$

The weight is defined as:  $W = (SA^{-1}P_cS^\top)^{-1} = (SP_c^\top A^{-1}P_cS^\top)^{-1}$  [Park, 2006]. Since  $A^{-1}P_c = P_c^\top A^{-1} = P_c^\top A^{-1}P_c$  [Sentis, 2007], the equivalence between (A.4) and (A.5) is brought to prove that:

$$JA^{-1}P_cS^\top (SA^{-1}P_cS^\top)^{-1}SP_c^\top A^{-1}J^\top = (JP_c^\top A^{-1}P_cJ^\top)$$

We can recognize the form  $(SP_c^\top)^{\#A^{-1}} = A^{-1}P_cS^\top (SA^{-1}P_cS^\top)^{-1}$  in the previous equality. It thus reduces to:

$$J(SP_c^\top)^{\#A^{-1}}SP_c^\top A^{-1}J^\top = (JP_c^\top A^{-1}P_cJ^\top) \quad (\text{A.6})$$

In [Sentis, 2007], it is proven that  $(SP_c^\top)^{\#}SP_c^\top = P_c^\top$ , which concludes the proof.

# Appendix B

## Visual Task (2D Task)

This task's objective is to move the head in such a way that a certain point in the 3D space is projected to a certain position in the image seen by the robot's camera located on its head. To this end, the relation between the task space and the joint space will be obtained using the interaction matrix and the proper Jacobian.

### B.1 Interaction Matrix

The Interaction Matrix  $L$  describes the relation between the velocity of the camera and the velocity of a 2D image point. Let a 3D point in the world be  $P_w = [X_w \ Y_w \ Z_w]^T$  and its corresponding image point be  $p_i$  as shown in Figure B.1. The projection of the 3D point in the camera frame  ${}^C P_w$  to a 2D point also expressed in terms of the camera frame is obtained according to the pinhole model as:

$$\begin{cases} {}^c x_i = f \frac{{}^c X_w}{{}^c Z_w} \\ {}^c y_i = f \frac{{}^c Y_w}{{}^c Z_w} \end{cases} \quad (\text{B.1})$$

Using the scaling factor  $(s_x, s_y)$  from metric units to pixels and adding an offset to the origin, the 2D point in the image frame assuming that there is no distortion is given by:

$$\begin{cases} {}^i x_i = u_0 + f s_x \frac{{}^c X_w}{{}^c Z_w} \\ {}^i y_i = v_0 + f s_y \frac{{}^c Y_w}{{}^c Z_w} \end{cases} \quad (\text{B.2})$$

where  $(u_0, v_0)$  is the intersection of the optical axis with the image plane,  $(s_x, s_y)$  is the size of the pixel and  $f$  is the focal length. For a treatment of the methods dealing with distortion see [Salvi et al., 2002]. The motion of a 3D point measured with respect to the camera frame is the same in magnitude but opposite in direction to the motion of

## B. VISUAL TASK (2D TASK)

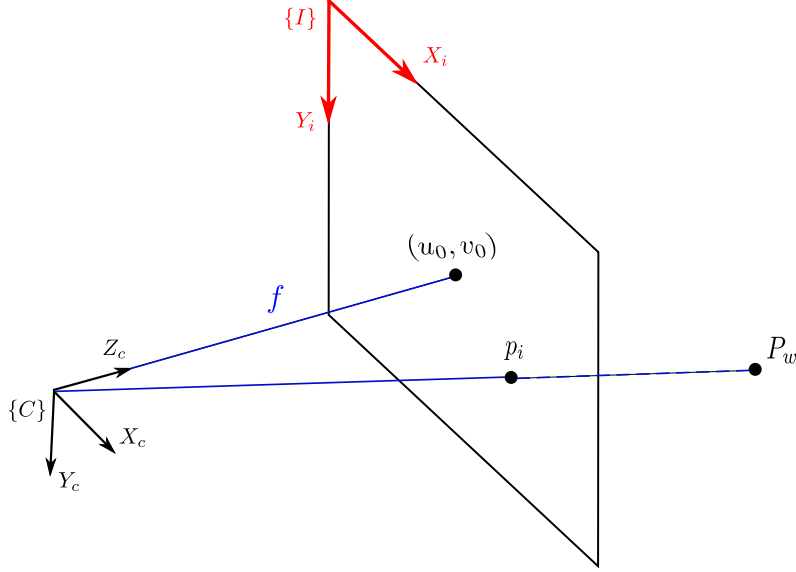


**Figure B.1:** Projection of a 3D point onto the image plane

the camera itself. For instance, if the camera moves right but the point remains still, it will seem to move left in the camera frame with the same speed. Let the velocity of the camera be  $V_c = [v_c \ \omega_c]^T$ , where the linear velocity of the camera is  $v_c = [v_x \ v_y \ v_z]^T$  and its angular velocity is  $\omega_c = [\omega_x \ \omega_y \ \omega_z]^T$ . The linear velocity of a 3D point  ${}^c\dot{P}_w$  is related to the camera velocity by [Chaumette and Hutchinson, 2006]:

$${}^c\dot{P}_w = -(v_c + \omega_c \times {}^cP_w) = \begin{cases} {}^c\dot{X}_w = -v_x - \omega_y {}^c\dot{Z}_w + \omega_z {}^c\dot{Y}_w \\ {}^c\dot{Y}_w = -v_y - \omega_z {}^c\dot{X}_w + \omega_x {}^c\dot{Z}_w \\ {}^c\dot{Z}_w = -v_z - \omega_x {}^c\dot{Y}_w + \omega_y {}^c\dot{X}_w \end{cases} \quad (\text{B.3})$$

Replacing (B.3) in the time derivative of (B.1) and setting the focal length to  $f = 1$ , without loss of generality, the relationship between the velocity of the camera and the velocity of the 2D image point in the camera frame is given by  $[{}^c\dot{x}_i \ {}^c\dot{y}_i]^T = {}^c\dot{p}_i = LV_c$ , where  $L$  is called the *interaction matrix* [Chaumette and Hutchinson, 2006] and is given by:

$$L = \begin{bmatrix} \frac{-1}{{}^cZ_w} & 0 & \frac{{}^c x_i}{{}^cZ_w} & {}^c x_i {}^c y_i & -(1 + {}^c x_i^2) & {}^c y_i \\ 0 & \frac{-1}{{}^cZ_w} & \frac{{}^c y_i}{{}^cZ_w} & 1 + {}^c y_i^2 & -{}^c x_i {}^c y_i & -{}^c x_i \end{bmatrix} \quad (\text{B.4})$$

## B.2 Frame system relations for the humanoid robot

The operational point  $x_h$  at the head has a reference frame  $\{H\}$  associated with it which has a different orientation than the one corresponding to the camera frame  $\{C\}$  as shown

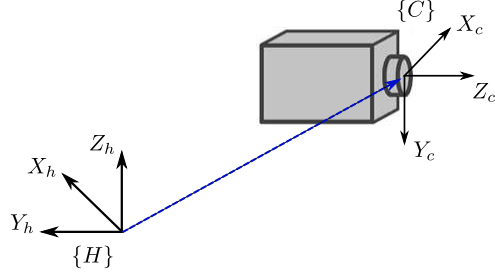


**Figure B.2:** Orientation of the camera frame  $\{C\}$  and the robot's head frame  $\{H\}$

in Figure B.2. Besides that, there is a constant offset between the position of the camera and the position of the head's operational point given by  ${}^h c = [{}^h c_x \ {}^h c_y \ {}^h c_z]^T$  in the head's reference frame. The matrix relating the frame of the head and the frame of the camera is then given by:

$${}^h M_c = \begin{bmatrix} 0 & 0 & 1 & {}^h c_x \\ -1 & 0 & 0 & {}^h c_y \\ 0 & -1 & 0 & {}^h c_z \\ 0 & 0 & 0 & 1 \end{bmatrix} \quad (\text{B.5})$$

which is a constant. At any time, the position and orientation of the head's frame with respect to the world  ${}^w M_h$  is known thanks to the forward kinematics model. Then, the relation between the camera frame and the world frame is  ${}^w M_c = {}^w M_h {}^h M_c$  and the desired 3D point  ${}^w P_w$  in the world frame is related to  ${}^c P_w$  in the camera frame by:

$${}^c P_w = {}^c M_w {}^w P_w = ({}^w M_h {}^h M_c)^{-1} {}^w P_w. \quad (\text{B.6})$$

After the 3D point has been converted to the camera frame, it can be projected to the image plane using (B.2). This point will be called  ${}^i p = {}^i p_i = [{}^i x_i \ {}^i y_i]^T$ .

## B.3 2D task specification

Considering an “infinite size” image plane, the current projection of a 3D point is  ${}^i p$  and  ${}^i p^*$  is its desired position on the image plane. The 2D visual task is then  $e = {}^i p - {}^i p^* = 0$  and its rate of change is characterized by the interaction matrix  $\dot{e} = \dot{{}^i p} = L V_c$ . The relation between  $V_c$  and the joints velocity  $\dot{q}_g$  is obtained using the basic Jacobian in the camera frame  ${}^c J$ , that is,  $V_c = {}^c J \dot{q}_g$ . The differential relation of the task is then

$$\dot{e} = L {}^c J \dot{q}_g \quad (\text{B.7})$$

with  $J_L = L {}^c J$  being the visual task Jacobian. This task is implemented using the acceleration referenced task model as in (3.37).

## B. VISUAL TASK (2D TASK)

---

# Bibliography

- ISO 11226 Ergonomie - évaluation des postures de travail statiques*, December 2000a. 36
- NF EN 614-2 Sécurité des machines - Principes ergonomiques de conception - Partie 2 : Interactions entre la conception des machines et les tâches du travail*, AFNOR, October 2000b. 36
- NF EN 614-1 Sécurité des machines - Principes ergonomiques de conception - Partie 1 : Terminologie et principes généraux*, AFNOR, July 2006. 36
- W. Abend, E. Bizzi, and P. Morasso. Human arm trajectory formation. *Brain* 105:331–348, 1982. 28
- J. Albus. The theory of cerebellar function. *Math. Biosci.* (10:25-61), 1971. 28
- R.M. Alexander. *Animal Mechanics*, volume 258. Blackwell Scientific, 1983. 25
- R.M Alexander. Walking and running. *American Scientist*, 72:348–354, 1984. 25
- R.M. Alexander. A minimum energy cost hypothesis for human arm trajectories. *Biological Cybernetics*, 76(2):97–105, 1997. 24, 30, 31
- R.M. Alexander. Bipedal animals, and their differences from humans. *Journal of Anatomy*, 204(5):321–330, 2004. 24
- David Amarantini, Guillaume Rao, and Eric Berton. A two-step emg-and-optimization process to estimate muscle force during dynamic movement. *Journal of Biomechanics*, 43(9):1827–1830, 2010. 26
- F. Anderson and M. Pandy. Dynamic optimization of human walking. *ASME Journal of Biomechanical Engineering*, 123:381–389, 2001a. 16

## BIBLIOGRAPHY

---

- F. Anderson and M. Pandy. Static and dynamic optimization solutions for gait are practically equivalent. *Journal of Biomechanics*, 34:153–161, 2001b. 16, 21, 144
- M. Aptel, S. Lafaurie, L. Tronchet, and J.J. Atain-Kouadio. Orege: un outil simple d'évaluation des facteurs de risque biomécanique de tms du membre supérieur. Technical report, INRS, 2000. 35
- H. Arisumi, J.-R. Chardonnet, A. Kheddar, and K. Yokoi. Dynamic lifting motion of humanoid robots. In *IEEE Int. Conf. on Robotics and Automation (ICRA'07)*, pages 2661–2667, Roma, April 2007. 18
- H. Arisumi, S. Miossec, J.-R. Chardonnet, and K. Yokoi. Dynamic lifting by whole body motion of humanoid robots. In *IEEE/RSJ Int. Conf. on Intelligent Robots and Systems (IROS'08)*, pages 668–675, September 2008. 18
- C. G. Atkeson and J. M. Hollerbach. Kinematic features of unrestrained vertical arm movements. *Journal of Neuroscience*, 5(9): 2318-2330, 1985. 28
- M. Audin. *Geometry*. Translated from the 1998 French original version. Springer-Verlag, 2002. 58
- P. Baerlocher and R. Boulic. Task-priority formulations for the kinematic control of highly redundant articulated structures. In *IEEE/RSJ Int. Conf. on Intelligent Robots and Systems*, Canada, October 1998. 9, 14, 143
- P. Baerlocher and R. Boulic. An inverse kinematic architecture enforcing an arbitrary number of strict priority levels. *The Visual Computer*, 6(20):402–417, August 2004. 17, 45
- B. Bardy, O. Ouillier, R. Bootsma, and T. Stroffregen. Dynamics of human postural transitions. *Exp. Psychol. Hum. Percept., Perform.*, 28:499–514, 2002. 61
- I. Belousov, C. Esteves, J.P. Laumond, and E. Ferre. Motion planning for the large space manipulators with complicated dynamics. *IEEE/RSJ Int. Conf. on Intelligent Robots and Systems (IROS'05)*, pages 3713–3719, 2005. 41, 151
- A. Ben-Israel and T. Greville. *Generalized inverses: theory and applications*. CMS Books in Mathematics. Springer, 2nd edition, 2003. 43, 44

- N. Bernstein. *The Coordination and Regulation of Movements*. Oxford: Pergamon Press, 1967. 21, 28, 144
- A. Berthoz. *Le sens du mouvement*. Odile Jacob, 1997. 24
- A. Berthoz. *La Décision*. Odile Jacob, 2003. 21, 145
- L.J. Bhargava, M.G. Pandy, and F.C. Anderson. A phenomenological model for estimating metabolic energy consumption in muscle contraction. *Journal of Biomechanics*, 37(1): 81–88, 2004. 21, 144
- L. Bianchi, D. Angelini, G.P. Orani, and F. Lacquaniti. Kinematic coordination in human gait: relation to mechanical energy cost. *Journal of Neurophysiology*, 79(4):2155–2170, 1998. 24, 25
- V. Bonnet, P. Fraisse, N. Ramdani, J. Lagarde, S. Ramdani, and B. Bardy. Modeling postural coordination dynamics using a closed-loop controller. In *IEEE-RAS International Conference on Humanoid Robots (Humanoid'08)*, Daejeon, Korea, December 2008. 64, 65
- R. Boulic, N.M. Thalmann, and D. Thalmann. A global human walking model with real-time kinematic personification. In *The Visual Computer*, volume 6, pages 344–358. Springer, 1990. 25
- K. Bouyarmane and A. Kheddar. Static multi-contact inverse problem for multiple humanoid robots and manipulated objects. In *IEEE-RAS International Conference on Humanoid Robots (Humanoid'10)*, pages 8–13, dec. 2010. 41, 151
- K. Bouyarmane and A. Kheddar. Multi-contact stances planning for multiple agents. In *IEEE Int. Conf. on Robotics and Automation (ICRA'11)*, Shanghai, China, May 2011a. 41, 151
- K. Bouyarmane and A. Kheddar. Using a multi-objective controller to synthesize simulated humanoid robot motion with changing contact configurations. In *IEEE/RSJ Int. Conf. on Intelligent Robots and Systems (IROS'11)*, San Fransisco, CA, USA, September 2011b. 41, 151
- S. Boyd and L. Vandenberghe. *Convex Optimization*. Cambridge University Press, 2004. 46

## BIBLIOGRAPHY

---

- D.C. Brogan, R.A. Metoyer, and J.K. Hodgins. Dynamically simulated characters in virtual environments. *IEEE Computer Graphics and Applications*, 18(5):58–69, 1998. 25
- A. Bruderlin and T.W. Calvert. Goal-directed, dynamic animation of human walking. In *ACM SIGGRAPH Computer Graphics*, volume 23, pages 233–242. ACM, 1989. 25
- G.E. Caldwell and L.W. Forrester. Estimates of mechanical work and energy transfers: demonstration of a rigid body power model of the recovery leg in gait. *Medicine & Science in Sports & Exercise*, 24(12):1396–1412, 1992. 24
- J.F. Canny. *The Complexity of Robot Motion Planning*. MIT Press, Cambridge, MA, USA, 1988. 11
- T. Chang and R. Dubey. A weighted least-norm solution based scheme for avoiding joints limits for redundant manipulators. *IEEE Trans. on Robotics and Automation*, 11(2):286–292, April 1995. 17
- F. Chaumette and S. Hutchinson. Visual servo control, part i: Basic approaches. *IEEE Robotics and Automation Magazine*, 13(4):82–90, December 2006. 168
- H. Choset, K. Lynch, S. Hutchinson, G. Kantor, W. Burgard, L. Kavraki, and S. Thrun. *Principles of Robot Motion: Theory, Algorithms and Implementations*. MIT Press, 2005. 10
- C.K. Chow and D.H. Jacobson. Studies of human locomotion via optimal programming. *Mathematical Biosciences*, 10(3-4):239–306, 1971. 23
- C. Collette, A. Micaelli, C. Andriot, and P. Lemerle. Dynamic balance control of humanoids for multiple grasps and noncoplanar frictional contacts. In *IEEE-RAS International Conference on Humanoid Robots (Humanoid'07)*, Pittsburgh, USA, 2007. 18, 40, 150
- B. Dariush, M. Gienger, A. Arumbakkam, C. Goerick, Y. Zhu, and K. Fujimura. Online and markerless motion retargeting with kinematic constraints. In *IEEE/RSJ Int. Conf. on Intelligent Robots and Systems (IROS'08)*, page 191198, 2008. 79, 81
- S.L. Delp and J.P. Loan. A computational framework for simulating and analyzing human and animal movement. *Computing in Science Engineering*, 2(5):46–55, sep/oct 2000. ISSN 1521-9615. doi: 10.1109/5992.877394. 21, 144

- 
- S.L. Delp, J.P. Loan, M.G. Hoy, F.E. Zajac, E.L. Topp, and J.M. Rosen. An interactive graphics-based model of the lower extremity to study orthopaedic surgical procedures. *IEEE Transactions on Biomedical Engineering*, 37(8):757–767, 1990. 31
- E. Demircan and O. Khatib. Robotics-based human dynamic performance analysis. In *Elsevier, Journal of Biomechanics Vol 43, Suppl 1. International Conference on Orthopaedic Surgery, Biomechanics and Clinical Applications, London, UK*, (June) 2010. 16
- J. B. Dingwell, C. D. Mah, and F. A. Mussa-Ivaldi. Experimentally confirmed mathematical model for human control of a non-rigid object. *J Neurophysiol*, 91(3):1158–1170, 2004. 30
- K. Doty, C. Melchiorri, and C. Bonivento. A theory of generalized inverses applied to robotics. *Int. J. of Robotics Research*, 12(1):1–19, December 1993. 49, 166
- S. Engelbrecht. Minimum principles in motor control. *J. Math Psychol.*, 45:497–542, 2001. 30
- A. Escande, A. Kheddar, and S. Miossec. Planning support contact-points for humanoid robots and experiments on hrp-2. *IEEE/RSJ Int. Conf. on Intelligent Robots and Systems (IROS'06)*, pages 2974–2979, 2006. 40, 150
- A. Escande, N. Mansard, and P-B. Wieber. Fast resolution of hierarchized inverse kinematics with inequality constraints. In *IEEE Int. Conf. on Robotics and Automation (ICRA '10)*, Anchorage, USA, May 2010. 3, 17, 18, 41, 46, 47, 59, 151
- B. Espiau, F. Chaumette, and P. Rives. A new approach to visual servoing in robotics. *IEEE Trans. on Robotics and Automation*, 8(3):313–326, June 1992. 43
- P. Evrard, F. Keith, J.-R. Chardonnet, and A. Kheddar. Framework for haptic interaction with virtual avatars. In *IEEE Int. Symp. on Robot and Human Interactive Communication*, Munich, Germany, August 2008. 59
- R. Featherstone. Robot dynamics algorithms. Kluwer academic publishers, 1987. 15, 101
- R. Featherstone. A divide-and-conquer articulated-body algorithm for parallel  $o(\log(n))$  calculation for rigid-body dynamics. part 1: Basic algorithm. *Int. J. Robotics Research*, 18:867–875, 1999. 15

## BIBLIOGRAPHY

---

- R. Featherstone. *Rigid body dynamics algorithms*. Springer, 2008. 49
- R. Featherstone and D. Orin. Robot dynamics: Equations and algorithms. In *IEEE Int. Conf. Robotics and Automation*, pages 826–834, 2000. 15
- A. G. Feldman. Functional tuning of the nervous system with control of movement or maintenance of a steady posture, ii : Controllable parameters of the muscles. *Biophysics*, 11:565–578, 1966. 28
- M. Flanders, J.J. Pellegrini, and S.D. Geisler. Basic features of phasic activation for reaching in vertical planes. *Exp Brain Res*, 1996. 28
- M. Flanders, L. Daghestani, and A. Berthoz. Reaching beyond reach. *Exp Brain Res*, 126:19–30, 1999. 28
- T. Flash and B. Hochner. Motor primitives in vertebrates and invertebrates. *Current Opinion in Neurobiology* 15 (6), pp. 660–666, 2005. 30
- T. Flash and N. Hogan. The coordination of arm movements: An experimentally confirmed mathematical model. *Journal of neuroscience*, 5:1688–1703, 1985. 21, 29, 144
- R. Fletcher. A general quadratic programming algorithm. *IMA Journal of Applied Mathematics*, 7:76–91, 1971. 46
- J-Y. Fourquet, V. Hue, and P. Chiron. Olarge: on kinematic schemes and regularization for automatic generation of human motion and ergonomic evaluation of workplaces. *33rd Annual Conf. of the IEEE Indust. Electronics Soc., IECON 07*, 2007. 8, 36, 142
- M. Gleicher. Retargetting motion to new characters. In *Proceedings of the 25th annual conference on Computer graphics and interactive techniques (SIGGRAPH 98)*, pages 33–42, Orlando, FL, USA, July 1998. 76
- G. Golub and C. Van Loan. *Matrix computations*. John Hopkins University Press, 3rd edition, 1996. 44
- K. Grochow, S.L. Martin, A. Hertzmann, and Z. Popović. Style-based inverse kinematics. *ACM Transactions on Graphics (TOG)*, 23(3):522–531, August 2004. 76
- E. Guigon, P. Baraduc, and M. Desmurget. Computational motor control: Redundancy and invariance. *Journal of Neurophysiology* 97(1):331–347, 2007. 30

- 
- C.M. Harris and D.M. Wolpert. Signal-dependent noise determines motor planning. *Nature*, 394(6695):780–784, 1998. 29
- H. Hatze. A comprehensive model for human motion simulation and its application to the take-off phase of the long jump. *Journal of Biomechanics*, 14(3):135–142, 1981. 25
- K. Hauser, T. Bretl, and J.C. Latombe. Non-gaited humanoid locomotion planning. *IEEE-RAS Int. Conf. on Humanoid Robots (Humanoid'05)*, pages 7–12, 2005. 40, 151
- A.V. Hill. The heat of shortening and the dynamic constants of muscle. *Proceedings of the Royal Society B Biological Sciences*, 126(843):136–195, 1938. 103
- J.K. Hodgins. Three-dimensional human running. 4:3271–3276, 1996. 25
- J.K. Hodgins and N.S. Pollard. Adapting simulated behaviors for new characters. *Proceedings of the 24th annual conference on Computer graphics and interactive techniques SIGGRAPH 97*, 31(Annual Conference Series):153–162, 1997. 25
- J.K. Hodgins, W.L. Wooten, D.C. Brogan, and J.F. OBrien. Animating human athletics. *Proceedings of the 22nd annual conference on Computer graphics and interactive techniques SIGGRAPH 95*, pages 71–78, August 1995. 25
- A. Hofmann, M. Popović, and H. Herr. Exploiting angular momentum to enhance bipedal center-of-mass control. In *IEEE Int. Conf. on Robotics and Automation (ICRA'09)*, Kobe, Japan, 2009. 17
- D. Hsu, J.C. Latombe, and R. Motwani. Path planning in expansive configuration spaces. *Int. J. Computational Geometry & Applications*, 9:495512, 1999. 11
- V. Hue. *Simulation de Mouvement Humain sur Postes de Travail pour le Diagnostic et l'aide la Conception*. PhD thesis, ENI, Tarbes, 2008. 7, 141
- V. Hue, J. Y. Fourquet, P. Chiron, and J. Gagne. OLARGE: A tool for automatic generation of human motion and ergonomic evaluation of workplace and tasks. *13th IEEE IFAC International Conference on Methods and Models in Automation and Robotics*, 2007. 36
- K. Ikeuchi and T. Suehiro. Toward an assembly plan from observation. task recognition with polyhedral objects. *IEEE Transactions on Robotics and Automation*, 10(3):368–385, 1994. ISSN 1042-296X. 19, 75, 79, 155

## BIBLIOGRAPHY

---

- P. Indyk and J. Matousek. *Low-distorsion embeddings of finite metric spaces*, *Handbook of Discrete and Computational Geometry*. MIT Press, Cambridge, MA, USA, 2004. 11
- V. Ivancević and T. Ivancević. *Natural Biodynamics*. World Scientific, 2005. 27
- V.G. Ivancević. Nonlinear complexity of human biodynamics engine. *Nonlinear dynamics*, 61(1-2):123–139, 2010. 26
- V.G. Ivancević and T.T. Ivancević. *Human-like Biomechanics A unified Mathematical Approach to Human Biomechanics and Humanoid Robotics*, volume 28 of *International Series on Microprocessor-Based and Intelligent Systems Engineering*. Springer, 2006. 26
- J. Järvinen and W. Karwowski. Applications of knowledge-based expert systems in industrial ergonomics: a review and appraisal. *Computer application in ergonomics, occupational safety and health*, Elsevier Science Publishers, pages 45–54, 1992. 33, 146
- E.S. Jung and A. Freivald. Development of an expert system for designing workplaces in manual handling jobs. In *W. Karwowski, A. Genaidy, S. Asfour (Eds) Computer-Aided Ergonomics - A researcher's guide*, pages 279–298, 1990. 35
- S. KAGAMI, K. NISHIWAKI, T. KITAGAWA, T. SUGIHARA, M. INABA, and H. IN-OUE. A fast generation method of a dynamically stable humanoid robot trajectory with enhanced zmp constraint. In *IEEE-RAS International Conference on Humanoid Robots (Humanoid'00)*, 2000. 19
- M.E. Kahn and B. Roth. The near minimum-time control of open-loop articulated kinematic chains. *Journal of Dynamic Systems, Measurement, and Control*, 94:164–172, 1971. 15
- S. Kajita, F. Kanehiro, K. Kaneko, K. Fujiwara, K. Harada, K. Yokoi, and H. Hirukawa. Biped walking pattern generation by using preview control of zero-moment point. In *IEEE Int. Conf. on Robotics and Automation (ICRA'03)*, pages 1620–1626, Taipei, Taiwan, September 2003. 9, 42, 78, 142, 152
- S. Kajita, H. Hirukawa, K. Harada, and K. Yokoi. *Introduction à la commande des robots humanoïdes*. Translated from the Japanese original version by S. Sakka. Springer, 2009. 57

## BIBLIOGRAPHY

---

- F Kanehiro, W Suleiman, F. Lamiroux, E. Yoshida, and J.P. Laumond. Integrating dynamics into motion planning for humanoid robots. In *IEEE/RSJ Int. Conf. on Intelligent Robots and Systems (IROS'08)*, pages 660–667, September 2008. 18
- K. Kaneko, F. Kanehiro, S. Kajita, H. Hirukawa, T. Kawasaki, M. Hirata, K. Akachi, and T. Isozumi. Humanoid robot hrp-2. *IEEE Int. Conf. on Robotics and Automation (ICRA '04)*, 2004. 10, 19, 60, 144
- K. Kaneko, F. Kanehiro, , M. Morisawa, K. Miura, S. Nakaoka, and S. Kajita. Cybernetic human hrp-4c. *IEEE-RAS International Conference on Humanoid Robots (Humanoid'09)*, pages 7–14, 2009. 7, 20, 88, 94, 141
- T. Kang, J. He, and S. I. H. Tillery. Determining natural arm configuration along a reaching trajectory. *Exp Brain Res*, 167:352–361, 2005. 30
- O. Kanoun, F. Lamiroux, F. Kanehiro, E. Yoshida, and Laumond J-P. Prioritizing linear equality and inequality systems: application to local motion planning for redundant robots. In *IEEE Int. Conf. on Robotics and Automation (ICRA'09)*, Kobe, Japan, May 2009. 3, 17, 41, 45, 46, 151
- W. KARWOWSKI, N. O. MULHOLLAND, T. L. WARD, V. JAGANNATHAN, and R. L. KIRCHNER. Liftan: An experimental expert system for analysis of manual lifting tasks. *Ergonomics*, 29(10):1213–1234, 1986. 35
- T. Kashima and Y. Isurugi. Trajectory formation based on physiological characteristics of skeletal muscles. *Biol Cybern*, 78(6):413–422, 1998. 30
- L. Kavraki, P. Svestka, J-C. Latombe, and M. Overmars. Probabilistic roadmaps for path planning in high-dimensional configuration spaces. *IEEE Trans. on Robotics and Automation*, 12:566–580, 1996. 11
- M. Kawato, Y. Maeda, Y. Uno, and R. Suzuki. Trajectory formation of arm movement by cascade neural network model based on minimum torque-change criterion. *Biological Cybernetics*, 62:275–288, 1990. ISSN 0340-1200. 21, 144
- M. Kaya, H. Minamitani, K. Hase, and N. Yamazaki. Motion analysis of optimal rowing form by using biomechanical model. In *Engineering in Medicine and Biology Society, 1995., IEEE 17th Annual Conference*, volume 2, pages 1281 –1282, September 1995. 101

## BIBLIOGRAPHY

---

- B. Kayis and K. Alimin. *Knowledge-based expert system approach to manual lifting*. Computer Applications in Ergonomics, Occupational Safety and Health, 1992. 35
- R.E. Kearney and I.W. Hunter. System identification of human joint dynamics. *Critical Reviews in Biomedical Engineering*, 18(1):55–87, 1990. 23
- F. Keith. *Optimisation de séquence de tâches avec lissage du mouvement dans la réalisation de missions autonomes ou collaboratives d'un humanoïde virtuel ou robotique*. Phd thesis, Université Montpellier 2, Montpellier, France, December 2010. 129, 159
- F. Keith, P.B. Wieber, N. Mansard, and A. Kheddar. Analysis of the discontinuities in prioritized task-space control under discrete task scheduling operations. In *IEEE/RSJ Int. Conf. on Intelligent Robots and Systems (IROS'11)*, San Francisco, USA, September 2011. 129, 159
- O. Khatib. Real-time obstacle avoidance for manipulators and mobile robots. *Int. Journal of Robotics Research*, 5(1):90–98, March 1986. 17
- O. Khatib. A unified approach for motion and force control of robot manipulators: The operational space formulation. *International Journal of Robotics Research*, 3(1):43–53, February 1987. 3, 10, 42, 49, 143
- O. Khatib, O. Brock, K.S. Chang, D. Ruspini, L. Sentis, and S. Viji. Human-centered robotics and interactive haptic simulation. *The International Journal of Robotics Research*, 23:167–178, 2004. 14
- O. Khatib, L. Sentis, and J. Park. A unified framework for whole-body humanoid robot control with multiple constraints and contacts. In *European Robotics Symposium*, pages 303–312, Prague, Czech Republic, March 2008. 16, 51, 52
- T. Komura, Y. Shinagawa, and T.L. Kunii. Creating and retargetting motion by the musculoskeletal human body model. *The Visual Computer*, 16(5):254–270, 2000. 101
- A. Konno, T. Myojin, T. Tsujita, and M. Uchiyama. Optimization of impact motions for humanoid robots. In *IEEE/RSJ Int. Conf. on Intelligent Robots and Systems (IROS'08)*, pages 647–652, September 2008. 18
- K.P. Kording and D.M. Wolpert. Bayesian decision theory in sensorimotor control. *Trends in Cognitive Sciences*, 10(7):319–326, 2006. 25

- J. Kuffner and S.M. LaValle. Prt-connect: An efficient approach to single-query path planning. *icra00*, 2, 2000. 11
- J. Kuffner, S. Kagami, K. Nishiwaki, M. Inaba, and H. Inoue. Dynamically-stable motion planning for humanoid robots. *Autonomous Robots*, 12(1):1–21, 2002. 41, 151
- J.J. Kuffner. Goal-directed navigation for animated characters using real-time path planning and control. In *Proceedings of the International Workshop on Modeling and Motion Capture Techniques for Virtual Environments, Captech'98*, pages 171–186, Geneva, Switzerland, 1998. 9, 143
- R. Kulpa. *Adaptation interactive et performante des mouvements d'humanoïdes synthétiques : aspects cinématiques, cinétiques et dynamiques*. Phd thesis, INSA Rennes, Rennes, November 2005. 76
- J-C. Latombe. *Robot Motion Planning*. Kluwer Academic Publishers, 1991. 10, 40
- J-P. Laumond. *Robot Motion Planning and Control*. Springer-Verlag, New York, NY, USA, 1998. 10, 11
- Jean-Paul Laumond. Feasible trajectories for mobile robots with kinematic and environment constraints. In *Intelligent Autonomous Systems, An International Conference*, pages 346–354, Amsterdam, The Netherlands, The Netherlands, 1987. North-Holland Publishing Co. ISBN 0-444-70168-0. 11
- J. Lauring. *Ergonomic workplace design - Development of a practitioner's tool for enhanced productivity*. Phd thesis, Chalmers University of Technology, Gothenburg, Sweden, 2004. 33, 146
- S. LaValle. *Planning Algorithms*. Cambridge University Press, 2006. 10
- H Lee, Y Huang, J Chen, and I Hwang. Quantitative analysis of the velocity related pathophysiology of spasticity and rigidity in the elbow flexors. *Journal of Neurology, Neurosurgery & Psychiatry*, 72(5):621–629, 2002. 23
- S. Lengagne, P. Mathieu, A. Kheddar, and E. Yoshida. Generation of dynamic motions under continuous constraints: Efficient computation using b-splines and taylor polynomials. In *IEEE/RSJ Int. Conf. on Intelligent Robots and Systems (IROS'10)*, pages 698 –703, October 2010. 10, 41, 143, 151

## BIBLIOGRAPHY

---

- Z. Li and J.F. Canny. *Nonholonomic Motion Planning*. Kluwer Academic Publishers, 1992. 11
- A. Liégeois. Automatic supervisory control of the configuration and behavior of multibody mechanisms. *IEEE Trans. on Systems, Man and Cybernetics*, 7(12):868–871, December 1977. 14, 43
- T. Liu and M.Y. Wang. Computation of three-dimensional rigid-body dynamics with multiple unilateral contacts using time-stepping and gaussseidel methods. *IEEE Transactions on Automation Science and Engineering*, 2(1):19–31, 2005. 71
- D.G. Lloyd and T.F. Besier. An emg-driven musculoskeletal model to estimate muscle forces and knee joint moments in vivo. 36(6):765–776, 2003. 23
- N. Mansard and F. Chaumette. Task sequencing for sensor-based control. *IEEE Trans. on Robotics*, 23(1):60–72, February 2007. 14
- N. Mansard, O. Khatib, and A. Kheddar. Integrating unilateral constraints inside the stack of tasks. *IEEE Trans. on Robotics and Automation*, 2009a. 17, 40, 150
- N. Mansard, O. Stasse, P. Evrard, and A. Kheddar. A versatile generalized inverted kinematics implementation for collaborative working humanoid robots: The stack of tasks. In *Int. Conf. on Advanced Robotics*, number 119, Munich, Germany, June 2009b. 41, 59, 152
- E. Marchand and G. Hager. Dynamic sensor planning in visual servoing. *IEEE/RSJ Int. Conf. on Intelligent Robots and Systems (IROS'98)*, 3:1988–1993, May 1998. 17
- E.J. Marey. *La machine animale*. 1872. 23
- E.J. Marey. *Le mouvement*. Springer, 1894. 23
- D. Marr. A theory of cerebellar cortex. *J. Physiol. (202:437-470)*, 1969. 28
- J. Marsot and L. Claudon. Etat de l'art des méthodes et outils utilisés pour l'évaluation en conception d'un poste de travail. Technical report, INRS, PERF-RV 2 Lot 1.1, 2006. 33, 35, 146
- S. Ménardais. *Fusion et adaptation temps réel de mouvements acquis pour l'animation d'humanoides synthétiques*. Phd thesis, Université Rennes 1, Rennes, France, January 2003. 76

- R. Merletti and P. di Torino. Standards for reporting emg data. *Journal of Electromyography and Kinesiology*, 9(1), February 1999. 103
- T.T. Minh. *Approche neuro-robotique pour la commande de gestes d'atteinte sur les robots humanoïdes*. Phd thesis, Université Toulouse III - Paul Sabatier, Toulouse, France, November 2009. 30
- S. Miossec, K. Yokoi, and A. Kheddar. Development of a software for motion optimization of robots - application to the kick motion of the hrp-2 robot. *IEEE International Conference on Robotics and Biomimetics*, 2006. 10, 18, 143
- S. Miossec, S. Lengagne, and K. Yokoi A. Kheddar and. Motion optimization of robotic systems and validation of hrp-2 robot. In *RSJ National Conference*, 2008. 18
- A. Mital, A. Nicholson, and M. Ayoub. *A guide to manual materials handling*. 1993. 35
- K. Miura, M. Morisawa, S. Nakaoka, F. Kanehiro, K. Harada, K. Kaneko, and S. Kajita. Robot motion remix based on motion capture data towards human-like locomotion of humanoid robots. *IEEE-RAS International Conference on Humanoid Robots (Humanoid'09)*, pages 596–603, December 2009. 19, 79, 155
- T.B. Moeslund, A. Hilton, and V. Kruger. A survey of advances in vision-based human motion capture and analysis. *Computer vision and image understanding*, 104(2-3): 90–126, 2006. ISSN 1077-3142. 82
- K. Mombaur and M.N. Sreenivasa. HRP-2 plays the yoyo: From human to humanoid yoyo playing using optimal control. In *Robotics and Automation (ICRA), 2010 IEEE International Conference on*, pages 3369–3376. IEEE, 2010. 79, 155
- F. Montecillo-Puente and M. Sreenivasa. On real-time whole-body human to humanoid motion transfer. *International Conference on Informatics in Control, Automation and Robotics*, 2010. 79
- P. Morasso. Spatial control of arm movements. *Exp Brain Res* 42:223–227, 1981. 28
- Analysis. Motion. Motion analysis. <http://www.motionanalysis.com/>. 82
- F. Multon. *Contrle du Mouvement des Humanoïdes de Synthèse*. PhD thesis, Université Rennes I, Rennes, France, 1998. 25

## BIBLIOGRAPHY

---

- F. Multon. *Analyse, modélisation et simulation du mouvement humain*. Université Rennes 2, IRISA, Rennes, 2006. 24, 76
- A. Murai, K. Yamane, and Y. Nakamura. Modeling and identifying the somatic reflex network of the human neuromuscular system. In *Engineering in Medicine and Biology Society, 2007. EMBS 2007. 29th Annual International Conference of the IEEE*, pages 2717–2721, August 2007. 26
- Y. Nakamura. *Advanced Robotics: Redundancy and Optimization*. Addison-Wesley Longman Publishing, Boston, 1991. 14
- Y. Nakamura and H. Hanafusa. Inverse kinematics solutions with singularity robustness for robot manipulator control. *ASME Journ of Dyn. Sys., Measures and Control*, 108: 163–171, September 1986. 3, 10, 12, 42, 143
- Y. Nakamura, K. Yamane, I. Suzuki, and Y. Fujita. Dynamics computation of musculoskeletal human model based on efficient algorithm for closed kinematic chains. *Animals*, pages 8656–8656, 2003. 101
- Y. Nakamura, K. Yamane, Y. Fujita, and I. Suzuki. Somatosensory computation for man-machine interface from motion-capture data and musculoskeletal human model. *IEEE Transactions on Robotics*, 21(1):58 – 66, feb. 2005. 26, 31, 101, 102
- Y. Nakamura, K. Yamane, and A. Murai. Macroscopic modeling and identification of the human neuromuscular network. In *Engineering in Medicine and Biology Society, 2006. EMBS '06. 28th Annual International Conference of the IEEE*, pages 99 –105, September 2006. 27
- J. Nakanishi, R. Cory, M. Mistry, J. Peters, and S. Schaal. Operational space control: A theoretical and empirical comparison. *Int. Journal of Robotics Research*, 27(6):737–757, June 2008. 16
- E. Nakano, H. Imamizu, R. Osu, Y. Uno, H. Gomi, T. Yoshioka, and M. Kawato. Quantitative examinations of internal representations for arm trajectory planning : minimum commanded torque change model. *J Neurophysiol*, 81(5):2140–2155, 1999. 30
- S. Nakaoka, A. Nakazawa, K. Yokoi, H. Hirukawa, and K. Ikeuchi. Generating whole body motions for a biped humanoid robot from captured human dances. In *IEEE Int. Conf.*

- 
- on Robotics and Automation (ICRA'03)*, pages 3905–3910, Taipei, Taiwan, September 2003. 19, 79, 155
- S. Nakaoka, A. Nakazawa, K. Yokoi, and K. Ikeuchi. Leg motion primitives for a dancing humanoid robot. In *IEEE International Conference on Robotics and Automation (ICRA'04)*, USA, April 2004. 79, 155
- S. Nakaoka, A. Nakazawa, F. Kanehiro, K. Kaneko, M. Morisawa, and K. Ikeuchi. Task model of lower body motion for a biped humanoid robot to imitate human dances. *iros05*, 2005. 10, 79, 144, 155
- S. Nakaoka, A. Nakazawa, F. Kanehiro, K. Kaneko, M. Morisawa, H. Hirukawa, and K. Ikeuchi. Learning from observation paradigm: Leg task models for enabling a biped humanoid robot to imitate human dances. *The International Journal of Robotics Research*, 26(8):829, 2007. ISSN 0278-3649. 19, 75, 79, 153, 155
- S. Nakaoka, F. Kanehiro, K. Miura, M. Morisawa, K. Fujiwara, K. Kaneko, S. Kajita, and H. Hirukawa. Creating facial motions of cybernetic human hrp-4c. In *Humanoid Robots, 2009. Humanoids 2009. 9th IEEE-RAS International Conference on*, pages 561–567, December 2009. 7, 141
- W. L. Nelson. Physical principles for economies of skilled movements. *Biol Cybern*, 46(2):135–147, 1983. 30
- O. Neo, K. Yokoi, S. Kajita, and K. Tanie. Whole-body motion generation integrating operator's intention and robot's autonomy in controlling humanoid robots. *IEEE Transactions on Robotics* 23, 4(3):763–775, 2007. 14
- K.M Newell. Motor skill acquisition. *Annual Reviews in Psychology*, 42, 213-237, 1991. 28
- J. Nilsson, A. Thorstensson, and J. Halbertsma. Changes in leg movements and muscle activity with speed of locomotion and mode of progression in humans. *Acta Physiologica Scandinavica*, 123(4):457–475, 1985. 25
- NIOSH. Work practice guide for manual lifting, technical report n°. Technical report, NIOSH Department of Health and Human service, 1991. 35
- J. Nishii and T. Murakami. Energetic optimality of arm trajectory. *Int. Conf. Biomechanics of Man*, 30–33, 2002. 30

## BIBLIOGRAPHY

---

- K. C. Nishikawa, S. T. Murray, and M. Flanders. Do arm postures vary with the speed of reaching? *J. Neurophysiol* 81:2582-2586, 1999. 28
- Sharratt M. Pezzack J. & Noble E. Norman, R. Reexamination of the mechanical efficiency of horizontal treadmill running. *Biomechanics V-B. International Series on Biomechanics*, pages 87–93, 1976. 24
- C.A. Oatis. The use of a mechanical model to describe the stiffness and damping characteristics of the knee joint in healthy adults. *Physical Therapy*, 73(11):740–749, 1993. 23
- R. Osu and H. Gomi. Multijoint muscle regulation mechanisms examined by measured human arm stiffness and emg signals. *Journal of Neurophysiology*, 81(4):1458–1468, 1999. 23
- C. Papaxanthis, T. Pozz, and M. Schieppati. Trajectories of arm pointing movements on the sagittal plane vary with both direction and speed. *Exp Brain Res*, 148(4):498–503, 2003. 28
- J. Park. *Control Strategies for Robots in Contact*. PhD thesis, Stanford University, California, USA, March 2006. 49, 50, 166
- J. Peters, M. Mistry, F. E. Udwardia, J. Nakanishi, and S. Schaal. A unifying framework for robot control with redundant dofs. *Autonomous Robots*, pages 1–12, 2008. 49
- M.R. Pierrynowski, D.A. Winter, and R.W. Norman. Transfers of mechanical energy within the total body and mechanical efficiency during treadmill walking. *Ergonomics*, 23(2):147–156, 1980. 24
- N.S. Pollard and F. Behmaram-Mosavat. Force-based motion editing for locomotion tasks. In *IEEE Int. Conf. on Robotics and Automation (ICRA '00)*, volume 1, pages 663–669, April 2000. 79
- N.S. Pollard, J.K. Hodgins, M.J. Riley, and C.G. Atkeson. Adapting human motion for the control of a humanoid robot. In *IEEE Int. Conf. on Robotics and Automation (ICRA '02)*, pages 1390–1397, Washington D.C., USA, May 2002. 19, 79
- Z. Popović. Editing dynamic properties of captured human motion. In *IEEE International Conference on Robotics and Automation (ICRA '00)*, San Francisco, CA, USA, April 2000. 76

- T. Pozzo, A. Berthoz, and L. Lefort. Head stabilization during various locomotor tasks in humans. i. normal subjects. *Exp Brain Res*, 82(1):97–106, 1990. 24
- O. Ramos, L. Saab, S. Hak, and N. Mansard. Dynamic motion capture and edition using a stack of tasks. In *IEEE-RAS International Conference on Humanoid Robots (Humanoid'11)*, October 2011. 77, 154
- J. Rasmussen, M. Damsgaard, E. Surma, S.T. Christensen, M. de Zee, and V. Vondrak. Anybody - a software system for ergonomic optimization. *Fifth World Congress on Structural and Multidisciplinary Optimization*, 2003. 21, 144
- D. Raunhardt and R. Boulic. Progressive clamping. In *IEEE Int. Conf. on Robotics and Automation*, Roma, Italy, April 2007. 17
- R. Reemtsen and J.J. Ruckmann. *Nonconvex optimization and its applications: Semi-infinite Programming*. Eds. R. Reemtsen and J.-J. Ruckmann. Springer, 1st edition, 1998. 41, 151
- M. J. E. Richardson and T. Flash. Comparing smooth arm movements with the two-thirds power law and the related segmented-control hypothesis. *J Neurosci*, 22(18):8201–8211, 2002. 30
- M. Riley, A. Ude, and C.G. Atkeson. Methods for motion generation and interaction with a humanoid robot: Case studies of dancing and catching. In *AAAI and CMU Workshop on Interactive Robotics and Entertainment 2000*, pages 35–42, 2000. 19
- J.M. Ritchie and D.R. Wilkie. The dynamics of muscular contraction. *The Journal of Physiology*, 143(1):104–113, 1958. 103
- D. Roetenberg, H. Luinge, and P. Slycke. Xsens mvn : Full 6dof human motion tracking using miniature inertial sensors. pages 1–7, 2009. URL <http://www.xsens.com/>. 81
- V. Rombach and W. Laurig. *ERGON-EXPERT: A modular knowledge-based approach to reduce health and safety hazards in manuel material handling tasks*. Taylor and Francis, 1990. 35
- M. Ruchanurucks, S. Nakaoka, S. Kudoh, and K. Ikeuchi. Humanoid robot motion generation with sequential physical constraints. In *IEEE International Conference on Robotics and Automation (ICRA 2006)*, pages 2649–2654, Orlando, FL, USA, May 2006. 78

## BIBLIOGRAPHY

---

- L. Saab, N. Mansard, F. Keith, J.Y. Fourquet, and P. Soueres. Generation of dynamic motion for anthropomorphic systems under prioritized equality and inequality constraints. In *IEEE Int. Conf. on Robotics and Automation (ICRA '11)*, Shanghai, China, May 2011a. 41, 50, 52, 151
- L. Saab, O. Ramos, N. Mansard, P. Soueres, and J.Y. Fourquet. Generic dynamic motion generation with multiple unilateral constraints. In *IEEE/RSJ Int. Conf. on Intelligent Robots and Systems (IROS'11)*, San Francisco, USA, 2011b. 41, 152
- A. Safonova, N.S. Pollard, and J.K. Hodgins. Optimizing human motion for the control of a humanoid robot. *Proc. Applied Mathematics and Applications of Mathematics*, 2003. 78
- J. Salini, S. Barthélemy, and P. Bidaud. Lqp controller design for generic whole body motion. *Climbing and Walking Robots*, 3, 2009. 14, 17
- J. Salvi, X. Armangué, and J. Batlle. A comparative review of camera calibrating methods with accuracy evaluation\* 1. *Pattern recognition*, 35(7):1617–1635, 2002. ISSN 0031-3203. 167
- C. Samson, M. Le Borgne, and B. Espiau. *Robot Control: the Task Function Approach*. Clarendon Press, Oxford, United Kingdom, 1991. 9, 14, 42, 59, 143
- S. Schaal. Is imitation learning the route to humanoid robots? *Trends Cognit. Sci.* 3: 223–231, 3:233–242, 1999. 19
- J. T. Schwartz and M. Sharir. *On the 'piano movers' problem II: General techniques for computing topological properties of real algebraic manifolds*. Courant Institute of Mathematical Sciences, New York University in New York, 1982. 10
- L. Sciaviacco and B. Siciliano. *Modelling and Control of Robot Manipulators*. Springer, 2009. 12
- L. Sentis. *Synthesis and Control of Whole-Body Behaviors in Humanoid Systems*. PhD thesis, Stanford University, USA, July 2007. 16, 40, 49, 50, 52, 150, 165, 166
- L. Sentis, J. Park, and O. Khatib. Compliant control of multicontact and center-of-mass behaviors in humanoid robots. *IEEE Trans. on Robotics*, 26(3), June 2010. 52

- T. Shiratori, S. Kudoh, S. Nakaoka, and K. Ikeuchi. Temporal scaling of upper body motion for sound feedback system of a dancing humanoid robot. In *IEEE/RSJ International Conference on Intelligent Robots and Systems (IROS 2007)*, pages 3251–3257, San Diego, USA, October 2007. 79
- B. Siciliano and O. Khatib, editors. *Springer Handbook of Robotics*. Springer, 2008. 13
- B. Siciliano and J-J. Slotine. A general framework for managing multiple tasks in highly redundant robotic systems. In *IEEE Int. Conf. on Advanced Robot*, Pisa, Italy, June 1991. 9, 14, 43, 44, 45, 49, 143
- M. Slater and M. Usoh. Presence in immersive virtual environments. In *IEEE Virtual Reality Annual International Symposium*, pages 90–96, September 1993. 23, 146
- S. Snook and V. Ciriello. The design of manual handling tasks: revised tables of maximum acceptable weights and forces. *Ergonomics*, pages 1197–1213, 1991. 35
- J. F. Soechting and F. Lacquaniti. Invariant characteristics of a pointing movement in man. *J Neurosci* 1:710–720, 1981. 28
- J. F. Soechting, C. A. Buneo, U. Herrmann, and M. Flanders. Moving effortlessly in three dimensions : does donders’ law apply to arm movement ? *J Neurosci*, 15(9):6271–6280, 1995. 30
- S Stroeve. Learning combined feedback and feedforward control of a musculoskeletal system. *Biological Cybernetics*, 75(1):73–83, 1996. URL <http://www.springerlink.com/index/X0110272T1681746.pdf>. 23
- W. Suleiman, E. Yoshida, J.P. Laumond, and A. Monin. On Humanoid Motion Optimization. In *IEEE-RAS 7th International Conference on Humanoid Robots*, Pittsburgh, Pennsylvania, USA, December 2007. 18, 20
- W. Suleiman, E. Yoshida, F. Kanehiro, J.P. Laumond, and A. Monin. On human motion imitation by humanoid robot. In *Robotics and Automation, 2008. ICRA 2008. IEEE International Conference on*, pages 2697–2704. IEEE, 2008a. 78
- W. Suleiman, E. Yoshida, J.P. Laumond, and A. Monin. Optimizing humanoid motions using recursive dynamics and lie groups. In *Proceedings of International Conference on Information and Communication Technologies: From Theory to Applications*, pages 1–6, Damascus, Syria, 2008b. 18

## BIBLIOGRAPHY

---

- H.C. Sun and D.N. Metaxas. Automating gait generation. In *Proceedings of the 28th annual conference on Computer graphics and interactive techniques SIGGRAPH 01*, pages 261–270. ACM Press, August 2001. 25
- N. Suzuki and A. Takatsu. *3d and 4d visualization of Morphological and Functional Information from the Human Body using Noninvasive Measurement Data citation*. Atlas of visualization. CRC Press, 1997. 101
- Y. Tamiya, M. Inaba, and H. Inoue. Realtime balance compensation for dynamic motion of full-body humanoid standing on one leg. *Journal of the Robotics Society of Japan*, 17(2):268–274, 1999. 19
- D. Thelen, F. Anderson, and S. Delp. Generating dynamic simulations of movement using computed muscle control. *Journal of Biomechanics*, 36(3):321–328, 2003. 16
- E. Todorov. Optimality principles in sensorimotor control. *Nat Neurosci*, 7(9):907–915, 2004. 30
- E. Todorov and Z. Ghahramani. Unsupervised learning of sensory-motor primitives. *IEEE Int. Conf. EMBS*, 2003. 31
- T. Tsujita, A. Konno, S. Komizunai, Y. Nomura, T. Owa, T. Myojin, Y. Ayaz, and M. Uchiyama. Humanoid robot motion generation for nailing task. In *IEEE/ASME International Conference on Advanced Intelligent Mechatronics, 2008.*, pages 1024 – 1029, july 2008a. 18
- T. Tsujita, A. Konno, S. Komizunai, Y. Nomura, T. Owa, T. Myojin, Y. Ayaz, and M. Uchiyama. Analysis of nailing task motion for a humanoid robot. In *IEEE/RSJ Int. Conf. on Intelligent Robots and Systems (IROS'08)*, pages 1570 –1575, Nice, France, September 2008b. 18
- J.J. Uicker. Dynamic force analysis of spatial linkages. *Transactions of the ASME journal of applied mechanics*, 34:418–424, 1967. 15
- Y. Uno, M. Kawato, and R. Suzuki. Formation and control of optimal trajectory in human multijoint arm movement: Minimum torque-change model. *Biol. Cybern.* 61:89–101, 1989. 29

- M.S. Valle, A. Casabona, R. Sgarlata, R. Garozzo, M. Vinci, and M. Cioni. The pendulum test as a tool to evaluate passive knee stiffness and viscosity of patients with rheumatoid arthritis. *BMC Musculoskelet Disord*, 7:89–100, 2006. 23
- J. Vedder and W. Laurig. Ergonlift a computer based tool for evaluation and design of manual materials handling task. *Proceedings of the 12th Triennial Congress of the International Ergonomics Association*, 2:293–295, 1994. 35
- G. Venture, K. Yamane, and Y. Nakamura. In-vivo estimation of the human elbow joint dynamics during passive movements using musculo-skeletal model computations. In *Biomedical Robotics and Biomechatronics, 2006. BioRob 2006. The First IEEE/RAS-EMBS International Conference on*, pages 205–210, February 2006. 26
- G. Venture, Y. Nakamura, K. Yamane, and M. Hirashima. A painless and constraint-free method to estimate viscoelastic passive dynamics of limbs’ joints to support diagnosis of neuromuscular diseases. In *Engineering in Medicine and Biology Society, 2007. EMBS 2007. 29th Annual International Conference of the IEEE*, pages 5362 –5365, August 2007. 7, 26, 141
- B. Vereijken, R.E.A. van Emmerick, H.T.A. Whiting, and K.M Newell. Free(z)ing degrees of freedom in skill acquisition. *Journal of Motor Behavior*, 24, 133-142, 1992. 21, 28, 144
- M. Vukobratović and B. Borovac. Zero moment point - thirty fives years of its life. *International Journal of Humanoid Robotics*, pages 157–173, 2004. 27, 57
- M. Vukobratović, B. Borovac, D. Surla, and D. Stokic. *Scientific Fundamentals of Robotics*, volume 1–7. Springer-Verlag, 1982–1988. 24
- M. Vukobratović, V. Potkonjak, and S. Tzafestas. Human and humanoid dynamics. *Journal of Intelligent and Robotic Systems*, 41(1):65–84, 2004. 27
- M.W Walker and D.E Orin. Efficient dynamic computer simulation of robotic mechanisms. *Trans. ASME, J. Dynamic Systems, Measurement & Control*, 104:205–211, 1982. 15
- X. Wang. Three-dimensional kinematic analysis of influence of hand orientation and joint limits on the control of arm postures and movements. *Biological Cybernetics*, 80: 449–463, 1999. 34

## BIBLIOGRAPHY

---

- J.H. Ward. Hierarchical grouping to optimize an objective function. *Journal of the American Statistical Association*, 58(301):236–244, 1963. 78
- T.R. Waters, Putz-Anderson V., Garg A., and Fine L. J. Revised NIOSH equation for the design and evaluation of manual lifting tasks. *Ergonomics*, 36(7):749–776, 1993. 35
- R.L Watts, A.W Wiegner, and R.R Young. Elastic properties of muscles measured at the elbow in man: Ii. patients with parkinsonian rigidity. *J. Neurol Neurosurg Psychiatry*, 49(10):1177–81, 1986. 23
- D.R. Wilkie. The mechanical properties of muscle. *British medical bulletin*, 12(3):177–182, 1956. 103
- K.R. Williams and P.R. Cavanagh. A model for the calculation of mechanical power during distance running. *Journal of Biomechanics*, 16(2):115–128, 1983. 24
- D.A. Winter. A new definition of mechanical work done in human movement. *Journal of Applied Physiology*, 46(1):79–83, 1979. 24
- D. M. Wolpert and Z. Ghahramani. Computational principles of movement neuroscience. *Nat Neurosci*, 3 Suppl:1212–1217, 2000. 29
- Xu Y. and J.M. Hollerbach. Identification of human joint mechanical properties from single trial data. *Biomedical Engineering, IEEE Transactions on*, 45(8):1051 –1060, August 1998. ISSN 0018-9294. doi: 10.1109/10.704874. 23
- K. Yamane and J. Hodgins. Simultaneous tracking and balancing of humanoid robots for imitating human motion capture data. *Data Processing*, pages 2510–2517, 2009. 79
- K. Yamane and Y. Nakamura. Dynamics filter-concept and implementation of online motion generator for human figures. *IEEE Transactions on Robotics and Automation*, 19(3):421–432, 2003a. 19, 79
- K. Yamane and Y. Nakamura. Natural motion animation through constraining and de-constraining at will. *IEEE Transactions on visualization and computer graphics*, 9(3): 352–360, July 2003b. 76
- K. Yamane and Y. Nakamura. Robot kinematics and dynamics for modeling the human body. *International Symposium on Robotics Research*, 2007. 16, 101, 103

- K. Yamane, J.K. Hodgins, and H.B. Brown. Controlling a marionette with human motion capture data. In *Proceedings of the 2003 IEEE International Conference on Robotics and Automation*, volume 3, pages 3834–3841, Taipei, Taiwan, September 2003. 19
- K. Yamane, Y. Fujita, and Y. Nakamura. Estimation of physically and physiologically valid somatosensory information. In *Proceedings of the 2005 IEEE International Conference on Robotics and Automation, ICRA 2005.*, pages 2624 – 2630, April 2005. 26, 101, 103
- K. Yamane, Y. Yamaguchi, and Y. Nakamura. Human motion database with a binary tree and node transition graphs. *Autonomous Robots*, 30(1):87–98, 2011. ISSN 0929-5593. 78, 155
- P.F. Yang, J. Laszlo, and K. Singh. Layered dynamic control for interactive character swimming. *Proceedings of the 2004 ACM SIGGRAPH Eurographics symposium on Computer animation SCA 04*, page 39, 2004. 25
- M.R. Yeadon, J. Atha, and F.D. Hales. The simulation of aerial movement—iv. a computer simulation model. *Journal of Biomechanics*, 23(1):85–89, 1990. 31
- E. Yoshida, I. Belousov, C. Esteves, and J.P. Laumond. Humanoid motion planning for dynamic tasks. *IEEE-RAS Int. Conf. on Humanoid Robots (Humanoid'05)*, pages 1–6, 2005. 41, 151
- E. Yoshida, O. Kanoun, C. Esteves, J.P. Laumond, and K Yokoi. Task-driven support polygon reshaping for humanoids. In *Proceedings of 6th IEEE-RAS International Conference on Humanoid Robots*, pages 827–832, 2006. 14
- D. Zeltzer. Motor control techniques for figure animation. *Computer Graphics and Applications, IEEE*, 2(9):53 –59, nov. 1982. 25
- J. Zhao and N. Badler. Inverse kinematics positioning using nonlinear programming for highly articulated figures. *ACM Transactions on Graphics*, 13, 1994. 17
- X. Zhao, Q. Huang, Z. Peng, and K. Li. Kinematics mapping and similarity evaluation of humanoid motion based on human motion capture. In *IEEE/RSJ International Conference on Intelligent Robots and Systems (IROS 2004)*, pages 840–845, Sendai, Japan, September 2004. 79, 155